Coordinating growth arrest and myogenesis in muscle stem cells : a molecular and cellular analysis

Despoina Mademtzoglou

Coordinating growth arrest and myogenesis in muscle stem cells: A molecular and cellular analysis

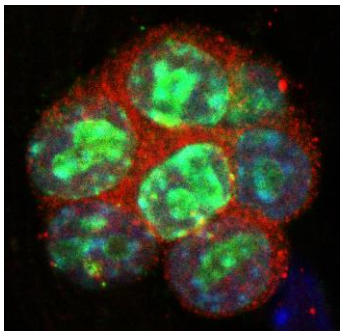

Defended on 02/09/2016

by

Despoina MADEMTZOGLOU

Jury

Prof. Miranda GROUNDS	***UWA, Perth (Australia)***	***UPMC reviewer***
Dr. Pascal MAIRE	***Institut Cochin, Paris (France)***	***UPMC reviewer***
Prof. Simone SPULER	***FU, Berlin (Germany)***	***FU reviewer***
Prof. Fritz RATHJEN	***FU, Berlin (Germany)***	***FU reviewer***
Prof. Frederic RELAIX	***UPEC, Créteil (France)***	***Thesis director***
Dr. Delphine DUPREZ	***UPMC, Paris (France)***	
Dr. Ezequiel MENDOZA	***FU, Berlin (Germany)***	

TABLE OF CONTENTS

ACKNOWLEDGMENTS

This co-tutelle Thesis was defended on 02/09/2016, in the presence of an international jury of distinguished scientists whom I would like to acknowledge. I wish to thank them for accepting to examine my work and for the helpful discussions to get a better understanding of the field and to improve my work.

Firstly I would like to thank my four reviewers Prof. **Miranda Grounds**, Dr. **Pascal Maire**, Prof. **Simone Spuler**, and Prof. **Fritz Rathjen** for the time they spent to read my manuscript, write their reports, and attend the defense, which included travelling from Australia and Germany.

- A special thanks to Prof. **M.Grounds**, whom I only met late during my PhD, but through stimulating discussions, her passion for science, and her influential work, inspires me in my future career.
- Merci à Dr. **P.Maire** for accepting to participate in my Jury. I much admire his scientific rigor since I first met him at MyoGrad's summer school and I am grateful to receive his input on my work.
- Prof. **S.Spuler** has followed me in the course of my Thesis in the Thesis Committee meetings and through MyoGrad, the PhD program she directs and in which I am enrolled. I would like to thank her for her continuous efforts to improve MyoGrad.
- I would like to thank Prof. **F.Rathjen** for taking time from his busy schedule to review my work and come to France for the defense.

Dr. **Delphine Duprez**, as part of my Thesis Committee, helped me at critical points of my PhD to evaluate my work and define the next steps. I would like to thank her for her feedback and for redacting the Committee meeting reports. I would also like to thank her for hosting us in her lab last summer for a very insightful workshop on chick embryology.

Muchas gracias to Dr. **Ezequiel Mendoza** for coming to Paris to attend one more MyoGrad defense and for the interesting discussions that preceded the defense.

In the second part of the acknowledgments I would like to thank the people who directly or indirectly participated in this project and, more generally, in my formation as a researcher.

Following a … geographical (Créteil→Paris→Berlin→Thessaloniki→Madrid) order:

I would like to thank Prof. **Fred Relaix** for trusting me with a project irrelevant to my previous lab background and for the "fred request" to join his group. He gave me the chance to work on the kind of projects that I admired since the first conferences I attended! His expertise, insightful comments, and patience added considerably to my graduate experience. I'd also like to thank him for taking time out of his busy agenda whenever I needed his guidance. I appreciate his vast knowledge and his way to present ideas and results. De ce fait, un grand merci for encouraging me to present my work in meetings. Especially the Gordon's conference just a few months after starting my project, was a great opportunity to get familiar with key players and recent advancements of the muscle field. Finally, his assistance in writing reports, his calm and pleasant character, his positive and supportive approach towards his team members have set an example for me.

Muchas gracias to Dr. **Sonia Alonso-Martin** for her continuous help throughout my thesis. Starting or completing my PhD would not be possible without the technical skills she taught me and the theoretical aspects she helped me grasp! I recognize how much effort and patience this takes and I understand por qué prefirió evitar desempeñar el mismo cargo en mi español-aprendizaje. Even after my initial learning period, it was a great relief to know that she would be around whenever I had a question (or lacked a protocol or was threatened by deadlines). Her constant good mood and enthusiasm make it very enjoyable to be in the lab (and very difficult to get angry if you somehow get trapped in a black room, counting fibers, at 10 pm). Her input and encouragement were critical many times, as were her recognition and her caring. Equally important was that she decided to include me in her projects, giving me the chance to learn and participate in things ranging from bioinformatics to graft experiments. I consider her my scientific big sister and I feel very lucky to have had her valuable guidance all these years.

I would like to express my gratitude to Dr. **Philippos Mourikis** (Φίλιππο Μουρίκη, to be grammatically correct). His continuous support, motivation, and constructive comments were essential to develop my project, to make the best use of obtained data, and to find alternatives to failed experiments. With his immense knowledge and guidance he provided me with direction. I much appreciate his patience, encouragement, and availability when it comes to new&ignorant lab members. Κι ένα μεγάλο ευχαριστώ for involving me in different aspects of the academic life and for encouraging me to interact with the people that have the expertise on the questions I needed to answer.

After four years of interaction with Dr. **Frederic Aurade**, I can confidently tell him “aie nide iou” when it comes to any aspect of molecular biology! I would like to thank him for his help sofar and for all the clonings for the p57 project (and the upcoming support for his beloved nucleo-cytoplasmic trafficking?). His magical troubleshooting abilities and extensive knowledge set a (very welcome) safety pillow for our molecular problems. Finally, it is very important to know that there is somebody in the lab to share geeky jokes with.

Mèsi **Bernie Drayton** for the immense help to organize our mice, “resurrect” our lines in the new animal facilities, and follow all necessary trainings. And all this in a permanent good-humored state, (*transcriptionally*?) primed to sing! I would also like to thank Bernie for her help during stressful periods as well as her student, **Thomas Marius**, for performing much of my genotyping.

I would like to acknowledge the work of **Bernie**, Dr. **Ted Chang**, and Dr. **Keren Bismuth** for setting the pillar of my PhD project by generating the p57-floxed mice. I am very happy to continue this project with Dr. **Matthew Borok**. His enthousiasm, creativity, and aptitude to rapidly start working independently are of great value. I would like to thank him for his understanding for my recent overwhelmed program and for his help to avoid ceasing the project while I was writing.

I want to thank Dr. **Marianne Gervais-Taurel**, **Marie Quetin**, and **Lina Gomez** for their continuous efforts and interest in solving our single fiber problems (or share our grief over clusterless fibers). Un

grand merci for **Marie**, **Zeynab Koumaiha**, and **Anikó Szegedi** for their ideas and creativity to make such a great atmosphere in the lab and help enrich the writing experience.

I would also like to thank some past members of Fred's group. Σ'ευχαριστώ Dr. **Amalia Stantzou** for all the things we shared: protocols, advice-to-freshman, ~~χώσιμο για~~ lab meeting presentations κάθε δυο βδομάδες το 2013, pineapple pizzas, and in general all the fun moments in and out of the lab! It was a pleasure to have a friend like you when starting! Merci Dr. **Antoine Zalc**, ありがとうございました Dr. **Shin Hayashi** for your advice to handle embryos and develop the developmental part of my project. Merci Dr. **Vanessa Ribes** for your persistent advice to define "what is my question".

As tutor and scientific expert of my Thesis Committee, Dr. **Benedicte Chazaud** and Dr. **Shahragim Tajbakhsh** contributed to advancing my work. Particularly I would like to thank Shahragim for helpful discussions and for giving me the chance to participate in a very informative and exceptionally well-prepared stem cell course that he co-organizes. I must add that I admire his way of thinking and his creative and enjoyable presentations.

Merci Dr. **Bruno Cadot**, **Petra Gimpel**, **Jean-François Darrigrand** for adopting me in your team until the new lab at Créteil was ready. It was very helpful to have a bench and to be in such a nice environment the last few stressful months of experiments. A special thanks to **Bruno** for giving me access to the super-microscopes that helped me see p57 in the cytoplasm for the first time! With his extensive knowledge and calm personality he is ready to help everyone at anytime. Vielen Dank **Petra** for the immense help with C2C12 culture and westerns, but also for serving as an example of how professional you can be even as a first year student. Also thanks for the psychological support, the funny atmosphere, all the german-greek exchange, and for helping me get started in Berlin!

Un clin d'oeil tout particulier à **Petra** and Dr. **Audrey Der Vartanian** for their help to communicate my results to the German and French audience. Un grand merci a **Petra**, **Audrey**, **Valerie Vilmont**, **Joana Esteves de Lima**, and **Matthew** for all the nice moments in the lab (or in Paris in general). I admire you all for proving that being a good researcher is compatible with not being arrogant.

I also wish to acknowledge **Bénédicte Hoareau** from the Flow Cytometry Core CyPS as well as the animal care facilities at UPMC and CDTA, and especially **Olivier Brégerie** and **Kim Nguyen** for the excellent collaboration. I'd also like to thank **Lila Bendameche**, **Susanne Wissler**, and **Michael Strehle** for (very efficiently) taking a big administrative burden from our shoulders.

Prof. **Carmen Birchmeier** möchte ich ganz herzlich bedanken, for accepting me in her lab in Berlin and including me in her team's projects. Her critical thinking, our discussions over the paper, and her stimulating questions incented me to widen my background. I enjoyed the interesting talks that she was organizing and the impressive meeting that her colleagues organized for her birthday, inviting speakers from all around the world!

Vielen Dank for Dr. **Dominique Bröhl** for giving me the chance to work by his side and for teaching me how to take 10^6 satellite cells from just a few mice. His calm and efficient way of working along with his amusing comments make him a very pleasant person to work with.

This list of people who helped me or forged me in the past few "lab years" would not be complete without Prof. **Penelope Mavragani-Tsipidou** and Dr. **Paloma Morales**. κ. Mavragani recruited me in her team for my dissertation back in 2008 and I am very grateful for having such a great first lab experience as well as for our interaction all these years. Her guidance and her personality were crucial in my early steps in research and I hope to always keep in mind the important lessons she taught me. Σας ευχαριστώ για την αμέριστη συμπεράσταση εντός κι εκτός εργαστηρίου και για την υποστήριξή σας όλα αυτά τα χρόνια! Muchas gracias to Paloma for accepting me in her lab as an Erasmus student, for giving me the first insights in cell culture, and for guiding me through writing the first paper! I am very happy to meet her every time I have the chance to go back to Madrid.

It's very difficult to thank in just a few sentences Dr. **Myrto Manolaki** for her support. Her eagerness to solve problems, her μεράκι in science, το πηγαίο χιούμορ της gave her a great potential to help me approximate the post-doc universe. Even though our fields exclude us from a mutual Nobel prize or

Fields medal I still hope that we'll get the chance to collaborate in one of her brilliant ideas to combine mathematics and life sciences.

Finally, I wish to thank my friends for ~~tolerating~~ cheering me up when the failed recombinations were striking. Especially **Nestoras**, **Magda**, **Elma** for the nice memories I have with them in Paris, **Maria**, **Matina** για τις ξέγνοιαστες βόλτες μας το ~~SugarAngel~~ Thessaloniki, and **Marietta** for our expeditions in Athens&Roma. Last but not least, I would like to thank my parents **Prodromos** and **Anastasia** for being supportive to my decisions and for giving me the strength to chase my dreams.

LIST OF ABBREVIATIONS

bHLH	basic Helix-Loop-Helix
BMP	Bone Morphogenetic Protein
BWS	Beckwith-Wiedemann Syndrome
CAK	Cdk-Activating Kinase
CDK	Cyclin-Dependent Kinase
CDKI	Cyclin-Dependent Kinase Inhibitor
DKO	Double Knock-Out
DTA	Diphtheria Toxin Fragment
DP	Differentiation-regulated transcription factor-1 Polypeptide
EMT	Epithelial–Mesenchymal Transition
ECM	ExtraCellular Matrix
FAP	Fibro/Adipogenic Progenitor
Fucci	Fluorescent Ubiquitynation-based Cell Cycle Inditator
HGF	Hepatocyte Growth Factor
KID	Kinase Inhibitory Domain
LIMK	LIM domain Kinase
MRF	Myogenic Regulatory Factor
MyHC	Myosin Heavy Chain
NICD	Notch IntraCellular Domain
NLS	Nuclear Localization Signal
PDGFR	Platelet-Derived Growth Factor Receptor
PP	Pocket Protein
PIC	PW1+ interstitial cell
Rb	RetinoBlastoma protein
SF	Scatter Factor
SP	Side Population
VEGF	Vascular Endothelial Growth Factor

ABSTRACT

Tightly controlled growth arrest coordinates the equilibrium between cell proliferation and cell differentiation during embryonic tissue formation as well as in adulthood during stem cell-mediated tissue regeneration. Myogenic differentiation requires a coordinated course of tissue-specific gene expression and irreversible cell cycle exit. However, I contributed to showing -using genetic manipulation in the mouse embryo- that these processes can be uncoupled. During development, growth arrest in myogenic cells is mediated by the cyclin-dependent kinase inhibitors (CDKIs) p21 and p57, which act redundantly to promote cell cycle exit. We demonstrated that skeletal muscle progenitors require a direct interaction with the differentiating myoblasts via the Notch signaling pathway to maintain their pool. We also identified a muscle-specific regulatory element of p57 that directly receives the input of Myogenic Regulatory Factors (MRFs) and Notch downstream targets. During my Ph.D. I examined whether this regulatory mechanism is also involved in postnatal myogenesis.

Adult skeletal muscle has a remarkable regenerative capacity, involving a stem cell population, called satellite cells (SCs), located on close contact to the myofibers under the basal lamina. At the transition from juvenile to adult state (around 3-4 week during postnatal growth in mice) they enter a non-cycling, quiescent state. Upon injury the SCs rapidly get activated, expand by proliferation and provide differentiated progeny for muscle repair, while a subpopulation self-renews and re-enters quiescence, allowing the support of additional rounds of muscle damage. To understand the mechanisms regulating acquisition of quiescence, we explored the role of the aforementioned CDKIs in adult muscle. Although absent from quiescent SCs, they become rapidly expressed upon activation (even in proliferating myoblasts) and their levels remain high in the differentiating muscle cells. Strikingly, during the course of differentiation p57 translocated from the cytoplasm of activated myoblasts to the nuclei of differentiating cells. Since p57 deficient mice die at birth, we generated a conditional knock-out allele to perform functional studies at the postnatal stages. This new allele, in which the coding region can be removed by the loxP/Cre recombination system, also contains a β-galactosidase reporter allowing the identification of p57-expressing cells. We generated a complete

loss of function allele using a ubiquitously expressed Cre, and observed developmental and perinatal phenotypes similar to previously described germline knock-outs. Furthermore, we showed that the reporter inserted in the p57 conditional allele faithfully recapitulates p57 expression profile at embryonic and adult tissues. Conditional ablation of p57 in adult SCs resulted in reduced myogenic differentiation in primary myoblast culture. Similarly, p21-null myoblasts exhibited proliferation and differentiation defects in single myofiber cultures. In vivo regeneration studies with p21 mutants showed an early impact on the SC pool, while both SCs and muscle structure were re-established by the end of the regeneration process. My Ph.D. work suggests that p21 and p57 are at play during adult myogenesis and cell cycle exit, although via different mechanisms compared to the developmental scenario. They both work at the early steps of satellite cell activation but do not compensate for each other's loss. Future studies will elucidate whether they lie genetically downstream of the MRFs and Notch targets during postnatal myogenesis.

RÉSUMÉ

Au cours du développement embryonnaire, tout comme chez l'adulte, la formation ainsi que la régénération des tissus nécessitent une régulation fine du cycle cellulaire afin de maintenir l'équilibre entre la prolifération et l'entrée en différenciation des cellules. La différenciation myogénique nécessite une coordination parfaite entre l'expression des gènes spécifiques au développement musculaire et la sortie irréversible du cycle cellulaire des cellules constitutives du tissu. Cependant, j'ai contribué à montrer que ces processus peuvent être découplés chez l'embryon via la génération de modèles murins génétiquement modifiés.

Au cours de la différenciation myogénique chez l'embryon, l'arrêt du cycle cellulaire est contrôlé par les inhibiteurs de kinases cyclines-dépendantes (CDKI) p21 et p57 qui présentent une activité redondante. Nous avons démontré que les cellules progénitrices du muscle squelettique requièrent une communication directe avec les myoblastes en différentiation via la voie de signalisation cellulaire Notch afin de maintenir cette population dans un état indifférenciée. De plus, nous avons mise en évidence la présence d'un élément de régulation spécifique du muscle dans la séquence du

gène p57 répondant aux facteurs myogéniques (Myogenic Regulatory Factors, MRFs) et aux gènes cibles de la voie de Notch. Dans la poursuite de ces travaux, j'ai ensuite étudié l'implication de ce mécanisme de régulation au cours de la myogenèse postnatale pendant mon travail de thèse.

Les cellules souches du muscle, ou cellules satellites, sont localisées sous la lame basale au contact des myofibres et confèrent une capacité de régénération remarquable au tissu musculaire. Chez la souris, au cours de la transition entre le stade juvénile et le stade adulte (c'est à dire 3-4 semaines après la naissance) les cellules satellites rentrent en état de quiescence. Sous l'action d'un stimuli externe ou lors d'une blessure musculaire, les cellules satellites s'activent et prolifèrent. Au cours de la régénération du muscle, une sous-population va se différencier pour réparer le muscle lésé alors qu'une partie de cette population va s'auto-renouveler afin de maintenir le stock de cellules souches quiescentes.

Dans le but de comprendre les mécanismes qui régissent l'entrée en quiescence de ces cellules, nous avons étudié le rôle de p21 et p57 et dans le muscle adulte. Bien que l'expression des gènes codants pour ces CDKIs ne soit pas détectée dans les cellules satellites quiescentes, ils sont rapidement détectés dès leur activation mais également dans les myoblastes et les cellules musculaires en différentiation où ils sont fortement exprimés. Au cours de la différenciation myogénique p57 est transloqué depuis le cytoplasme des myoblastes jusqu´au noyau des cellules en différenciation.

Chez la souris, l'ablation du gène p57 est létale à la naissance. Afin de pouvoir étudier le rôle fonctionnel de cette protéine après la naissance, nous avons généré un modèle murin présentant une modification génique conditionnelle permettant de muter le gène p57. Cette construction conditionnelle utilise le système de recombinaison Cre/LoxP qui permet d'exciser la séquence codante du gène p57. Elle contient également le gène rapporteur β-galactosidase afin de pouvoir identifier les cellules qui expriment p57. La perte totale de fonction générée par l'utilisation d'une Cre recombinase exprimée de manière ubiquitaire a permis de caractériser les phénotypes observés au cours du développement embryonnaire et au cours de la période périnatale. Les phénotypes observés sont identiques aux phénotypes décrits précédemment chez les souris présentant une perte

de fonction du gène p57. De plus, nous avons pu caractériser le profile d'expression de ce gène au cours du développement embryonnaire et dans les différents tissus chez l'adulte grâce au gène rapporteur.

Dans les cultures primaires de cellules satellites adultes, la délétion de p57 conduit à une diminution de la différenciation myogénique. De même, les cultures de fibres isolées issues des myoblastes mutants pour le gène p21, présentent des défauts de prolifération et de différenciation. In vivo, l'étude de régénération chez les mutants p21 montre une réduction précoce de la population satellitaire. Paradoxalement, la population des cellules souches du muscle ainsi que la structure du tissu musculaire sont entièrement reconstituées à la fin du processus de régénération.

Mon travail de thèse suggère que p21 et p57 jouent un rôle important dans la myogenèse et la régulation du cycle cellulaire. Ces protéines ont une action similaire qui est déterminante sur l'activation des cellules satellites et agissent de manière précoce sur ces dernières. Cependant, chez l'adulte leur activité semble distincte lorsqu'un des deux CDKIs est manquant contrairement au stade embryonnaire. Mes travaux ouvrent des perspectives nouvelles sur le rôle de p21 et p57 en aval de la voie de signalisation de Notch et des MRFs au cours de la myogenèse post-natale.

ABSTRAKT

Das Gleichgewicht zwischen Zellproliferation und Zelldifferenzierung wird während der embryonalen Gewebebildung sowie während der stammzellvermittelten Geweberegeneration im Adultstadium durch einen streng kontrollierten Wachstumsarrest koordiniert. Die myogene Differenzierung erfordert sowohl eine koordinierte Abfolge von gewebespezifischer Genexpression als auch einen irreversiblen Zellzyklusaustritt. Jedoch konnte ich durch genetische Manipulation von Mausembryos dazu beitragen, aufzuzeigen, dass diese beiden Prozesse voneinander entkoppelt werden können. Ein Wachstumsarrest myogener Zellen wird während der Entwicklung durch die Cyclin-abhängigen Kinaseinhibitoren (CDKIs) p21 und p57 vermittelt. Letztere wirken dabei redundant, um einen Zellzyklusaustritt zu fördern. Wir konnten bereits nachweisen, dass skelettale Muskelvorläuferzellen

eine direkte Interaktion mit differenzierenden Myoblasten über den Notch-Signalweg benötigen, um ihren Pool aufrecht zu erhalten. Des Weiteren haben wir ein muskelspezifisches regulatorisches Element von p57 identifiziert, das direkten Input von myogenen Regulationsfaktoren (MRFs) und Notch Stromabwärts-Zielen erhält. Im Rahmen meiner Doktorarbeit habe ich untersucht, ob dieser regulatorische Mechanismus auch in der postnatalen Myogenese involviert ist.

Der adulte skelettale Muskel hat eine bemerkenswerte regenerative Kapazität, die eine Stammzellpopulation, sogennante Satellitenzellen (SCs, engl. für "satellite cells") involviert. Diese befinden sich zwischen der Basallamina und der Muskelfaser. Beim Übergang zwischen juvenilen und adultem Stadium (zwischen 3-4 Wochen während des postnatalen Wachstums in Mäusen), gehen die Satellitenzellen in einen nicht-zyklischen Ruhezustand über. Satellitenzellen werden nach einer Verletzung schnell aktiviert, expandieren und stellen differenzierte Abkömmlinge für die Muskelreparatur zur Verfügung. Eine Subpopulation der Satellitenzellen erneuern sich selbst und gehen zurück in den Ruhezustand, so dass bei erneuter Muskelverletzung Unterstützung gewährleistet ist. Um die Mechanismen verstehen zu können, die den Übergang in den Ruhezustand regulieren, haben wir die Rolle der zuvor genannten CDKIs im adulten Muskel untersucht. Obwohl CDKIs in ruhenden Satellitenzellen abwesend sind, werden sie nach Aktivierung der Satellitenzellen schnell exprimiert, und ihr Expressionslevel bleibt in differenzierenden Muskelzellen aufrecht erhalten. Erstaunlicherweise transloziert p57 während des Differenzierungsprozesses vom Zytosplasma in den Zellkern. Da p57-defiziente Mäuse bei Geburt sterben, haben wir eine konditionelle Mausmutante generiert, um funktionale Studien im postnatalen Stadium durchführen zu können. Dieses neue Mausmodell hat ein modifiziertes p57-Allel, in dem die codierende Region von p57 durch loxP/Cre-Rekombination entfernt werden kann. Des Weiteren beinhaltet es auch das Reportgen β-Galactosidase, um p57-exprimierende Zellen identifizieren zu können. Wir haben durch eine ubiquitär exprimierte Cre-Rekombinase vollständige Knockout-Mäuse generiert und dabei entwicklungsorientierte und perinatale Phänotypen, ähnlich wie bei bereits beschriebenen Knockout-Mäusen, beobachtet. Des Weiteren konnten wir zeigen, dass der in das konditionelle p57-Allel eingefügte Reporter dem Expressionsprofil von p57 im embryonalen und adulten Gewebe entspricht. Konditionelle Ablation von p57 in Satellitenzellen resultierte in einer reduzierten myogenen

Differenzierung von primären Myoblastenkulturen. p21-defiziente-Myoblasten wiesen ähnliche Proliferation- und Differenzierungsdefekte in einzelnen Muskelfaser-Kulturen auf. In-vivo-Regenerationsstudien mit p21-Mutanten haben eine initiale Reduktion der Satellitenzellenanzahl gezeigt. Zum Ende des Regenerationsprozesses waren die Anzahl der Satellitenzellen sowie die Muskelstruktur jedoch re-etabliert. Meine Doktorarbeit lässt darauf schließen, dass p21 und p57 während der adulten Myogenese und des Zellzyklusaustritts eine Rolle spielen, jedoch unterscheidet sich der Mechanismus im Vergleich zum pränatalem Stadium. Beide fungieren bei frühzeitigen Schritten der Satellitenzellenaktivierung, aber kompensieren sich nicht für den gegenseitigen Verlust. Künftige Studien werden zeigen, ob p21 und p57 von MRFs und Notch während der postnatalen Myogenese reguliert werden.

INTRODUCTION

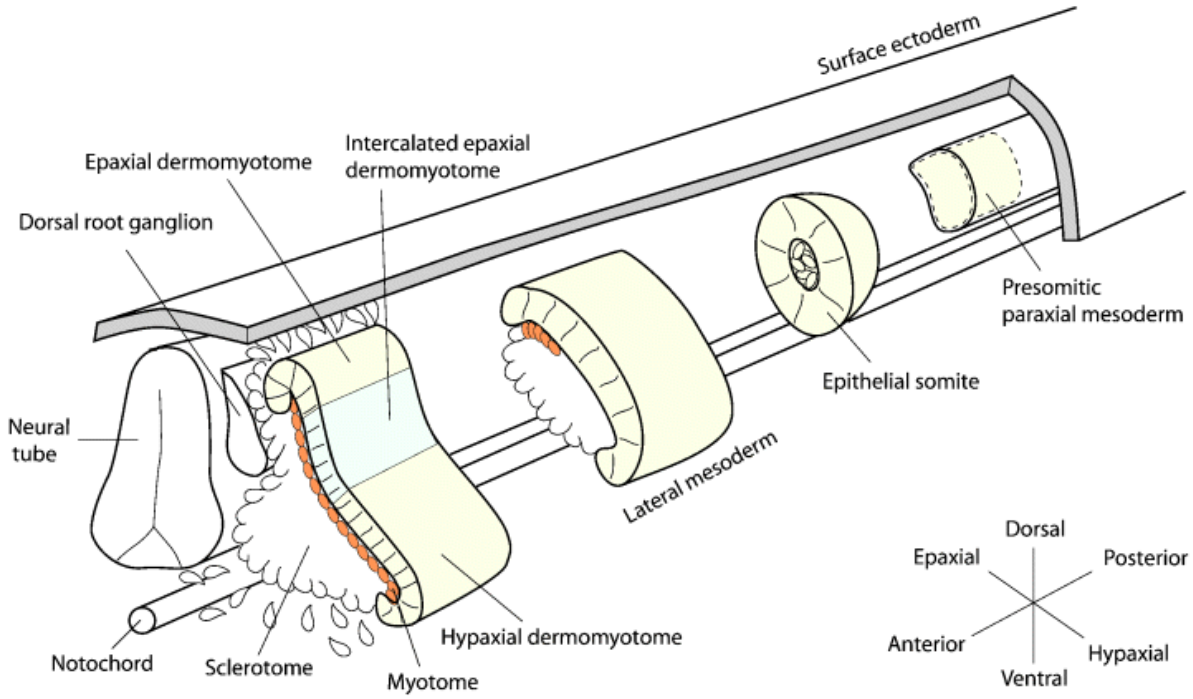

Figure 1.1. From somites to myotome.

Trunk and limb muscle derive from the paraxial mesoderm. The presomitic mesoderm will get progressively segmented into distinct, epithelially enclosed units, termed somites, which undergo several steps of specification and differentiation in a posterior-to-anterior orientation. As maturation proceeds they are compartmentalized into sclerotome and dermomyotome in response to signals from the adjacent structures. Cells from the dermomyotome migrate later to form the underlying myotome, the first differentiated skeletal muscle, as well as to distal myogenic sites, such as the developing limbs, diaphragm, and tongue.

Adapted from: Buckingham et al., 2003

Chapter 1. Skeletal muscle development, growth, and regeneration

1.1 Embryonic myogenesis: from somites to the first muscle masses

1.1.1 Somitogenesis: formation of multipotent mesodermal structures

Starting as a unicellular totipotent zygote the nascent organism develops into a multitude of differentiated, functionally interacting tissues and organs. During gastrulation, cells produced by consecutive divisions of the zygote and its descendants ingress through the blastopore/primitive streak to generate the three germ layers of the embryo, namely ectoderm, mesoderm and endoderm that will contribute all embryonic tissues. Skeletal muscle is of mesodermal origin and its emergence and organization is a complex process starting soon after gastrulation (E8 at mouse) [1].

Among the mesodermal compartments (axial, paraxial, intermediate, and lateral plate), the paraxial mesoderm gives rise to all the muscles of the limbs and ventral body [Christ & Ordahl, 1995], while branchiomeric and ocular muscles derive from cranial/pharyngeal and prechordal cranial mesoderm [Scaal & Christ, 2004; Buckingham & Mayeuf, 2012]. The paraxial mesoderm constitutes two longitudinal columns of mesoderm on each side of the neural tube/notochord [Pourquié, 2001]. It will undergo somitogenesis, meaning generation of somites, which are segmented epithelial units that develop stepwise to give rise to the ventral mesenchymal sclerotome and the dorsal epithelial dermomyotome (**Fig. 1.1**). Apart from the differences in origin of body (trunk, limb) and head musculature, distinct genetic networks operate in each of them [Tajbakhsh, 2009; Bismuth & Relaix, 2010] and diverse turnover has been reported [McLoon et al., 2004; Keefe et al., 2015; Pawlikowski et al., 2015]. Limb and trunk musculature are, in general, more extensively studied and of more relevance to my PhD work and, thus, will be on focus in this section.

Somitogenesis occurs in coordination with embryo extension along the antero-posterior axis. Within the presomitic mesoderm, cellular arrangements of prospective somites point to a segmental pattern prior to somitogenesis and in response to intrinsic signals [Pourquié, 2001]. During gastrulation, new

Table 1.1. Somitogenesis across species [Hubaud & Pourquié, 2014].

Organism	Frequency of new pair addition	Final number of somite pairs
zebrafish	25 minutes	33
mouse	2 hours	65
human	4-5 hours	38-44

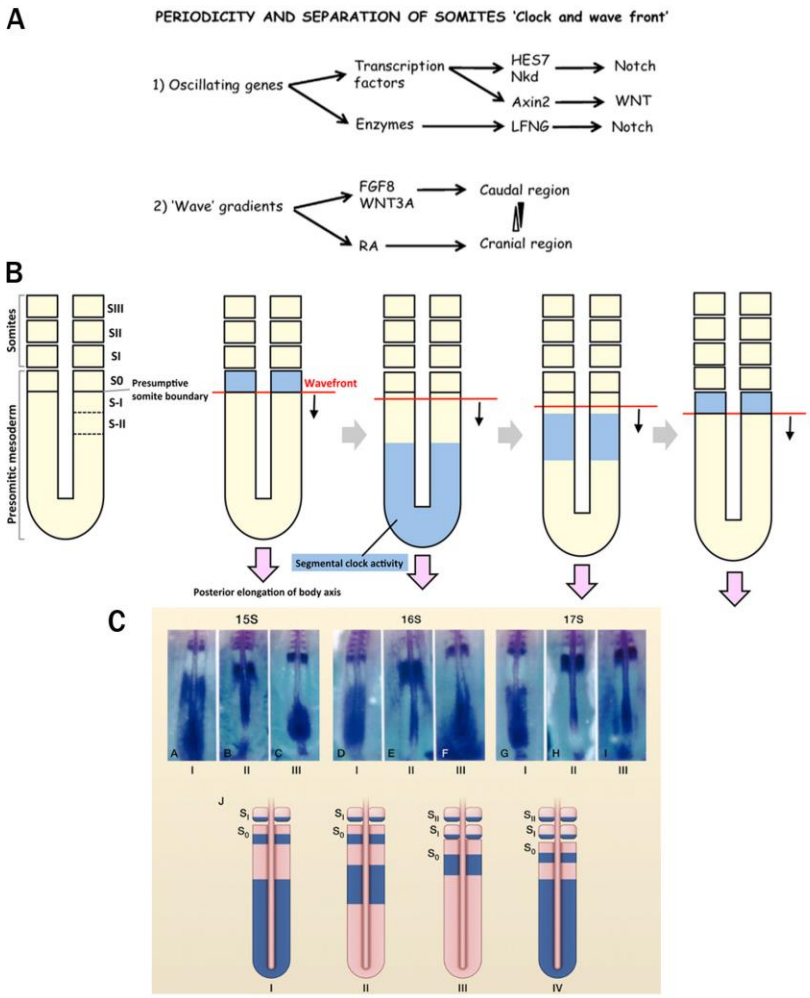

Figure 1.2. The "clock and wavefront" model for periodic somite generation

A. Major molecular contributors to the oscillation (clock) and gradient (wavefront) components of the model. B. Schematic representation of the location of activity of the clock and wavefront. C. Oscillatory expression of *c-hairy1* (*in situ* hybridization during formation of somites 15 to 17).

Adapted from: Pourquié, 2011; Musumeci et al., 2015; Yabe & Tanaka, 2016

mesenchyme cells enter the paraxial mesoderm leading to the addition of bilaterally symmetrical somite pairs at the anterior end of the presomitic mesoderm [Christ & Ordahl, 1995]. Convergence-extension movements of this phase produce the future anterior somitic mesoderm, while later on the tail bud contributes caudal somites [Pourquié, 2001]. Somitogenesis is a stepwise procedure involving periodic formation, separation, epithelialization, specification, and differentiation (with additional Epithelial–Mesenchymal Transition (EMT) transitions to form the sclerotome and myotome) [Musumeci et al., 2015].

Somites emerge periodically in a species-specific frequency (**Table 1.1**). To explain this feature, a theoretical model, the "clock and wavefront" model, was proposed in the 1970s (**Fig. 1.2**) [Cooke & Zeeman, 1976]. The clock refers to intrinsic oscillator(s) that make(s) presomitic mesoderm fluctuate between permissive and non-permissive states of somite formation (**Fig. 1.2B**) [Kalcheim & Ben-Yair, 2005]. The wavefront of competence to generate somites lays at a defined position with regard to the tail bud (**Fig. 1.2B**) [Saga, 2012]. On a molecular level, the idea of the clock was supported by the discovery of cyclic waves of *c-hairy1* linking it with somitogenesis (**Fig. 1.2C**) [Palmeirim et al., 1997]. This was followed by the identification of several other transcription factors (e.g. HES7, AXIN2) or enzymes (e.g. LFNG), mainly belonging to the Notch, FGF and Wnt pathways, which are periodically expressed at defined time intervals imitating the segmentation rounds (**Fig. 1.2A**) [Pourquié, 2011; Musumeci et al., 2015]. Notch, a key player of intercellular communication of neighboring cells, is further suggested to act by synchronizing the oscillations of individual cells [Horikawa et al., 2006]. The clock is mainly considered to act through the activation of the MESP transcription factors [Saga, 2012]. Different segment periodicities in the anterior and posterior presomitic mesoderm of zebrafish were revealed by recent live imaging experiments [Shih et al., 2015]. Another recent study challenged the role of the clock, counter-suggesting that cell-cell interactions drive somitogenesis [Dias et al., 2014]. However, they described somite-like structures [Dias et al., 2014] which were later criticized as being expected self-organizing differentiating derivatives, missing several somite characteristics [Hubaud & Pourquié, 2014]. The wavefront corresponds at the molecular level to a threshold of different signaling gradients, with Wnt and FGF signaling being highest at the posterior unsegmented paraxial mesoderm and retinoic acid following a counter-gradient (**Fig. 1.2A**) [Hubaud & Pourquié,

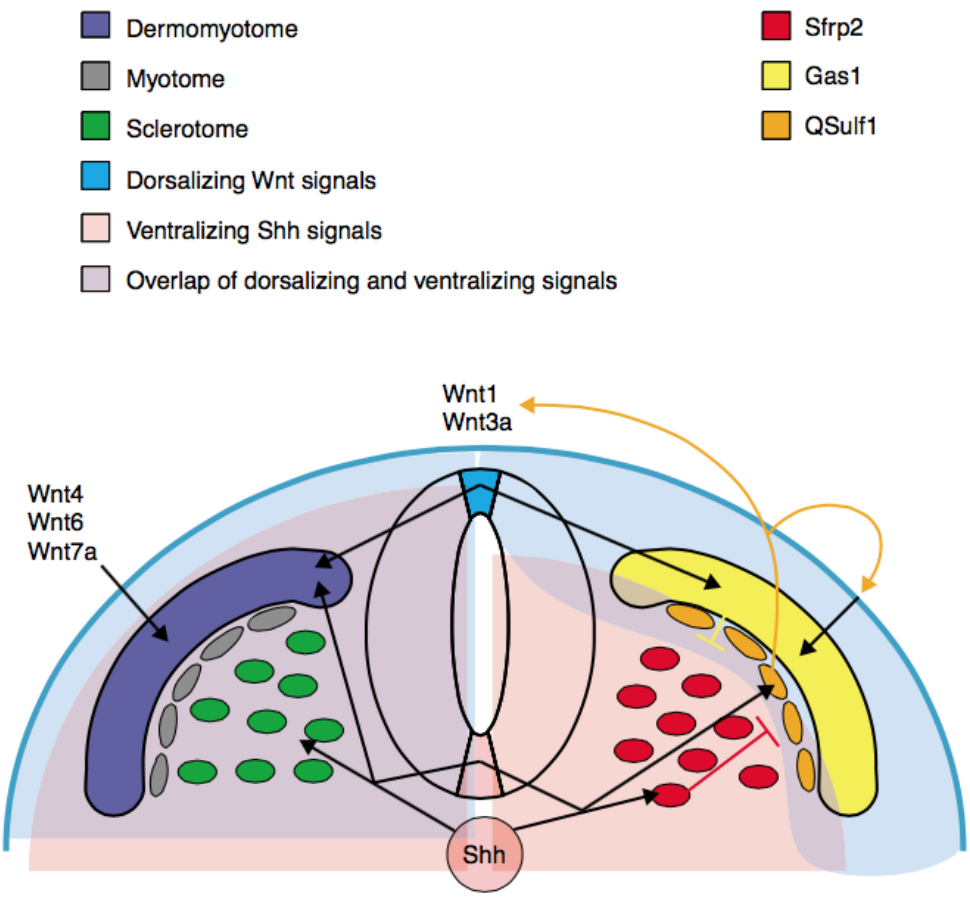

Figure 1.3. Dorsalizing and ventralizing signals involved in somite differentiation.

Left half simplistically focuses on the major dorsalizing (Wnt) and ventralizing (Shh) signals that act on the developing somites. Right half underlines the necessary activity of further factors for the final fine gradient driving the formation of dermomyotome in the dorsal somite and sclerotome in the ventral moiety.

Source: Brent & Tabin, 2002

2014; Mallo, 2016]. These gradients depend on mRNA decay or gradients of synthesizing and degrading enzymes, respectively [Aulehla & Pourquié, 2009]. Retinoic acid is also suggested to participate in synchronically generating left and right somites [Sirbu & Duester, 2006].

Once the new somite pair is signaled to be formed, it needs to undergo detachment and epithelialization. Separation of consecutive somites and formation of an acellular intersomitic border depend on the families of cadherins and ephrins and their receptors [Kalcheim & Ben-Yair, 2005]. Before complete detachment, mesenchymal-epithelial transition takes place, driven by the bHLH transcription factor PARAXIS and the GTPases CDC42 and RAC1 [Burgess et al., 1996; Nakaya et al., 2004]. Adhesion molecules (e.g. N-cadherin) and Fibronectin, an extracellular matrix protein were also found to participate in epithelialization [Duband et al., 1987; Linask et al., 1998]. Interestingly, in *Paraxis*-null mice epithelial somites are substituted by mesenchymal blocks, uncoupling segmentation and epithelialization [Burgess et al., 1996].

The next steps of somitogenesis involve specification and differentiation. Somite specification appears to depend on HOX genes, with maintenance of the HOX profile even after heterotopic transplantation [Nowicki & Burke, 2000]. Differentiation is largely attributed to interactions and molecular signals originating from the surrounding tissues. The ectoderm and notochord mediate dorsalization with signals such as Wnt proteins and Bone Morphogenetic Proteins (BMP), while the neural tube provides ventralizing signals, such as Sonic hedgehog homolog (Shh) or the BMP antagonist Noggin [Christ & Brand-Saberi, 2002; Scaal & Christ, 2004]. Further factors, such as SFRP2 or GAS1 antagonize Wnt and Shh, respectively, to prevent their long-range signaling and induce gradients of dorsalizing and ventralizing signals (**Fig. 1.3**) [Brent & Tabin, 2002].

Somites bud off the paraxial mesoderm at its rostral extremity, so that the caudalmost somite is the youngest or somite number I, according to the applied dynamic staging system with consecutive Roman numbers (**Fig. 1.2B**) [Scaal & Christ, 2004]. At early stages somites show developmental plasticity, as evidenced by single cell transplantation experiments [Kato & Gurdon, 1993]. Moreover, transplantations of groups of cells demonstrate a community effect [Gurdon et al., 1993]. Both cases

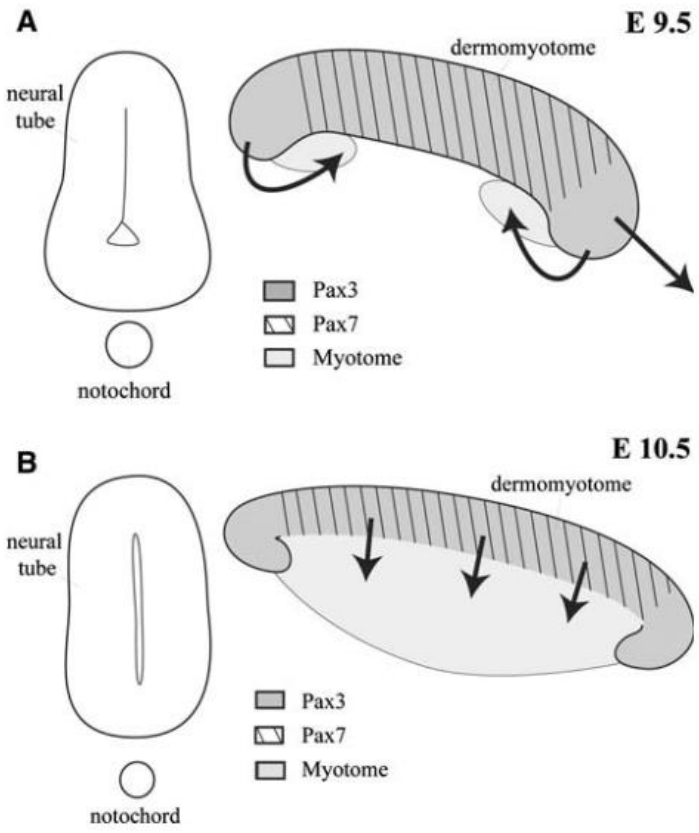

Figure 1.4. Myotome formation.

Myotome formation depends on cells migrating from the dermomyotome, initially from the lips (A) and subsequently from the central region (B).

Source: Buckingham et al., 2006

underline the influence of the surrounding microenvironment. Up to somites III-IV, they are shaped as epithelial spheres enclosing mesenchymal cells. Later on, the adjacent structure provide the aforementioned ventralizing and dorsalizing signals to compartmentalize somites into sclerotome and dermomyotome, respectively [Christ & Brand-Saberi, 2002; Scaal & Christ, 2004]. The ventral moiety undergoes EMT to form the sclerotome, which is mainly the source of the cartilage and bone of vertebral column and ribs (axial skeleton), but also contributes tendons, and joints [Musumeci et al., 2015]. The dorsal dermomyotome remains epithelial and stretches to form a sheet that roofs sclerotome. At later steps and while it adapts its rectangular-like form, dermomyotome develops a central mesenchymal sheet adjacent to the ectoderm and four inwardly curved epithelial lips. Dermomyotome gives rise to the dermis of the back and skeletal muscle, with their precursors originating in asymmetric divisions at the dorsal-ventral axis during EMT of the central part (see section 1.1.2) [Ben-Yair & Kalcheim, 2005]. Somites are divided in epaxial and hypaxial domains, lying dorsally and ventrally, respectively, to the horizontal septum of the vertebrae. The epaxial compartment generates muscles of the back, while the hypaxial part is the source of the muscles of the ventral body and limbs [Birchmeier & Brohmann, 2000; Musumeci et al., 2015].

1.1.2 Myotome: the first skeletal muscle

As the somite matures, cells delaminate and migrate underneath to form a third compartment, called myotome (**Fig. 1.4**), which corresponds to the first differentiated skeletal muscle. The groups of Ordahl and Kalcheim came to contradictory results when trying to elucidate the starting points and movements of myotomal precursors [Brent & Tabin, 2002], but a more recent stepwise model described by Gros et al. [2004] helped resolve the controversy. According to these findings, at a first phase cells translocate from the dorso-medial lip to the myotome and once there, they elongate along the rostral-caudal axis. At a second phase, cells invade myotome starting from all four lips and elongate along the anterior-posterior axis. Elongation can be unidirectional (cells from rostral or caudal lip) or bidirectional (cells from dorso-medial or ventro-lateral lip).

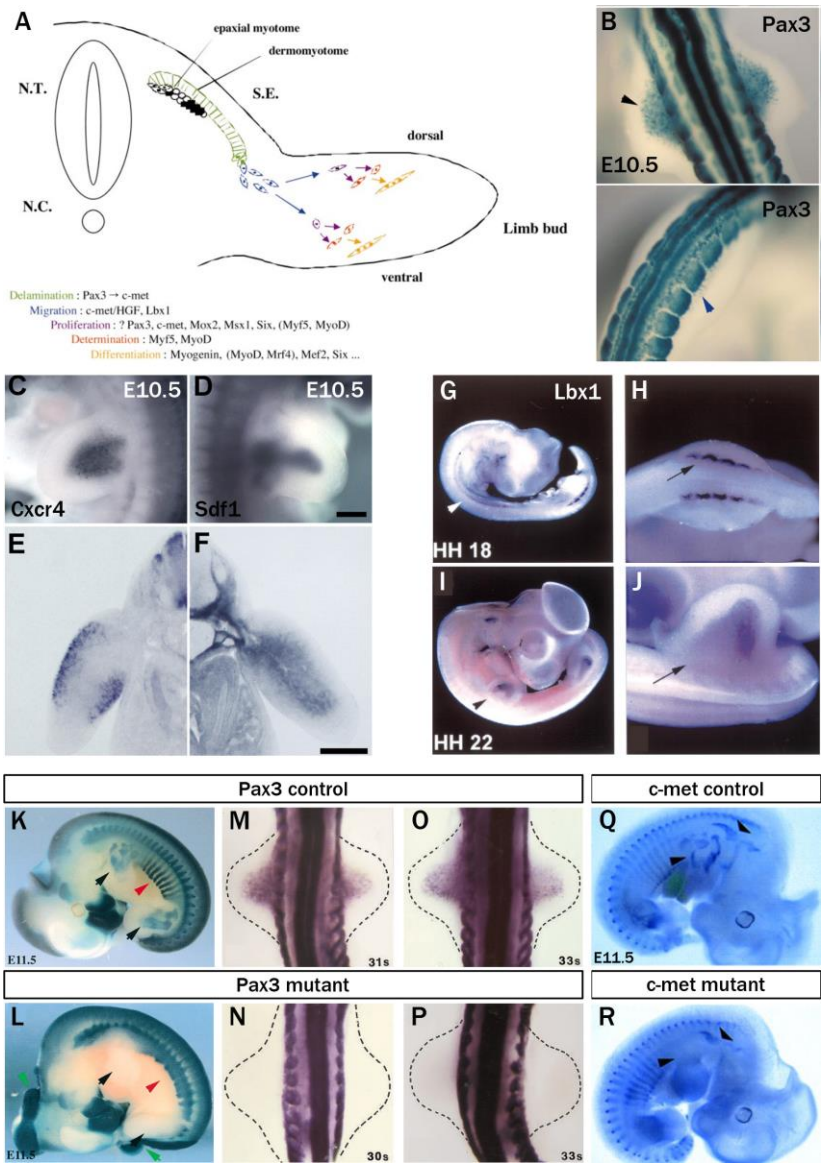

Figure 1.5. Progenitor migration for limb myogenesis.

A) Major factors controlling the consecutive steps of limb myogenesis. B) At E10.5 in the mouse embryo, Pax3-LacZ progenitors have migrated to the forelimb (up) and begin to migrate to the hindlimb (down). C,E) *Cxcr4* expression in limb at E10.5 mouse embryo. D,F) *Sdf1* expression in limb at E10.5 mouse embryo. G-J) *Lbx1* expression in somites and limbs of chick embryos at HH18 and HH22 stages. K-L) Limb muscles (black arrows) are absent from and somites are fused and truncated (red arrowheads) in *Pax3*$^{IRESnLacZ/Sp}$ E11.5 mouse embryos as opposed to *Pax3*$^{IRESnLacZ/+}$ control embryos at the same stage. M-P) PAX3-expressing cells do not colonize the forelimbs of *Splotch* mutants at 30-33 somite stages. Q-R) Lack of muscle (identified with *MyoD*) in the forelimbs of *c-Met* mutant E11.5 mouse embryos, in contrast to controls. NC: notochord, NT: neural tube, SE: surface ectoderm.
Adapted from: Bober et al., 1994; Maina et al., 1996; Mennerich et al., 1998; Buckingham et al., 2003; Relaix et al., 2003; Vasyutina et al., 2005.

Once the primary myotome is formed, a second population of myogenic progenitor cells originating from the central dermomyotome is colonizing the underlying myotome, rendering its initial name "dermatome" erroneous (**Fig. 1.4**). At later stages of embryonic and fetal life, muscle growth was found to depend on progenitors originating from the central dermomyotome, rather than the lips (see session 1.2.1) [Ben-Yair & Kalcheim, 2005; Gros et al., 2005; Kassar-Duchossoy et al., 2005; Relaix et al., 2005]. Of note, embryonic and fetal progenitors are mitotically active and have not engaged to the myogenic program. They maintain their proliferative status in embryonic and fetal muscles of trunk and limbs throughout development. They depend on transcription factors of the PAX family and they contribute to the forming muscles as well as their associated stem cells, as discussed in the following sections.

1.1.3 Migration of muscle progenitors to support limb myogenesis

Distant sites of myogenesis, such as the developing limb, depend on long-range migration of progenitors from the hypaxial dermomyotome to the limb buds, where they proliferate and subsequently commit to the myogenic lineage and undergo differentiation into skeletal muscle (**Fig. 1.5 A**) [Buckingham et al., 2003].

The transcription factor LBX1 is considered a bona fide marker of long-range migrating muscle precursors [Dietrich et al., 1998]. *Lbx1* starts to be expressed in the dispersing dermomyotomal lips, meaning prior to delamination. It then follows the migrating population (**Fig. 1.5 G-J**) and declines only when these progenitors arrive at the target sites and start to differentiate [Jagla et al., 1995; Dietrich et al., 1998; Mennerich et al., 1998]. In its absence, migratory precursors manage to form and delaminate but they display defective routing, demonstrating that LBX1 is critical for migration [Schäfer & Braun, 1999; Brohmann et al., 2000; Gross et al., 2000].

The migratory behavior of muscle progenitors is also controlled by PAX3, which is essential for the initiation of their migration. *Splotch* and other PAX3 mutant embryos show a number of developmental phenotypes in dorsal neural regions, neural crest cells and derivatives and muscle

tissues [Auerbach, 1954; Relaix et al., 2004]. Strikingly, PAX3-deficient embryos are devoid of myogenic migrating cells, leading to complete absence of muscular diaphragm, tongue and limb muscles (**Fig. 1.5 K-P**) [Mennerich et al., 1998; Relaix et al., 2004]. PAX3-expressing migrating progenitor cells also express LBX1 [Vasyutina et al., 2005].

Central in the genetic hierarchy controlling delamination and migration are the c-MET tyrosine kinase receptor - expressed by hypaxial muscle precursors - and its ligand scatter factor/ hepatocyte growth factor (SF/HGF) - lining the migratory route in the limb mesenchyme and other sites of migratory myogenesis [Birchmeier & Brohmann, 2000]. In their absence, migrating myogenic progenitors and, subsequently, muscle masses are missing from the limbs, tongue and diaphragm (**Fig. 1.5 Q-R**) [Bladt et al., 1995; Maina et al., 1996; Dietrich et al., 1999]. *c-Met* transcription depends on PAX3 [Epstein et al., 1996; Relaix et al., 2003]; *c-Met* expression as well as migratory progenitors and limb muscles are absent from *Splotch* embryos [Bober et al., 1994; Epstein et al., 1996; Yang et al., 1996; Tajbakhsh et al., 1997]. The *c-Met* promoter contains a PAX3 binding site [Epstein et al., 1996] and *c-Met* has been established as PAX3 target *in vitro* and *in vivo* [Epstein et al., 1996; Relaix et al., 2003]. *Cxcr4* and *Sdf1* constitute a further receptor-ligand pair affecting progenitor migration to the limbs [Vasyutina et al., 2005]. Similarly to c-MET and SF/HGF, CXCR4 receptor-expressing muscle progenitors are guided by a SDF1-paved route to the limb (**Fig. 1.5 C-F**). However, CXCR4/SDF1 seems to be required only for a subset of cells and to have a transient expression [Vasyutina et al., 2005].

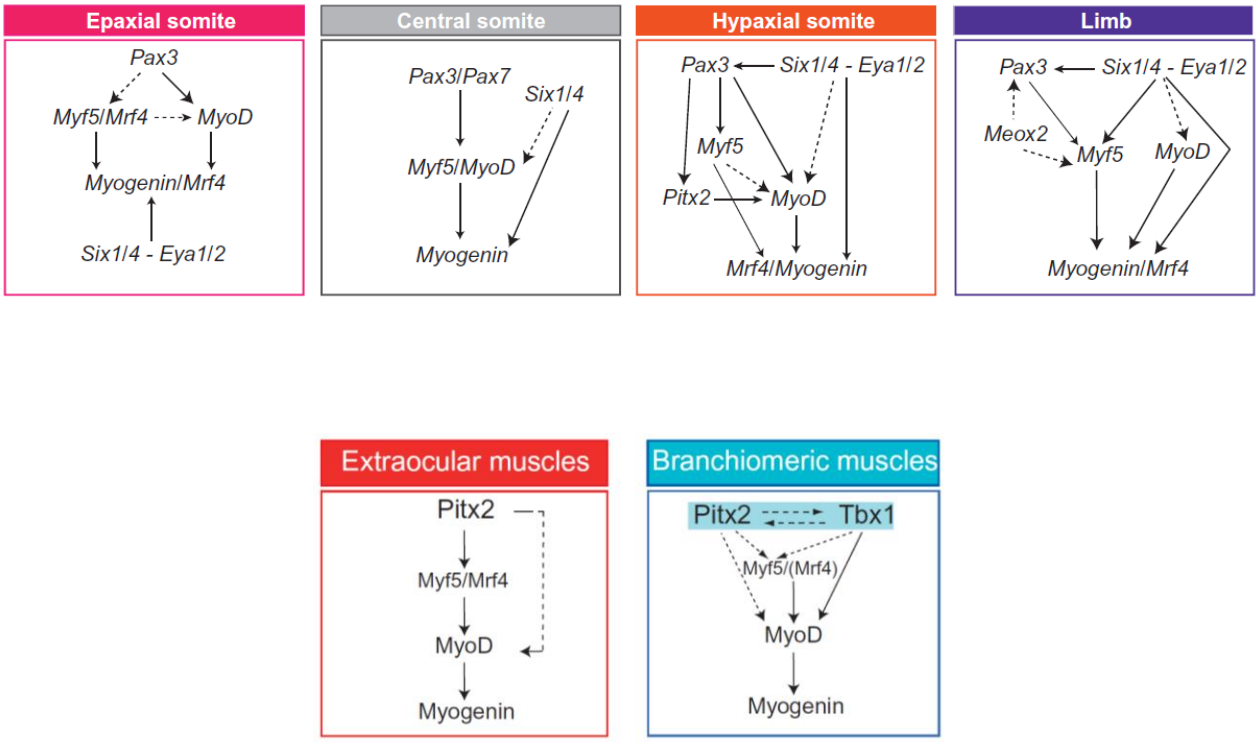

Fig. 1.6. Distinct genetic hierarchies control trunk, limb, and head myogenesis.

Adapted from: Buckingham & Mayeuf, 2012

1.2 Genetic hierarchies in head and body musculature establishment

A complex repertoire of transcription factor is crucial for the acquisition of the myogenic fate and skeletal muscle differentiation. Myogenic determination and differentiation rely on the Myogenic Regulatory Factors (MRFs), a family of basic helix-loop-helix (bHLH) transcription factors, including MYF5, MYOD, MRF4, and MYOGENIN. Upstream transcription factors act in the activation of MRFs as well as by regulating the proliferation and survival of progenitor cells. The upstream regulators differ between head/neck and trunk/limb muscles (**Fig. 1.6**) [Bismuth & Relaix, 2010; Braun & Gautel, 2011; Buckingham & Mayeuf, 2012].

In the body musculature PAX3/7 play a central role (see section 1.3), while a similar upstream role, linked to that of PAX3, was shown for the SIX homeodomain transcription factors and EYA cofactors [Buckingham & Rigby, 2014]. SIX1/4 or EYA1/2 deficient mice show a pronounced downregulation of MRFs and lacked limb and many trunk muscles [Grifone et al., 2005; Grifone et al., 2007]. Accordingly, SIX proteins were found to control *Myf5* [Giordani et al., 2007], *MyoD* [Relaix et al., 2013] and *Myogenin* [Spitz et al., 1998] expression, the first two in synergy with PAX3.

Head muscle development follows a distinct program, not requiring PAX3/7 but depending on four transcription factors -MYOR, Capsulin, PITX2, and TBX1- acting on different head muscle groups. PAX3 is not expressed in mesodermal derivatives in the head, while PAX7 is expressed in some head muscles, but its absence does not cause any head muscle phenotype [Bismuth & Relaix, 2010]. MYOR and Capsulin are bHLH transcription factors that redundantly function in specifying masticatory muscles [Bismuth & Relaix, 2010]. PITX2 is central in the regulation of non-somitic myogenic progenitors, controlling the survival and differentiation of muscle progenitors from the first branchial arches as well as progenitors that will form extraocular muscles [Buckingham & Mayeuf, 2012]. Finally, TBX1 has been described as “genetically equivalent to PAX3 during branchial arch development”, as it is expressed in the mesodermal cores of branchial arches and it is involved in bilateral branchiomeric myogenesis [Bismuth & Relaix, 2010].

Table 1.2. Pax transcription factors structure and control of development [Buckingham & Relaix, 2007].

Pax genes	Structural characteristics	Expression in developing tissues/organs
Pax3	PD OP HD1/HD2/3	CNS, craniofacial tissue, trunk neural crest, somites/skeletal muscle
Pax7		CNS, craniofacial tissue, somites/skeletal muscle
Pax4		Pancreas, gut
Pax6		CNS, pancreas, gut, nose, eye
Pax2		CNS, kidney, ear
Pax8		CNS, kidney, thyroid
Pax5		CNS, B-lymphocytes
Pax1		Skeleton, thymus, parathyroid
Pax9		Skeleton, thymus, craniofacial tissue, teeth

CNS: central nervous system, HD: homeodomain, OP: octapeptide, PD: paired domain.

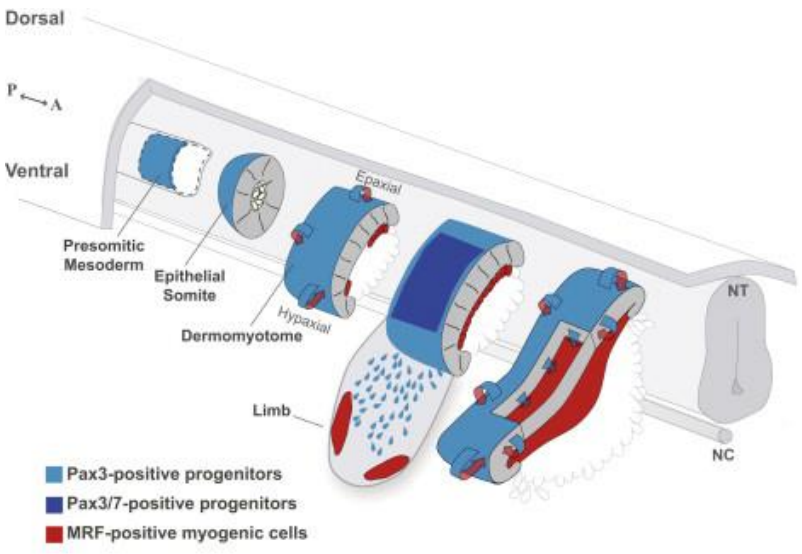

Figure 1.7. Pax and MRF expression during development of trunk and limb muscles.

PAX3+ progenitors first appear in the presomitic mesoderm and remain present until late stages of somitogenesis. *Pax7* starts to be expressed later and is restricted to the central dermomyotome. MRF+ myogenic cells are initially found in the forming myotome and the nascent muscle masses of ventral and dorsal limb areas. A: anterior, NC: notochord, NT: neural tube, P: posterior.
Source: Buckingham & Rigby, 2014

1.3 PAX proteins and bHLH MRFs play a central role in the myogenic program

My PhD work focuses on limb and trunk musculature and, thus, this section will cover general aspects of the function of PAX and MRFs in body musculature (**Fig. 1.7**) as well as their essential participation in embryonic myogenesis. Their role in postnatal growth and adult regeneration will be included in the session presenting satellite cells, which are the stem cells providing muscle precursors after birth.

1.3.1 PAX3 and PAX7 as upstream myogenic regulators

PAX proteins control the development of many lineages during embryogenesis (**Table 1.2**), with PAX3 and PAX7 acting as key regulators in the muscle lineage [Buckingham & Relaix, 2007]. In mammals, nine PAX proteins have been described, structurally characterized by a common paired box domain offering sequence-specific DNA binding. Some of them (including PAX3/7) also possess an octapeptide motif and an entire or truncated homeodomain (**Table 1.2**) [Buckingham & Relaix, 2007; Olguín & Pisconti, 2012]. *Pax* genes encode transcription factors and both PAX3 and PAX7 were shown to act as transcriptional activators *in vivo* [Relaix et al., 2003; Relaix et al., 2004] and orchestrate various biological aspects of myogenic progenitors and stem cells, including survival, proliferation, migration, self-renewal and triggering the myogenic program [Buckingham & Relaix, 2015]. Apart from their essential role in the muscle tissue, they are also important for neural crest derivatives and the central nervous system [Buckingham & Relaix, 2007].

As early as in the somite, compartmentalization and lineage specification are accompanied by alterations in the expression patterns of *Pax* genes [Christ & Ordahl, 1995]. PAX3 is mainly functioning during early embryonic myogenesis and gets downregulated in most muscles after birth, while PAX7 prevails in the post-natal growth phase as well as during adult muscle regeneration [Buckingham & Relaix, 2015]. Genetic replacement of PAX3 by PAX7 rescues most of the phenotypes of PAX3 mutants, but also shows that PAX7 cannot fully substitute PAX3 function in delamination, migration and proliferation of limb muscle progenitors (**Fig. 1.8**) [Relaix et al., 2004]. Furthermore, despite some overlapping functions of PAX3 and PAX7 in triggering the adult myogenic program, PAX7 has a distinct

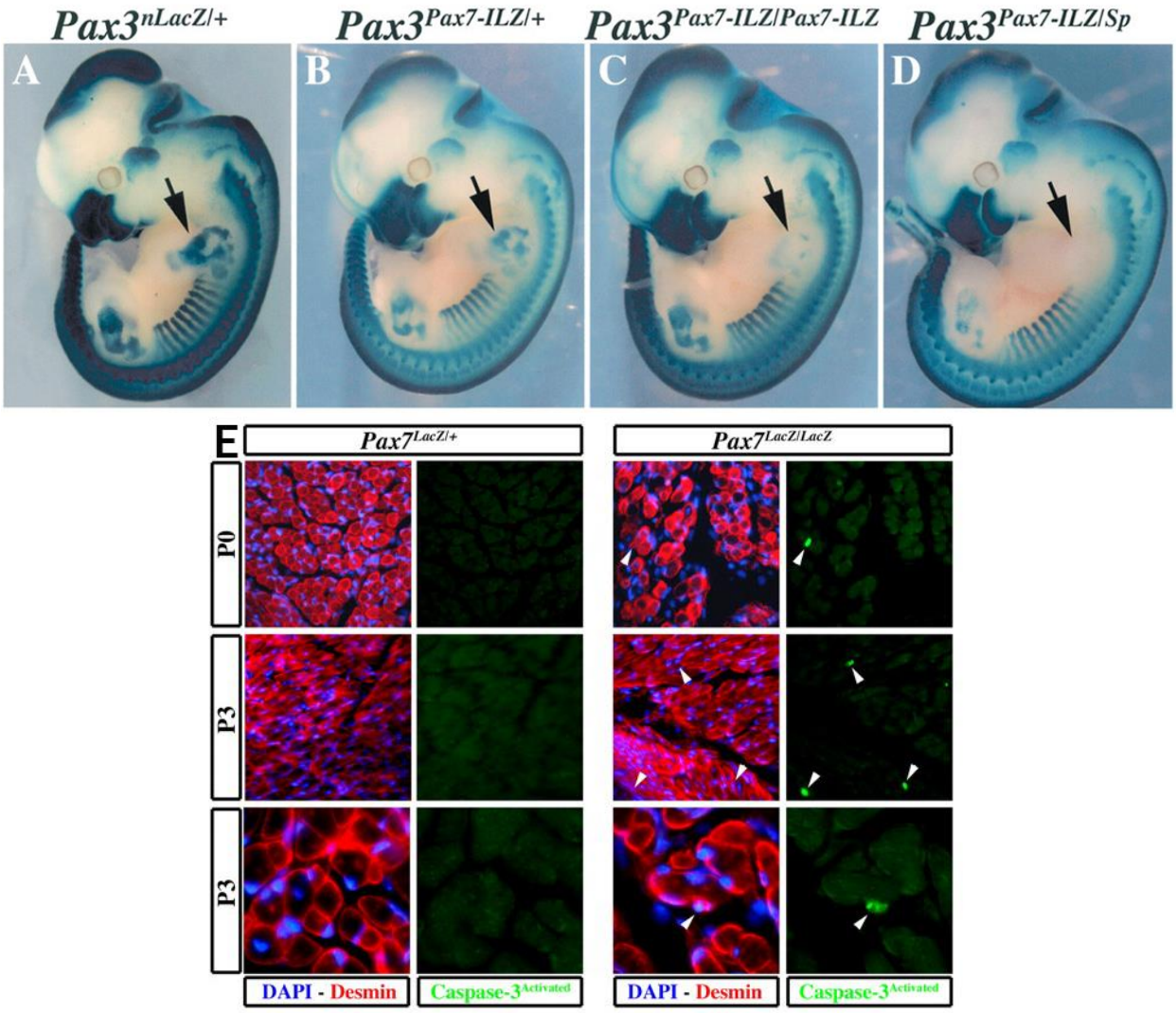

Figure 1.8. PAX3 and PAX7 have only partially overlapping functions.

A-D) PAX7 cannot rescue limb defects of *Pax3*-mutant embryos, when knock-in in the *Pax3* locus. E) In the absence of PAX7, PAX3 cannot replace its antiapoptotic function.

Adapted from: Relaix et al., 2004; Relaix et al., 2006

role in survival (**Fig. 1.8**) and cell cycle progression [Relaix et al., 2006]. Large scale analysis of PAX3 and PAX7 binding profiles revealed several factors that could account for these differences, such as a) differential binding affinities for paired (PAX3) versus homeobox (PAX7) motifs, b) PAX3 binding only a subset of PAX7 targets (~5K sites for PAX3 vs ~53K sites for PAX7, with ~3.5K common sites), c) PAX7 occupying in the adult sites bound by PAX3 in the embryo, d) unique PAX3 targets involved in embryonic myogenesis (i.e. enrichment in ontology terms of skeletal muscle morphogenesis and neural and epithelial tube formation) [Soleimani et al., 2012].

PAX3 and PAX7 expression begins early in the nascent myogenic lineage and their absence leads to a complete arrest of skeletal muscle development. Transcript and reporter analyses revealed that PAX3 expression initiates in the presomitic mesoderm prior to segmentation (around E8 in the mouse) and its expression is progressively confined to the dermomyotome covering the epaxial and hypaxial extremities, while PAX7 appears later (around E9 in the mouse) and is concentrated in the central dermomyotome [Murphy & Kardon, 2011]. In the limb, PAX3+ progenitors migrate to the limb buds, where they are transiently present from E10 to E12.5 [Bober et al., 1994], while PAX7 appears later (E11.5), in PAX3-expressing myogenic progenitors and persists until fetal/neonatal stages [Relaix et al., 2004]. Later on, PAX3 gets downregulated but PAX7 persists [Kassar-Duchossoy et al., 2005]. In adult muscles, PAX7 is a universal marker of satellite cells, the progenitor/stem cell population responsible for postnatal growth/regeneration (see section 1.3), while PAX3 is restricted to a subset of trunk and limb muscle satellite cells [Seale et al., 2000; Relaix et al., 2006; Calhabeu et al., 2013].

Importantly, in 2005 a PAX3/PAX7+ progenitor population was identified in both chick and mouse embryos as the major source of myogenic cells for the forming muscle fibers in the trunk and limb [Ben-Yair & Kalcheim 2005; Gros et al., 2005; Kassar-Duchossoy et al., 2005; Relaix et al., 2005]. They are maintained in a proliferative state and lack MRFs or other muscle-specific markers. Reporter- or quail-to-chick-based genetic tracing place these dermomyotome-derived progenitors in lineage continuum with the forming MRF+, post-mitotic cells that enter the myogenic program. Strikingly, satellite cells also derive from the same dermomyotome population once cells become embedded under the basal lamina at E18.5 acquiring the characteristic “satellite” position [Gros et al., 2005;

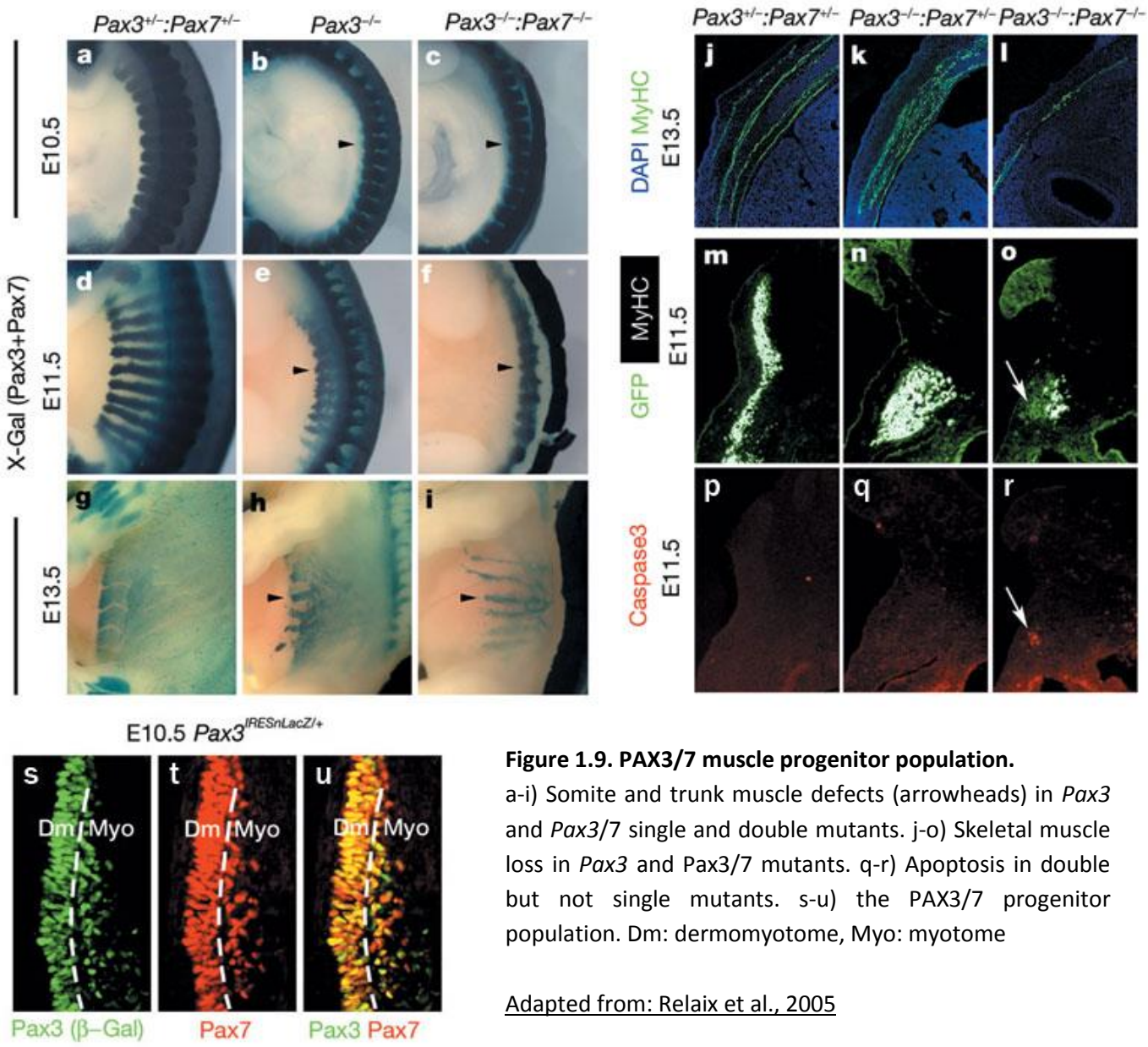

Figure 1.9. PAX3/7 muscle progenitor population.
a-i) Somite and trunk muscle defects (arrowheads) in *Pax3* and *Pax3*/7 single and double mutants. j-o) Skeletal muscle loss in *Pax3* and Pax3/7 mutants. q-r) Apoptosis in double but not single mutants. s-u) the PAX3/7 progenitor population. Dm: dermomyotome, Myo: myotome

Adapted from: Relaix et al., 2005

Kassar-Duchossoy et al., 2005; Relaix et al., 2005]. PAX3/7 compound deficiency demonstrated their unequivocal role in the survival and specification of embryonic myogenic progenitors. Specifically, in the absence of PAX3/7, the progenitor cells either undergo cell death or fail to enter the myogenic program and get integrated to other tissues (**Fig. 1.9**) [Relaix et al., 2005]. PAX3 mutants, also known as splotch-mice (Auerbach, 1954), show defects in somitogenesis and segmentation, later affecting hypaxial trunk musculature. Furthermore, their migratory muscle progenitors are absent and they lack limb musculature (**Fig. 1.9**) [Bober et al., 1994; Tajbakhsh et al., 1997; Relaix et al., 2003; Relaix et al, 2004]. PAX7-null mice do not manifest any overt embryonic muscle phenotype and their trunk, limb, and facial muscles seem to develop normally [Mansouri et al., 1996; Relaix et al., 2004]. Embryonic lethality of splotch mice leaves PAX3 role uncharacterized in later stages; conversely, PAX7 exerts principal and indispensable functions at postnatal stages (see section 1.3).

1.3.2 MRFs play a central role in myogenic determination and differentiation

Skeletal muscle identity is conferred by the MRF family of transcription factors, which are expressed solely in skeletal muscle. In order to activate muscle-specific genes via direct binding to an E-box -a specific DNA sequence (CANNTG)-, MRFs heterodimerize with the ubiquitously expressed E proteins [Singh & Dilworth, 2013]. The MRF family consists of four members, MYOD [Davis et al., 1987], MYF5 [Braun et al., 1989], MRF4 [Rhodes & Konieczny, 1989], and MYOGENIN [Wright et al., 1989], which were originally identified by their ability to trigger conversion of non-muscle cell types into myogenic fate when ectopically expressed [Olson & Klein, 1994]. All four MRFs share a bHLH domain, mediating DNA binding as well as dimerization to form transcriptional complexes [Maroto et al., 2008]. The bHLH domain is characterized by ~80% amino acid identity among the four members, while limited sequence similarity is observed in the transcriptional activation domains, residing in the amino- and carboxyl-termini [Olson & Klein, 1994]. Target binding and expression profiling revealed shared targets between some members of the family and, in the case of MYOD and MYOGENIN, suggested a model whereby MYOD establishes an open chromatin structure at muscle-specific genes and MYOGENIN enhances transcription once chromatin is rendered accessible [Blais et al., 2005; Cao et al., 2006]. A further study implicated MYOD in chromatin loop dynamics regulation [Battistelli et al.,

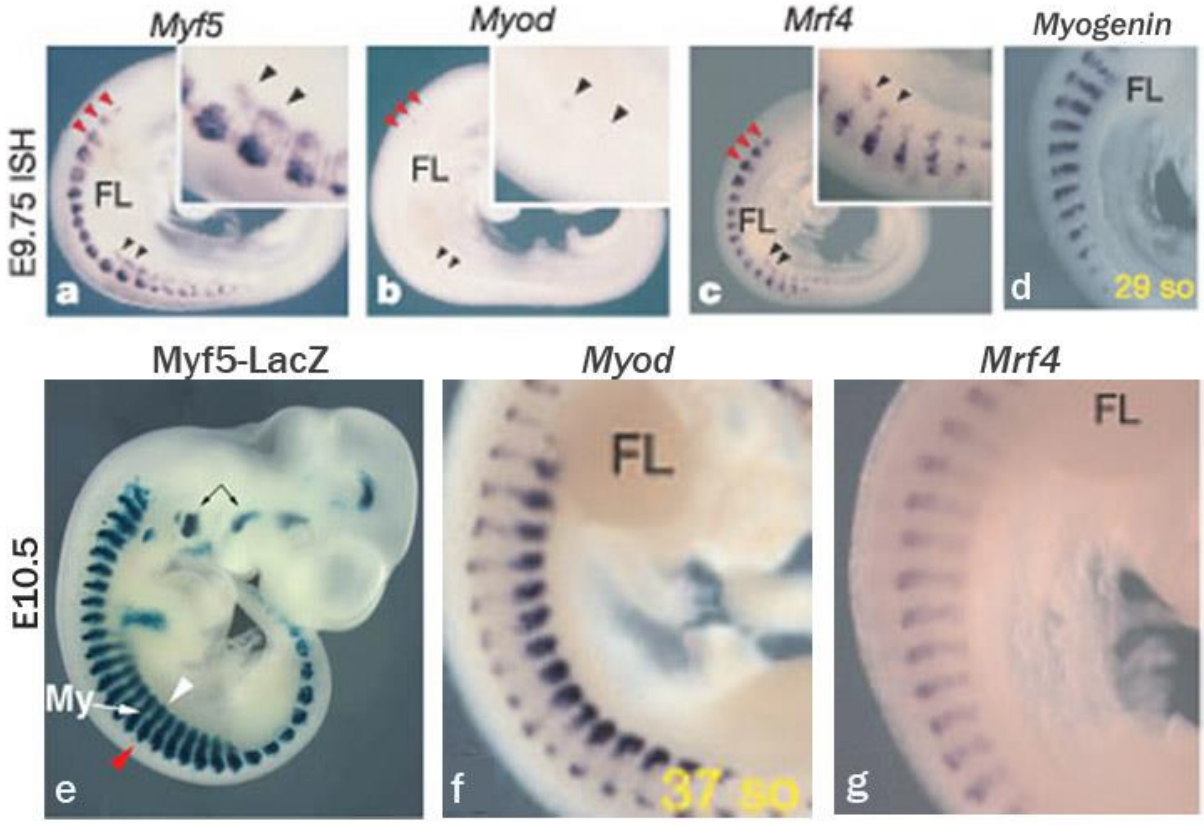

Figure 1.10. MRF expression profile at early embryonic myogenesis.

a-d) MRF transcripts at somites of E9.75 mouse embryos. e-g) MYF5 (reporter-based) and *MyoD/Mrf4* (transcript-based) expression at E10.5 mouse embryos. FL: forelimb, My: myotome.

Adapted from: Kassar-Duchossoy et al., 2004

2014], while MYOD and MYOGENIN targets include chromatin remodeling factors [Cao et al., 2006].

The specific expression of MRFs transcripts is initiated early during muscle development and follow distinct spatio-temporal patterns (**Fig. 1.10**) [summarized in Murphy & Kardon, 2011; Singh & Dilworth, 2013]. *Myf5* is the first MRF expressed, with its transcripts being observed from E8 in the epaxial dermomyotome and showing declining levels from recently formed (caudal) to mature (rostral) somites [Ott et al., 1991]. *Myf5* expression decreases from E14 onwards [Ott et al., 1991]. Of note, some PAX7+ cells do not express MYF5 and represent progenitors with slower proliferation and earlier exit from the cell cycle [Picard & Marcelle, 2013]. *Myogenin* is found from E8.5, accumulating in the most rostral somites and coinciding with differentiating muscle cells [Sassoon et al., 1989; Ott et al., 1991]. MYOD appears at E10.25-E10.5 [Sassoon et al., 1989; Kablar et al., 1997; Zabludoff et al., 1998]. In the limb, *Myf5* is detected in forelimb and hindlimb from E10.5 and E11, respectively, and gets downregulated by E11.5 when MYOD and MYOGENIN accumulate [Sassoon et al., 1989; Ott et al., 1991; Kablar et al., 1997]. *Mrf4* shows a biphasic pattern, with its transcripts appearing from E9 until E12 and then again from E16 onwards [Bober et al., 1991]. Adult myonuclei will maintain the expression of MRF4, which becomes the predominant MRF in adult muscle [Hinterberger et al., 1991; Gayraud-Morel et al., 2007].

Genetic ablation during embryonic and fetal myogenesis established MYF5, MYOD, and MRF4 as myogenic determination factors and MYOD, MYOGENIN, and MRF4 as myogenic differentiation factor [Murphy & Kardon, 2011]. MYF5-null mice form myotome with a 2-day delay [Braun et al., 1992; Tajbakhsh et al., 1997; Kassar-Duchossoy et al., 2004] and a MYF5-driven LacZ reporter revealed the presence of progenitors which activated *Myf5* in MYF5-null mice, but remained multipotent, failed to localize correctly and eventually differentiated into non-muscle derivatives according to their local environment [Tajbakhsh et al., 1996]. Despite the delayed myotome initiation in MYF5-deficient embryos, the myogenic program gets rescued around E11.5 by the delayed activation of MYOD [Braun et al., 1994] and muscles of MYF5 mutants become structurally and functionally normal until birth (**Figs. 1.11-1.12**) [Braun et al., 1992; Tajbakhsh et al., 1997]. It has been proposed that MYF5-independent MYOD- expressing myoblasts sustain myogenesis in the absence of a distinct, MYF5-

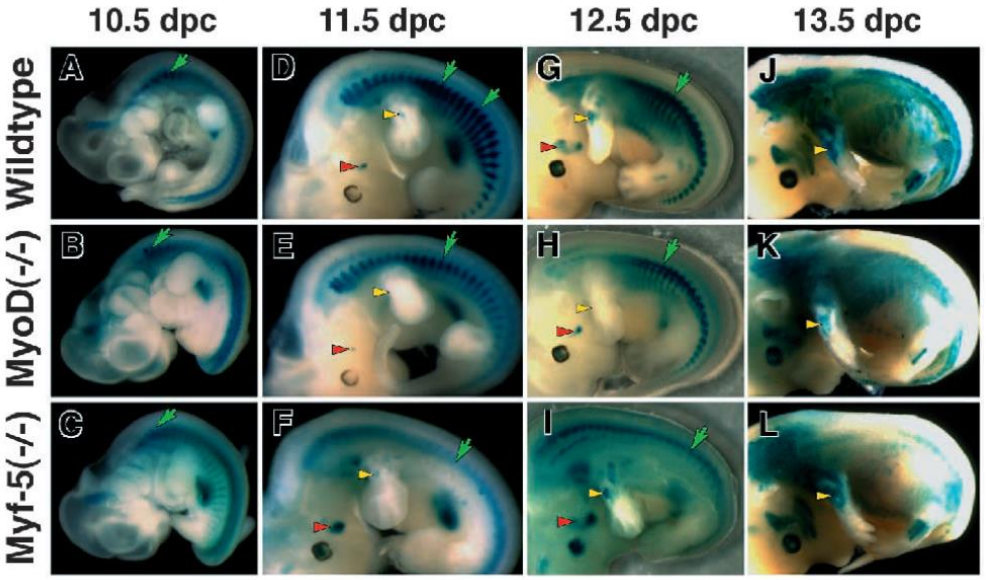

Figure 1.11. Embryonic myogenesis in the absence of MyoD or Myf5.

Developing muscles marked by MD6.0-LacZ reveal subtle differences in the absence of either *MyoD* (B, E, H, K) or *Myf5* (C, F, I, L) compared to age-matched control embryos (A, D, G, J).
Source: Kablar et al., 1997

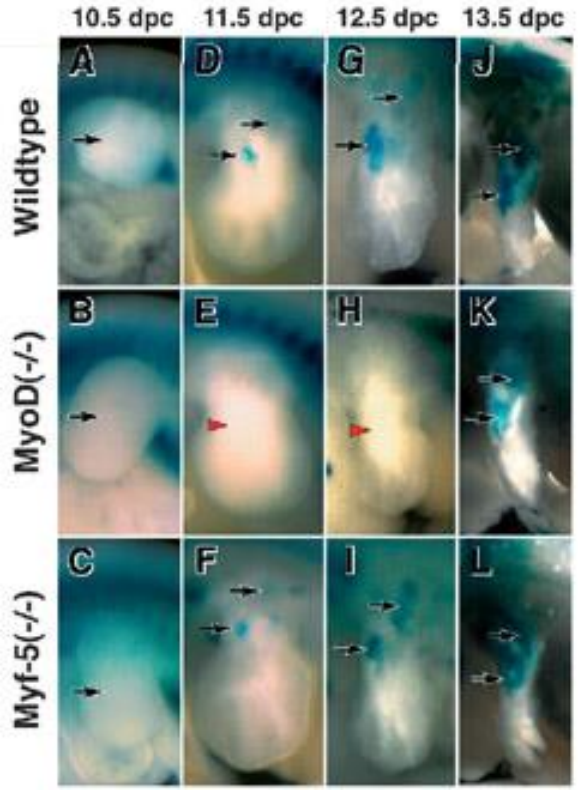

Figure 1.12. Limb myogenesis in the absence of MyoD or Myf5.

Delayed muscle development in the limbs of *MyoD* mutant (B, E, H, K), but not *Myf5* mutant embryos (C, F, I, L) compared to age-matched controls (A, D, G, J) as evidenced by MD6.0-LacZ expression. dpc: days post coitum
Source: Kablar et al., 1997

dependent lineage [Haldar et al., 2008]. Conversely, mice lacking MYOD have morphologically normal muscles (albeit showing 2-day delayed differentiation in the limb [Kablar et al., 1997]) (**Figs. 1.11-1.12**) and maintain high levels of MYF5 [Rudnicki et al., 1992; Kablar et al., 1998]. In the absence of both factors, newborns are completely devoid of skeletal muscles in both trunk and limbs [Rudnicki et al., 1993]. However, this effect appears to depend on compromised *Mrf4* expression, since skeletal muscle manages to differentiate in MYF5/MYOD double knockouts with functional MRF4 [Kassar-Duchossoy et al., 2004]. It has been proposed that the proximity of *Mrf4* and *Myf5* (the former residing 8kb 5' of the latter) likely account for cis-regulatory interactions [Olson et al., 1996], that are diversely affected in different MYF5 nulls. Thus, *Mrf4* was also identified as a determination gene, while genetic manipulation of the three factors placed both MYF5 and MRF4 upstream of *MyoD* [Kassar-Duchossoy et al., 2004]. Specific ablation of *Myf5*-expressing cells using $Myf5^{Cre}$; $R26R^{DTA/+}$, suggested the presence of distinct *Myf5*-dependent and *Myf5*-independent *MyoD*-expressing myoblasts [Gensch et al., 2008; Haldar et al., 2008]. However, when *Myf5*-expressing cells were eliminated in a *MyoD* null background, no muscles were formed, indicating that the previously observed *Myf5*-independent myoblasts were in fact MYF5+ escaper cells [Comai et al., 2014].

Myogenic differentiation was found to depend on MYOGENIN, MYOD, and MRF4 [Murphy & Kardon, 2011]. MYOGENIN did not overlap with MYOD or MYF5 in specification of the myogenic lineage [Rawls et al., 1995]. However, its deficiency led to compromised muscle-specific gene expression and differentiation, including a generalized fusion defect so that mutant mice presented with severely reduced muscle masses associated with lethality at birth [Hasty et al., 1993; Nabeshima et al., 1993; Rawls et al., 1995; Rawls et al., 1998]. These defects are phenocopied in MYOD/MRF4 double knockout mice [Rawls et al., 1998], implying that either MYOGENIN or MYOD and MRF4 need to be present to drive differentiation. Finally, single MRF4 loss-of-function overall did not jeopardize muscle development [reviewed in Olson et al., 1996], although different strategies for *Mrf4* disruption resulted in phenotypes as different as ranging from perinatal lethality to normal survival [Braun & Arnold, 1995; Patapoutian et al., 1995; Zhang et al., 1995], again likely due to interrelated cis-regulatory interactions with Myf5 [Olson et al., 1996].

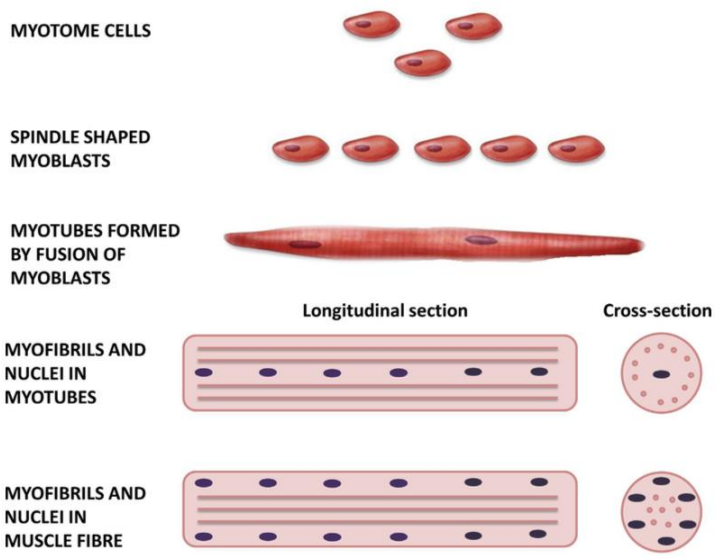

Figure 1.13. Myofiber formation.

Round myotomal cells undergo a step-wise differentiation and fusion procedure into long myotubes that further mature to myofibers with peripherally-positioned myonuclei.

Source: Musumeci et al., 2015

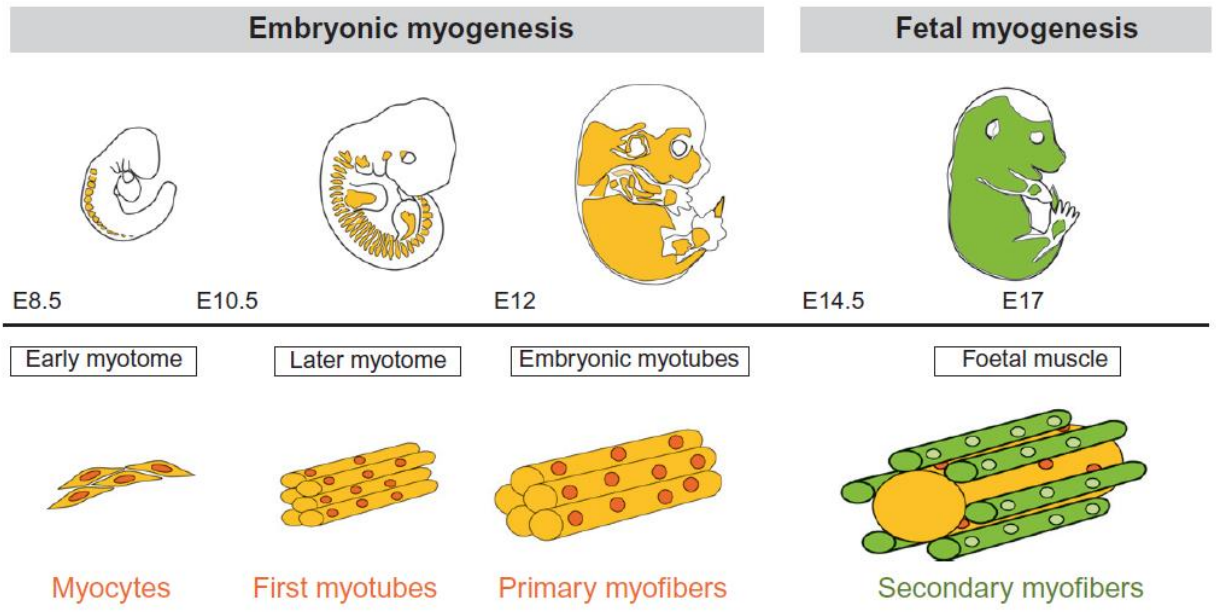

Fig. 1.14. Embryonic and fetal waves of myogenesis.

Source: Buckingham & Mayeuf, 2012

In vivo genetic manipulations abrogating PAX3, MYF5 or both, complemented by *in vitro* cultures in the presence of dominant negative forms, established that *Pax3* and *Myf5* define two distinct pathways, with *MyoD* lying genetically downstream [Tajbakhsh et al., 1997; Relaix et al., 2003]. *Pax3* and *Pax7* seem to act similarly in MYOD activation and skeletal muscle differentiation [Relaix et al., 2006].

1.4 From embryonic myogenic development to postnatal muscle

1.4.1 Embryonic and fetal waves of myogenesis

During development, myoblasts progressively differentiate and fuse to form the myofibers present in adult skeletal muscles [reviewed in Musumeci et al., 2015]. Differentiation includes increased synthesis of myofibrillar proteins (e.g. myosin heavy and light chains, skeletal muscle actin, tropomyosin, troponin) and increased activity of enzymes, such as creatine phosphokinase. Prior to fusion, myoblasts' shape and metabolic status undergo changes, including elongation, mitochondria amount increase, and sarcoplasmic reticulum development. The next step is a cadherin- and cell-adhesion-molecule-mediated adherence to fibronectin and alignment in chains. Eventually they fuse to give rise to myotubes, and further mature in myofibers, which are long syncytia consisting of postmitotic nuclei that will ultimately be located to the myofiber periphery (**Fig. 1.13**) [Musumeci et al., 2015]. Using the Fucci system (Fluorescent ubiquitynation-based cell cycle inditator), it was shown that myonuclei in terminally differentiated muscle fibers in fetal limb muscles as well as in adult myofibers have exited the cell cycle in G1 phase and are blocked in a G1-like state [Esteves de Lima et al., 2014].

The first muscle fibers start appearing at E11 in the mouse, and correspond to the so-called embryonic or primary myogenesis (**Fig. 1.14**) [Buckingham et al., 2003; Buckingham & Mayeuf, 2012]. This is followed by a second wave of myofiber formation after E14, around the previously formed primary myofibers [Buckingham et al., 2003; Buckingham & Mayeuf, 2012]. Primary and secondary fibers differ in their transcriptome and contractile proteins [Buckingham & Mayeuf, 2012].

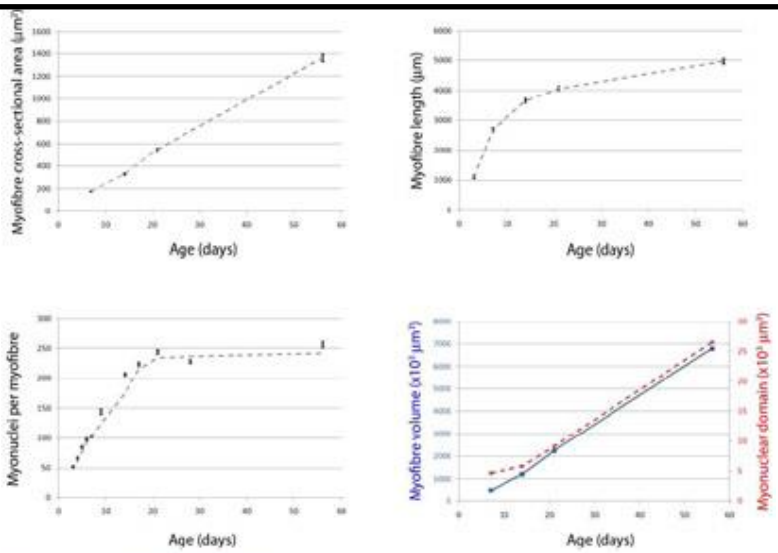

Figure 1.15. Postnatal muscle growth dynamics.

Hypertrophy and hyperplasia parameters from birth to adulthood (upper panel) and photos of growing myofibers (lower panel).

Adapted from: White et al., 2010

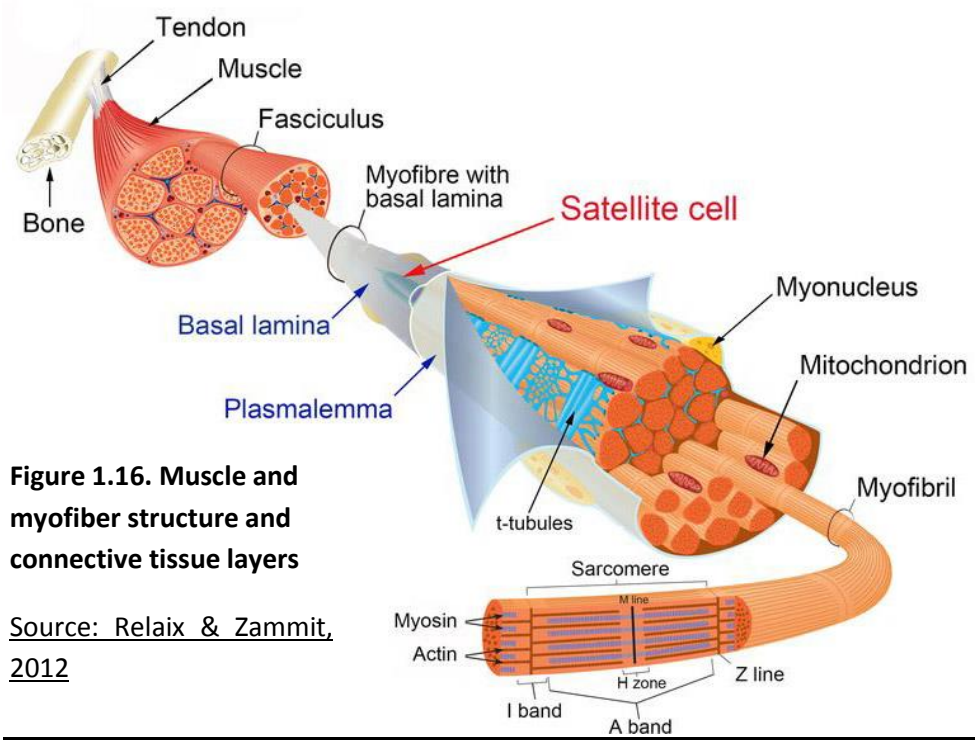

Figure 1.16. Muscle and myofiber structure and connective tissue layers

Source: Relaix & Zammit, 2012

Furthermore, Secondary/fetal myogenesis is associated with the establishment of definitive neuromuscular junctions and excitation-contraction coupling [Buckingham & Mayeuf, 2012]. Growth and patterning events prefigure the complex organization that persists from fetal to adult muscles [Relaix, 2006].

1.4.2 Postnatal muscle growth

Muscle growth is achieved by an increase in the number (hyperplasia) and/or size (hypertrophy) of myofibers. In the mouse, the number of myofibers is settled by birth, while subsequent muscle growth occurs by hypertrophy of existing myofibers, including increase in length, volume, and, importantly, myonuclei number (**Fig. 1.15**) [Moss & Leblond, 1971; White et al., 2010]. Myonuclei per myofiber increase by 5-fold between P3 and P21 [White et al., 2010]. Satellite cells support this hypertrophic phase (see section 1.5).

1.4.3 Adult muscle: structure & function

The entire adult muscle is ensheathed in a layer of connective tissue, called epimysium, while sets of neighboring myofibers are arranged in fasciculi covered by a further layer of connective tissue, called perimysium. Individual fibers are coated by the basal lamina (also called basement membrane or endomysium) [Tajbakhsh, 2009; Yin et al., 2013]. The interstitial stromal cell population residing between the epimysium and the basal lamina is mostly comprised by fibroblasts. Skeletal muscle also involves a microvascular network and neurons establishing neuromuscular junctions. Furthermore, a few immune cells reside within intact muscles [Yin et al., 2013].

Myofibers consist of myofibrils (bundles of myosin and actin filaments) subdivided in repetitive units (sarcomeres) giving a striated appearance. Within the myofiber, sarcoplasmic reticulum connects transverse tubules (t-tubules) and provides the calcium needed for muscle contraction and force generation (**Fig. 1.16**) [Cooper, 2000; Tajbakhsh, 2009; Yin et al., 2013]. Slow-contracting and fast-contracting muscle fibers (**Fig. 1.17**) differ in their myosin heavy chain expression profile and in

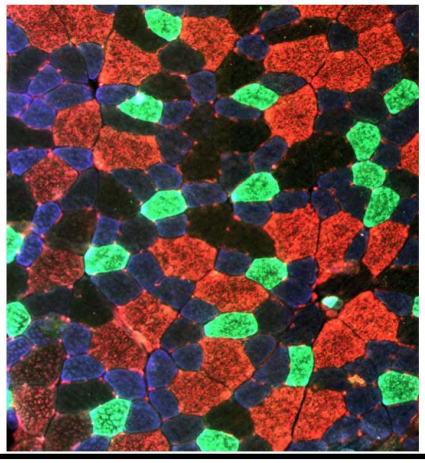

Figure 1.17. Skeletal muscle fiber types.

Muscle fiber typing based on different myosin heavy isoforms. Fiber types are as follows: MHC1 (green)-slow type I fibers, MHC2a (blue)-fast type IIA fibers, MHC2b (red)-fast type IIB fibers, MHC2x (unstainted)-fast type IIX fibers.

Source: Liu et al., 2015

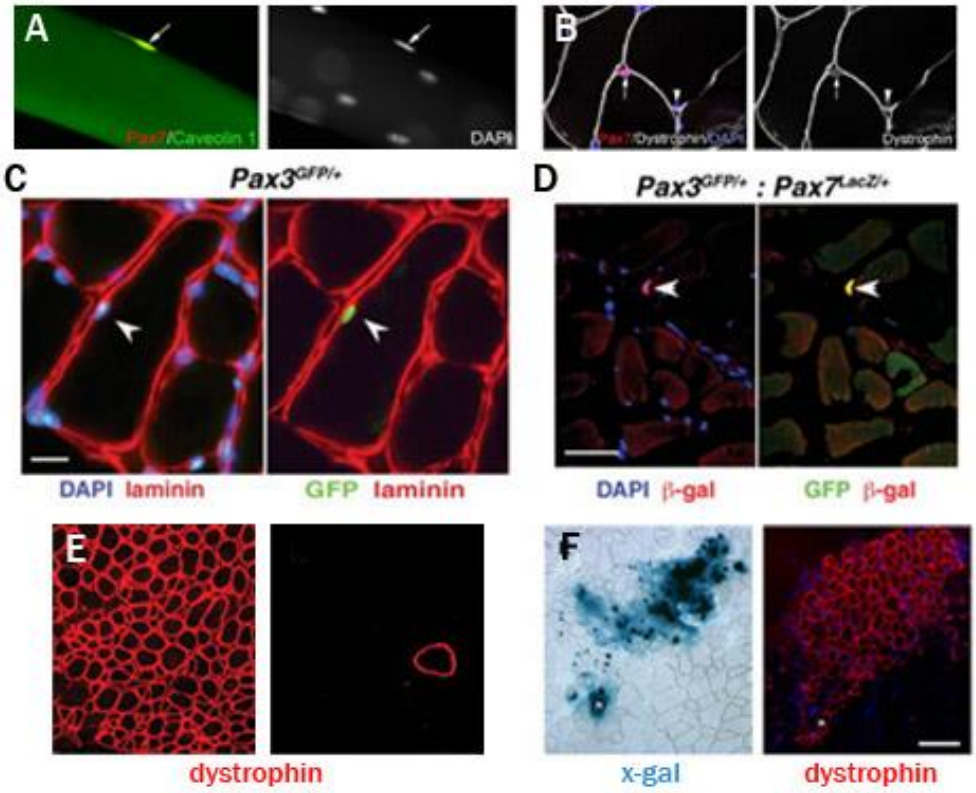

Figure 1.18. Satellite cells are skeletal muscle stem cells.

A) Satellite cell on isolated myofiber marked by PAX7/Calveolin-1. B) PAX7-marked satellite cell on muscle section, residing outside the dystrophin-outlined myofiber. C-D) Sublaminar PAX3+ or PAX3/7+ satellite cells in diaphragm. E-F) DYSTROPHIN restoration in *dystrophin*-deficient *mdx* mice three weeks following grafting of satellite cells (GFP+ cells of *Pax3*$^{GFP/+}$ mice; E) or myofibers of 3F-nLacZ-2E mice (areas with donor-derived cells are detected by b-gal activity; F).

Adapted from: Collins et al., 2005; Montarras et al., 2005; Relaix & Zammit, 2012

physiological properties (e.g. oxidative metabolism and fatigue resistance in slow fibers) and they appear in varying proportions at different muscles [Haizlip et al., 2015; Luna et al., 2015]. Apart from contraction to support voluntary movement, skeletal muscle is also essential for breathing, posture maintenance, and metabolic aspects (e.g. heat production, storage of carbohydrates and amino acids) [Kharraz et al., 2013]. Loss of functionality – caused by disorders (i.e. myopathies) or naturally occurring during aging – has detrimental effects in strength, locomotion, and metabolic status, and can even result in lethality [Kharraz et al., 2013; Chang & Rudnicki, 2014].

Postnatal muscle growth, homeostasis, and repair depend on a population of resident muscle stem cells, termed satellite cells. They reside under the basal lamina of their adjacent myofiber, accounting for 2.5-6% of the muscle's nuclear content [Tedesco et al., 2010].

1.5 Satellite cells: the skeletal muscle stem cells

Originally described as "wedged between the plasma membrane of the muscle fiber and the basement membrane" by A. Mauro in 1961, satellite cells were named after their anatomical position in the periphery of the myofibers (**Fig. 1.18A-B**), under the basal lamina (**Fig. 1.18C**). They were predicted to represent dormant myoblasts ready to recapitulate the embryonic developmental myogenic program for myofiber repair [Katz, 1961; Mauro, 1961]. However, it was not until 2005 that their stem cell potential was proven, by virtue of a) providing differentiated progeny for muscle regeneration (**Fig. 1.18E-F**) and b) self-renewing their pool, upon engraftment of FACS-sorted satellite cells [Montarras et al., 2005] or single myofibers [Collins et al., 2005] into the muscles of *mdx* mice that lack dystrophin and undergo continuous regeneration. Recently, human satellite cells were also shown to support regeneration and repopulation of the satellite cell compartment after transplantation [Marg et al., 2014]. Importantly, muscle fails to regenerate in the absence of satellite cells. DTA (diphtheria toxin fragment A)-mediated ablation of satellite cells demonstrated the absolute requirement of satellite cells for muscle regeneration [Lepper et al., 2011; McCarthy et al., 2011; Murphy et al., 2011; Sambasivan et al., 2011]. The term stem cell often entails mutlipotency, although this is not an obligate criterion for stem cells [Tajbakhsh, 2003]. Indeed, satellite cells can be

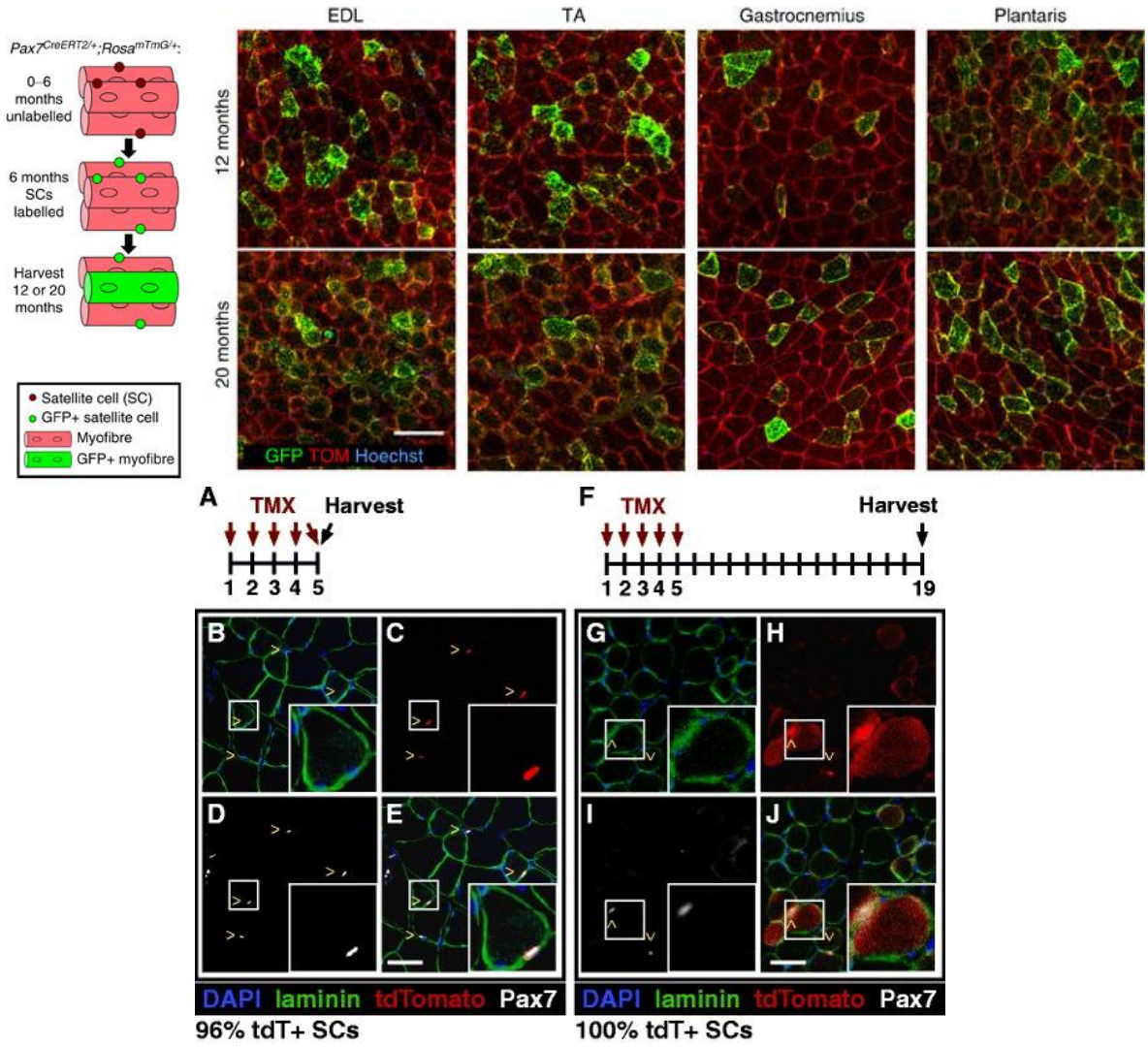

Figure 1.19. Adult satellite cell contribute to resting muscle.

Genetic tracing of PAX7+ satellite cells fusing with adult uninjured myofibers by TMX-inducible membrane-GFP (upper panel) or tdTomato (lower panel). EDL: *Extensor digitorum longus* muscle, TA: *Tibilialis anterior* muscle, TMX: tamoxifen

Adapted from: Keefe et al., 2015; Pawlikowski et al., 2015

driven to adipogenic and osteogenic fates in culture [Asakura et al., 2001], arguing for multipotent nature. However, culture contamination by other lineages cannot be excluded and satellite cells are generally considered monopotent cells in physiological conditions [Relaix & Zammit, 2012].

1.5.1 Establishment during development

At late fetal stages (E16.5-E18.5) satellite cells become embedded under the basal lamina that forms and surrounds the muscle fibers, while remaining outside of the myofibers [Kassar-Duchossoy et al., 2005; Relaix et al., 2005]. Reporter-based tracing as well as quail-to-chick grafts place the origin of satellite cells back to the dermomyotome, similarly to the muscles in which they reside [Gros et al., 2005; Kassar-Duchossoy et al., 2005; Relaix et al., 2005]. These findings on shared developmental origin between muscles masses and their associated satellite cells were later extended to limb [Schienda et al., 2006] and head musculature [Harel et al., 2009]. PAX3/7 proteins are marking the progenitor cells that will give rise the satellite cells. While PAX7 is maintained and provides a reliable marker for the emerging and adult satellite cells, *Pax3* is downregulated in some muscles [Kassar-Duchossoy et al., 2005; Relaix et al., 2005; Relaix et al., 2006; Calhabeu et al., 2013].

1.5.2 Satellite cells in the control of postnatal growth and homeostasis

Postnatal muscle growth depends on myofiber size increase, in the mouse (see section 1.4.2). Of note, the number of myonuclei per myofiber undergoes a 5-fold increase within the first three weeks of life [White et al., 2010]. Satellite cells are the main contributors to this hypertrophic phenomenon. They proliferate rapidly and extensively and are the source of new myoblasts that fuse with existing myofibers, while myonuclei have stopped dividing [Moss & Leblond, 1971; Lepper et al., 2009; White et al., 2010].

Satellite cell fusion reaches a plateau around three weeks postnatally [White et al., 2010]. Thereafter, satellite cells were hypothesized to contribute to adult skeletal muscle homeostasis even in the

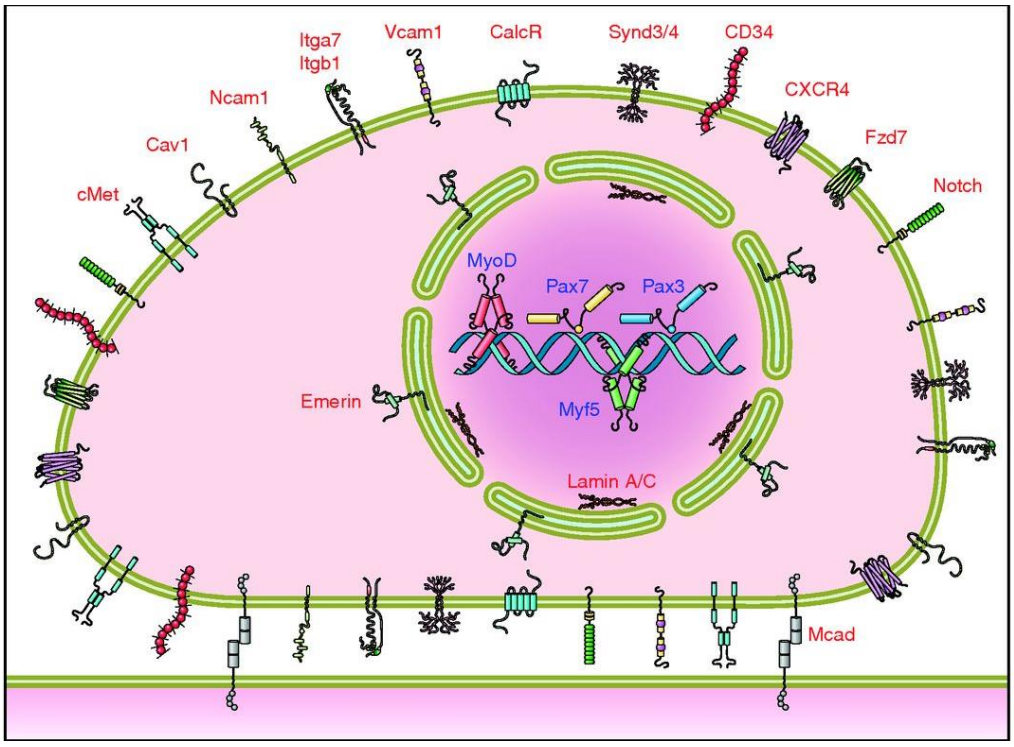

Figure 1.20. Satellite cell markers

Adapted from: Yin et al., 2013

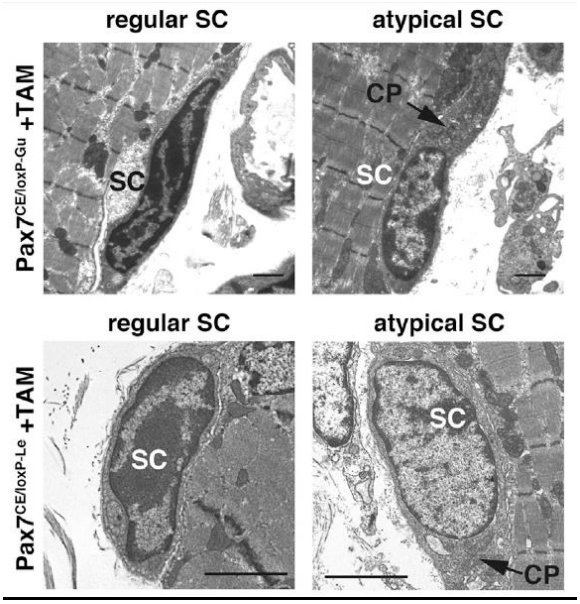

Figure 1.21. Chromatin state of quiescent satellite cells and PAX7.

Quiescent satellite cells have tightly packed heterochromatin (left). Different conditional tamoxifen-inducible *Pax7* mutants acquire a euchromatic state (right). TAM: tamoxifen, SC: satellite cell

Adapted from: Günther et al., 2013

absence of injuries. Indeed, genetic lineage studies provided experimental evidence for the predicted low rate fusion that constantly occurs (**Fig. 1.19**) [Keefe et al., 2015; Pawlikowski et al., 2015]. It should be stressed, however, that in general adult myofibers persist throughout the life in the absence of injury or myopathies that trigger a regeneration response resulting to new muscle formation [Grounds & Shavlakadze, 2011].

1.5.3 Acquisition of quiescence for function preservation

At three weeks of age (i.e. P21) there is a critical period of change from juvenile muscle/satellite cells to their form observed in the adult. Postnatally, satellite cells undergo a progressive number diminution and loss of proliferative capacity, which culminates in entering into a quiescent, non-cycling state around P21 [Lepper et al., 2009; White et al., 2010]. Long-standing efforts have described a series of markers (**Fig. 1.20**) to identify quiescent satellite cells, with PAX7 being central. Active Notch is fundamental to maintain quiescence (see Chapter 3), while Angiopoieitin-1/TIE2 is a further signaling promoting this state [Abou-Khalil et al., 2009]. On the DNA level, the histone methyltransferase Suv4-20H1 was recently found to maintain satellite cell quiescence by promoting a heterochromatic state [Boonsanay et al., 2016]. Moreover, PAX7 has a rather unappreciated role in chromatin architecture modifications, with its loss leading to euchromatic morphology (**Fig. 1.21**) [Günther et al., 2013]. Quiescence preservation is also ensured by translation repression, via phosphorylation of the translation initiation factor eIF2a [Zismanov et al., 2016].

It is widely accepted, that the dormant quiescent state is adopted to preserve key functional features, since it is accompanied by low metabolism and higher resistance to DNA damage [Cheung & Rando, 2013; Wang et al., 2014]. As opposed to other forms of growth arrest (i.e. differentiation, senescence), quiescence is reversible (see section 2.1). This allows fast activation and reentry into the cell cycle upon specific needs, such as exercise or injury, in the case of muscle.

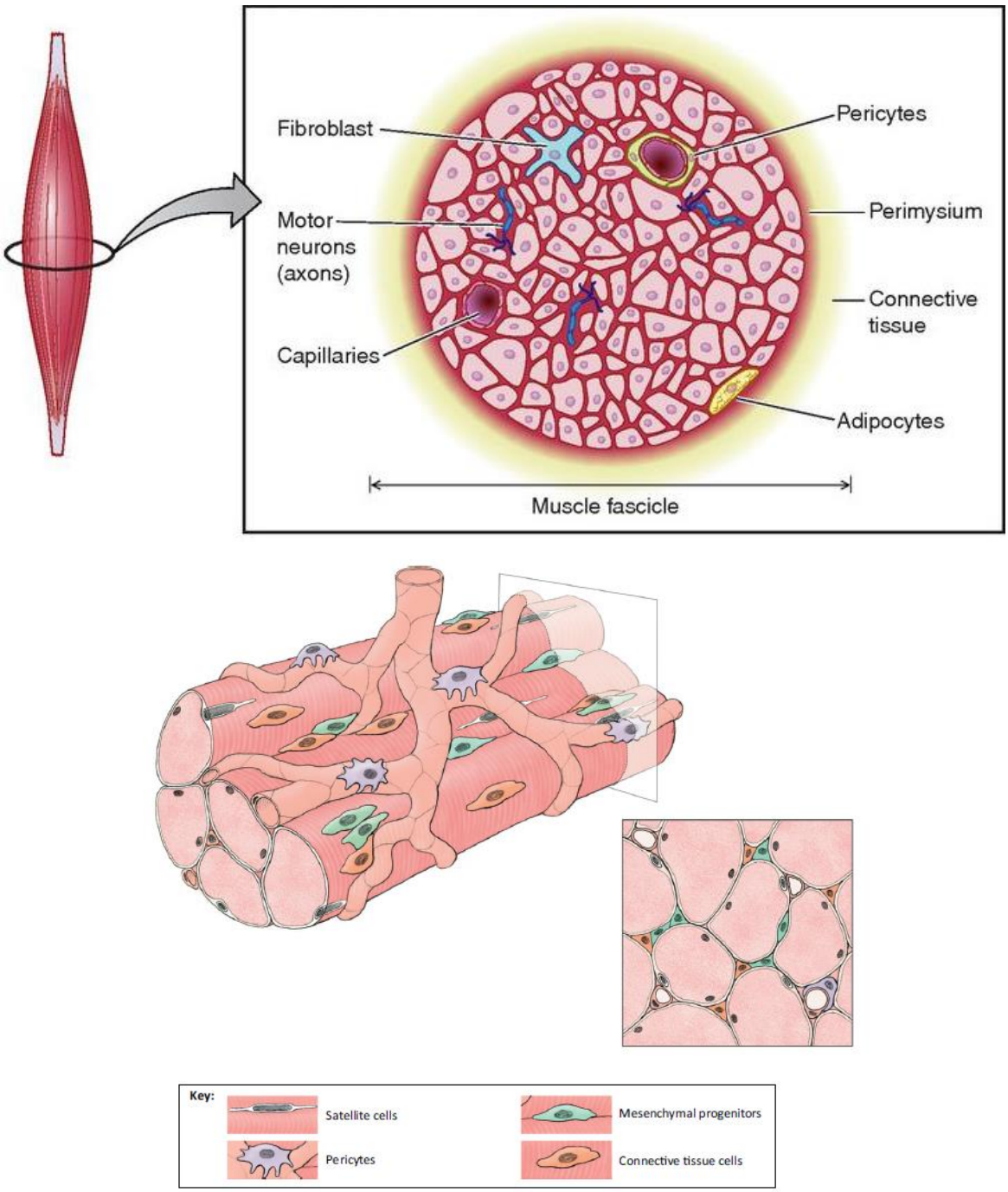

Figure 1.22. Satellite cell niche.

Adapted from: Pannérec et al., 2012; Yin et al., 2013

1.5.4 Satellite cell niche

Stem cells reside in a microenvironment that profoundly affects their properties and behavior, termed niche. It encompasses both anatomical and functional dimensions, meaning that it is in a defined anatomical location where a) the stem cells can proliferate yet remain in limited numbers and b) "stemness" maintenance is assured via differentiation inhibition [Scadden, 2006; Brack & Rando, 2012]. It is composed by heterologous cell types providing structural and biochemical cues that influence the stem cells. Satellite cell niche consists of extracellular matrix (ECM) and various types of surrounding cells, including interstitial cells, motor neurons, and blood vessels (**Fig. 1.22**) [reviewed in Pannérec et al., 2012; Yin et al., 2013]. ECM deposition defines its stiffness, which in turn impacts on satellite cell proliferation and differentiation as shown by *in vitro* studies with primary myoblast cultures and the C2C12 myogenic cell lines. Among the interstitial cells, there is a population of connective tissue fibroblasts, identified by TCF4, which interact with satellite cells during regeneration, while ablation of any of the two dysregulates the dynamics of the other. Platelet-derived growth factor receptor (PDGFR)a+ mesenchymal progenitors and fibro/adipogenic progenitors (FAPs) also reside in the muscle interstitium, and may overlap with the TCF4 population. The balance between PDGFRa+cells/FAPs-mediated adipogenesis and satellite cell-dependent myogenesis drives normal muscle homeostasis and regeneration. Muscle contraction is directed by a neuronal network that signals to individual fibers. Finally, the muscle is nourished by a microvascular network, with satellite cells residing in close proximity to capillaries and their associated pericytes [session based on informative reviews by Pannérec et al., 2012; Yin et al., 2013].

1.5.5 Satellite cells in the control of regeneration

Skeletal muscle shows a remarkable regenerative capacity, with rapid functional and structural reestablishment (within three weeks) even after multiple rounds of severe injury that cause widespread necrosis [Relaix & Zammit, 2012]. Under both physiological (e.g. accidental injuries) and pathological (e.g. toxin-induced injury or diseases such a s muscular dystrophies) conditions, satellite

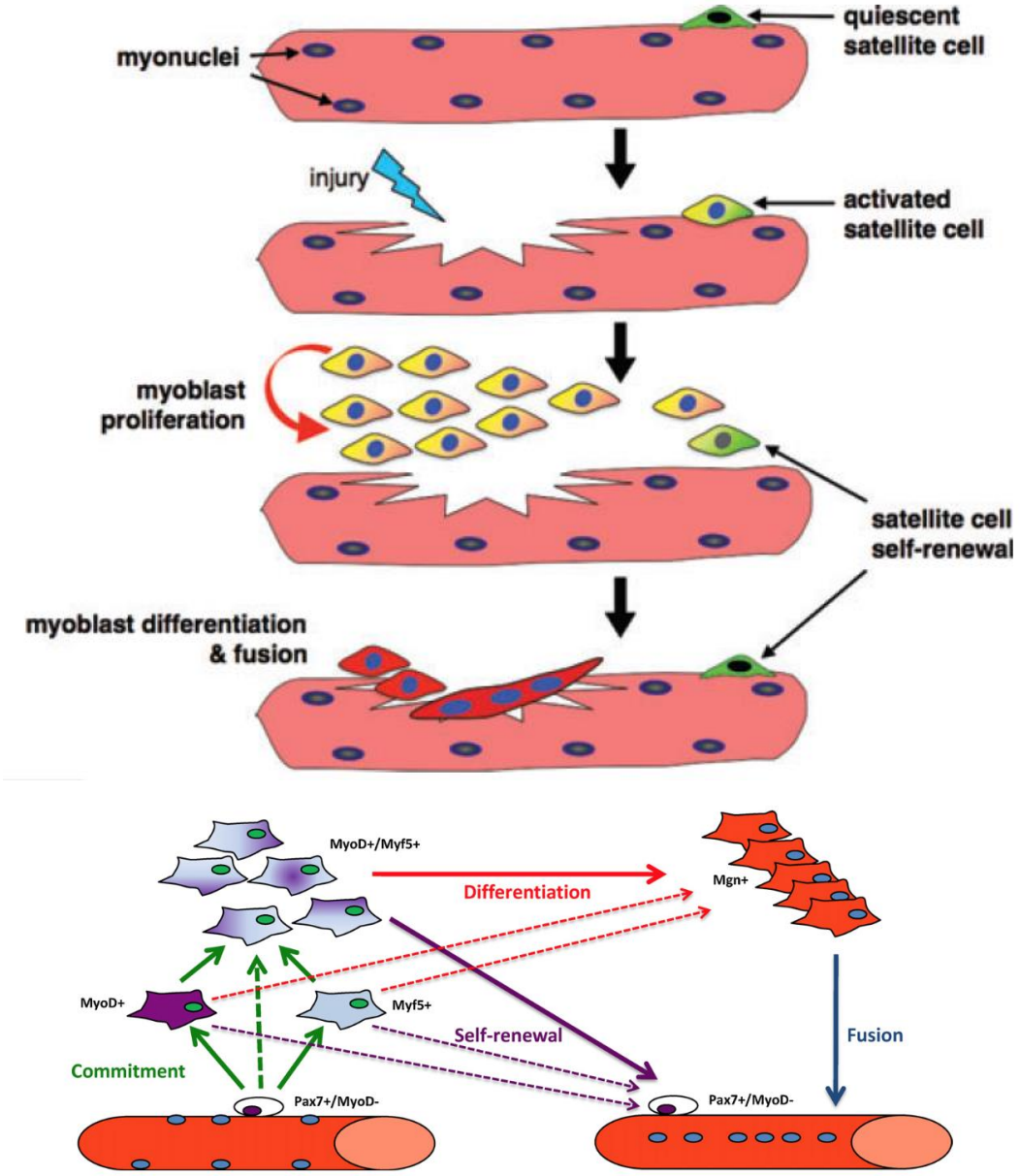

Figure 1.23. Activation of quiescence satellite cells supports muscle regeneration.

of PAX7/MYOD activated myoblasts proceeds to differentiation, downregulating *Pax7* and activating *Myogenin*, inducing fusion and new myofiber formation. A small subpopulation loses the MFRs but keeps PAX7 and self-renews the satellite cell pool.

Adapted from: Biressi & Rando, 2010; Olguín & Pisconti, 2012

cells play a pivotal role during the remodeling and regeneration process. They are rapidly activated, reenter the cell cycle, expand, and express MRFs (MYF5 and MYOD, succeeded by MYOGENIN). The activated population initially co-expresses PAX7 and MYOD. Subsequently, most myoblasts downregulate *Pax7* but maintain MYOD, express MYOGENIN, and follow the myogenic program to supply differentiated progeny for muscle repair (**Fig. 1.23**). Importantly, a subpopulation of activated satellite cells does not engage into terminal differentiation, maintains PAX7 (while losing MYOD) and returns to the quiescent state. Hence, they replenish the satellite cell pool by self-renewal in order to support future needs (**Fig. 1.23**). Similarly, satellite cells activated *in vitro,* either by primary culture of satellite cell-derived myoblasts [Abou-Khalil et al., 2010] or by culture of isolated fibers with their associated satellite cells [Zammit et al., 2004], are induced to proliferate and (upon certain culture stimuli) differentiate, while a subpopulation bypasses differentiation and returns to quiescence. Signaling molecules and pathways crucial functioning during development are redeployed for regeneration, implying that this process recapitulates many, yet not all, aspects of embryonic myogenesis [discussed in Tajbakhsh, 2009].

While disturbed homeostasis and minor forms of muscle tissue injury can activate satellite cells (without myogenic fusion with myofibres), damage that results in myofibre necrosis can regularly result from accidents, surgical and orthopaedic situations and some degenerative neuromuscular disorders [Grounds, 2014]. The *in vivo* modelling and study of myofibre necrosis (and subsequent myogenesis and regeneration) employs many forms of experimental injury or transplantation, including intramuscular myotoxin administration or cryoinjury in rodents [compared in Lee et al., 2013; Hardy et al., 2016]. Muscle necrosis ignites the following four phases for reconstitution of structurally and functionally normal muscle tissue: degeneration/necrosis, inflammation, myogenesis and fusion as essential components of regeneration (that may sometimes also require revascularisation and re-innervation), and subsequent remodelling and maturation (**Fig. 1.24A**) [reviewed in Barberi et al., 2013; Yin et al., 2013]. Extracellular calcium influx induces myofiber proteolysis and necrosis, while muscle proteins and microRNAs are released from the cytosol. Necrotic material stimulates an inflammatory response to remove tissue debris from the lesion site and activate stem cell-mediated muscle repair and regeneration. Neutrophils, M1 macrophages, and

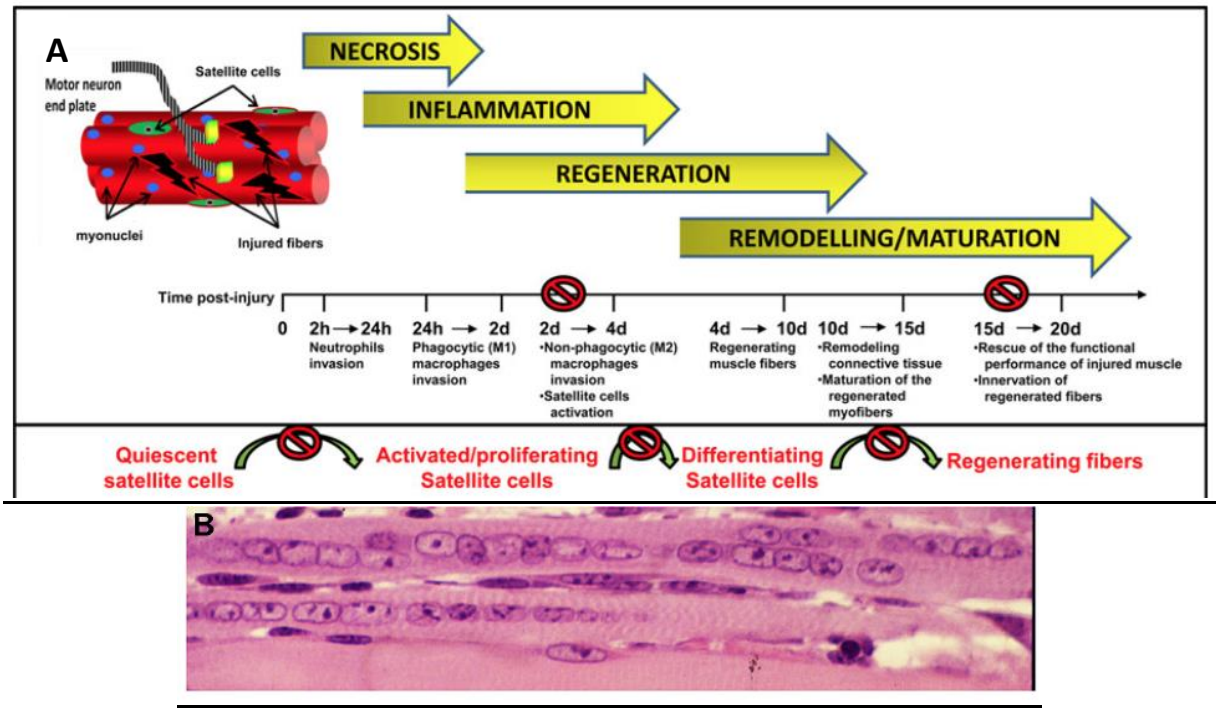

Figure 1.24. Muscle regeneration.

A) Timeline and satellite cells state of four major steps of the muscle regeneration procedure. Restrictive signs indicated stages susceptible to defects during aging. B) Characteristic central nuclei of regenerating muscle.

Adapted from: Barberi et al., 2013; Grounds, 2014

M2 macrophages sequentially invade the injured muscle, with macrophages being predominant. M2 macrophages progressively replace M1 and they are the ones that tune the inflammatory response, remove the debris, and promote remodeling. Inflammation is followed by a phase of active regeneration, characterized by satellite cell activation and expansion. Subsequently, a small proportion of satellite cells will replenish the quiescent pool, while the vast majority will provide committed myoblasts that fuse to form myotubes that later fuse with ends of remaining segments of damaged myofibres, or mature to form new myofibres as required, all with typical centrally located nuclei (**Fig. 1.24B**) [Grounds, 2014]. These steps of myogenesis with fusion to form myotubes can be reproduced in culture, helping thorough study of early myogenic events but often leading to misuse of the term regeneration [Grounds, 2014]. Recently, 3D time-lapse intravital imaging revealed that basal lamina remnants serve as "ghost fibers" to orient satellite cells and preserve muscle architecture [Webster et al., 2016]. Upon activation, satellite cells switch from an immobile to a migratory state *in vitro* [Siegel et al., 2009; Marg et al., 2014] and *in vivo* [Webster et al., 2016], which enables them to invade the lesion sites. The final steps of regeneration involve contractile apparatus maturation and reestablishment of innervation, vascular network, and extracellular matrix to ensure recovery of the functional performance. If any of these four phases is disrupted or missregulated, myofiber formation and muscle architecture are compromised, while excessive deposition of fibrotic and adipose tissue may also be observed, further hindering regeneration [Brzoska et al., 2011].

Satellite cells seem to be primed for myogenesis and quickly convert from a quiescent to an activated state. The observations of Crist et al. [2012] might explain this phenomenon, as they describe a model, whereby satellite cells transcribe *Myf5*, but post-translationally suppress it (through sequestration in messenger ribonucleoprotein granules by mir-31) to maintain quiescence. Accordingly, quiescent satellite cells in muscle sections and isolated myofibers of *Myf5*^{nlacZ} mice express β-galactosidase, further confirming the *Myf5* locus transcription [Gayraud-Morel et al., 2007; Kuang et al., 2007a; Tajbakhsh, 2009]. These results can also be interpreted as indicative of myogenic commitment by the majority of satellite cells before returning to quiescence. Satellite cells were shown *in vivo* to progress from G0 quiescence to the so-called G_{Alert} phase, in which they are primed for activation [Rodgers et al., 2014]. Upon activation, they upregulate *c-Met*, *Pax7*, and *M-cadherin* as

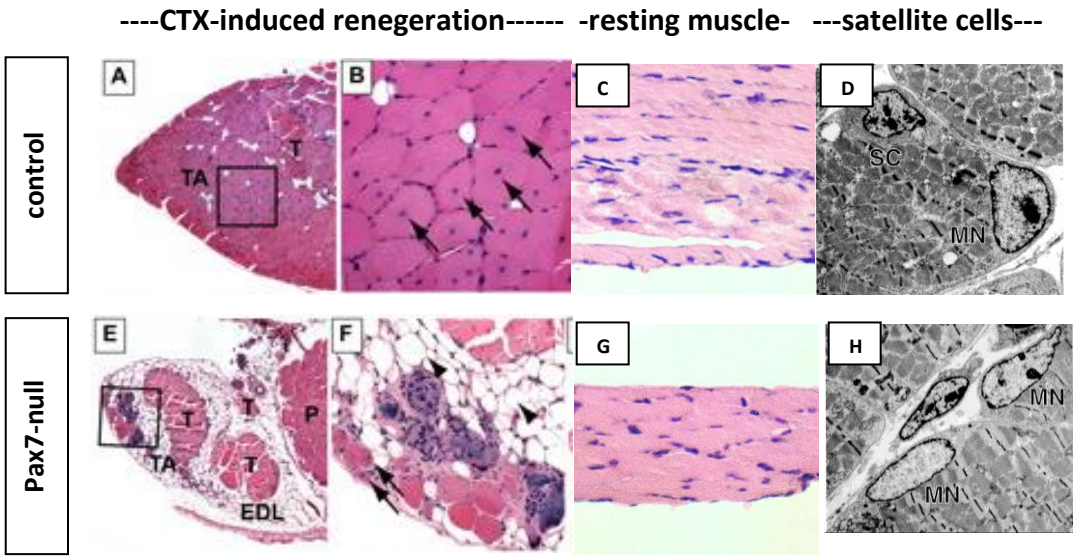

Figure 1.25. Regeneration deficit, muscle atrophy, and loss of satellite cells in the absence of *Pax7*. Regenerative response, resting muscle and satellite cells of wild-type mice (A-D) or *Pax7*-deficient mice (E-H) reveal differences in muscle structure reestablishement post-injury (A, B, E, F), muscle mass (C, G) and satellite cell specification (D, H). CTX: cardiotoxin, EDL: *Extensor digitorum longus* muscle, MN: myonucleus, P: *Plantaris* muscle, SC: satellite cells, T: tendon, TA: *Tibilialis Anterior* muscle.

Adapted from: Seale et al., 2000; Kuang et al., 2006

well as specification factors, such as *Myf5* and *MyoD* [summarized in Barberi et al., 2013]. *MyoD* upregulation correlates with post-injury [Grounds et al., 1992; Yan et al., 2003] or culture-triggered [Zammit et al., 2004] satellite cell activation. This possibly represents an early activation event, since *MyoD* is detectable as early as six hours post-trauma [Grounds et al., 1992]. Interestingly, when the methyltransferase Suv4-20h1, which is involved in heterochromatin formation and quiescence maintenance, is depleted, the *MyoD* locus is repositioned away from heterochromatic sites and transcriptionally activated [Boonsanay et al., 2016]. At the onset of differentiation, cells withdrawing from the cell cycle, express *Myogenin* and *Mrf4* and down-regulate *Pax7*, the latter possibly mediated by MYOGENIN [Seale et al., 2000; Zammit et al., 2004; Olguín & Olwin, 2004; Gayraud-Morel et al., 2007; Olguín et al., 2007]. Recent studies showed that the ubiquitin-ligase NEDD4 drives proteasome-dependent PAX7 degradation upon differentiation [Bustos et al., 2015], while casein kinase 2-dependent PAX7 phosphorylation ensures its maintenance in proliferating progenitors [González et al., 2016]. Either PAX3/7, acting through MYOD, or MYF5 is required for satellite cell-driven myogenesis [reviewed in Buckingham, 2007]. Intriguingly, PAX3/7+ satellite-like cells also support muscle regeneration in arthropods, extending the vertebrate findings and suggesting early evolution of this repair strategy [Konstantinides & Averof, 2014].

PAX7 is essential for satellite cells function during adult muscle growth and regeneration. In its absence, postnatal muscle growth and regeneration are severely affected, due to the progressive loss of satellite cells (**Fig. 1.25**), even in muscles expressing *Pax3*, the paralogue of *Pax7* [Seale et al., 2000; Oustanina et al., 2004; Kuang et al., 2006; Relaix et al., 2006]. Specifically, body weight and muscle mass are reduced, muscles consist of smaller myofibers with less myonuclei, and upon injury there is negligible fiber formation accompanied by extensive adipocyte, calcium, and fibrotic deposition. The Braun group reported that *Pax7* mutant phenotype is sensitive to the genetic background. In a sv129 background, Pax7-deficient juvenile muscles are nearly normal and do not present with a complete lack of satellite cells; nevertheless, adult muscles display severe deficiencies in homeostasis or regeneration associated with delayed loss of satellite cells [Oustanina et al., 2004]. Conditional ablation of PAX7+ satellite cells in adult mice using different tamoxifen-inducible Cre lines, demonstrated its critical role for adult satellite cell function, as in its absence skeletal muscle repair

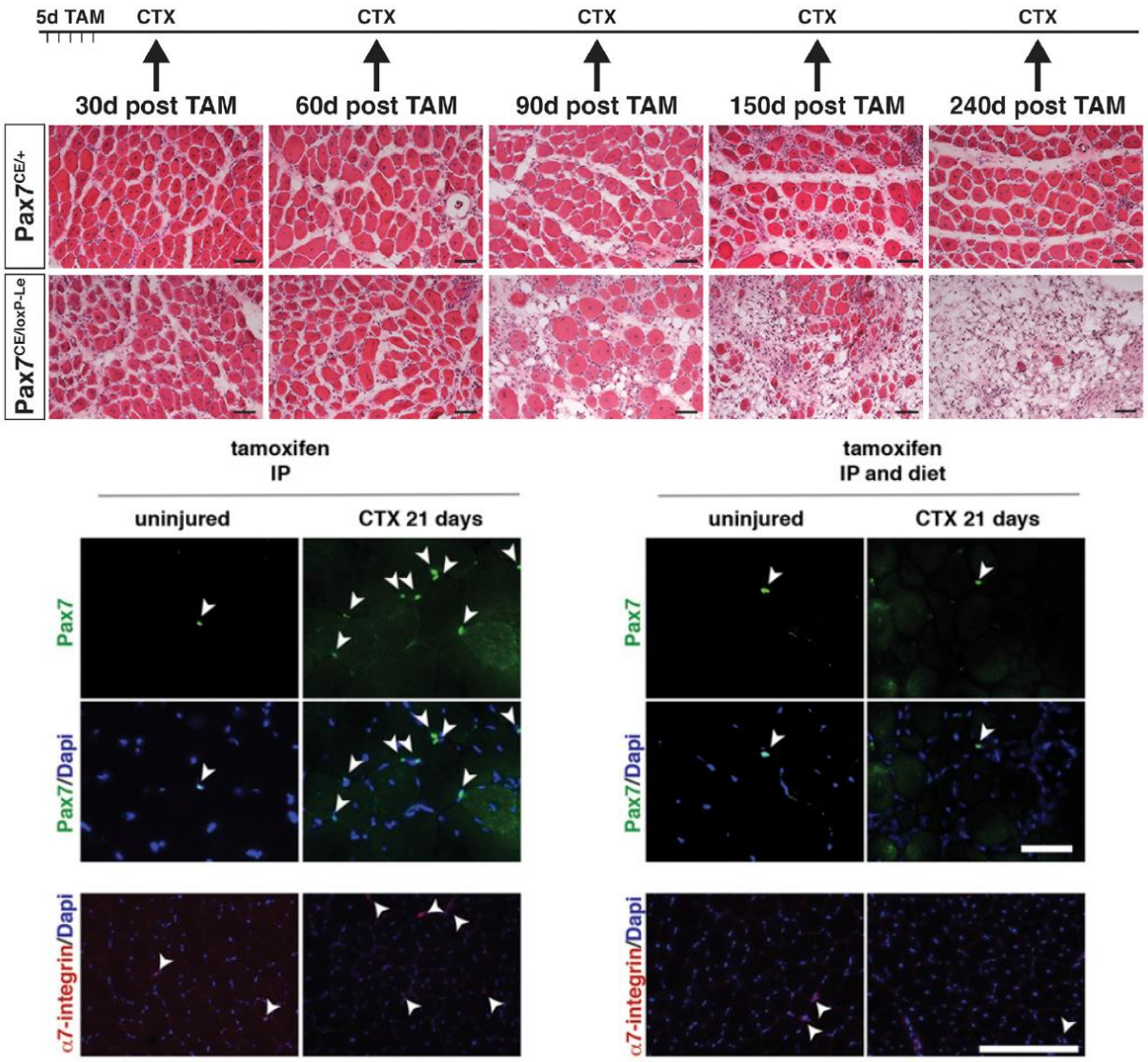

Figure 1.26. Applying tamoxifen scheme might musk the limitations of the loxP-Cre system.

Different chase periods (upper, lower panel) and tamoxifen administration during regeneration (lower panel) have diverse outcomes on PAX7+ satellite cell elimination (PAX7+ cells marked with arrowheads in lower panel) and subsequent regeneration. CTX: cardiotoxin, TAM: tamoxifen.

Adapted from: Günther et al., 2013; von Maltzahn et al., 2013

was strongly compromised [Günther et al., 2013; von Maltzahn et al., 2013]. These studies ignited a debate with the first work with conditionally Pax7-depleted muscles which reported functional satellite cells and efficient regeneration [Lepper et al., 2009]. The differences have been attributed to (a) the inefficient CreERT2-mediated recombination in quiescent satellite cells, (b) the limitations of the Cre-LoxP technology and the presence of "escaper" cells; suboptimal gene targeting occurred when the chase period was not long or tamoxifen was not administered during regeneration (**Fig. 1.26**), (c) the possible generation of truncated PAX7 by one of the used alleles [discussed in Brack, 2014; Buckingham & Relaix, 2015]. Even few wild-type satellite cells are capable of replenishing the satellite cell pool and out-compete the recombined majority [von Maltzahn et al., 2013].

A subset of MRFs is also important for muscle homeostasis and regeneration in the adult, as revealed by genetic manipulations in mice. Opposite to the embryo situation, MYF5 and MYOD do not seem to effectively compensate for each other in the adult. MYF5 deficiency results in delayed muscle regeneration after injury, possibly due to delayed transition from proliferation to differentiation [Gayraud-Morel et al., 2007; Ustanina et al., 2007]. Resting muscles of young MYF5-deficient adults are comparable to controls, while satellite cell amount and quiescent state (evaluated by electron microscopy) are preserved [Gayraud-Morel et al., 2007; Ustanina et al., 2007]. However, old MYF5 mutant muscles show increased fibrosis and centrally-located nuclei, indicative of a cumulative defect following chronic regeneration [Gayraud-Morel et al., 2007]. MYOD-null mice have more satellite cells, but they show a defective balance in proliferation/self-renewal and myogenic progression resulting in delayed regeneration [Megeney et al., 1996; Yablonka-Reuveni et al., 1999; White et al., 2000]. MYOD-deficient donor myoblasts show increased migrations, possibly as a side effect of the proliferation/differentiation dysregulation [Smythe & Grounds, 2001]. MYOGENIN deficiency at post-embryonic-myogenesis stages does not compromise muscle postnatal growth in terms of structure or function [Knapp et al., 2006]. Satellite cell-derived myoblasts lacking MYOGENIN grow and differentiate in culture as controls [Meadows et al., 2008]. However, muscles have not been challenged with injury to evaluate the full potential of their satellite cells in repair. Finally, MRF4 is absent from quiescent satellite cells or their activated progeny until differentiation initiation and there are no signs of upregulation upon MYF5 deficiency; thus, its participation at the early stages of

satellite cell function was excluded and no further analyses have been performed [Gayraud-Morel et al., 2007].

Apart from the critical contribution of satellite cells in muscle regeneration, several other populations have myogenic potential [reviewed in Pannérec et al., 2012; Yin et al., 2013]. *In vitro* or upon transplantation in compromised muscles, they have myogenic capacity, participate in the repair procedure by myofiber formation, and some even contribute to the satellite cell compartment. Initiated with experiments with bone-marrow-derived cells, these findings were later expanded in several more populations, including a hematopoietic population referred to as side population (SP), CD133+ cells, PW1+ interstitial cells (PICs), mesangioblasts, and the vessel-associated pericytes. However, none of these cell types is able to form new muscle or replenish the satellite cell pool in the absence of satellite cells, as demonstrated by regeneration analyses in muscles depleted of satellite cells. In fact, the defective regeneration was only rescued by wild-type satellite cell engraftment [Sambasivan et al., 2011].

Since satellite cell characterization as adult skeletal muscle stem cells, their studying progressed immensely, with implications in regenerative medicine. However, technical challenges hold their therapeutic promise back, since they are isolated in small amounts from muscle biopsies and expansion in culture is challenging due to rapid and irreversible differentiation *in vitro* [Bentzinger et al., 2012]. Similarly, *in vitro* genetic corrections and subsequent autologous transplantation cannot be accomplished [Bentzinger et al., 2012]. Amelioration of culture conditions resembling the characteristics of the niche might resolve these problems, raising hopes for implementation in humans. For instance, substrate elasticity mimicking the one of muscle favors self-renewal *in vitro* and efficient regeneration after transplantation [Gilbert et al., 2010]. Similarly, enhanced performance can be achieved by treatment with the bisperoxovanadium, a phosphotyrosine phosphatase inhibitor [Smeriglio et al., 2016].

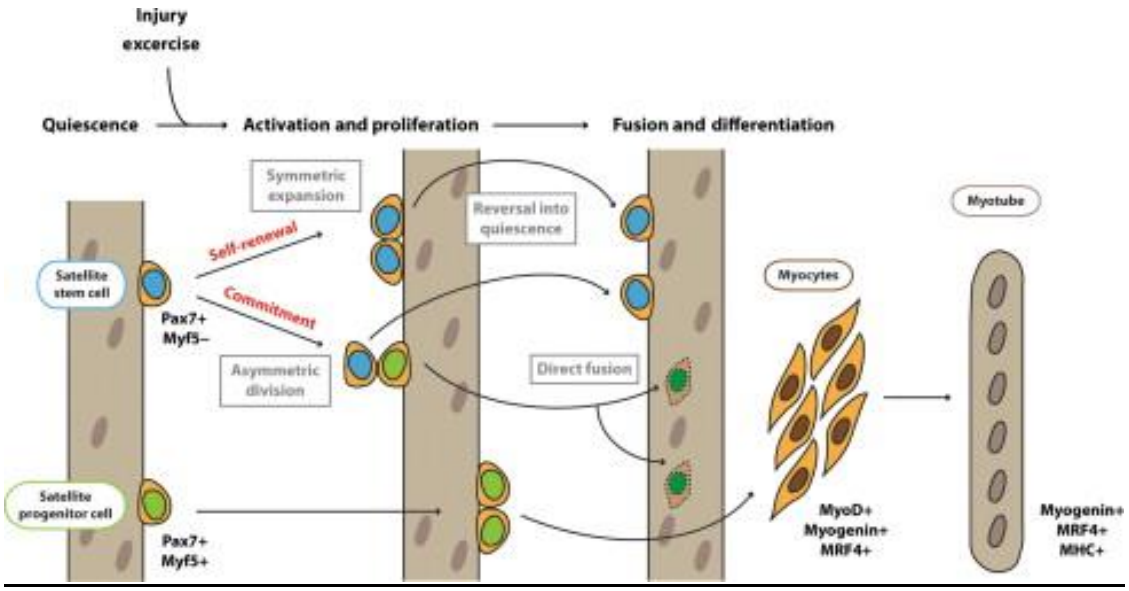

Figure 1.27. Symmetric and asymmetric divisions of Myf5- or Myf5+ satellite cells.

PAX7+MYF5- satellite cells represent a more stem population able to provide the more committed PAX7+MYF5+ satellite cells but also self-renew, undergoing apico-basal/asymmetric or planar/ symmetric division, respectively. On the contrary, PAX7+MYF5+ satellite cells provide only committed progeny (by symmetric division) that will sustain differentiation.

Source: Chang & Rudnicki, 2014

1.5.6 Satellite cell heterogeneity

Satellite cells are considered a heterogeneous population, in terms of gene expression signatures, proliferation rate, differentiation propensity, and, importantly, stemness. Satellite cells originating from different muscles show variations (e.g. in amount, gene expression profile, proliferation/differentiation kinetics) [Ono et al., 2010]; however, the above properties are also subject to intra-muscle variations. Live imaging revealed differences in the rates of cell cycle reentry and subsequent divisions [Siegel et al., 2011; Webster et al., 2016]. Other groups have linked this variation to subpopulations defined by different markers. A subset of satellite cell markers are not expressed by the entire population [Beauchamp et al., 2000; Gnocchi et al., 2009], including *Pax3*, which is postnatally restricted to a subset of muscles [Relaix et al., 2006; Calhabeu et al., 2013]. Furthermore, markers that are considered universal, such as PAX7, do not have uniform levels [Rocheteau et al., 2012]. Higher *Pax7* expression characterizes a more stem/less committed subpopulation, with lower metabolic rates, delayed activation, and higher self-renewal ability and regeneration capacity. At cell division, $PAX7^{Low}$ cells segregate their chromosomes randomly and provide two committed daughters, while $PAX7^{High}$ cells perform asymmetric DNA segregation, with the template-DNA-retaining daughter exhibiting a more stem-like phenotype [Rocheteau et al., 2012]. This is in line with early reports of asymmetric divisions leading to inheritance of the older template strand to the daughter cell with more immature and self-renewing phenotype [Shinin et al., 2006; Conboy et al., 2007]. A further intrinsic factor with asymmetric distribution and preferential transmission to the self-renewing daughter cell is the cilium, a structure present in quiescent satellite cells but disassembled in activated ones [Jaafar Marican et al., 2016].

Variability in *Myf5* locus activity has also been noted among satellite cells, but their possible origin from the embryonic co-existing PAX7+MYF5+ and PAX7+MYF5- populations [Picard & Marcelle, 2013] has not been investigated. Following muscle damage and induction of regeneration, a subset of satellite cells undergoes activation, proliferation, and early differentiation phases, presumably without ever activating MYF5 [Cooper et al., 1999]. Similarly, only 87-90% of quiescent adult satellite cells are β-galactosidase+ and YFP+ in $Myf5^{nLacZ}$ and $Myf5^{Cre}$; $Rosa26^{YFP}$ mice, respectively [Kuang et

al., 2007a]. The reporter-negative cells may represent a more stem population [Kuang et al., 2007a], although after *Myf5*-Cre ablation of PAX7+ satellite cells, surviving satellite cells do not replenish the pool and cannot rescue the regeneration phenotype [Günther et al., 2013]. MYF5- satellite cells are able to give rise to both compartments, as opposed to their MYF5+ counterparts [Kuang et al., 2007a]. Asymmetric divisions seem to account for the generation of the latter (**Fig. 1.27**). Symmetric divisions give rise to two identical daughter cells, while asymmetric ones contribute daughter cells with distinct fates. Mitotic spindle orientation perpendicular to the myofiber drives an asymmetric apico-basal division, whereby a PAX7+MYF5- cell gives rise to an apical PAX7+MYF5+ and a basal PAX7+MYF5- daughter [Kuang et al., 2007a]. Non canonical Wnt pathway was shown to promote symmetric expansion of satellite cells [Le Grand et al., 2009], while dystrophin cooperates with Par proteins to drive asymmetric divisions [Dumont et al., 2015] in addition to its well-defined traditional role in maintaining sarcolemma integrity. Time lapse imaging revealed that cells resulting from vertical divisions remain associated longer than cells from planar divisions [Siegel et al., 2011]. Notably, recent intravital imaging studies render these observations unlikely in the *in vivo* situation, where divisions predominantly occur in parallel to the axis of the myofibers [Webster et al., 2016].

The histone H2B-GFP pulse/chase system allowed a further classification of satellite cells based on label retention [Chakkalakal et al., 2014]. Label-retaining cells (LRCs) present with a more stem signature, associated with ability to self-renew, earlier entry into quiescence, rare divisions, and lower propensity for expansion and differentiation. They can give rise to both LRCs and differentiation-competent non-LRCs. The two populations are already established at birth.

While different assays classify satellite cells into a more stem and/or a more committed compartment, the degree of overlap between the subpopulations defined by different methods still remains to be established.

1.5.7 Aging effect in muscle and satellite cells

Advanced age results in sarcopenic muscles, characterized by reduced mass and function, with implications on personal (e.g. independence, quality of life) and socio-economical levels (e.g. health costs) [Grounds, 2014]. Sarcopenia has a multifactorial etiology and both intrinsic (e.g. satellite-cell-related) and extrinsic (e.g. microenvironment, inflammatory status, innervation) factors contribute to the observed regenerative decline (**Fig. 1.22A**) with aging. Reduced numbers, proliferative capacity, and telomere length of satellite cells have been associated to the defective phenotype [reviewed in Barberi et al., 2013]. As opposed to young (2-6 months) or old (20-24 months) satellite cells, geriatric ones (28-32 months) undergo a so-called geroconversion, shown by p16-mediated switch into an irreversible pre-senescent state, which severely affects their intrinsic regenerative and self-renewal potential [Sousa-Victor et al., 2014]. The same group later linked age-related decline in autophagy with the quiescence-to-senescence shift upon aging [García-Prat et al., 2016]. Furthermore, compromised function of the neuromuscular function and myofiber denervation are associated to sarcopenia [Barns et al., 2014; Krishnan et al., 2016]. Heterochronic parabiosis experiments (linking the blood supply of young and old mice) rescue the regenerative defects of aged mice, underlining the importance of systemic factors [Conboy et al., 2005]. However, the intrinsic defects such as senescence marker expression and increased p38α/β MAPK signaling cannot be counteracted by the young microenvironment and rather depend on pharmacological treatment [Bernet et al., 2014; Cosgrove et al., 2014]. Study design seems to be an unappreciated factor strongly influencing the reported conclusions. Several factors affect the final outcome, including short-term (5 days post-injury) or long-term (28 days post-injury, when regeneration procedure is complete) follow-up, applied methodologies to induce a regenerative response (preserving or not the neurovascular supply), age range (including or not geriatric individuals), and assessed endpoints (e.g. overt muscle architecture reestablishment, satellite cell status and self-renewal).

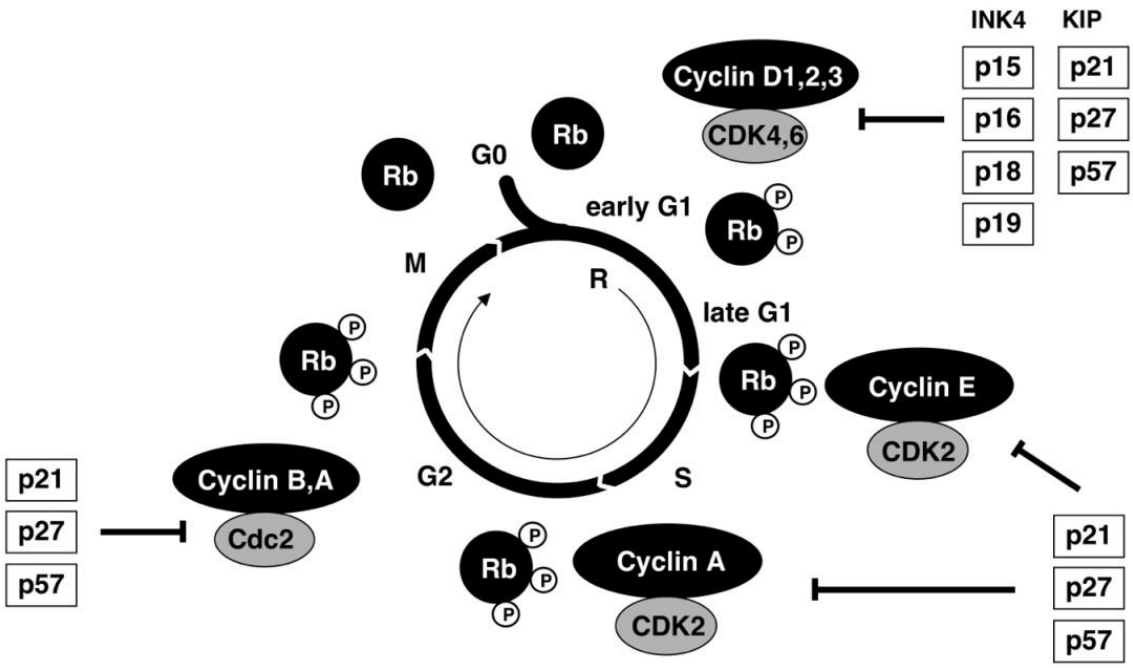

Figure 2.1. Cell cycle progression and arrest.

Non-cycling cells are maintained at the resting, non-proliferating phase called G0, while cycling cells undergo S-phase (Synthesis; DNA replication step) and M-phase (Mitosis; division step), which are separated by two "gap phases" (G1, G2). Cell cycle progression depends on the activity of various complexes of Cyclin-Dependent Kinases (CDKs) and cyclins, acting on different cell cycle transitions. When active, these complexes phosphorylate the retinoblastoma protein (Rb), blocking its inhibitory activity on proliferation. Two families of Cyclin-Dependent Kinase Inhibitors counteract the activity of CDK-cyclin complexes at G1 phase (family INK4, encompassing p15, p16, p18, p19) or throughout the cell cycle (family Cip/Kip, including p21, p27 and p57).

Source: Müller, 2010

Chapter 2. Cell cycle and growth arrest in skeletal muscle and beyond

Tightly controlling cell cycle is imperative throughout the live of complex organisms. Dysregulated cell cycle has been associated with developmental abnormalities [Yan et al., 1997; Zhang et al., 1997], severe organ malfunction and defective stem cell self-renewal [Matsumoto et al., 2011; Sherr, 2012] or stem cell loss [Kozar et al., 2004]. Moreover, perturbations of the cell cycle are linked to cancer [Sherr, 2012], aging [Matheu et al., 2009] and age-related pathologies [Sherr, 2012; Chandler & Peters 2013]. Cell cycle regulation and differentiation are intimately linked, although they can be uncoupled [Zalc et al., 2014]. Appropriate embryonic growth and patterning depend on a balance between proliferation and differentiation, to ensure sufficient propagation but not at the expense of forming differentiated structures [Ciemerych et al., 2011]. Once growth or tissue repair are completed, cell division is no longer required to guarantee a healthy homeostasis. Yet, in the absence of proper cell cycle control, cancer may develop. Notably, among the hallmarks of cancer are sustained proliferation, limitless replicative potential, and evasion of growth suppressors or apoptosis [Khabar, 2016]. Thus, interrupting cell cycle holds therapeutic promise to arrest cancer growth [Blachly et al., 2016].

Cell cycle progression is primarily achieved by an array of Cyclin-Dependent Kinases (CDKs) and their activating subunits named cyclins [Malumbres, 2014]. The regulation of these CDK-Cyclin complexes depends on the Cyclin-Dependent Kinase Inhibitors (CDKIs), which are classified in two families based on their structural homology and specificity of action (Borriello et al., 2011): INK4 [including $p15^{Ink4b}$ (p15), $p16^{Ink4a}$ (p16), $p18^{Inc4c}$ (p18), $p19^{Ink4d}$ (p19)] and Cip/Kip [including $p21^{Cip1}$ (p21), $p27^{Kip1}$ (p27), $p57^{Kip2}$ (p57)]. In case of CDKI-mediated inhibition, the CDK-Cyclin complexes lose the capacity to phosphorylate the retinoblastoma protein (pRB) [Cobrinik, 2005]. In its hypophosphorylated form, pRB can target factors of the E2F family, negatively affecting E2F-responsive genes, which are maintaining the cell in cycle (**Fig. 2.1**) [reviewed in van den Heuvel & Dyson, 2008].

A more in-depth presentation of the molecules described above is provided in the sub-sessions to follow. Relevant discoveries in the muscle field are summarized in the end of each sub-session.

Substantial work has identified essential participants of *in vitro* cell cycle exit and differentiation of muscle cells. Nevertheless, less data are available to confirm this interplay *in vivo* and, most importantly, to unravel the mechanism of satellite cell entry into quiescence.

2.1 Cell cycle overview

During the cell cycle, cells consecutively pass through four phase (**Fig. 2.1**):
- G1 (Gap 1), during which the cells are metabolically being prepared for division. They grow in size, produce RNA and proteins and increase their supply in organelles. The G1 checkpoint safeguards that everything is ready for DNA synthesis.
- S (Synthesis), during which DNA replication occurs. The genetic material is duplicated guaranteeing that each daughter cell will inherit a complete copy of the mother cell genome.
- G2 (Gap 2), during which the cells continue to grow. The G2 checkpoint is the control mechanism ensuring that the cell is ready to divide.
- M, during which the cells undergo nuclear division (mitosis), followed by cell division (cytokinesis).

After division, cells return to G1 and will either proceed to a further division or enter G0 phase. The latter is a resting phase characterizing cells that withdraw from the cell cycle either permanently (differentiation, senescence) or reversibly (quiescence). It is a post-mitotic, non-proliferative state. Quiescence allows cells to start cycling upon specific needs. For instance, following tissue damage, quiescent myogenic stem cells get activated, proliferate to amplify their population, and are available for fusion and muscle regeneration where necrosis has occurred. In contrast, cells driven to terminal differentiation post-mitotically, such as myonuclei, do not re-enter the cell cycle in physiological conditions [Cheung & Rando, 2013]. Similarly, cells may cease to divide and enter into (irreversible) senescence, in response to developmental cues/regeneration (physiological context) [Muñoz-Espín et al., 2013; Storer et al., 2013; Le Roux et al., 2015] or damage/stress (pathological context) [Muñoz-Espín & Serrano, 2014].

Apart from the temporal orchestration of the molecules forming the core cell cycle machinery, chromatin changes are intimately linked to cell cycle regulation. Global and local chromatin architecture and packaging dictate transitions between chromatin compaction and decompaction and render the chromatin non-permissive or permissive, respectively, to DNA-templated processes, such as transcription, replication, and repair [Yu et al., 2016]. Thus, chromatin accessibility and condensation are coordinated with the cell cycle to tune specific genome activities.

2.2 CDK-Cyclin complexes: cell cycle progression

General features in cell cycle regulation

The cell cycle is orchestrated by a cascade of CDKs and their associated cyclin subunits. The importance of these complexes in promoting transitions through the cell cycle was established in the late 90s. Less than a decade later, the Nobel prize in Physiology or Medicine (LH Hartwell, T Hunt, PM Nurse; 2001) internationally acknowledged the characterization of these key cell cycle players of all eukaryotic organisms, identified across the eukaryote kingdom, from yeasts to plants and animals.

CDKs are serine/threonine kinases that acquire their catalytic activity via binding of a cyclin molecule and the resulting conformational modifications [reviewed in Malumbres, 2014]. There is considerable specificity in CDK-Cyclin interactions as well as in the cell cycle phase to be controlled (**Fig. 2.1**). The first, and most important, restriction point is the G1 checkpoint, that has to be overcome for cells to proliferate. At early G1, complexes of Cyclin D with CDK4 [Quelle, 1993] or CDK6 suppress the antiproliferative effects of pRb protein, while CDK2-Cyclin E complexes act at later G1 in a pRb-independent way [Resnitzky & Reed, 1995]. CDK2 further participates in S-phase interaction, but at that phase it binds with Cyclin A [Pagano et al., 1992]. Mitosis is then initiated by the complexes of CDC2 (CDK1) with Cyclin B or Cyclin A [Draetta et al., 1989; Pagano et al., 1992; Kishimoto & Okumura 1997].

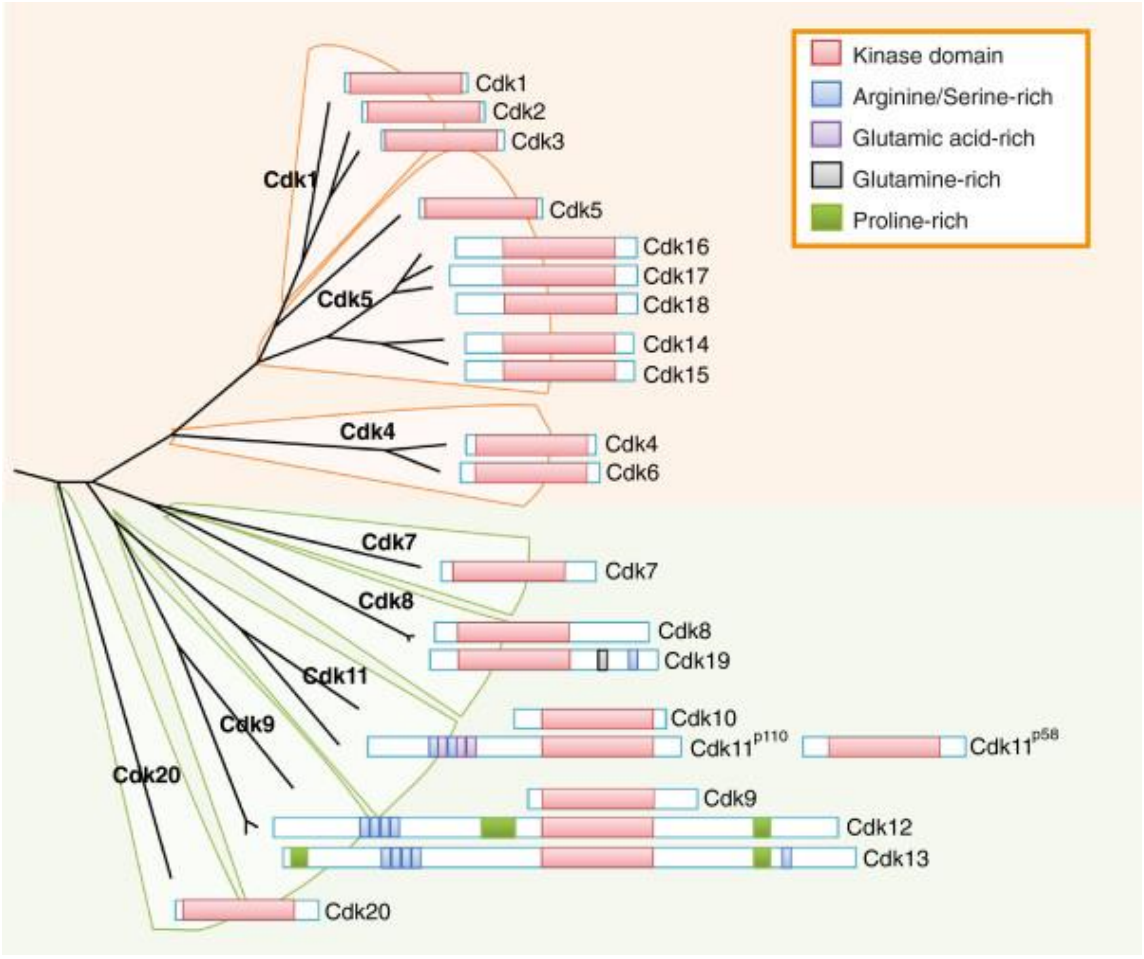

Figure 2.2. Phylogenetic tree of mammalian CDK families.

Eight CDK families (left part of the tree) encompass 20 CDKs (right part of the tree), functioning in cell cycle (orange; top) or transcription (green; bottom). All CDKs share a conserved kinase domain (red), while some possess further domains (as indicated in key).

Source: Malumbres, 2014

The mechanisms governing CDK activity involve i) activation by cyclin binding and by CDK phosphorylation at a conserved threonine and ii) repression by CDKI binding (subsession 2.3) or by phosphorylation at inhibitory sites near the N terminus. Like other kinases, CDKs have a two-lobed structure with the active site for ATP binding and catalysis being in a deep cleft at the junction of the lobes [de Bondt et al., 1993]. Although the biochemical features of different CDK-Cyclin complexes may vary, the model arising from CDK2 studies is well accepted to mirror how the CDK-Cyclin association is the key step for CDK activation. Structural analyses of monomeric and cyclin-bound CDK showed that the CDK catalytic cleft of the cyclin-free form is closed, preventing enzymatic activity. However, cyclin binding reorients key side chains, restoring active sites to their correct position [de Bondt et al., 1993]. To acquire full activation, the CDK-Cyclin complex is then phosphorylated by the Cdk-Activating Kinase (CAK), which is believed to be the complex CDK7-Cyclin H-Mat1 in higher eukaryotes [Fisher & Morgan, 1994; Devault et al., 1995]. Moreover, CAK-mediated phosphorylation promotes the formation of high-affinity complexes in some CDK-Cyclin cases [Desai et al., 1995]. Inhibitory phosphorylation is, by definition, non-CAK-induced. CDK4 and CDC2 are phosphorylated during G1 and G2 progression, respectively, and their dephosphorylation is required for S-phase and mitosis entry, respectively [Terada et al, 1995; Mueller et al., 1997]. Increased CDK4 phosphorylation is observed following DNA damage, causing G1 arrest [Terada et al., 1995].

Cyclins constitute a large, diverse family, ranging in size from 35 to 90 kDa [Malumbres, 2014]. Despite the substantial sequence differences, considerable structural similarities are suggested [Nugent et al., 1991]. Cyclins are structurally defined by a 100-residue domain called cyclin box, which is required to bind and activate CDKs [Nugent et al., 1991; Kobayashi et al., 1992; Lees & Harlow, 1993]. Different cyclins appear at different phases of the cell cycle, with D/E functioning at G1, E/A at S phase, and A/B at mitosis (**Fig. 2.1**). As implicated by their name, cyclins are subject to oscillations during the cell cycle. These fluctuations depend on gene transcription and protein degradation [Morgan, 1977]; remarkably, proteolysis of mitotic cyclins is essential for mitosis exit [King et al., 1996]. In the case of cyclin B there is additional regulation by subcellular translocation [Gallant et al., 1995].

Apart from the three CDK families regulating the cell cycle, there are a few more that are functioning in transcription. Those are more conserved (**Fig. 2.2**) and they are regulated by mechanisms different from cyclin level oscillations [Malumbres, 2014].

Implications in skeletal muscle cell cycle regulation

Dividing and differentiating myoblasts have been extensively analyzed for the presence and activity of various CDK-Cyclin complexes. Both early G1 CDKs (i.e. CDK4/6) levels were constant during myocyte differentiation [Wang & Walsh, 1996b]. Their cyclin partners showed divergent patterns: i) Cyclin D1 was high in the proliferating population and low in the differentiating one, ii) Cyclin D2 was not detectable in any population, and iii) Cyclin D3 unexpectedly increased upon differentiation [Rao et al., 1994; Kiess et al., 1995; Skapek et al., 1995; Wang & Walsh, 1996b]. Among the CDKs, CDK4 has been extensively studied. It was found to be expressed in both myoblasts and myotubes [Shapek et al., 1995]; however, in myotubes it appeared to not be associated with cyclins but interacted with the inhibitors p21 and p27 [Wang & Walsh, 1996b]. Moreover, Cyclin D1-dependendent subcellular localization has been shown. CDK4 was nuclear in the dividing Cyclin D1-expressing myoblasts, but translocated to the cytoplasm of the forming myotubes, that lacked Cyclin D1 [Zhang et al., 1999a]. Chemical inhibition of CDK4/6 promoted G1 accumulation and enhanced muscle-specific expression [Saab et al., 2006]. Conversely, forced expression of CDK4 and cyclin D1 in C2C12 or primary myoblast cultures triggered DNA synthesis in myotubes [Latella et al., 2001]. As far as differentiation is concerned, ectopic CDK4-CyclinD impaired muscle-specific gene expression [Latella et al., 2001] and repressed MEF2 activity, without affecting all transcriptional activation [Lazaro et al., 2002], while ectopic Cyclin D1 inhibited MyoD-induced activation of muscle gene transcription [Rao et al., 1994]. Zhang and colleagues showed that CDK4 can bind MYOD and block its DNA binding capacity [Zhang et al., 1999a], while MYOD can bind CDK4 and inhibit its ability to phosphorylate pRb [Zhang et al., 1999c]. These seemingly contradictory observations might depend on differences in MYOD/CDK4 levels, on subcellular trafficking or on the involvement of further partners in the MYOD/CDK4 complexes.

Fewer studies focused on the other CDK/Cyclin complexes. The mitotic complex of CDC2/Cyclin B was found to phosphorylate MYOD, leading to repression of MYOD-dependent transactivation as well as to diminished MYOD amount during mitosis [Tintignac et al., 2004]. Muscle-specific expression of different CDKs-Cyclins in *C.elegans* activated the cell cycle transcriptional program, without loss of the differentiated state. Under those experimental conditions, cell cycle reentry and S-phase induction was not driven by CDK2/Cyclin E but rather CDK4/Cyclin D [Kotzelius et al., 2011]. In line with this observation, ectopic CDK2/Cyclin E did not reinforce cell cycle reentry in differentiated myotubes, as opposed to the other G1 CDK/Cyclin complex [Latella et al., 2001]. CDK2-associated kinase activity was observed in lysates from proliferating C2C12 myoblasts, but not differentiating ones, while inactive CDK2/Cyclin E seemed to persist in the latter [Mal et al., 2000]. CDK2 immunoprecipitated with Cyclin A in proliferating myoblasts [Chu & Lim, 2000], in agreement with this complex's role in S-phase (**Fig. 2.1**). However, upon differentiation there is evidence that CDK2 is sequestrated from Cyclin A into inactive Cyclin D3-p27-CDK2 complexes [Chu & Lim, 2000]. As previously mentioned, Cyclin D3 was the only G1 cyclin surprisingly found to be upregulated upon myogenic differentiation [Rao et al., 1994; Skapek et al., 1995; Wang & Walsh, 1996b]. In fact, MYOD was found to activate its expression, assisted by the co-activator p300 [Cenciarelli et al., 1999]. Cyclin D3 was suggested to participate in the induction but not maintenance of muscle differentiation. In line with this, Cyclin D3 was highly expressed at late fetal stages, but disappeared in terminally differentiated skeletal muscle [Bartkova et al., 1998]. Furthermore, Cyclin D3 primes myoblasts for differentiation when overexpressed [Gurung & Parnaik, 2012]. *In vitro* and *in vivo* studies of Cyclin D3 knock-out muscles showed defects under homeostatic conditions as well as reduced satellite cell renewal following activation [de Luca et al., 2014].

Regarding the CDK families that are implicated in transcription rather than cell cycle progression, scarce data are available. In contrast to cell cycle-related CDK/Cyclin complexes, CDK9/Cyclin T2a seemed to enhance MYOD function and promote differentiation [reviewed in de Falco & de Luca, 2009], consistent with a role distant from supporting proliferation.

2.3 The Pocket Protein- E2F network: downstream effectors of Cdk/Cyclins

General features in cell cycle regulation

The pocket protein (PP) family is comprised by pRB and the pRB-related p107 and p130. They are known to inhibit G1-S transition by controlling E2F-induced genes. The classical model includes a) PP-mediated inhibition of activator E2F or b) formation of repressive E2F/PP complexes, both leading to cell cycle suppression. CDK-induced phosphorylation of PPs promotes its dissociation from E2F, allowing entry into S phase.

Among PPs, pRb has a leading role as implicated by single and compound knock-outs [reviewed in Lin et al., 1996]. Tissue-specific pRb loss contributes to various proliferation and differentiation defects [Cobrinik, 2005]. pRb-lacking mice die at mid-gestation (E13.5-E16.5), while *Mox2*^{Cre}-mediated ubiquitous pRb loss from E5.5 causes perinatal death [Lee et al., 1996; Berman et al., 2009]. In both cases mice display a series of phenotypes (e.g. apoptosis in liver and central nervous system) which are exacerbated by additional deletion of p107 [Lee et al., 1996; Berman et al., 2009]. Compound deficiency of pRb/p107 or pRb/p107/p130 results in earlier embryonic lethality (E11.5 and E9-E11, respectively) and in even more elevated proliferation and apoptosis compared to pRb abrogation [Lee et al., 1996; Berman et al., 2009; Wirt et al., 2010]. In contrast, p107 and p130 single knockouts are viable, healthy and fertile. Yet combined ablation of both factors results in perinatal lethality associated with breathing abnormalities and maternal rejection [Cobrinik et al., 1996; Lee et al., 1996]. One study reported strain-dependent phenotypes upon p130 ablation; p130 loss resulted in multiple defects (abnormal growth, increased apoptosis/proliferation and impaired myogenesis/neurogenesis) culminating to embryonic lethality, but this phenotype was completely suppressed in C57BL/6J background, in which the mice were viable, fertile and without detectable phenotypes [LeCouter et al., 1998].

Given the eminent role of pRb, data regarding this PP will mainly be presented hereafter. pRb is synthesized throughout the cell cycle, but its phase-specific Cdk-driven phosphorylation renders it

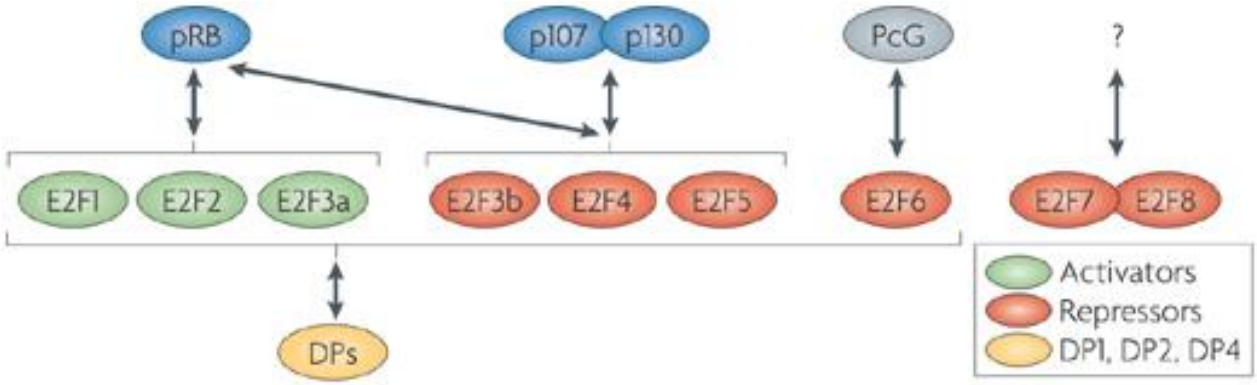

Figure 2.3. Interactions of Pocket Protein and E2F families.

The Pocket Protein (PP) family includes retinoblastoma protein [pRb; acting on several E2F factors (E2F1-5)], and p107 and p130 (limited to E2F3b-5). PP binding to activatory E2Fs (green) inhibits their positive effect on targets. On the other hand, PP or other protein binding to repressive E2Fs (orange) consists complexes that suppress target expression. Some E2F members need to associate with Differentiation-regulated transcription factor-1 Polypeptide (DP; yellow) to exert their action.

Source: van den Heuvel & Dyson, 2008

inactive at S/G2/M [Buchkovich et al., 1989; Zarkowska & Mittnacht, 1997]. Resting cells express the hypo-phosphorylated form of pRb, but it is increasingly phosphorylated during progression through G1 and is maintained hyperphosphorylated until late mitosis, while dephosphorylation precedes total growth arrest during differentiation [Buchkovich et al., 1989; Chen et al., 1989]. pRb is shown to restrict cell cycle progression at a specific, early G1 point [Goodrich et al., 1991]. Loss of pRb function is associated with loss of proliferative control, which is rescued by pRb restoration [Huang 1988; Qin et al., 1992]. Furthermore, reintroduction of pRb in carcinoma cell lines not only suppresses the neoplastic phenotype *in vitro*, but it also halts the tumor forming ability in nude mice [Huang et al., 1988; Bookstein et al., 1990].

The two growth-suppressing pRb domains are also identified as necessary for E2F binding [Qin et al., 1992]. Direct physical association of the two factors is revealed by a series of experiments including overexpression of pRb or mutant pRb as well as transactivation assays with E2F1 mutants incapable of pRb binding [Flemington et al., 1993; Helin et al., 1993]. Although PPs mostly restrain the cell cycle by affecting E2F-regulated transcription, there is also evidence that they directly (p107) or indirectly (pRB) inhibit Cdk activity [Zhu et al., 1995; Alexander and Hinds, 2001].

Eight mammalian E2F transcription factor genes have been identified. *In vivo* abrogation of one or multiple closely related E2F proteins suggested partial redundancy [Gaubatz et al., 2000; Li et al., 2003]. As illustrated in **Fig. 2.3**, the family contains activators (E2F1-E2F3a) and repressors (E2F3b-E2F8), some of which (E2F1-E2F6) form heterodimeric complexes with Differentiation-regulated transcription factor-1 Polypeptide (DP) before binding to DNA in a sequence-specific manner. E2F1-E2F3a are transcriptional activators, preferentially inhibited by pRb. They occupy promoters when the genes are being transcribed and they stimulate cells to pass the G1/S transition [reviewed in van den Heuvel & Dyson, 2008]. On the other hand, E2F3b-E2F8 form repressive complexes with unphophorylated PPs (E2F1-5) or further factors (E2F6-8) at quiescence or at early G1 and they bind to promoters, while the targets are being repressed [reviewed in van den Heuvel & Dyson, 2008]. It is further known that E2F4 and E2F5 are expressed throughout the cell cycle, but -due to their lack of

nuclear localization signal- they remain cytoplasmic until p107 and p130 bind them and recruit them to the nucleus to repress targets [Allen et al., 1997].

E2F proteins regulate genes important for multiple processes during the cell cycle. Since myc, the first E2F cellular target to be described [Hiebert et al., 1989; Thalmeier et al., 1989], a multitude of cell cycle-associated factors has been demonstrated to be regulated by E2F, including cyclins, CDKs, CDKIs, Ki67, PCNA, and E2F themselves [summarized in Bracken et al., 2004]. Furthermore, E2F as well as PPs control cell fate decisions, impact stem cell maintenance and differentiation, and participate in procedures such as DNA damage response/apoptosis/development, often without simultaneous effect on cell cycle dynamics [Cobrinik, 2005; Julian & Blais, 2015].

Implications in skeletal muscle cell cycle regulation

The expression levels and phosphorylation status of pRb changed upon myogenic differentiation, with MYOD participating in both processes. More precisely, MYOD was found to enhance pRb expression during myogenic differentiation [Martelli et al., 1994] and to bind CDK4 to inhibit its ability to phosphorylate pRb [Zhang et al., 1999c]. Although pRb was present in both growing myoblasts and differentiating myocytes, the hypo-phosphorylated form prevailed in the latter populations [Kiess et al., 1995; Wang & Walsh, 1996b; Carnca et al., 2000].

The requirement for pRb in myogenesis is well-established. Unphosphorylated pRb was shown to be bound by MYOD, with the interaction requiring the bHLH domain of MYOD and the C-terminal half of pRb [Gu et al., 1993a]. In differentiating myoblasts pRb was found to cooperate with MYOD to promote MEF2 transcritptional activity [Novitch et al., 1999]. pRb overexpression blocked S-phase entry and induced myogenesis, as evidenced by MYOGENIN expression [Carnca et al., 2000]. Abrogation of pRb was studied *in vitro* in C2C12 muscle cell line, primary myoblasts, and MYOD-mediated myogenically converted fibroblasts. pRb-null mice die at early embryonic stages, before myogenesis is completed, by severe anemia attributed to placental abnormalities. Thus, *in vivo* pRb ablation was studied by (a) generation of mice carrying a hypomorphic pRb minigene expressed in

placenta and nervous system but not in skeletal muscle [Zacksenhaus et al., 1996; Ciavarra et al., 2011], (b) conditional knock-out mice, in which pRb excision was induced by the Mox-Cre (acting from E5.5 onwards) [de Bruin et al., 2003] or the muscle-specific Myf5-Cre and MCK-Cre [Huh et al., 2004]. A series of abnormalities was observed in all *in vitro* and *in vivo* systems. Firstly, no post-mitotic stage was reached and growth factor re-stimulation of $Rb^{-/-}$ differentiated myotubes resulted in S-phase re-entry [Schneider et al., 1994; Novitch et al., 1996; Camarda et al., 2004; Huh et al., 2004; Ciavarra et al., 2011]. pRb deletion in differentiating C2C12 was sufficient to cause cell cycle reentry without growth factor re-stimulation [Pajcini et al., 2010]; however, in primary myoblast cultures, BrdU was incorporated in myotubes only when *pRb* and *Arf* (an alternative product encoded by the *Ink4a* locus) were concomitantly suppressed [Camarda et al., 2004; Pajcini et al., 2010]. The non-maintained cell cycle arrest was evidenced *in vivo* by accumulation of elongated nuclei that actively synthesized DNA within the myotubes of hypomorphic pRb mice [Zacksenhaus et al., 1996]. Reversibility of the terminally differentiated stated is a unique phenotype, which was never noted upon the modulation of any other cell cycle factor. Secondly, pRb removal was associated with enhanced proliferative potential. It resulted in molecular events associated with transition into S phase, including reactivation of E2F, upregulation of Cyclins A and E, re-induction of PCNA, MCM2 and replication protein A, accumulation of Cyclin A, Cyclin B1, CDK2 and CDC2 in the nuclei [Peschiaroli et al., 2002; Camarda et al., 2004]. Thirdly, there was increased susceptibility to apoptosis [Zacksenhaus et al., 1996; Wang et al., 1997; Peschiaroli et al., 2002; Ciavarra et al., 2011]. Finally, the myogenic differentiation was severely affected *in vitro* and *in vivo* [Novitch et al., 1996; Zacksenhaus et al., 1996; de Bruin et al., 2003; Huh et al., 2004; Ciavarra et al., 2011]; even though differentiation could be initiated (e.g. *Myogenin* expression), there was a failure to progress and complete the myogenic program (e.g. reduction in late muscle-specific genes, including MyHC, MCK, MRF4, Troponin T). Mutant mice exhibited shorter myotubes with fewer myofibrils and enlarged nuclei (pRb minigene), hypoplastic and dysplastic myofibers within the intercostal muscles, diaphragm, limbs (Mox2-Cre;$Rb^{f/-}$) or dramatic reduction in muscle mass accompanied by complete absence of mature fibers (Myf5-Cre;$Rb^{f/f}$). Some of these phenotypes were even associated to the respiratory problems and early perinatal death of the mutants. Interestingly, pRb did not seem to be required for the maintenance or regeneration of differentiated skeletal muscle as implied by two independent systems. Firstly, MCK-

Cre;$Rb^{f/f}$ mice are viable, healthy, with normal muscle tissue and without deficits in regenerative capability of damaged muscles [Huh et al., 2004]. Secondly, when pRb deletion was performed in myotubes rather than before differentiation initiation, the post-mitotic status was not challenged by growth factor re-stimulation [Camarda et al., 2004].

Other pocket proteins have also been shown to play some functions in muscle differentiation . p107 is high in proliferating myoblasts but sharply drops upon differentiation [Kiess et al., 1995; Carnca et al., 2000]. In the absence of pRb this downregulation did not occur, but neither did it inverse the defective phenotype, implying lack of compensation [Schneider et al., 1994]. p130 exhibited the opposite pattern of p107 [Kiess et al., 1995; Carnca et al., 2000]. Unlike pRb, the differentiation-induced upregulation of p130 mainly occurred in reserve cells rather than multinucleated myotubes [Carnca et al., 2000]. Indeed, when overexpressed it blocked S-phase entry but repressed myogenesis, through inhibition of MYOD and its transactivation ability [Carnca et al., 2000]. Initial studies of *in vivo* p130 loss did not report any muscle phenotype [Cobrinik et al., 1996], while later reduction in myotomal myocytes was demonstrated [LeCouter et al., 1998]; however, the latter effect was strongly dependent on the genetic background and was completely suppressed in certain strains.

The complexes of pocket proteins with E2F transcription factors were analyzed in proliferation and differentiation conditions *in vitro*. p107 was the most prominent component in the complexes appearing in undifferentiated cells, while it was reported to be replaced by p130 in E2F complexes upon differentiation [Corbeil et al., 1995; Kiess et al., 1995; Shin et al., 1995]. E2F4 appeared to be sequestered in a complex with pRb2/p130 and to accumulate in the nucleus when growth arrest occurred [Puri et al., 1997; Puri et al., 1998]. Undifferentiated C2C12 lacked pRb-E2F complexes [Corbeil et al., 1995], consistent with the presence of hyper-phosphorylated pRb in this proliferating group [Kiess et al., 1995; Wang & Walsh, 1996b; Carnca et al., 2000]. Similarly, pRb/E2F repressor complexes did not form in myotonic dystrophy patients, whose muscle differentiation is affected, but they are abundant in differentiated cells of control subjects [Timchenko et al., 2001]. However, only few such complexes appeared in fully differentiated C2C12 myotubes [Corbeil et al., 1995], in

agreement with the proposed unimportant role of pRb in maintenance of that population [Camarda et al., 2004; Huh et al., 2004]. Permanent silencing of E2F targets during muscle differentiation was driven by Suv39h1-dependent H3K9 tri-methylation and positioning close to heterochromatin nuclear compartment [Guasconi et al., 2010], but this tri-methylation and silencing was not directly specified by pRb binding [Vandromme et al., 2008], as is the case for senescent cells.

E2F levels do not show a uniform behavior upon differentiation. E2F1 and E2F3a were strongly down-regulated, dropping to undetectable levels in mature myotubes, while E2F2, E2F3b and E2F4 remained unchanged [Wang et al., 1995; Asp et al., 2009]. Furthermore, the subcellular distribution of these factors was subject to changes. When myogenic cells were induced to differentiate, E2F1 and E2F5 became exclusively cytoplasmic, E2F3 remained cytoplasmic, E2F2 was primarily nuclear and E2F4 appeared in both compartments [Gill & Hamel, 2000]. In contrast, even weak mitogenic signals could cause nuclear import of E2F1 and E2F4 [Gill & Hamel, 2000]. Ablation of each of these factors established E2F3b as a critical regulator of myogenic differentiation through the transcriptional control of developmental and differentiation genes in myotubes [Asp et al., 2009]. E2F4 ablation caused a milder differentiation impairment [Asp et al., 2009]. In contrast, E2F1 overexpression inhibited cell cycle exit and MYOD- or MYOGENIN-mediated transcription activation [Wang et al., 1995; Wang et al., 1996] or caused S-phase entry in myocytes [Chen & Lee, 1999]. Furthermore, ectopic nuclear E2F1 and E2F4 promoted cell cycle reentry and opposed the differentiation program [Gill & Hamel, 2000]. Whether the same effects occur *in vivo* remains to be confirmed. Upon *in vivo* E2F1 ablation and muscle injury, the regeneration procedure was severely compromised, as shown by rough histological analysis [Yan et al., 2003]. However, the reasons causing this defect as well as the potential role of E2F factors during embryonic and postnatal myogenesis are still uncharacterized.

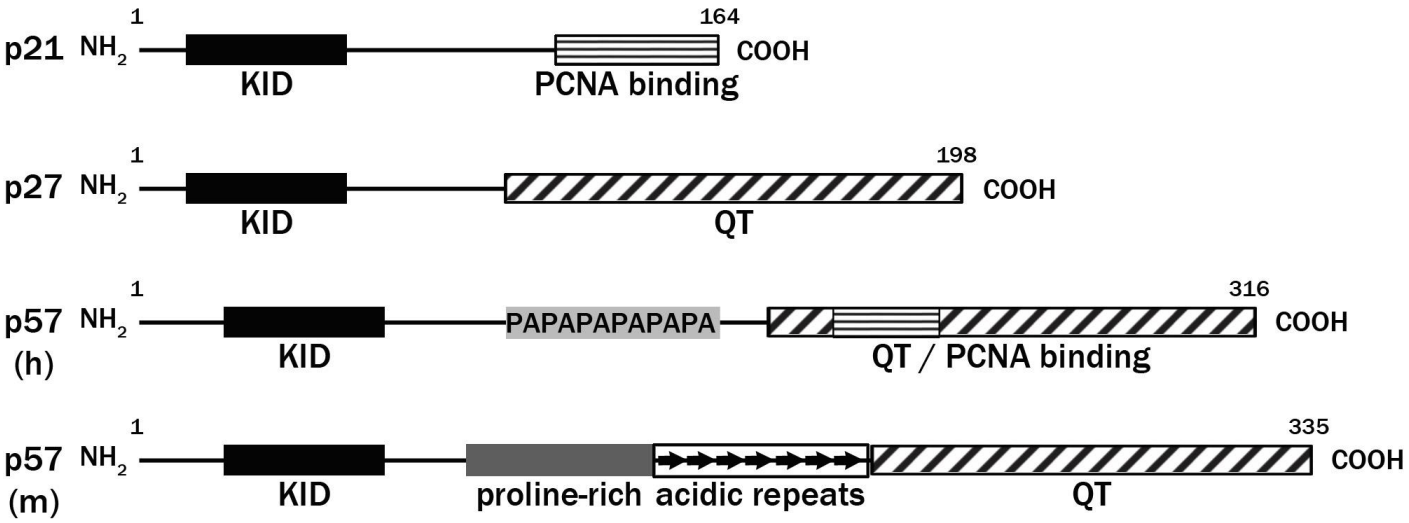

Figure 2.4. Domain structure of Cip/Kip family of CDKIs.

p21, p27 and p57 share conserved regions (indicated as boxes), including an N-terminal CDK inhibitory domain (KID-black box; all members), a C-terminal PCNA binding domain (horizontally stripped box; p21 and p57) and a C-terminal QT box (diagonally stripped box; p27 and p57). Human and mouse p57 further possess a unique central domain, implicated in functions not shared with p21 and p27. This region consists of PAPA repeats (human p57 - h) or a proline-rich and acidic domain (mouse p57 - m). Numbers indicated first and last amino acid of each protein [Scheme based on: Matsuoka et al., 1995; Galea et al., 2008; Pateras et al., 2009].

2.4 CDKIs: major negative regulators of Cdk-Cyclin activity

General features in cell cycle regulation

The control of formation and activity of CDK-Cyclin complexes largely depends on the CDKIs, which belong to two broad categories on the basis of their structural and functional profile. The INK4 family includes p15, p16, p18, and p19, which contain conserved ankyrin repeats [Serrano et al., 1993; Hannon & Beach, 1994; Hirai et al., 1995], a motif participating in protein recognition and interaction [Michaely & Bennett, 1992]. The Cip/Kip family involves p21, p27, and p57, which show partial structural homology (**Fig. 2.4**). They share a 60-residue kinase inhibitory domain in their N-terminal region and a nuclear localization signal (NLS) within their C-terminal region [Polyak et al., 1994; Lee et al., 1995; Matsuoka et al., 1995]. In addition, p21 and p57 contain a C-terminal PCNA-binding domain, allowing interaction with PCNA and prevention of DNA replication [Li et al., 1994; Waga et al., 1994; Watanabe et al., 1998]. Moreover, p27 and p57 include a C-terminal QT box with a consensus CDK phosphorylation site [Polyak et al., 1994; Lee et al., 1995; Matsuoka et al., 1995], involved in their SCF/Skp2-mediated degradation [Lu & Hanter, 2010]. Finally, p57 possesses a unique central region (**Fig. 2.4**), consisting of PAPA repeats (human p57) or proline-rich and acidic-rich domains (mouse p57) [Lee et al., 1995; Matsuoka et al., 1995].

These structural differences underlie the divergent specificity of action between the two CDKI families. This functional variation is two-fold. Firstly, INK4 members are selective inhibitors of CDK4 and CDK6, leaving other CDKs unaffected [Serrano et al., 1993; Hannon & Beach, 1994; Guan et al., 1994; Chan et al., 1995; Hirai et al., 1995]. In contrast, Cip/Kip proteins bind and inhibit all CDK-Cyclin complexes that are formed throughout the cell cycle [Gu et al., 1993b; Harper et al., 1993; Xiong et al., 1993; Polyak et al., 1994a, b; Lee et al., 1995; Matsuoka et al., 1995], in line with the finding that they show intrinsic flexibility and they are largely disordered prior to binding to other proteins [Galea et al., 2008]. In fact, they belong to a group of intrinsically unstructured proteins, meaning that they are devoid of secondary and/or tertiary structure under physiological conditions. Structural analysis of free and CDK/Cyclin-bound p21 and p27 demonstrates a disorder-to-order transition following

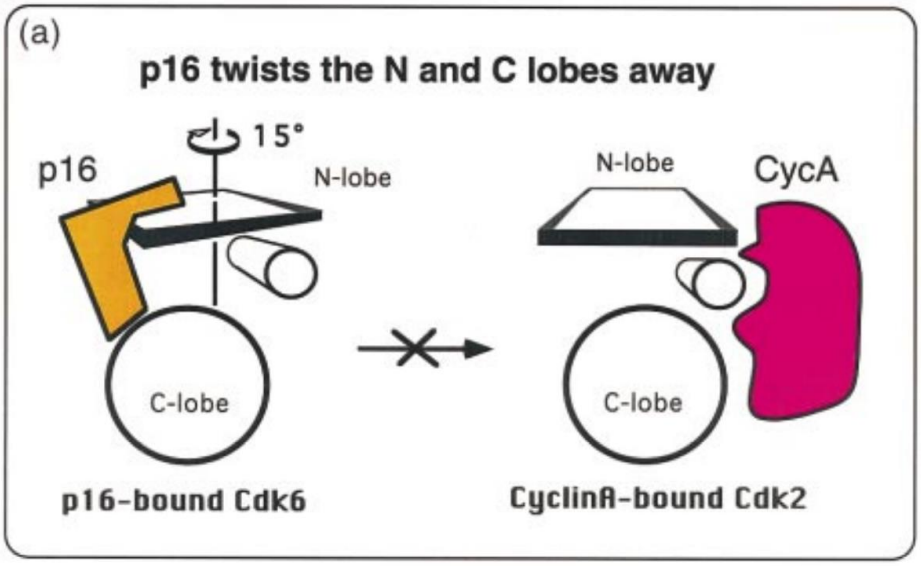

Figure 2.5. Differential CDKI and Cyclin binding to Cdk.

For CDK binding, p16 (left) and Cyclin A (right) interact with both Cdk lobes but depending on different relative orientation. p16-mediated allosteric changes inhibit ATP and cyclin binding, interfering with CDK kinase activity.

Source: Pavletich, 1999

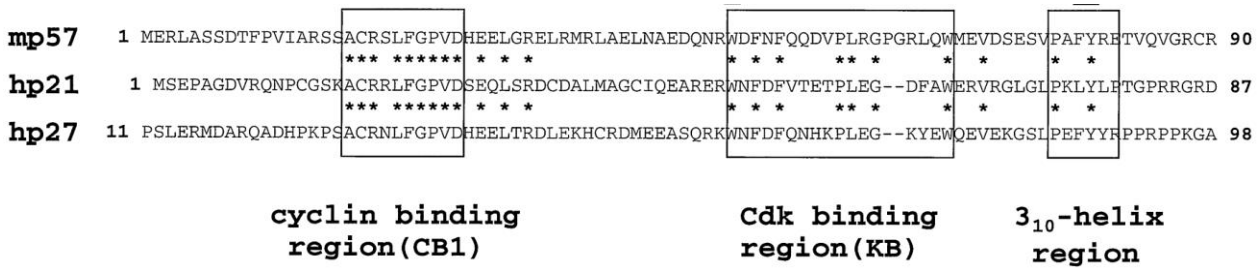

Figure 2.6. Regions of Cip/Kip Cdk-inhibitory domain.

Aligned N-terminal regions of p21, p27 and p57 proteins with highlighted subregions of the CDK-inhibitory domain, includes regions for CDK and cyclin binding and a 3_{10}-helix. (*modified from Hashimoto et al., 1998*)

Source: Hashimoto et al., 1998

binding [Kriwacki et al., 1996; Russo et al., 1996; Lacy et al., 2004] that is achieved in a stepwise manner [Lacy et al., 2004]. Even though most structural data come from p27 studies, acquisition of secondary structure is observed in several subdomains with homology among the three family members. Secondly, INK4 inhibitors can bind to untethered or cyclin-associated CDK subunits, causing a strong inhibition of CDK catalytic activity and inducing G1 arrest [Serrano et al., 1993; Hannon & Beach, 1994; Guan et al., 1994; Chan et al., 1995; Hirai et al., 1995]. They promote conformational changes that interfere with both ATP and cyclin binding, by changing the relative orientation of the two CDK lobes (**Fig. 2.5**) [Brotherton et al., 1998; Russo et al., 1998]. In contrast, p21, p27, and p57 bind CDK-Cyclin heterodimers, with the affinity for CDKs increasing by Cyclin association [Gu et al., 1993b; Harper et al., 1993; Xiong et al., 1993; Polyak et al., 1994a, b; Harper et al., 1995; Matsuoka et al., 1995]. In fact, their N-terminal CDK inhibitory domain involves a cyclin binding site, a CDK binding site and a 3_{10} helix (**Fig. 2.6**); however, the last is indispensable only in p57-dependent inhibition [Hashimoto et al., 1998]. Moreover, structural examination of p27-bound complexes reveals that p27 intrudes the CDK catalytic cleft and interferes with ATP binding [Russo et al., 1996]. Considering their ability to bridge CDKs and cyclins, members of the Cip/Kip group would be expected to promote CDK-cyclin assembly. Indeed, at low concentrations p21 stabilized this interaction, while addition of extra p21 molecules to the complex leads to inhibition [Michieli et al., 1994; Zhang et al., 1994; Harper et al., 1995; LaBaer et al., 1997]. p57 is found to stabilize early G1 complexes only in the absence of p21 and p27 [Cerqueira et al., 2014], while CDK4-Cyclin D1 inhibition premises p57 homodimerization [Reynaud et al., 2000a]. Furthermore, p27 binding to CDK-Cyclin complexes was compatible with kinase activity [Soos et al., 1997]. Thus, Cip/Kip might function as titratable buffers and repress CDKs in a concentration-dependent manner.

CDKI expression is mostly linked to cell cycle withdrawal that accompanies differentiation, but additional functions have been described. An expression pattern that correlates with terminal differentiation of multiple lineages during organogenesis (e.g. skeletal muscle, kidney, brain, gonads, cartilage, cranio-facial structures) has been described for all INK4 and Cip/Kip inhibitors except p15 and p16 [Parker et al., 1995; Zindy et al., 1997; Westbury et al., 2001; Susaki et al., 2009]. Furthermore, all CDKIs have been related to cellular senescence [Erickson et al., 1998; Zhu et al.,

1998; Tsugu et al., 2000; Alexander & Hinds, 2001; Gagrica et al., 2012; Giovannini et al., 2012; García-Fernández et al., 2014], with the major CDKI-involving pathways being the p16/pRb, the $p19^{ARF}$/p53/p21, and the PTEN/p27 pathways [reviewed by Bringold & Serrano, 2000]. Although it is traditionally associated with aging, senescence has also been detected during embryonic development, with p21 and p15 playing a leading role [Muñoz-Espín et al., 2013; Storer et al., 2013]. Moreover, CDKIs, mainly from the Cip/Kip family, have been reported to modulate apoptosis [reviewed in Besson et al., 2008] and transcription [Pippa et al., 2012; Orlando et al., 2015].

Implications in skeletal muscle cell cycle regulation

The expression of CDKIs is, generally, upregulated during myogenesis, as evidenced by developing mouse embryos and myogenic cells. When the equilibrium is shifted to or against one of these factors, the differentiation and proliferation capacities are rapidly affected *in vitro*. More recently, *in vivo* data started to support the unique and redundant roles of CDKIs for muscle development, homeostasis and regeneration. Further studies are expected to elucidate the currently poorly understood role of CDKIs in the entry (early postnatally) or re-entry (post-regeneration) of satellite cells into quiescence.

A limited number of studies have evaluated the impact of the INK4 family on the muscle lineage. Terminally differentiated adult muscles or C2C12-derived myotubes lacked p15 [Franklin & Xiong, 1996]. However, p15 was found elevated in satellite cells from aged animals along with other CDKIs and this could contribute to the defective regeneration of old muscle [Li et al., 2015]. Same as p15, p16 was also absent from proliferating C2C12 cells, myotubes or adult muscle samples [Franklin & Xiong, 1996; Reynaud et al., 1999]. However, ectopic p16 was associated with increased muscle-specific gene expression [Skapek et al., 1995] as well as with protecting differentiating C2C12 from apoptosis [Wang & Walsh, 1996a], the latter only in the presence of pRb [Wang et al., 1997]. p16 transcripts and protein levels increased with aging, with the promoter exhibiting a more open chromatin pattern following injury-induced satellite cell activation [Li et al., 2015]. In addition, p16 derepression ignited a switch of resting geriatric satellite cells from reversible quiescence to

irreversible pre-senescence state, compromising muscle regenerative capacity [Sousa-Victor et al., 2014]. p18 showed a remarkable increase upon C2C12 differentiation, that was regulated transcriptionally (promoter switch to produce a different transcript) and translationally [Franklin & Xiong, 1996; Phelps et al., 1998]. Furthermore, there was a continuing increase of p18-associated CDK4 and CDK6 [Franklin & Xiong, 1996]. In adult muscle tissue, p18 was very abundant and it was associated with all CDK6 and half CDK4 (shared with p27) [Franklin & Xiong, 1996]. *In vivo* regeneration studies showed an early transient increase in p18 levels, although this effect was not further followed [Yan et al., 2003]. p19 was the only CDKI found at high levels in proliferating myoblasts and declining following differentiation [Franklin & Xiong, 1996]. The reciprocal p19 decrease and p18 increase raised the possibility of p19 replacement by p18 as CDKI during differentiation.

Members of the Cip/Kip family have been more extensively explored. Historically, most studies focused on p21, the first family member to be identified. When C2C12 myoblasts were maintained in proliferation conditions, p21 was generally low [Mal et al., 2000]. p21 reached detectable levels close to G1, but at mitosis entry it rapidly decreased [Tintignac et al., 2004]. After switching to differentiation conditions, p21 sharply increased [Halevy et al., 1995; Franklin & Xiong, 1996; Reynaud et al., 1999; Mal et al., 2000]. Consistent with a role in differentiation-associated growth arrest, myotubal p21 (a) immunoprecipitated with CDK2 and CDK4, (b) showed increased interaction with CDK2, CDK4, and CDK6 compared to myoblasts, and (c) exceeded the quantity of active CDK4/Cyclin [Franklin & Xiong, 1996; Wang & Walsh, 1996b; Wang et al., 1997; Figliola & Maione, 2004]. In fact, p21 overexpression in C2C12 was sufficient for cell cycle withdrawal under growth conditions [Guo et al., 1995], while p21-deficient primary myoblasts showed increased proliferation [Hawke et al., 2001]. Forced p21 promoted muscle-specific gene expression, rescued Cyclin D1-mediated *MyoD* repression and exerted protection against apoptosis [Skapek et al., 1995; Wang & Walsh, 1996a]. Conversely, primary myoblast culture of $p21^{-/-}$ animals showed problematic differentiation and increased apoptosis [Hawke et al., 2001]. MYOD transcriptionally activated *p21* [Halevy et al., 1995; Tintignac et al., 2004] and p21 was able to inhibit MYOD phosphorylation, stabilizing it [Reynaud et al., 1999]. Non-phosphorylable MYOD sustained *p21* expression, interfering

with M-phase entry [Tintignac et al., 2004], while in the absence of MYOD, p21 expression was delayed during muscle development [Parker et al., 1995]. MYOD-mediated p21 induction and p21 expression in the developing muscle are p53-independent [Halevy et al., 1995; Parker et al., 1995], although p21 is transcriptionally regulated by p53 [El-Deiry et al., 1993]. Overexpression and silencing approaches established Cyclin D3 as a further factor that enhanced p21 expression [Gurung et al., 2012; de Luca et al., 2014], in agreement with the notion that Cyclin D3 is the only G1 cyclin to promote myogenic differentiation rather than proliferation. A direct MYOGENIN-mediated induction of p21 would be anticipated because (a) MYOGENIN binding sites were detected in the *p21* promoter [Singh & Dilworth, 2013] and (b) on a protein level, p21 expression follows MYOGENIN upon differentiation [Andres & Walsh, 1996]. However, when myoblasts are induced to differentiate, *p21* transcripts appear before *Myogenin*, while MYOGENIN knock-out embryos provided unequivocal evidence that MYOGENIN is not required for p21 induction [Parker et al., 1995].

The *in vivo* profiling of p21 expression in muscle revealed age-related differences. During embryonic development and the establishment of the muscle lineage, *p21* mRNA first appears in the forming myotome of E8.5 somites [Parker et al., 1995]. From E10 it followed the *Myogenin* pattern [Parker et al., 1995]. In the adult, no protein was found in skeletal muscles [Franklin & Xiong, 1996; Mademtzoglou et al., submitted-2], while the mRNA expression is controversial. Very high [Parker et al., 1995; Park & Chung, 2001] or undetectable [Macleod et al., 1995] transcripts were reported in adult skeletal muscles; differences in analyzed muscles, mouse background, age window, or probes could partially explain these differences. *p21* mRNA in skeletal muscle increased up to 5 months, followed by a continuing decline until 23 months [Park & Chung, 2001]. However, the protein seemed to be absent from adult skeletal muscle. Satellite cell-focused analysis revealed p21 rise with aging along with increased chromatin accessibility post-injury [Li et al., 2015]. Notably, p21 loss did not affect the development of muscle or the establishment of the satellite cell compartment [Deng et al., 1995; Hawke et al., 2003; Chakkalakal et al., 2014; Chinzei et al., 2015; Mademtzoglou et al., submitted-2], while AAV-mediated transient *p21* suppression did not impact the genetic status or differentiation capacity of myoblasts [Biferi et al., 2015]. During injury-induced activation of satellite cells and muscle regeneration, p21 seemed to exert its function during the early period of the

regeneration procedure [Yan et al., 2003; Hawke et al., 2003; Chakkalakal et al., 2014; Chinzei et al., 2015; Mademtzoglou et al., submitted-2].

Searching for alternative cell cycle regulators in cells undergoing G1 arrest and myogenic differentiation, the groups of Maione, Lanfranchi and Leibovitch independently identified p57 [Reynaud et al., 1999; Figliola & Maione, 2004; Bean et al., 2005]. p57 increased remarkably as C2C12 cells were stimulated to differentiate [Reynaud et al., 1999] or as embryonic muscle progenitors proceeded to myogenic determination and differentiation [Zalc et al., 2014]. During development it was present in most nuclei of limb and abdominal wall muscles [Zhang et al., 1997; Zalc et al., 2014], but p57 knockout mice did not manifest any severe muscle phenotype [Yan et al., 1997; Zhang et al., 1997], implying compensatory pathways (see below). Postnatally, p57 progressively decreased as mice aged [Park & Chung, 2001] and it was barely detectable in satellite cells [Chakkalakal et al., 2014; Mademtzoglou et al., submitted-2]. However, p57 peaked soon after muscle regeneration was initiated and it was maintained at higher than baseline levels throughout regeneration [Yan et al., 2003; our unpublished observation].

p57 and MYOD have been implicated in a positive feedback loop *in vitro* and *in vivo*, whereby MYOD induced p57 which then enhanced MYOD activity and stabilization. Although three putative MYOD -boxes proximal and downstream from the transcription start site were not functional [Bean et al., 2005], MYOD -responsive regions upstream of the transcription start site were identified by us and others [Bean et al., 2005; Zalc et al., 2014]. *In vitro* studies, based mostly on fibroblasts converted to the myogenic lineage, suggested that MYOD plays a dual function in inducing p57. Firstly, it counteracted a cis-acting repression, by sequentially interacting with CTCF, disrupting the CTCF-mediated chromatin loop and releasing the p57 promoter, and secondly, it assisted up-regulation by the intermediate factors p73, SP1 and EGR1 [Vaccarello et al., 2006; Figliola et al., 2008; Busanello et al., 2012; Battistelli et al., 2014]. Our data provide evidence for E-box-dependent MYOD binding and transactivation of a muscle-specific *p57* regulatory element [Zalc et al., 2014]. *MyoD* knockdown in zebrafish embryos reduced p57, while MYOD over-expression promoted ectopic p57 in somatic and head mesoderm [Osborn et al., 2011]. Notably, MYOD -induced myogenic conversion of fibroblasts

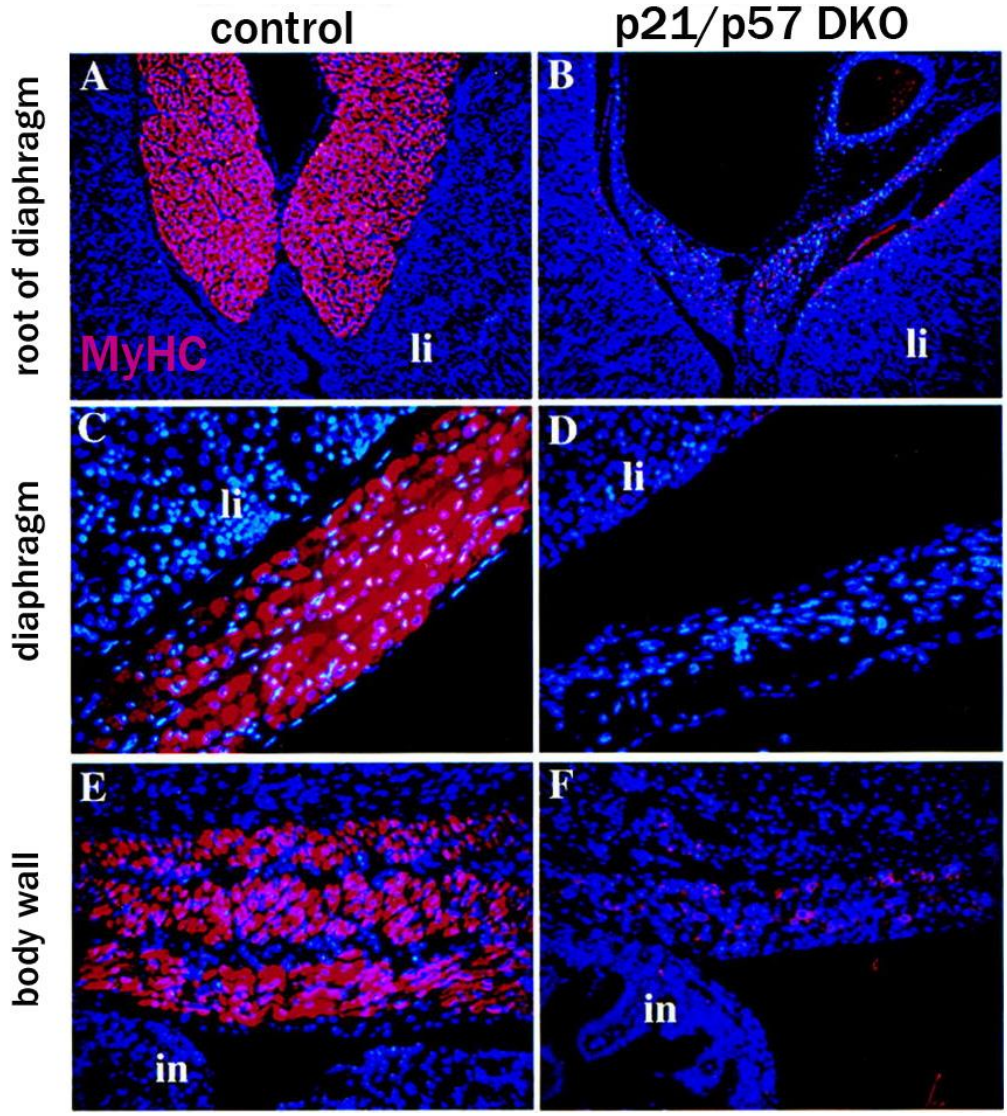

Figure 2.7. p21 and p57 loss severely affects skeletal muscle during embryogenesis.

p21/p57 double knock-out (DKO; right) fetuses had diminishes muscle masses compared to controls (left), as evidenced by myosin heavy chain staining (MyHC). Muscle masses from the root of diaphragm (A, B), diaphragm (C, D), and body wall (E, F) are shown. in: intestine; li: liver.

Adapted from: Zhang et al., 1999b

upregulated p57 only in the absence of p21 [Figliola & Maione, 2004; Zhang et al., 1999c], implying intrinsic differences between that lineage and muscle. On the other way round, p57 was found to promote MyoD accumulation in adaxial cells of zebrafish embryos [Osborn et al., 2011]. Co-immunoprecipitation assays showed that p57 directly binds to MYOD, through the basic region of MYOD and the amino-terminal domain of p57 [Reynaud et al., 2000b]. Remarkably, the same p57 helix domain (**Fig. 2.6**) that was indispensable for CDK/Cyclin inhibition was also important for MYOD binding [Hashimoto et al., 1998; Reynaud et al., 2000b]. *In vitro* dissection of the underlying mechanism revealed that p57 increased MYOD stability by inhibiting its phosphorylation by CDK2/CyclinE complexes [Reynaud et al., 1999], while p57- MYOD binding was competed by CDK4/Cyclin D1 complexes [Reynaud et al., 2000b].

Based on the similarities of the profiles of p21 and p57 during myogenesis as well as the lack of muscle phenotypes in p21 or p57 knock-out embryos, their possible redundancy during development was evaluated by concomitantly ablating both factors [Zhang et al., 1999b]. Simultaneous abrogation of p21 and p57 boosted CDK2 activity toward pRb, increased myoblast proliferation and apoptosis, and induced endoreduplication of residual myotubes. Head, trunk and limb muscles as well as diaphragm of double knock-out embryos were severely diminished (**Fig. 2.7**). Fewer and smaller myotubes were present, indicative of fusion defects. Somitogenesis and primary myogenesis appeared normal, suggesting a secondary myogenesis defect. p21/p57 mutant muscles phenotypically resemble the ones from embryos lacking *Myogenin*. p21/p57 levels in MYOGENIN mutants were comparable to controls, while *Myogenin* expression was not impaired in p21/p57 double knock-outs. Furthermore, MYOGENIN failed to induce p21 or p57 when applied to fibroblasts for myogenic conversion. Thus, the two CDKIs are placed in parallel to MYOGENIN rather than upstream or downstream of this MRF. Whether the redundant functions of p21 and p57 in myogenic cell growth arrest are at play during adult myogenesis remains to be shown and is part of my PhD studies.

Studies on the last member of the Cip/Kip family in muscle development and maintenance revealed p27 participation both in the differentiation program and in maintaining a certain satellite cell

subpopulation. During *in vitro* myogenic differentiation, p27 protein levels increased, even though the mRNA amount remained constant, implying posttranslational regulation [Halevy et al., 1995; Franklin & Xiong, 1996; Reynaud et al., 1999; Chu et al., 2000]. Ectopic p27 inhibited proliferation and promoted differentiation, while p27 repression had the opposite effect [Chakravarthy et al., 2000; Messina et al., 2005]. An in-depth *in vivo* analysis of satellite cell subpopulations revealed that p27 was required to maintain the primitive fate of a subpopulation with label-retaining dormant behavior [Chakkalakal et al., 2014]. The authors also showed that p21 was acting in the non-label-retaining satellite cells to promote lineage commitment [Chakkalakal et al., 2014]. These *in vivo* findings are in agreement with early *in vitro* observations, whereby p21 was enriched in differentiated myotubes and p27 in renewing reserve cells [Cao et al., 2003]. Further supporting this model, p27 was only transiently expressed in the developing muscle masses between E10.5 and E11.5 and all p27+ cells co-expressed MYOD, while only a subset had MYOGENIN [Zabludoff et al., 1998].

2.5 p57 – "KI P"layer in cell physiology and pathology

p57 was identified in 1995 as the last member of the Cip/Kip family of CDKIs [Lee et al., 1995; Matsuoka et al., 1995]. Structural (e.g. N-terminally-located Cdk inhibitory domain, PCNA binding domain, C-terminal QT box) and functional (inhibition of a broad spectrum of CDK-Cyclin complexes) criteria place it in the Cip/Kip family, close to p21 and p27. However, it is distinguished from its siblings in terms of structure (non-shared central domain; **Fig. 2.4**), distribution pattern throughout development and adult life, and multifunction. Furthermore, it is the only CDKI that is subjected to imprinting, with preferential expression of the maternally transmitted allele [Hatada & Mukai, 1995; Matsuoka et al., 1996; Li et al., 2012].

Apart from its well-established role in cell cycle by G1 arrest (see section 2.4), it is emerging as a multifaceted protein participating in several cellular processes [reviewed in Pateras et al., 2009; Rossi & Antonangeli, 2015]. p57 function is critical during embryogenesis, evidenced by the gross developmental defects and perinatal lethality of mice lacking or having excess p57 [Yan et al., 1997; Zhang et al., 1997; Takahashi et al., 2000; Andrews et al., 2007; Susaki et al., 2009]. In contrast to p21

Table 2.1. Defects of p57 knock-out mice

TISSUE	DEFECTS	REFERENCES*
survival	perinatal lethality	1, 2, 4, 5
palate	apoptosis on the surface of palatal shelves (E14.5) cleft palate	1, 2, 4, 5
skeleton	sternum closure defect limb bone shortening and thickening delayed differentiation/ossification	1, 2, 4, 5
gastro-intestinal tract	absent, shortened and/or inflated stomach/intestine increased apoptosis in smooth muscle of intestinal wall omphalocele	1, 2, 4, 5
abdominal wall	thinner body wall muscle dysplasia	2, 4, 5
umbilical region	umbilical hernia	1, 5
kidney	renal medullary dysplasia	2, 4
eye lens	vacuolization cataracts	2, 4
adrenal gland	hyperplasia cytomegaly	2, 4

*1, Yan et al., 1997; 2, Zhang et al., 1997; 3, Takahashi et al., 2000; 4, Susaki et al., 2009; 5, Mademtzoglou et al., submitted-1

and p27, p57 is broadly expressed in developing mice, with levels peaking at key differentiating steps of specific organs [Matsuoka et al., 1995; Westbury et al., 2001]. Loss of p57 affects the proliferation, apoptosis, and differentiation status of a multitude of tissues and organs, including skeletal elements, cranio-facial structures, kidney, adrenal gland, reproductive system, gastro-intestinal tract, and sensory organs (**Table 2.1**) [Yan et al., 1997; Zhang et al., 1997; Takahashi et al., 2000; Susaki et al., 2009]. p27 knock-in rescues many of these abnormalities, supporting the idea that their conserved regions are essential during organogenesis. Nevertheless, many defects, including perinatal lethality, persist, suggesting additional roles for p57 or cell type-dependent differences in p27 and p57 stability [Susaki et al., 2009]. Although in adult life p57 seems less abundant, it has an emerging importance in stem cell homeostasis, promoting acquisition of quiescence [Matsumoto et al., 2011; Zou et al., 2011; Furutachi et al., 2013].

The putative roles in senescence and apoptosis of p57 have been explored. p57 expression increases upon progressive cell passages and it induces senescence when over-expressed in a variety of cell types (e.g. human astrocytoma cells, human hepatocellular carcinoma cells, human prostate epithelial cells, and human uroepithelial cells) [Schwarze et al., 2001; Tsugu et al., 2000; Giovannini et al., 2012; Valcheva et al., 2014]. It seems to have a dual role in programmed cell death, since both pro-apoptotic and anti-apoptotic function have been described. On one hand, p57 is found to sensitize cells to apoptosis [Samuelsson et al., 2002; Gonzalez et al., 2005; Vlachos et al., 2007], by translocating to mitochondria and triggering the intrinsic apoptotic pathway [Vlachos et al., 2007]. Interestingly, the methylation status of its promoter could influence the impact on apoptosis [Kuang et al., 2007b]. On the other hand, increased apoptosis of palate, intestine, and lens upon p57 loss imply anti-apoptotic potential [Yan et al., 1997; Zhang et al., 1997; Zhang et al., 1998]. p57 anti-apoptotic role is mediated by inhibition of the JNK/SAPK pathway, with p57 C-terminal QT box being central to this function [Chang et al., 2003]. However, JNK/SAPK suppression is not observed with p27, despite possessing a QT box as p57 [Chang et al., 2003]. Notably, pro-apoptotic effects are mostly observed in a cancer context, while the anti-apoptotic function is associated with physiological conditions (i.e. development, JNK pathway regulation).

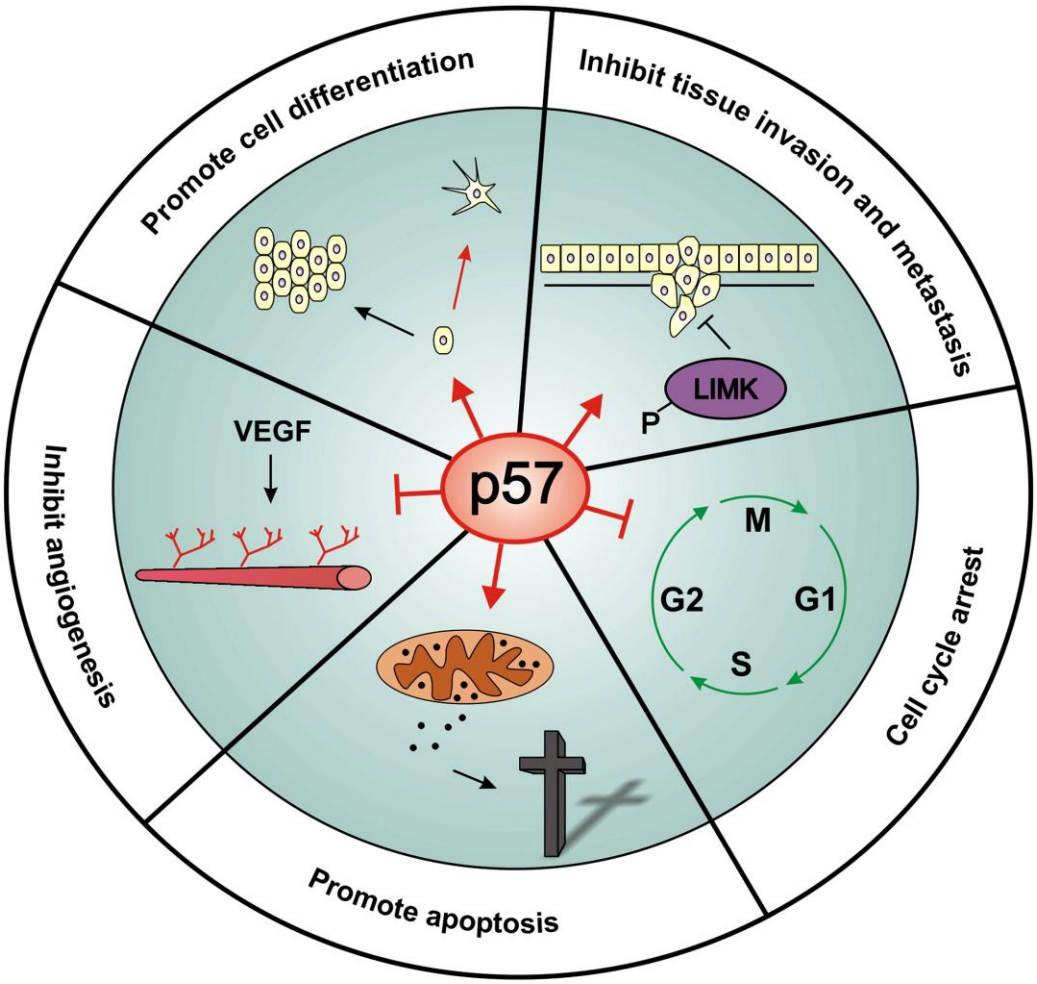

Figure 2.8. p57 implication in cancer hallmarks.

p57 functions that associate its dysregulation with carcinogenesis include growth arrest induction, apoptosis promotion via the mitochondrial pathway, angiogenesis inhibition by negatively regulating Vascular Endothelial Growth Factor (VEGF), cell differentiation advancement, invasion/metastasis repression by interaction with LIM domain Kinase (LIMK) [Kavanagh & Joseph, 2011].

Source: Kavanagh & Joseph, 2011

Cell cycle-independent p57 functions also include participation in actin cytoskeleton dynamics and cell migration. p57 negatively affects cell mobility by interacting with LIM-kinase 1 and regulating cofilin, an actin depolymerization factor [Vlachos & Joseph, 2009; Chow et al., 2011; Guo et al., 2015]. This activity appears independent of the CDK inhibitory ability but connected to the unique central region that p57 does not share with any other CDKI [Yokoo et al., 2003; Vlachos & Joseph, 2009]. The effect on mobility is associated with cytoplasmic p57 presence and is linked to p57 pro-apoptotic effect [Vlachos & Joseph, 2009; Kavanagh et al., 2012]. In contrast, cytosolic p21 and p27 are putative oncogenic factors, involved in tumor invasion and metastasis, and their retention in the cytoplasm is negative prognostic factor in certain tumors [reviewed in Besson et al., 2004; Besson et al., 2008].

p57 implication in carcinogenesis and growth disorders underlines its impact on human pathology [reviewed in Guo et al., 2010; Borriello et al., 2011; Kavanagh & Joseph, 2011; Soejima & Higashimoto, 2013]. Participating in cell cycle arrest, apoptosis, and cell mobility makes p57 a putative tumor suppressor (**Fig. 2.8**) [Kavanagh & Joseph, 2011]. Remarkably, p57 was downregulated in several malignancies and its deficiency or overexpression correlated with proliferative and invasive capacities of cancer cells or tumor formation [Jin et al., 2008; Guo et al., 2011; Xu et al., 2012; Guo et al., 2015]. p57 loss is associated with poor patient prognosis [Xu et al., 2012; Hu et al., 2013; Yang et al., 2015]. Furthermore, p57 is located at a site of frequent loss of heterozygosity in sporadic and familial cancers [Matsuoka et al., 1995]. In fact, p57 loss and gain of function were found to cause two clinically opposite growth disorders, namely BWS (Beckwith-Wiedemann syndrome) and IMAGE (intrauterine growth restriction, metaphyseal dysplasia, adrenal hypoplasia congenita, and genital anomalies), respectively [Soejima & Higashimoto, 2013].

p57 is the most recently discovered CDKI and remains the least studied, partially owing to the lack of genetic tools. Its emerging importance in several cell traits, in stem cell function and in human pathology, prompted us to generate a new mouse model, allowing conditional ablation and reporter-dependent tracking of p57-expressing cells. This mouse is further expected to facilitate *in vivo* studies of p57 impact in postnatal myogenesis, circumventing the early perinatal lethality of germline knock-outs.

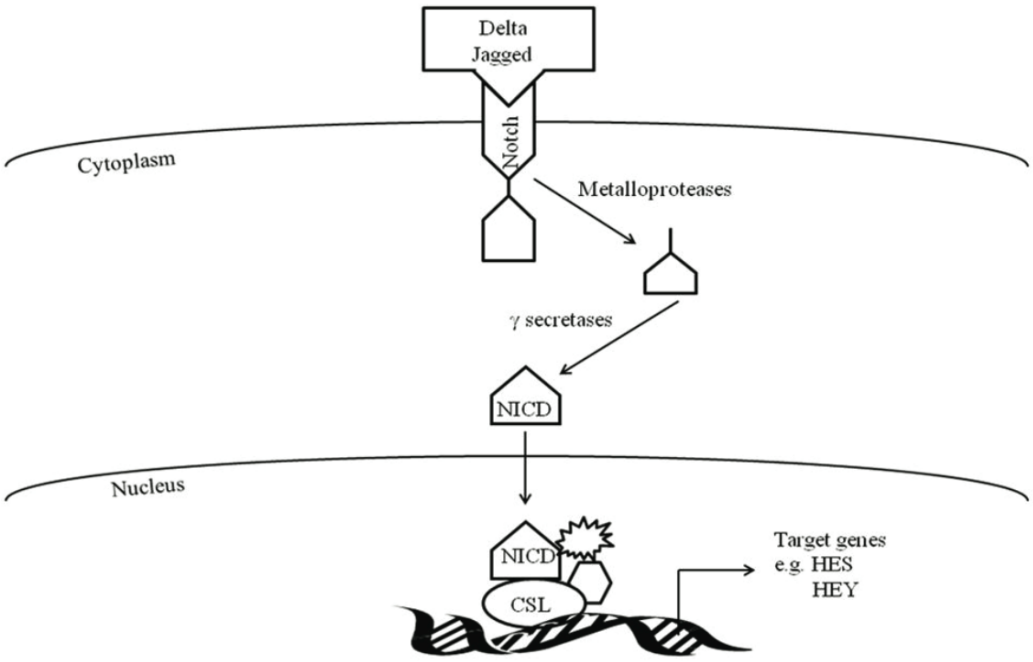

Figure 3.1. Core elements of Notch signaling pathway.

Transmembrane Notch receptors (Notch1-4 in mammals) and ligands (Delta-like, Jagged in mammals) interact to activate the pathway. As a result, a series of metalloprotase/γ-secretase-driven cleavages releases part of the receptor (Notch IntraCellular Domain, NICD) and allows it to translocate to the nucleus and form activatory complexes with CSL DNA-binding proteins leading to transcription of Notch-responsive genes, such as members of the Hes or Hey families.

Source: Tsivitse, 2010

Chapter 3. Notch signaling pathway: pleiotropic role of a master cell fate regulator in myogenesis

The Notch signaling pathway exerts fundamental functions in most cellular decision-making, including stem cell fate and maintenance in adult tissues, while its pertrubation is associated with several genetic disorders and cancer [Guruharsha et al., 2012]. By regulating the balance of proliferation and differentiation, it profoundly affects cell fates in multiple metazoan tissues [Artavanis-Tsakonas & Muskavitch, 2010]. Despite its crucial activity in almost all developing tissues and organs, its effects are highly pleiotropic and the final outcome is context-dependent. The spatial and temporal developmental context and the dosage of Notch activity will dictate the resulting cell fates [Artavanis-Tsakonas & Muskavitch, 2010]. For instance, its activation has an oncogenic effect in T-cells and breast cancer, but tumor suppressive effect in acute myeloblastic leukemia [Guo et al., 2011a; Hernandez Tejada et al., 2014].

Notch signaling depends on the physical interaction of ligand-expressing and receptor-expressing cells, linking the fates of cellular neighbors [Hori et al., 2013]. Thus, Notch was cleverly described as segregating specific lineages from developmentally equivalent cells as well as specifying borders between cellular fields [Hori et al., 2013]. Trans-interactions of apposing cells are activatory, while cis-interactions of receptors and ligands of the same cell are inhibitory [Guruharsha et al., 2012]. The core elements of Notch signaling include the trans-membrane Notch receptors (NOTCH1-4 in mammals), the ligands [Delta-like (DLL1, DLL4) and Jagged (JAG1, JAG2) in mammals], and CSL [CBF1–Su(H)–LAG1] DNA-binding proteins (e.g. CBF1, also known as RBPJ) mediating the transcriptional output of Notch signaling. Receptor-ligand binding ignites proteolytic cleavage and liberation of the Notch IntraCellular Domain (NICD), leading to its nuclear translocation and in the formation of a transcriptional complex including the CSL transcription factors. Upon NICD interaction with CSL, co-repressors are released and co-activators are recruited, leading to transcription of Notch-responsive genes, such as members of the Hes and Herp families (**Fig. 3.1**) [Iso et al., 2003 Guruharsha et al., 2012; Hori et al., 2013].

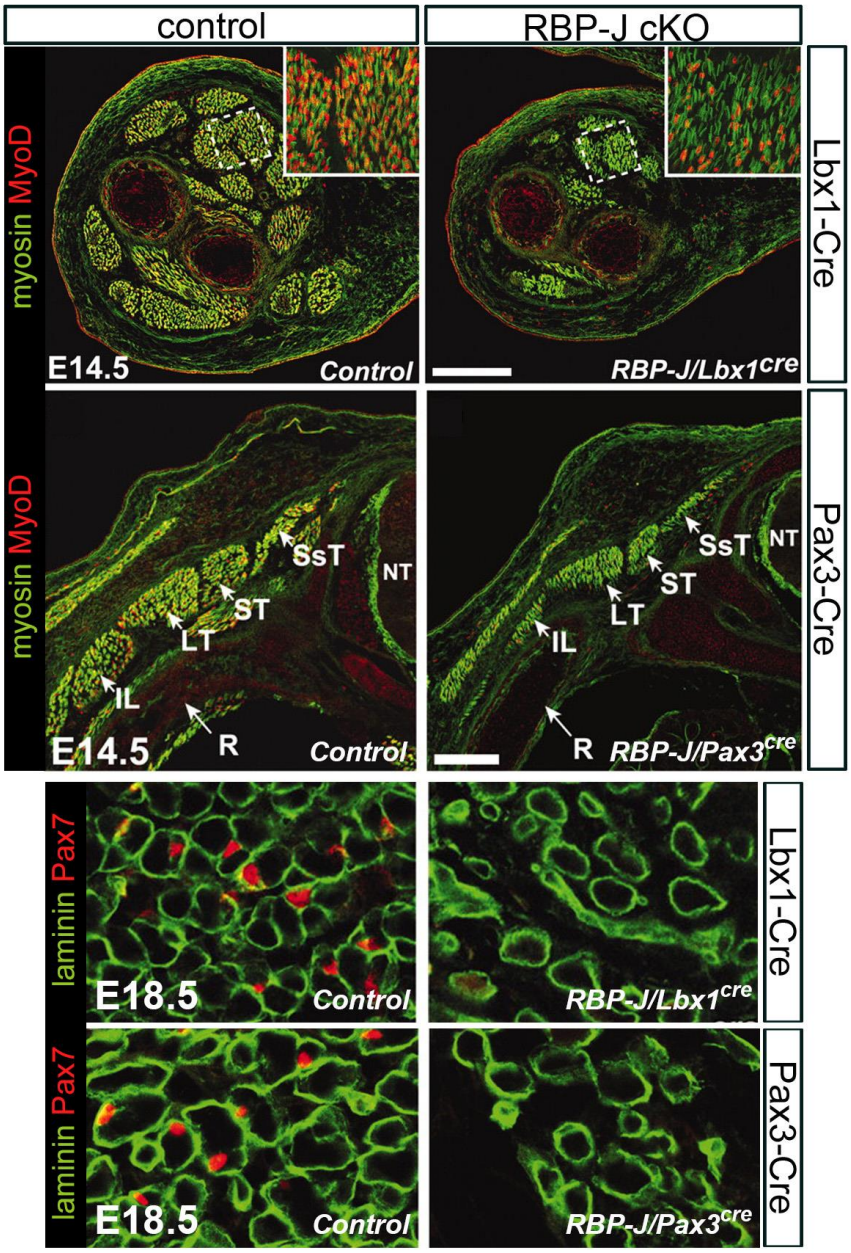

Figure 3.2. Defective myogenesis in Notch mutants.

Rbpj conditional ablation (cKO) in LBX1+ migrating muscle progenitors or PAX3+ non-migrating hypaxial and epaxial muscle progenitors resulted in diminished muscle mass formation (upper panel) and lack of satellite cells (lower panel). NT: neural tube; R: rib; SsT: *semispinalis thoracis*; ST: *spinalis thoracis*; LT: *longissimus thoracis*; IL: *ilicostalis lumborum*.

Adapted from: Vasyutina et al., 2007

Early *ex vivo* studies suggested that Notch controls myogenesis, by suppressing differentiation of cultured myoblasts. Exposure to activated NOTCH1 or DLL1 or activated RBPJ severely affected myotube formation as well as MYOD, MYOGENIN, and MYOSIN levels [Shawber et al., 1996; Nofziger et al., 1999; Kuroda et a., 1999; Buas et al., 2009]. The genetic manipulation of Notch elements *in vivo* in mouse and chick models rendered this notion indisputable, strongly supporting that the fine tuning of this pathway is central in the development, homeostasis and regeneration of skeletal muscle [reviewed in Vasyutina et al., 2007a; Mourikis & Tajbakhsh, 2014].

In both chick and mouse development models it was shown that postimitotic cells and muscle fibers expressed various ligands (e.g. *Dll1*, *Delta1*, *Serrate2*), while mononucleated immature myoblasts expressed receptors (e.g. *Notch1*, *Notch3*) [Delfini et al., 2000; Hirsinger et al., 2001; Schuster-Gossler et al., 2007; Mourikis et al., 2012a]. Some dorsal dermomyotomal chick myogenic progenitors transiently activated Notch by *Dll1*-expressing passing neural crest cells, pointing to a different ligand source [Rios et al., 2011]. Furthermore, in that case differentiation was promoted by Notch [Rios et al., 2011], in contrast with all the other reports of developmental or adult myogenesis. Given that Notch is context-dependent, these results imply that the time window and progenitor subpopulation might affect the final outcome.

The Notch signaling pathway plays key roles during developmental myogenesis. In the chicken embryo, DLL1-triggered Notch reduced the *MyoD*-expressing region, ultimately leading to smaller and disorganized muscles [Delfini et al., 2000; Hirsinger et al., 2001]. Similar conclusions were drawn from loss-of-function (i.e. interfering with DLL1 or RBPJ) and gain-of-function (NICD overexpression) approaches in mouse embryos. *Dll1* hypomorphs [Schuster-Gossler et al., 2007] and conditional RBPJ mutants [Vasyutina et al., 2007b] were used to overcome early embryonic lethality of DLL1 and RBPJ knock-out mice. In both cases, muscle masses were diminished and the remaining muscles were deprived of satellite cells (**Fig. 3.2**). This was due to early depletion of the progenitor pool by precocious differentiation [Schuster-Gossler et al., 2007; Vasyutina et al., 2007b]. On the contrary, constitutive Notch was sufficient to maintain a self-renewing progenitor population, to promote transition into a state with quiescent signature, and to inhibit lineage progression and myogenic

differentiation [Mourikis et al., 2012a]. Interestingly, the PAX3+MYF5+ fraction was unaltered both in the gain-of-function chick experiments and in the loss-of-function mouse approach [Delfini et al., 2000; Vasyutina et al., 2007b].

Apart from the well-characterized Notch-mediated regulation of muscle progenitor maintenance by differentiation inhibition, Notch exerts additional functions in the emerging muscle masses. It has been implicated in the correct homing of emerging satellite cells; Notch elimination affected satellite cell adhesion to myofibers and basal lamina assembly around them, a phenotype rescued by concomitant ablation of *MyoD* [Bröhl et al., 2012]. Furthermore, Notch promoted the endothelial/vascular versus skeletal muscle fate in PAX3+ multipotent progenitors of the somites prior to migration to the limb [Mayeuf-Louchart et al., 2014], consistent with the role of this pathway in cell fate decisions of early developmental precursors [Buas & Kadesch, 2010]. However, Notch is dispensable for dermis versus muscle fate of precursors of the central dermomyotome [Mourikis et al., 2012a], underlining again the context-dependent outcome of Notch activity.

Similarly to the developmental scenario, adult satellite cell populations showed a prevalence of DLL1 ligand in committed PAX7+MYF5+ progenitors and NOTCH3 receptor in the upstream PAX7+MYF5- cells [Kuang et al., 2007a]. In fact, under those conditions, Notch inhibition resulted in loss of the PAX7+MYF5- population [Kuang et al., 2007a]. Furthermore, it is reported that precursor divisions lead to daughter cells with asymmetric distribution of the Notch inhibitor NUMB [Conboy & Rando, 2002]. The asymmetrical NUMB localization linked Notch cessation with myogenic progression and sustained Notch with the maintenance of undifferentiated state [Conboy & Rando, 2002]. Furthermore, NUMB was shown to prevent p53-dependent senescence in injured skeletal muscle, while *Numb* elimination impaired muscle regeneration [Le Roux et al., 2015].

In the adult, Notch is essential for the satellite cell compartment. Conditional ablation of RBPJ leads to progressive depletion of the satellite cell pool of resting or regenerating muscles and severely impairs regeneration of injured muscles. Spontaneous activation, precocious differentiation, and failure to self-renew accounted for the satellite cell loss [Bjornson et al., 2012; Mourikis et al., 2012b].

Interestingly, it was shown there is a tendency to differentiate bypassing division [Bjornson et al., 2012; Mourikis et al., 2012b]. In a complementary approach, satellite cell-specific NICD overexpression promoted self-renewal and reduced proliferation and differentiation *ex vivo*. Moreover, satellite cell-specific NICD overexpression impaired regeneration and increased PAX7+ mononuclear cells post-injury [Wen et al., 2012]. Notch was found active in quiescent satellite cells, while it declined upon *in vitro* activation or right after muscle injury [Bjornson et al., 2012; Mourikis et al., 2012b]. Notch was restored around 20-30 days post-injury [Mourikis et al., 2012b], a time point when differentiated myofibers have been formed and the satellite cell compartment is being self-renewed. However, one report associates Notch activation with transition from quiescent to activated satellite cells *ex vivo* [Conboy & Rando, 2002]. *Notch3* receptor was found upregulated in quiescent and self-renewing versus activated satellite cells [Fukada et al., 2007; Kitamoto & Hanaoka, 2010; Mourikis et al., 2012b], suggesting that it might mediate Notch effects in satellite cells. However, knock-out mice had an expanded satellite cell compartment of resting or regenerating muscles, showed increased myoblast proliferation *ex vivo* and exhibited hypertrophic muscles following regeneration [Kitamoto & Hanaoka, 2010]. During aging, Notch activity declines, impairing muscle regeneration. This was rescued by forced Notch activation in old mice; on the contrary, Notch inhibition in young muscle diminished the regenerative capacity [Conboy et al., 2003]. Conditional deletion of the different Notch receptor, as well as combined and conditional ablation should help clarify the temporal and functional requirement of this pathway during myogenesis.

In conclusion, it is argued that Notch signaling allows maintenance and expansion of muscle progenitors by preventing precocious differentiation. It is a pathway with crucial role on myogenesis and satellite cell homeostasis, while cross-talks with other pathways is not excluded. Specifically, Notch and TGF-b/pSmad3 were shown to antagonize each other by favoring satellite cell proliferation and growth arrest, respectively [Carlson et al., 2008]. The declining competence of old satellite cells was partially attributed to Notch and TGF-b/pSmad3 imbalance, occuring with aging [Carlson et al., 2008]. The balance between Notch and Wnt signaling is also decisive and a transition to Wnt was associated with differentiation steps during postnatal myogenesis [Brack et al., 2008].

RESULTS

Aims and Hypotheses

Balanced cell proliferation and differentiation are crucial for embryonic tissue formation (during development) as well as for stem cell-mediated tissue regeneration (in adulthood). Muscle differentiation relies on tissue-specific gene expression and irreversible cell cycle exit, while their dysregulation might cause apoptosis or cancer. Although several key regulators of myogenic differentiation have been identified, less information is available on the molecular circuits controlling cell cycle arrest. Thus, the present project was planned to elucidate the molecular and cellular mechanisms of growth arrest in muscle progenitor and stem cells, with specific focus upon factors and signals involved in the cell cycle exit, such as the Cyclin-Dependent Kinase Inhibitors (CDKIs) p21 and p57.

The specific aims and hypotheses outlined in the following three papers are:

Aim 1: Identification of networks controlling growth arrest at embryonic and fetal stages of muscle development.

Hypothesis: The CDKIs p21 and p57 are suppressed in the proliferating muscle progenitors to allow sufficient propagation, while they are induced in the differentiating myoblasts to ensure cell cycle exit and subsequently differentiation.

Aim 2: Development of a genetic tool allowing postnatal functional studies of p57, given that p57 mutants show perinatal lethality.

Aim 3: Evaluation of cell cycle control following activation of adult quiescent satellite cells.

Hypothesis: When quiescent satellite cells are activated upon specific homeostatic or regenerative needs, the CDKIs p21 and p57 are implicated i) in the return into quiescence (to replenish the quiescent pool) and/or ii) in irreversible cell cycle exit (to provide differentiated progeny for muscle repair).

Preface

During organogenesis, normal tissue development relies on the equilibrium between cell proliferation and cell differentiation, while overt proliferation or precocious differentiation can jeopardize correct embryogenesis. In the developing skeletal muscle, we addressed how the balance of these two processes is coordinated by growth arrest signals (i.e. the CDKIs p21 and p57), the Notch signaling pathway, and Myogenic Regulatory Factors (MRFs). Using mouse molecular genetics we showed that although cell cycle exit and myogenic differentiation occur synchronously, they can be uncoupled. Furthermore, we demonstrated that progenitors and differentiating myoblasts of the nascent muscle masses interact via the Notch signaling pathway, which is essential to repress p57 and maintain the cycling status of muscle progenitors. Finally, we identified a muscle-specific regulatory element of p57, directly regulated by an interplay between Notch downstream targets and MRFs to influence the decision between progenitor propagation and myogenic differentiation.

© 2014. Published by The Company of Biologists Ltd | Development (2014) 141, 2780-2790 doi:10.1242/dev.110155

RESEARCH ARTICLE

STEM CELLS AND REGENERATION

Antagonistic regulation of p57kip2 by Hes/Hey downstream of Notch signaling and muscle regulatory factors regulates skeletal muscle growth arrest

Antoine Zalc[1,2,3,*], Shinichiro Hayashi[1,2,3,*], Frédéric Auradé[1,2,3,‡], Dominique Bröhl[4,‡], Ted Chang[1,2,3,‡], Despoina Mademtzoglou[1,2,3], Philippos Mourikis[1,2,3], Zizhen Yao[5,§], Yi Cao[5,§], Carmen Birchmeier[4] and Frédéric Relaix[1,2,3,¶]

ABSTRACT

A central question in development is to define how the equilibrium between cell proliferation and differentiation is temporally and spatially regulated during tissue formation. Here, we address how interactions between cyclin-dependent kinase inhibitors essential for myogenic growth arrest ($p21^{cip1}$ and $p57^{kip2}$), the Notch pathway and myogenic regulatory factors (MRFs) orchestrate the proliferation, specification and differentiation of muscle progenitor cells. We first show that cell cycle exit and myogenic differentiation can be uncoupled. In addition, we establish that skeletal muscle progenitor cells require Notch signaling to maintain their cycling status. Using several mouse models combined with *ex vivo* studies, we demonstrate that Notch signaling is required to repress $p21^{cip1}$ and $p57^{kip2}$ expression in muscle progenitor cells. Finally, we identify a muscle-specific regulatory element of $p57^{kip2}$ directly activated by MRFs in myoblasts but repressed by the Notch targets Hes1/Hey1 in progenitor cells. We propose a molecular mechanism whereby information provided by Hes/Hey downstream of Notch as well as MRF activities are integrated at the level of the $p57^{kip2}$ enhancer to regulate the decision between progenitor cell maintenance and muscle differentiation.

KEY WORDS: Myogenesis, Cell cycle regulation, $p57^{kip2}$, Cdkn1, Notch signaling, MRF

INTRODUCTION

The formation of functional organs of an appropriate size is highly controlled during development. Organ transplantation and regeneration studies have revealed that organ size relies on both intrinsic and extrinsic mechanisms (reviewed by Cook and Tyers, 2007). Systemic factors, such as growth hormones and nutritional status, have been known for many years to regulate organ size, while more recently the role of the Hippo and insulin/TOR pathways has emerged (Tumaneng et al., 2012). Of note, increasing evidence links these pathways with stem cell self-renewal and differentiation (Cherrett et al., 2012). Nevertheless, how cell fate decisions and differentiation programs are coordinated with cell cycle progression and arrest remains poorly understood.

[1]UPMC Paris 06, U 974, Paris, F-75013, France. [2]INSERM, Avenir Team, Pitié-Salpêtrière, Paris, F-75013, France. [3]Institut de Myologie, Paris, F-75013, France. [4]Max-Delbrück-Center for Molecular Medicine, Berlin 13125, Germany. [5]Human Biology Division, Fred Hutchinson Cancer Research Center, Seattle, WA 98109, USA.
*These authors contributed equally to this work
‡These authors contributed equally to this work
§These authors contributed equally to this work

¶Author for correspondence (frelaix@gmail.com)

Received 14 March 2014; Accepted 13 May 2014

Skeletal muscle provides a suitable model for such studies because the molecular pathways regulating differentiation and growth arrest have been identified. Muscle formation relies on a proliferating population of progenitor cells that express and require the Paired homeobox transcription factors Pax3 and Pax7 (Buckingham and Relaix, 2007). These resident progenitors are maintained in the developing muscles, where they provide a source of cells for muscle growth during development and eventually generate the adult stem cells population, termed satellite cells (Gros et al., 2005; Kassar-Duchossoy et al., 2005; Lepper and Fan, 2010; Relaix et al., 2006). Initially, muscle progenitor cells are located in the somite where they give rise to the trunk musculature of the myotome (Ben-Yair and Kalcheim, 2005; Kassar-Duchossoy et al., 2005; Relaix et al., 2005) or migrate out of the somitic dermomyotome to form limb skeletal muscles (Birchmeier and Brohmann, 2000; Schienda et al., 2006). During limb embryonic myogenesis, $Pax3/7^{+}$ progenitor cells undergo consecutive steps of differentiation via sequential expression of bHLH myogenic regulatory factors [MRFs; Myf5, Myod1 and myogenin (Myog)], and first form committed progenitor cells that express Pax3/7 and Myf5, which correspond to a transit amplifying population (Picard and Marcelle, 2013), followed by the generation of myoblasts that express Myf5 and Myod1, culminating in the appearance of differentiating myoblasts marked by Myog (Fig. 1) (Murphy and Kardon, 2011). The $Myog^{+}$ cells then fuse to form multinucleated muscle fibers. In the absence of Myod1, despite upregulated Myf5 expression, myogenic differentiation is delayed during early limb development, resulting in a transient absence of differentiating ($Myog^{+}$) myoblasts and fibers prior to E14.5 (Kablar et al., 1998). When both Myf5 and Myod1 are impaired, $Pax3/7^{+}$ cells do not enter the myogenic program and skeletal muscle formation is abolished at all sites of myogenesis (Rudnicki et al., 1993).

Building a tissue requires the coordination of cell cycle exit with differentiation. Despite the identification of key molecular regulators of myogenic specification and differentiation (Buckingham and Relaix, 2007), how cell cycle exit is synchronized with skeletal muscle differentiation is not well understood. Cell cycle exit in muscle cells is orchestrated by cyclin-dependent kinase inhibitors (CDKIs) belonging to the CIP/Kip family: $p21^{cip1}$ (Cdkn1a, $p21^{waf1}$), $p27^{kip1}$ (Cdkn1b) and $p57^{kip2}$ (Cdkn1c), abbreviated here as p21, p27 and p57, respectively. These CDKIs can bind and inhibit all combinations of cyclin-CDK complexes (reviewed by Besson et al., 2008). Most notably, in the absence of both *p21* and *p57*, skeletal muscle development is severely affected and fiber formation is impaired, with myogenic cells undergoing apoptosis. This points to an essential function of p21 and p57 in cell cycle arrest during myogenesis (Zhang et al., 1999). *In vitro*, Myod1 has been suggested to be a direct regulator of *p21*, thus controlling cell cycle exit during

RESEARCH ARTICLE Development (2014) 141, 2780-2790 doi:10.1242/dev.110155

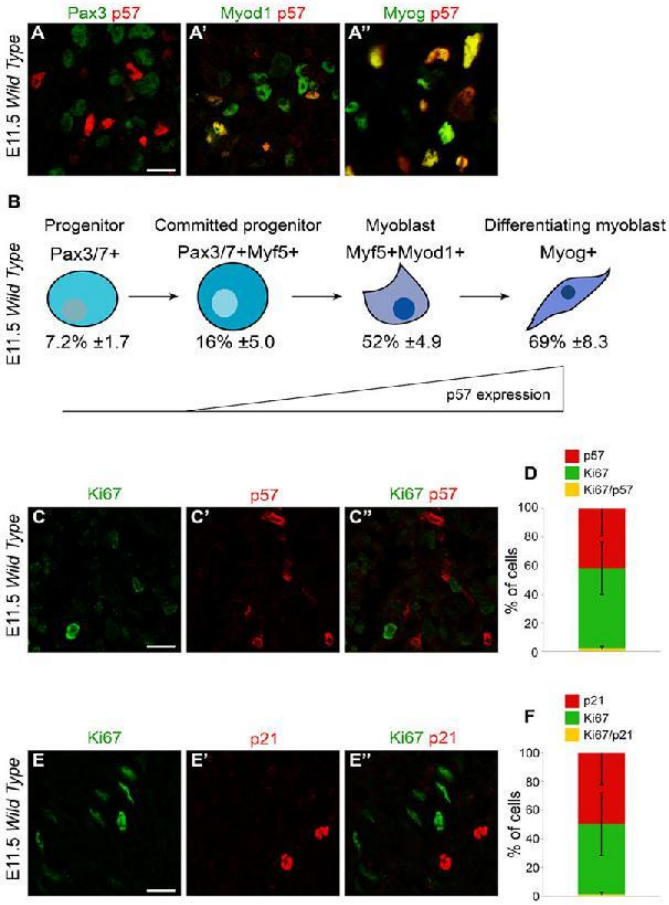

Fig. 1. Cell cycle exit occurs at the determination stage. (A-A″) Co-immunostaining for Pax3 (A), Myod1 (A′) and myogenin (Myog, A″) in green, and p57 (A′,A″) in red in E11.5 embryonic limb muscles. (B) Percentage of p57-expressing cells during forelimb myogenesis is given for each population. Progenitors and committed progenitors are mostly proliferating, whereas myoblasts and differentiating myoblasts are exiting the cell cycle. (C-C″) Co-immunostaining for Ki67 (C,C″, green) and p57 (C′,C″, red) in E11.5 embryonic limb muscles. (D) Quantification of C-C″. (E-E″) Co-immunostaining for Ki67 (E,E″, green) and p21 (E′,E″, red) in E11.5 embryonic limb muscles. (F) Quantification of E-E″. Ki67 is not expressed in cells expressing p21 or p57. For all experiments n=3 embryos; error bars indicate s.d. Scale bars: 10 μm.

adult muscle differentiation (Halevy et al., 1995). It has also been shown, both in mammalian cells (Reynaud et al., 2000) and in zebrafish (Osborn et al., 2010), that p57 interacts and stabilizes Myod1 to promote muscle differentiation, demonstrating a role for CDKIs beyond that in growth arrest. Analysis of *p21*; *p57* double-mutant mouse embryos suggested that cell cycle exit occurs in parallel to, but independently of, Myog-dependent terminal differentiation, while the lack of Mef2c expression in these mice suggested that late differentiation is defective (Zhang et al., 1999).

Previous studies have implicated the Notch signaling pathway as a key regulator of proliferation and differentiation of muscle progenitor cells (Buas and Kadesch, 2010; Mourikis and Tajbakhsh, 2014). This pathway is highly conserved during evolution and plays key roles during development, including the regulation of cell fate decisions, differentiation and homeostasis of progenitor cells in a wide variety of tissues (reviewed by Artavanis-Tsakonas and Muskavitch, 2010). Notch signaling requires direct interaction between a cell expressing at least one of the ligands [delta-like 1 (Dll1) and 4 and jagged 1 and 2 in mammals] with a cell expressing one of the receptors (notch 1-4 in mammals). This interaction leads to a proteolytic cleavage of the receptor that releases the Notch intracellular domain, which translocates into the nucleus and interacts with the Rbpj transcription factor to induce downstream effectors, such as the Hes/Hey family of bHLH transcriptional repressors (reviewed by Borggrefe and Liefke, 2012).

The role of Notch signaling in skeletal muscle development has been assessed in two mouse models: in a hypomorphic *Dll1* mutant (Schuster-Gossler et al., 2007) or in mice in which *Rbpj* expression was conditionally abrogated specifically in the myogenic lineage (Vasyutina et al., 2007). These *in vivo* models, along with studies performed in chick embryos, have demonstrated that Dll1-triggered canonical Notch signaling is required for the maintenance of muscle progenitor cells (Delfini et al., 2000; Hirsinger et al., 2001; Mourikis et al., 2012a; Schuster-Gossler et al., 2007; Vasyutina et al., 2007). Dll1 absence leads to early onset differentiation (Schuster-Gossler et al., 2007; Vasyutina et al., 2007), resulting in rapid exhaustion of the muscle progenitor cell pool and near complete absence of skeletal muscles at the fetal stage (Schuster-Gossler et al., 2007; Vasyutina et al., 2007). This is in part mediated by the repression of Myod1 target genes through direct binding of Hey1 to their promoters (Bröhl et al., 2012; Buas et al., 2010). Interestingly, the role of Notch can be context dependent, since in the young somite of the chick embryo, $Dll1^{+}$ neural crest cells provide a transient stimulation of Notch activity that is important for the initiation of early myogenesis (Rios et al., 2011).

Here, we evaluated the *in vivo* expression of p57 and its link with muscle cell differentiation. Although cell cycle exit is normally synchronous with cell differentiation, we show that these events can be uncoupled. In fact, we found that during embryonic myogenesis p57-mediated cell cycle arrest occurs earlier than

RESEARCH ARTICLE Development (2014) 141, 2780-2790 doi:10.1242/dev.110155

previously recognized, namely in determined muscle cells. Moreover, we demonstrate that in the absence of terminal differentiation muscle progenitor cells aberrantly induce p57 expression, leading to growth arrest. We further show that this growth arrest is associated with a loss of Notch signaling. This is confirmed by conditional genetic ablation of *Rbpj* that leads to upregulation of p21 and p57 in muscle progenitors associated with increased growth arrest. We finally identify a muscle-specific *p57* regulatory element and show that this enhancer is the target of both positive regulation by MRFs in myoblasts and negative regulation by Hes/Hey repressors downstream of Notch in progenitor cells. Our data therefore demonstrate that the regulation of cell cycle exit integrates both negative (via Hes/Hey downstream of Notch signaling) and positive (by MRFs) regulation at the same *p57* regulatory element during muscle differentiation, and that Notch signaling acts upstream, but independently, of both differentiation and cell growth arrest.

RESULTS

Cell cycle exit and differentiation can be uncoupled during skeletal muscle development

We first assessed whether myogenic progenitors leave the cell cycle at specific steps of the MRF-mediated differentiation program, by comparing p57 expression with that of MRFs in E11.5 mouse limbs by immunofluorescence (Fig. 1A-A″). As expected, p57 expression was very low in Pax3/7^{+} progenitors (7.2 ±1.7%). By contrast, a proportion of the Pax3/7^{+}/Myf5^{+} committed progenitor cells did express p57 (16±5%), and this proportion increased significantly in Myf5^{+}/Myod1^{+} (52±4.9%) and Myog^{+} (69±8.3%) populations (Fig. 1B). Similar results were obtained with p21 (data not shown). We verified that p21 and p57 are accurate markers of cell cycle exit of myogenic progenitors as their expression almost never co-localized with that of Ki67, a marker of cycling cells (Fig. 1C-F). Our data are consistent with the results of previous *in vivo* studies analyzing the proliferation of myogenic cells during development (Gros et al., 2005; Lagha et al., 2008; Relaix et al., 2005).

In order to test the existence of a link coupling cell cycle arrest with muscle differentiation, we first investigated whether muscle differentiation is affected when cell cycle exit is impaired. We examined whether the differentiation program proceeds normally in *p21: p57* double-null embryos, in which growth arrest is abolished (Zhang et al., 1999). In limb muscles of control mice, 4.7±1.4% of Myog-positive cells underwent proliferation as assessed by phospho-histone H3 (P-H3) (Fig. 2A-A″,C). By contrast, $p21^{-/-}$; $p57^{+/-m}$ double-mutant embryos displayed a marked increase in Myog^{+}/P-H3^{+} cells (25.2±3.2%; Fig. 2B-C). Taken together, we conclude that p21- and p57-mediated cell cycle exit and MRF-mediated myogenic differentiation can occur independently of each other.

We then examined whether the uncoupling of proliferation and differentiation that we observed in the $p21^{-/-}$; $p57^{+/-m}$ double-mutant embryos holds true in a complementary condition. Delayed myogenesis in *Myod1* mutant embryos provides a useful model for such analysis (Kablar et al., 1997). As expected, Myog and p57 co-localized in the forelimbs of control $Myod1^{+/-}$ mice at E12.5 (Fig. 2D-D″). By contrast, in the E12.5 $Myod1^{-/-}$ forelimbs, even

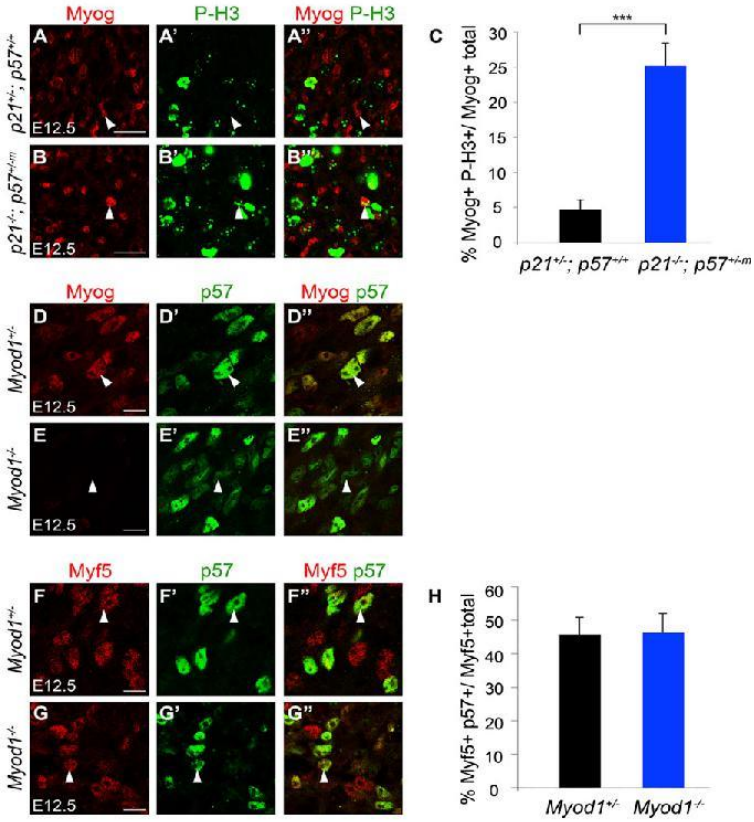

Fig. 2. Cell cycle exit can be uncoupled from cell differentiation. (A-B″) Co-immunostaining for Myog (A,A″,B,B″, red) and P-H3 (A′,A″,B′,B″, green) in $p21^{+/-}$; $p57^{+/+}$ (A-A″) or $p21^{-/-}$; $p57^{+/-m}$ (B-B″) forelimbs at E12.5. Myog^{+} cells (A) do not normally express P-H3 (A′,A″), whereas in $p21^{-/-}$; $p57^{+/-m}$ embryos Myog^{+} cells aberrantly proliferate (B-B″). (C) Quantification of A″,B″. (D-G″) Co-immunostaining for Myog (D,D″,E,E″, red), p57 (D′,D″,E′,E″,F′,F″,G′,G″, green) and Myf5 (F,F″, G,G″, red) in $Myod1^{+/-}$ (D-D″,F-F″) or $Myod1^{-/-}$ (E-E″, G-G″) embryonic limb muscles at E12.5. Myog^{+} cells express p57 in $Myod1^{+/-}$ embryos (D-D″, arrowheads). p57 is expressed in $Myod1^{-/-}$ embryos (E′) despite the absence of Myog (E). Myf5 is co-expressed with p57 in both $Myod1^{+/-}$ (F-F″, arrowheads) and $Myod1^{-/-}$ (G-G″) embryos. (H) Quantification of F″,G″. For all experiments n=3 embryos for each genotype; error bars indicate s.d.; ***P<0.001. Scale bars: 10 μm.

RESEARCH ARTICLE Development (2014) 141, 2780-2790 doi:10.1242/dev.110155

though Myog is not expressed, p57 is detected in the forming muscle masses (Fig. 2E-E″), where it labels nearly half of the Myf5^{+} cells in both *Myod1*$^{+/-}$ (Fig. 2F-F″,H) and *Myod1*$^{-/-}$ (Fig. 2G-H) forelimb (45.6±5.1% versus 46.3±5.5%). These data suggest that cell cycle exit coincides with Myf5 expression in myoblasts and is unaffected when Myod1/Myog-mediated differentiation is impaired.

In the absence of differentiated myoblasts, muscle progenitors precociously express p57 and exit the cell cycle

It has been previously shown that differentiating myoblasts are required for the survival of muscle progenitor cells throughout development (Kassar-Duchossoy et al., 2005). We examined in more detail the impact of differentiating myoblasts on the proliferation state of Pax3^{+} cells by analyzing different allelic combinations of *Myod1: Myf5* double-null embryos to allow key steps during myogenic commitment to be separated. In the absence of Myod1^{+} myoblasts but in the presence of Myf5^{+} myoblasts in *Myod1*$^{-/-}$; *Myf5*$^{+/nlacZ}$ mice (Rudnicki et al., 1993; Tajbakhsh et al., 1997) (supplementary material Fig. S1), the proliferation rate of Pax3^{+} cells was comparable to that observed in control mice at E12.5 (23.6±3.9% versus 25.6±4.6%; Fig. 3A-B″,D). By contrast, in the double-mutant *Myod1*$^{-/-}$; *Myf5*$^{nlacZ/nlacZ}$ forelimbs, which lack both committed progenitors and myoblasts (supplementary material Fig. S1), we observed a significant decrease in the proliferation of Pax3^{+} cells (12.8±3.6% versus 25.6±4.6%; Fig. 3C-D). These data suggest that committed progenitors are required to maintain the proliferation of muscle progenitor cells, whereas differentiated myoblasts are dispensable.

Consistent with the proliferation profile, the cell cycle inhibitor p57 was aberrantly expressed in Pax3^{+}/MRF^{-} progenitor cells of *Myod1*$^{-/-}$; *Myf5*$^{nlacZ/nlacZ}$ embryos compared with control embryos (28.4±2.7% versus 2.3±2.7%; Fig. 3E-G). These data suggested that myoblasts are required to maintain cycling muscle progenitor cells by preventing p57 expression and cell cycle arrest.

Impaired Notch signaling in *Myod1; Myf5* mutant embryos

Our analysis of *Myod1; Myf5* mutant embryos reinforced the notion that functional interactions are taking place between myoblasts and muscle progenitor cells. A strong candidate pathway to mediate these interactions is Notch signaling. It has been previously shown that differentiating myogenic cells express Dll1 and possibly signal to the upstream population that expresses higher levels of Notch receptors (mainly notch 1, 2 and 3) (Delfini et al., 2000; Hirsinger et al., 2001; Mourikis et al., 2012b; Schuster-Gossler et al., 2007). This feedback mechanism of receptor/ligand regulation is supported by many independent *in vivo* studies. However, it has not been formally shown that such cell-cell interactions occur during development, a prerequisite for Notch signaling.

To demonstrate an interaction between myoblasts and muscle progenitor cells, we analyzed the cellular organization on sections of embryonic forelimb muscle masses by co-immunostaining, and found that the majority of Pax7^{+} progenitor cells are in close proximity to Myod1^{+} myoblasts (Fig. 4A-B). Our analysis therefore suggests that direct cell-cell signaling via Notch can occur between progenitors and myoblasts.

To further assess the significance of differentiating muscle cells in Notch activation, we measured endogenous pathway activity in E12.5 *Myod1*; *Myf5* double-mutant embryos that lack differentiated muscle due to the MRF deficiency. It was previously shown that Pax7 expression is lost when Notch signaling is abrogated in myogenic progenitor cells (Vasyutina et al., 2007). Consistent with impaired Notch activity, Pax7 protein was undetectable by immunofluorescence at E12.5 in *Myod1*$^{-/-}$; *Myf5*$^{nlacZ/nlacZ}$ forelimbs (Fig. 4C-E), whereas it was expressed in *Myod1*$^{-/-}$; *Myf5*$^{+/nlacZ}$ embryos (Fig. 4C-E). In addition, we found downregulation of the Notch target genes *Hes1* and *Hey1* in the forelimbs of *Myod1*$^{-/-}$; *Myf5*$^{nlacZ/nlacZ}$ compared with *Myod1*$^{+/-}$; *Myf5*$^{+/nlacZ}$ or with *Myod1*$^{-/-}$; *Myf5*$^{+/nlacZ}$ at E12.5 (Fig. 4F,G).

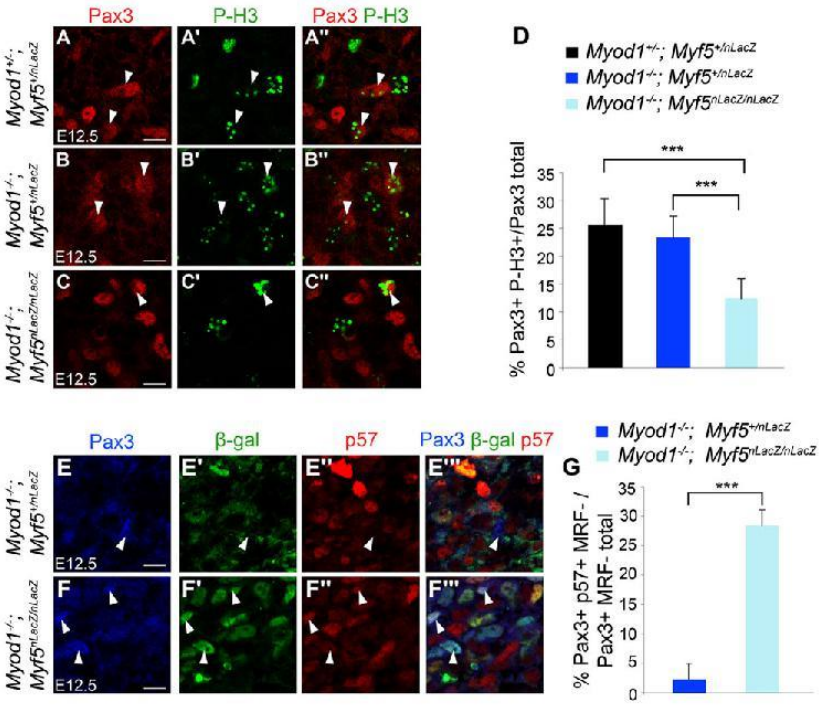

Fig. 3. Myoblasts control muscle progenitor cell proliferation by preventing cell cycle exit. (A-C″) Co-immunostaining for Pax3 (red) and P-H3 (green) in *Myod1*$^{+/-}$; *Myf5*$^{+/nlacZ}$ (A-A″), *Myod1*$^{-/-}$; *Myf5*$^{+/nlacZ}$ (B-B″) and *Myod1*$^{-/-}$; *Myf5*$^{nlacZ/nlacZ}$ (C-C″) embryos at E12.5. Arrowheads indicate Pax3^{+} cells undergoing mitosis. (D) Quantification of A″,B″,C″. (E-F‴) Co-immunostaining for Pax3 (blue), β-gal (green) and p57 (red) in *Myod1*$^{-/-}$; *Myf5*$^{+/nlacZ}$ (E-E‴) or *Myod1*$^{-/-}$; *Myf5*$^{nlacZ/nlacZ}$ (F-F‴) embryos at E12.5. Myf5^{-}/β-gal^{-} cells do not express p57 (arrowheads in E-E‴) in *Myod1*$^{-/-}$; *Myf5*$^{+/nlacZ}$ embryos, whereas in *Myod1*$^{-/-}$; *Myf5*$^{nlacZ/nlacZ}$ embryos Pax3^{+} cells are p57^{+} (arrowheads in F-F‴). (G) Quantification of E‴,F‴. For all experiments n=3 embryos for each genotype; error bars indicate s.d.; ***P<0.001. Scale bars: 10 μm.

RESEARCH ARTICLE Development (2014) 141, 2780-2790 doi:10.1242/dev.110155

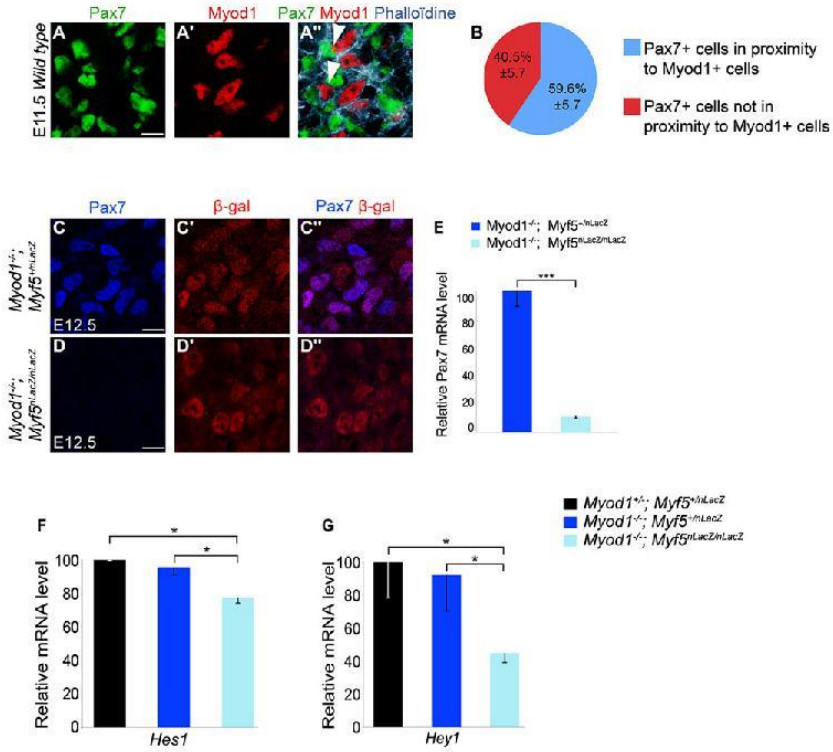

Fig. 4. Close proximity of Pax7$^+$ and Myod1$^+$ cells, with decreased Pax7 and Hes1/Hey1 expression in muscle progenitor cells of the *Myod1; Myf5* double mutant. (A-A″) Co-immunostaining for Pax7 (green) and Myod1 (red), with phalloidin (cyan) to label actin to visualize cell membranes, in wild-type limb muscles at E11.5. (B) Percentage of Pax7$^+$ cells in proximity to Myod1$^+$ cells in limb muscle masses. (C-D″) Co-immunostaining for Pax7 (blue) and β-gal (red) in *Myod1*$^{-/-}$; *Myf5*$^{+/nlacZ}$ (C-C″) and *Myod1*$^{-/-}$; *Myf5*$^{nlacZ/nlacZ}$ (D-D″) embryos at E12.5. (E-G) qRT-PCR for *Pax7* (E), *Hes1* (F) and *Hey1* (G) on E12.5 forelimbs of the genotypes indicated. For all experiments n=3 embryos for each genotype; error bars indicate s.e.m.; *P<0.05, **P<0.01, ***P<0.001. Scale bars: 10 μm.

Notch signaling prevents activation of p57 in muscle progenitor cells

Based on our results (Fig. 4) and previous reports (Georgia et al., 2006), we hypothesized that myoblasts control progenitor cell proliferation by activating the Notch/Hes1/Hey1 pathway, which would then repress p57 expression.

First, to establish whether Notch signaling participates directly in the coordinated control of cell cycle exit and differentiation, we used an *ex vivo* whole limb culture system (Zúñiga et al., 1999). We cultured E11.5 mouse forelimbs for 28 h, with or without 20 μM γ-secretase inhibitor DAPT, an inhibitor of Notch signaling. As expected, we saw decreased expression of the Notch target genes *Hes1* and *Hey1* after DAPT treatment (Fig. 5A). In addition, inhibition of Notch signaling led to reduced numbers of Pax7$^+$ cells (56.8±5.6% in control versus 27.7±7.0% in DAPT-treated limb explants; Fig. 5B′,C′,D), whereas the Myod1$^+$ cell population was increased (62.7±9.0% compared with 32.6±5.3% in control DMSO-treated explants; Fig. 5B″,C″,D), confirming previous reports (Schuster-Gossler et al., 2007; Vasyutina et al., 2007) and the robustness of our *ex vivo* model. Accordingly, we found decreased levels of *Pax7* mRNA and increased levels of *Myod1* mRNA in DAPT-treated samples (Fig. 5A). We next examined whether pharmacological inhibition of Notch signaling induces cell cycle arrest in cultured muscle progenitor cells. We found a 5-fold increase in p57 expression in Pax3$^+$/MRF$^-$ cells in DAPT-treated limb explants compared with controls (Fig. 5E-G).

To confirm these results *in vivo*, we genetically abrogated Notch signaling in progenitor cells by conditionally deleting *Rbpj*. RbpJ is a DNA-binding transcription factor and the major effector of all four Notch receptors (Fortini and Artavanis-Tsakonas, 1994; Jarriault et al., 1995; Kopan and Ilagan, 2009; Schweisguth and Posakony, 1992). We performed a conditional deletion of *Rbpj* in the Pax3 lineage by crossing *Rbpj*$^{flox/flox}$ mice (Han et al., 2002) with a *Pax3*$^{Cre/+}$ allele (Engleka et al., 2005). Ablation of *Rbpj* led to increased myogenic differentiation as previously reported (Vasyutina et al., 2007), with a severe loss of progenitor cells leading to tiny limb muscles at a fetal stage. Strikingly, both p57 and p21 were upregulated in the Pax3$^+$/Myf5$^-$ muscle progenitor cells in the forelimbs of *Rbpj*$^{flox/flox}$; *Pax3*$^{Cre/+}$ mice at E11.5, whereas Pax3 and these CDKIs were rarely co-expressed in such cells in control mice (Fig. 6A-D, see also Fig. 1). To demonstrate that expression of p21 and p57 is associated with growth arrest in these mutants, we analyzed the co-expression of Ki67 with either p57 or p21 in Pax3$^+$ muscle progenitors (Fig. 6E,F) in the forelimbs of *Rbpj*$^{flox/flox}$; *Pax3*$^{Cre/+}$ mice at E11.5. We found a small but significant increase of Pax3$^+$ cells co-expressing p21 or p57 with Ki67 in the mutant embryos; nevertheless, the large majority of the Pax3$^+$/p57$^+$ cells did not express Ki67, as predicted.

Altogether, these results demonstrate that in embryonic muscle progenitor cells Notch signaling antagonizes cell cycle exit by repressing p57 expression.

A *p57* muscle-specific enhancer is directly regulated by Notch signaling and MRFs

To gain insight into the molecular mechanisms of *p57* regulation, we used data generated by a Myod1 ChIP sequencing experiment (Cao et al., 2010) to identify Myod1 binding sites in the vicinity of the *p57* locus. A previous study had predicted that *p57* muscle-specific regulatory elements are located between +35 and +225 kb from the *p57* transcription start site (John et al., 2001). In keeping with this, a high density of Myod1 binding sites was found in a conserved region located +59 kb from *p57*. We isolated an evolutionarily conserved

RESEARCH ARTICLE Development (2014) 141, 2780-2790 doi:10.1242/dev.110155

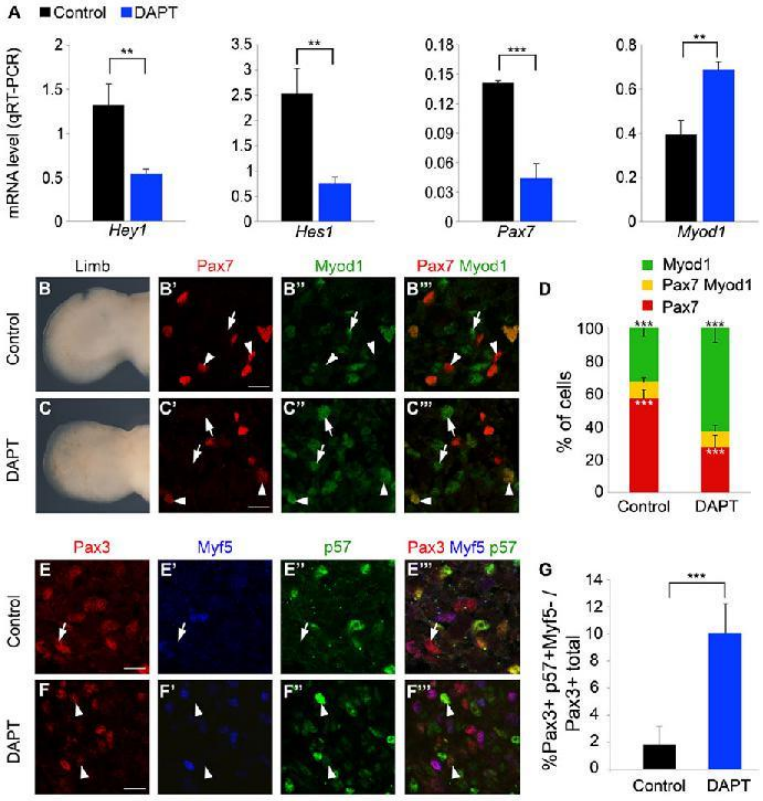

Fig. 5. The Notch pathway prevents activation of p57 in progenitor cells. (A) qRT-PCR for *Hey1*, *Hes1*, *Pax7* and *Myod1* mRNA in control (DMSO-treated) and DAPT-treated *ex vivo* whole limb culture. (B,C) An E11.5 forelimb kept in culture for 28 h treated with DMSO (B) or 20 μM DAPT (C). (B′-B‴,C′-C‴) Co-immunostaining for Pax7 (red) and Myod1 (green) in DMSO-treated (B′-B‴) or 20 μM DAPT-treated (C′-C‴) explants from E11.5 limb muscles. Arrowheads indicate Pax7^{+}/Myod1^{-} cells in B′-B‴ and Pax7^{+}/Myod1^{+} cells in C′-C‴; arrows indicate Myod1^{+}/Pax7^{-} cells. (D) Quantification of B‴,C‴. (E-F‴) Co-immunostaining for Pax3 (red), Myf5 (blue) and p57 (green) in DMSO-treated (E-E‴) or 20 μM DAPT-treated (F-F‴) explants from E11.5 limb muscles. Arrow in E-E‴ indicates a Pax3^{+}/Myf5^{-}/p57^{-} cell. Arrowheads in F-F‴ indicate Pax3^{+}/Myf5^{-}/p57^{+} cells. (G) Quantification of E‴,F‴. For all experiments n=3; error bars indicate s.d.; **P<0.01, ***P<0.001. Scale bars: 10 μm.

686 bp fragment that contains 15 E-boxes, which are binding sites for MRFs, Hey1 and Hes1 (supplementary material Fig. S2).

We first validated this *p57* muscle regulatory element (*p57MRE*) as a functional enhancer *in vivo* by generating transgenic embryos carrying a *p57MRE-tk-nlacZ* construct. Following analysis of *lacZ* expression at E12, we detected robust reporter expression in all myogenic domains (Fig. 7A,A′), with an expression profile that matched that of Myod1. Interestingly, this element is skeletal muscle specific, since no other sites of p57 expression, such as parenchymal organs and intestine (Westbury et al., 2001), were observed. In order to characterize the myogenic cell type that expresses the p57 reporter, we performed immunohistochemical analyses on limb buds from these transgenic embryos. β-Gal^{+} cells co-expressed p57 (Fig. 7B-B″) and Myod1 (Fig. 7C-C″) but not Pax7 (Fig. 7D-D″), defining the cellular specificity of the *p57MRE*.

We next hypothesized that this regulatory element integrates negative regulation by Hes/Hey proteins and positive regulation via direct activation by the MRFs. We performed ChIP experiments on E12.5 wild-type forelimbs and found that both Myod1 and Hes1 were bound *in vivo* to the *p57MRE* fragment (Fig. 8A). To ensure that our assay was specific, and given the lack of known positive controls for Hes1 in the myogenic lineage, we performed ChIP experiments in HEK293 cells transfected with either Hes1 or Myod1 and either wild-type *p57MRE* or containing mutations in the MRF and Hes binding sites (*p57MREΔE-Boxes*). Robust binding was observed for Hes1 (Fig. 8B) and Myod1 (Fig. 8C) on the *p57MRE* and this binding was abrogated on *p57MREΔE-Boxes* (Fig. 8B,C).

Finally, to further establish this interplay between positive and negative regulation, we tested the transcriptional activity of Myod1, Hes1 and Hey1 on *p57MRE-tk-nlacZ* in transient transfection experiments in C2C12 muscle cells. Myod1 enhanced the activation of the *p57MRE* (Fig. 8D), but was not able to activate the *p57MREΔE-Boxes* element. Furthermore, Myod1 transcriptional activation was abolished when exposed to increasing concentrations of Hes1 or Hey1 (Fig. 8D), suggesting that both are able to repress the Myod1-dependent activation of *p57MRE*.

We propose a model in which the integration of Notch and MRF activities at the level of a muscle-specific enhancer of the key cell cycle arrest gene *p57* provides a means to control the equilibrium between progenitor pool amplification and the establishment of definitive functions of skeletal muscle (Fig. 8E).

DISCUSSION

The generation of organs of a defined size requires a balance between proliferation and differentiation. This balance is ensured by regulated cell growth, which prevents prolonged proliferation or premature differentiation, both of which are deleterious for normal development.

During skeletal muscle development and postnatal regeneration, Notch signaling activity is crucial for sustaining stem/progenitor cell self-renewal and its downregulation is required to allow myogenic differentiation. Cell cycle exit was previously thought to be controlled by the differentiation program (Halevy et al., 1995). In this report we show that growth arrest is also negatively regulated by Notch signaling and demonstrate that these two events, despite appearing synchronous, can be uncoupled. In *Myod1*$^{-/-}$ forelimbs, myogenesis is paused between E11.5 and E14.5 (Kablar et al., 1998). Although Myf5 is unable to drive myogenesis and activate *Myog* at these stages,

RESEARCH ARTICLE

Development (2014) 141, 2780-2790 doi:10.1242/dev.110155

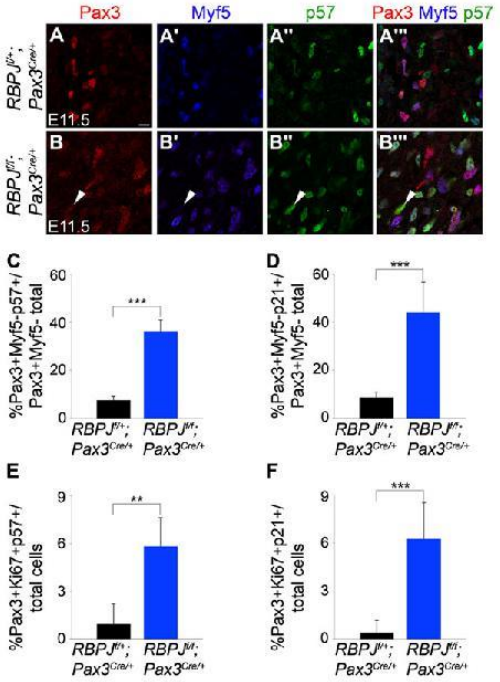

Fig. 6. Conditional ablation of *Rbpj* leads to upregulation of p57 and p21 and to cell cycle arrest in muscle progenitor cells. (A-B‴) Co-immunostaining for Pax3 (red), Myf5 (blue) or p57 (green) in $Rbpj^{flox/+}$; $Pax3^{Cre/+}$ (A-A‴) or $Rbpj^{flox/flox}$; $Pax3^{Cre/+}$ (B-B‴) forelimbs at E11.5. Arrowhead indicates a Pax3$^+$/Myf5$^-$/p57$^+$ cell. Scale bars: 10 μm. (C) Quantification of A″,B‴. (D) Quantification of co-immunostaining for Pax3, Myf5 or p21 in $Rbpj^{flox/+}$; $Pax3^{Cre/+}$ or $Rbpj^{flox/flox}$; $Pax3^{Cre/+}$ forelimbs at E11.5. (E) Quantification of co-immunostaining for Pax3, Ki67 or p57 in $Rbpj^{flox/+}$; $Pax3^{Cre/+}$ or $Rbpj^{flox/flox}$; $Pax3^{Cre/+}$ forelimbs at E11.5. (F) Quantification of co-immunostaining for Pax3, Ki67 or p21 in $Rbpj^{flox/+}$; $Pax3^{Cre/+}$ or $Rbpj^{flox/flox}$; $Pax3^{Cre/+}$ forelimbs at E11.5. For all experiments n=3 embryos for each genotype; error bars indicate s.d.; **P<0.01, ***P<0.001.

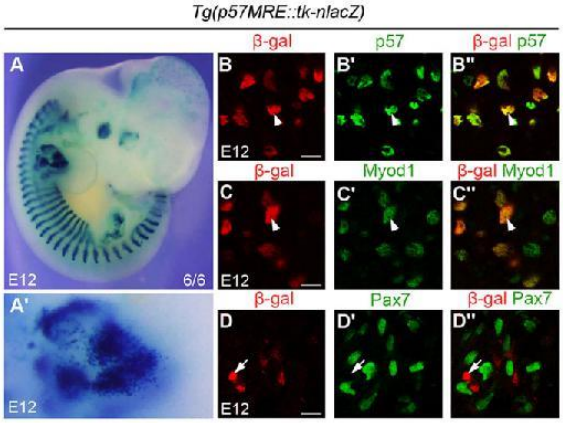

Fig. 7. Expression of a *p57* muscle regulatory enhancer (MRE) in transgenic mice. (A,A′) X-Gal staining on a transgenic *p57MRE-tk-nlacZ* embryo. A′ is a higher magnification of the forelimb region from A. (B-D″) Co-immunostaining for β-gal (B,C,D,B″,C″,D″, red), p57 (B′,B″, green), Myod1 (C′, C″, green) and Pax7 (D′,D″, green). Arrowheads indicate β-gal$^+$ /p57$^+$ (B-B″) and β-gal$^+$/Myod1$^+$ cells (C-C″); arrows indicate β-gal$^+$/Pax7$^-$ cells. Scale bars: 10 μm.

we found that Myf5$^+$/Pax3/7$^-$ cells expressed p57 at E12.5 and this did not prevent them from resuming differentiation at E14.5 (presumably when Mrf4 is activated). Given our finding that Myod1 directly binds and activates *p57* via the *p57MRE* sequence, we believe that Myf5 operates in the same way, thereby providing a functional uncoupling between MRF myogenic activity and growth arrest. Moreover, our study and those of others indicate that cell cycle exit occurs at the transition from committed progenitors to determined myoblasts (Fig. 1A). Consistently, we found that committed progenitor cells express Pax3/7 and Myf5, but neither p21 nor p57. This finding is consistent with the robust repressive activity exerted by Hes/Hey on MRF-mediated transactivation (Fig. 8D). The cycling status of committed progenitor cells is therefore of interest. A recent study showed that whereas the undifferentiated resident progenitor cells that express Pax7 represent a slow-cycling pool, the Pax3/7$^+$/Myf5$^+$ committed progenitors correspond to a fast-cycling population (Picard and Marcelle, 2013). Our study did not address the subtle cell cycle regulation of these progenitor cell populations and future studies will be required to determine whether these changes in cell proliferation are linked to Myf5 or to other, as yet unidentified, factors.

The model of coordinated regulation that we propose, with a single *p57* element integrating positive (from the MRFs) and negative (from Hes/Hey) regulatory information suggests that the interplay between Notch repression of *p57MRE* in Pax3/7 progenitors and its activation by MRFs in myoblasts is crucial for growth arrest. The molecular mechanisms regulating Notch signaling components during myogenesis are not fully characterized. It was reported that during *Xenopus* development Dll1 expression is regulated by Myod1 (Wittenberger et al., 1999) and that Myod1 expression is repressed by Hairy-1 (Umbhauer et al., 2001). It is unclear if these regulatory mechanisms also exist in amniotes, but our data are compatible with such a sequence of events. Resolving the precise molecular interplay between Pax gene expression, cell growth arrest, MRF regulation and the switch in Notch signaling will require additional investigations.

Notch signaling plays a key role in maintaining the homeostasis of muscle stem cells in the adult (Bjornson et al., 2012; Carlson et al., 2008; Fukada et al., 2011; Kitamoto and Hanaoka, 2010; Mourikis et al., 2012b) and in colonization of the satellite cell niche (Bröhl et al., 2012). In particular, Notch controls quiescence of muscle satellite cells (Bjornson et al., 2012; Mourikis et al., 2012b). This activity might be mediated by Hey1 and HeyL, which are required in the adult lineage for satellite cell homeostasis and skeletal muscle regeneration (Fukada et al., 2011). Conditional deletion of *Rbpj* in Pax7$^+$ satellite cells led to spontaneous differentiation without activation or division of the cells (Bjornson et al., 2012; Mourikis et al., 2012b). Strikingly, *RbpJ* ablation does not lead to an immediate and complete differentiation or growth arrest in the Pax3$^+$ population during embryonic development, leaving open the possibility that other pathways are involved. For instance, Notch activity on adult muscle stem cells is counteracted by TGFβ signaling (Carlson and Conboy, 2007). This is mediated through the activation of phosphorylated Smad3, which can directly bind and activate the *p15* (*Cdkn2b*), *p16* (*Cdkn2a*), *p21* and *p27* promoters (Carlson and Conboy, 2007) to favor muscle stem cell differentiation. Interestingly, during chicken myogenesis myostatin, which is a member of the TGFβ family, has also been implicated in the control of terminal differentiation through indirect activation of p21 (Manceau et al., 2008).

In addition to driving cell cycle exit during adult myogenesis, p57 has also been implicated in stabilization of Myod1 through direct association in C2C12 cells, resulting in enhanced myogenesis

RESEARCH ARTICLE Development (2014) 141, 2780-2790 doi:10.1242/dev.110155

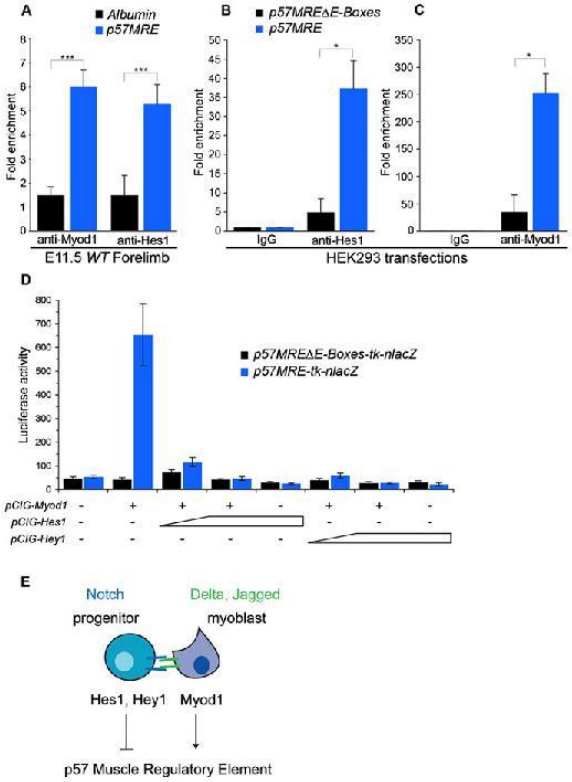

Fig. 8. Direct regulation of the *p57MRE* by Myod1 and Hes1/Hey1. (A) Chromatin immunoprecipitation followed by qPCR on wild-type forelimbs at E11.5. *p57MRE* is enriched when precipitated with anti-Myod1 or anti-Hes1 antibodies compared with an albumin gene control. (B,C) Validation of antibody ChIP capacities on transfected HEK293 cells: enrichment with anti-Hes1 (B) or anti-Myod1 (C) is obtained with the *p57MRE* compared with the construct in which all putative E-boxes have been mutated (*p57MREΔE-Boxes*). $n=3$; error bars indicate s.e.m.; *$P<0.05$, ***$P<0.001$. (D) Transactivation assay on C2C12 cells with the expression plasmids and reporters indicated ($n\geq3$). (E) Schematic representation of the regulation of cell cycle exit during myogenesis. In muscle progenitors, Notch downstream effectors Hes1 and Hey1 repress the activation of p57 to allow the amplification of the pool, while in the neighboring myoblasts that express the Notch ligands, Myod1 directly activates p57 expression.

(Reynaud et al., 2000). A similar mechanism has also been identified in zebrafish, in which p57 cooperates with Myod1 to drive the differentiation of several early zebrafish muscle fiber types (Osborn et al., 2010). It is not known if this positive-feedback loop also operates during early murine skeletal muscle formation. One could propose that, although the initiation of myogenic differentiation and growth arrest are independent, these events may synergize subsequently, for instance to enhance Myod1 activity and reinforce terminal differentiation. In zebrafish, p57 cooperates with Myod1 to drive *myog* expression (Osborn et al., 2010); nevertheless, proliferating Myod1$^+$ and Myog$^+$ cells are detected in $p21^{-/-}$; $p57^{+/-}$ mice (see Fig. 2A-C; our unpublished observations). Interestingly, expression of Mef2c is impaired in these mutant mice (Zhang et al., 1999), raising the possibility that p57 may also be involved in terminal differentiation in murine myogenesis during development.

In our study, the expression of p57 is firmly linked to an absence of cell cycle progression, since we observe no overlap between p57 (or p21) expression and Ki67 (Fig. 1C-F) under normal conditions. Strikingly, a small but significant proportion of the Pax3$^+$/p21$^+$ or Pax3$^+$/p57$^+$ cells are Ki67$^+$ in the $Pax3^{Cre/+}$; $Rbpj^{flox/flox}$ mutant context. Although this might correspond to a transitory state due to the differentiation phenotype of these mutant embryos, one cannot exclude the possibility that Notch might also be involved in both cell cycle progression and cell cycle arrest via a complex regulatory loop.

p57 expression has been reported previously in adult satellite cells (Fukada et al., 2007), but the precise timing of expression has yet to be characterized. The identification of *p57MRE* through a Myod1 ChIP-seq screen performed in C2C12 cells raises the possibility that this element is reused in adult muscle cells *in vivo*. Owing to the perinatal death of *p57* mutant mice, the role of p57 in postnatal myogenesis cannot be studied *in vivo*. *p21*-deficient mice display normal muscle development but impaired skeletal muscle regeneration (Hawke et al., 2003). Given the functional overlap between p21 and p57 during development, it would be interesting to evaluate the combined role of these two proteins in postnatal satellite cell homeostasis and skeletal muscle regeneration.

The recent identification of the role of p57 in the maintenance of quiescent hematopoietic (Matsumoto et al., 2011), neural (Furutachi et al., 2013) and lung (Zacharek et al., 2011) stem cells indicates that p57, along with other CDKIs, is important for stem cell function. Whether such a regulatory mechanism for CDKI expression is redeployed in other systems remains to be investigated. For example, Notch has been implicated in maintaining progenitor cell proliferation in intestinal stem cells (Riccio et al., 2008), in adult neural stem cells (Imayoshi et al., 2010) and in Rathke's pouch progenitors of the pituitary (Monahan et al., 2009) and, indeed, one proposed mechanism is the repression of CDKIs by the product of the Notch target gene *Hes1* (Monahan et al., 2009; Riccio et al., 2008). Unfortunately, these studies did not define which cells provide the ligands. Nevertheless, our data and the role of Notch and Hes1 in intestinal stem cells, neural stem cells and pituitary progenitor cells might suggest a general mechanism whereby the expansion of the progenitor cell population is regulated via modulation of CDKI genes. Such a regulatory mechanism could be used as a safeguard to prevent tumor formation by progenitor/stem cells, for instance when differentiation is impaired. It is also tempting to speculate that fine-tuning of this system could also be used for intrinsically regulating organ size.

MATERIALS AND METHODS

Mouse lines and harvest of embryos

$Myf5^{+/nlacZ}$, $Myod1^{+/-}$, $p21^{+/-}$, $p57^{+/-m}$ (*p57* is an imprinted gene; we indicate maternal origin of the allele by a superscript *m*), $Pax3^{Cre/+}$ and $Rbpj^{flox/+}$ lines have been described previously (Deng et al., 1995; Engleka et al., 2005; Han et al., 2002; Rudnicki et al., 1992; Yan et al., 1997). For explant and ChIP experiments, C57BL/6J embryos were used (Janvier). For timed pregnancies, the morning when a vaginal plug was found was defined as embryonic day (E) 0.5. All experiments were performed on three independent embryos for each genotype.

Immunohistochemistry and X-Gal staining

Embryos and forelimbs were harvested and fixed for 2 h and for 20 min, respectively, in PBS/4% paraformaldehyde at 4°C. Cryoprotection was performed by equilibration in PBS/15% sucrose overnight at 4°C. Frozen sections were permeabilized in PBS/0.1% Triton X-100, blocked in PBS/2% bovine serum albumin for 1 h at room temperature, then immunolabeled with primary antibodies overnight at 4°C. For X-Gal staining, embryos were collected in PBS, fixed 20 min in PBS/4% paraformaldehyde at room temperature and incubated in X-Gal solution (Life Technologies) overnight at 37°C on a rotary shaker.

RESEARCH ARTICLE Development (2014) 141, 2780-2790 doi:10.1242/dev.110155

Antibodies

The following antibodies were used: mouse anti-β-galactosidase 1/500 (Promega, Z378), mouse anti-Myod1 5.8A 1/200 (DAKO, M3512), mouse anti-Myog F5D 1/200 (DSHB, F5D), mouse anti-p21 1/100 (BD Pharmingen, 556431), mouse anti-p57 1/100 (Santa Cruz, sc-56341), mouse anti-Pax7-c 1/100 (DSHB, Pax7-c), mouse anti-Pax3-c 1/100 (DSHB, Pax3-c), rabbit anti-β-galactosidase 1/1000 (Life Technologies, A-11132), rabbit anti-Myod1 M318 1/100 (Santa Cruz, sc-760), rabbit anti-Myf5 C20 1/500 (Santa Cruz, sc-302), rabbit anti-p57 H91 1/100 (Santa Cruz, sc-8298), rabbit anti-phospho-histone 3 Ser10 1/1000 (Cell Signaling, 9701), goat anti-p57 M20 1/50 (Santa Cruz, sc-1039) and goat anti-Pax3 1/100 (Santa Cruz, sc-34916). Phalloidin (649 nm) 1/500 was from Life Technologies. Secondary antibodies were coupled to Alexa Fluor 488 1/250, 594 1/1000 (Life Technologies) or 649 1/250 (Jackson ImmunoResearch).

Explant and cell culture

Forelimbs from E11.5 wild-type embryos were cultured in 12-well plates in BGJb medium (Life Technologies), without serum, with 200 µg/ml ascorbic acid (Sigma) and 100 µg/ml penicillin/streptomycin (Life Technologies). For Notch inhibition, forelimbs were immediately treated with 20 µM N-[N-(3,5-difluorophenacetyl)-L-alanyl]-S-phenylglycine t-butyl ester (DAPT; Sigma) or DMSO carrier (Sigma) for 28 h. Treated and control forelimbs originating from the same embryo were compared in each experiment. C2C12 and HEK293 cells were cultured in proliferating medium comprising DMEM with 10% fetal bovine serum and 100 µg/ml penicillin/streptomycin (Life Technologies).

Plasmid construct for transgenesis

The *p57* muscle regulatory element (*p57MRE*) (chr7: 150,587,238-150,587,924) was isolated by PCR. For cloning convenience, *Eag*I restriction sites were added to the forward and reverse primers used for amplification: forward, 5′-AAGCGGCCGCACCCAGTTTGCCCAGT-GTAG-3′; reverse, 5′-AACGGCCGCCAGGTAAAGACACCCCAGA-3′. After *Eag*I digestion, the 686 bp fragment was cloned, respecting its genomic orientation, into the *Not*I site of p*tk*nlacZ(−) plasmid (Hadchouel et al., 2000) (*tk*, thymidine kinase). The *p57MRE-tk-nlacZ* fragment was released by *Sac*II/*Xho*I digestion and gel purified using the Nucleobond plasmid purification kit (Macherey-Nagel) before injection into pronuclei.

β-galactosidase assay

Hey1, *Hes1* cDNAs [gifts from S. Tajbakhsh (Pasteur Institute, Paris, France) and R. Kageyama (Institute for Virus Research, Kyoto University, Japan), respectively] and *Myod1* cDNA were cloned into the pCIG plasmid (Megason and McMahon, 2002). C2C12 cells were transfected with a total of 1.2 µg DNA using Lipofectamine LTX plus reagent (Life Technologies). Fixed concentrations of *p57MRE-tk-nlacZ* or *p57MREΔE-Boxes-tk-nlacZ* (0.6 µg), or pCIG-Myod1 (0.15 µg) were used. For pCIG-Hes1 and pCIG-Hey1, 0.15 or 0.3 µg was used. Each sample was co-transfected with 0.1 µg *tk*-Luciferase reporter for sample-to-sample normalization. Forty-eight hours after transfection, the cells were collected and the proteins were extracted and assayed for β-galactosidase activity (β-Gal assay Kit K1455-01, Life Technologies) and for luciferase activity (Luciferase assay system E1500, Promega) to normalize transfection variation. Measurements were made at least in triplicate and expressed as the mean (with s.e.m.) of the amount of β-galactosidase substrate (ONPG) hydrolyzed.

Reverse transcription and quantitative PCR (qPCR)

Total RNA from embryo forelimbs was extracted using the RNeasy mini kit (Qiagen). 1 µg RNA was used to generate cDNA using the Superscript II reverse transcriptase kit (Life Technologies). qPCR was performed using the Lightcycler 480 SYBR Green mix (Roche) and Lightcycler 480 II (Roche). RT-qPCR on FACS-isolated cells was performed using the Superscript III cell direct cDNA kit (Life Technologies). qPCR results are expressed as relative ratios of target cDNA to *Hprt*. The following oligonucleotides were used (5′-3′; forward and reverse): *Hes1*, ACACCGGACAAACCAAAGAC and AATGCCGGGAGCTATCTTTC; *Hey1*, CACCTGAAAATGCTGCACAC and ATGCTCAGATAACGGG-CAAC; *Myod1*, GGCTACGACACCGCCTACTA and GAGATGCGCT-CCACTATGCT; *Pax7*, AGGCCTTCGAGAGGACCCAC and CTGA-ACCAGACCTGGACGCG.

Chromatin immunoprecipitation (ChIP)

Myod1 ChIP-seq has been described in detail (Cao et al., 2010). For qPCR ChIP experiments, forelimbs from E11.5 embryos were frozen in liquid nitrogen and processed for ChIP according to the manufacturer's protocol (Active motif). 150 µg of chromatin was used for each experiment. 2 g of a rabbit anti-Myod1 M318 (Santa Cruz, sc-760) and 2 g of a goat anti-Hes1 (Santa Cruz, sc-13844) were used; 2 g of a rabbit anti-β-galactosidase (Life Technologies, A-11132) or 2 g of a goat anti-β-galactosidase (Santa Cruz, sc-19119) were used as the corresponding IgG negative control. The precipitated and input chromatins were analyzed by qPCR using *p57MRE* primers (forward, 5′-ATGTGCACACAG-CTCAGAGG-3′; reverse, 5′-GGAAGGATGGAGGGCTTTAC-3′) with albumin primers as negative control (forward, 5′-GGGACGAGATGGT-ACTTTGTG-3′; reverse, 5′-GATCAGTCCAAACTTCTTTCTG-3′).

For ChIP on transfected cells, HEK293 cells were transfected with a total of 7.5 µg DNA using FuGENE6 (Promega). A mutant *p57MRE* sequence, *p57MREΔE-Boxes*, was synthesized (GeneART) in which all putative E-boxes were mutated according to Iso et al. (2003). Fixed concentrations of *p57MRE-tk-nlacZ* or *p57MREΔE-Boxes-tk-nlacZ* (4 µg) were used together with either pCig-Myod1 or pCig-Hes1 (2 µg). After 48 h, chromatin was extracted and processed as above; 100 µg chromatin was used for each experiment. For ChIP, 2 µg normal mouse (Santa Cruz) and goat (Santa Cruz) IgG were used for negative controls for the Myod1 and Hes1 antibodies mentioned above. Results are expressed as fold change compared with IgG control.

Statistical test

Immunostainings were performed on at least three embryos of each genotype. Quantifications were performed using images of all muscle masses present in an embryo section (6-8 sections per slide, 2-3 frames per masse). All qPCR experiments were performed at least three times independently. Cell counting and qPCR results were analyzed by Mann–Whitney or Student's *t*-test. In Fig. 3D and Fig. 4F,G, quantifications were analyzed by ANOVA. In Fig. 5D, quantifications were analyzed by a chi-square test.

Acknowledgements

We are grateful to Drs Sonia Alonso-Martin, Edgar Gomes, Revital Rattenbach, Vanessa Ribes and David Sassoon for their assistance with this work and writing. We thank Catherine Bodin for histology. We also acknowledge the animal care facilities at UPMC and CDTA, and Catherine Blanc and Bénédicte Hoareau from the Flow Cytometry Core CyPS. We are grateful to Drs Tapscott and Fukada for sharing unpublished data, Drs Tajbakhsh and Kageyama for *Hey1* and *Hes1* cDNAs and F. Langa Vives for transgenic services.

Competing interests

The authors declare no competing financial interests.

Author contributions

A.Z. designed and performed experiments, analyzed data and wrote the paper. S.H. and F.A. designed and performed experiments, analyzed data and edited the manuscript. T.C., D.M. and P.M. designed and performed experiments, analyzed data. Z.Y. and Y.C. provided data on Myod1 ChIP-seq. D.B. provided *Rbpj* mutant embryos. C.B. analyzed data and edited the manuscript. F.R. oversaw the entire project, designed experiments, analyzed data and wrote the paper.

Funding

This work is supported by funding to F.R. from Institut National de la Santé et de la Recherche Médicale (INSERM) Avenir Program, Association Française contre les Myopathies (AFM), Association Institut de Myologie (AIM), Labex REVIVE, the European Union Seventh Framework Program in the project ENDOSTEM [grant # 241440], Ligue Nationale Contre le Cancer (LNCC), Association pour la Recherche contre le Cancer (ARC), Fondation pour la Recherche Médicale (FRM) [FDT20130928236], Institut National du Cancer

Development (2014) 141, 2780-2790 doi:10.1242/dev.110155

(INCa), Agence Nationale pour la Recherche (ANR) grant Epimuscle [grant # 11 BSV2 017 02] and Agence Nationale pour la Recherche Maladies Rares (MRAR) grant Pax3 in WS [grant # 06-MRAR-032]. This work was also funded by the German Research Foundation (DFG) [grant GK1631], French-German University (UFA-DFH) [grant CDFA-06-11] and the AFM as part of the MyoGrad International Research Training Group for Myology.

Supplementary material

Supplementary material available online at
http://dev.biologists.org/lookup/suppl/doi:10.1242/dev.110155/-/DC1

References

Artavanis-Tsakonas, S. and Muskavitch, M. A. T. (2010). Notch: the past, the present, and the future. *Curr. Top. Dev. Biol.* **92**, 1-29.

Ben-Yair, R. and Kalcheim, C. (2005). Lineage analysis of the avian dermomyotome sheet reveals the existence of single cells with both dermal and muscle progenitor fates. *Development* **132**, 689-701.

Besson, A., Dowdy, S. F. and Roberts, J. M. (2008). CDK inhibitors: cell cycle regulators and beyond. *Dev. Cell* **14**, 159-169.

Birchmeier, C. and Brohmann, H. (2000). Genes that control the development of migrating muscle precursor cells. *Curr. Opin. Cell Biol.* **12**, 725-730.

Bjornson, C. R. R., Cheung, T. H., Liu, L., Tripathi, P. V., Steeper, K. M. and Rando, T. A. (2012). Notch signaling is necessary to maintain quiescence in adult muscle stem cells. *Stem Cells* **30**, 232-242.

Borggrefe, T. and Liefke, R. (2012). Fine-tuning of the intracellular canonical Notch signaling pathway. *Cell Cycle* **11**, 264-276.

Bröhl, D., Vasyutina, E., Czajkowski, M. T., Griger, J., Rassek, C., Rahn, H.-P., Purfürst, B., Wende, H. and Birchmeier, C. (2012). Colonization of the satellite cell niche by skeletal muscle progenitor cells depends on Notch signals. *Dev. Cell* **23**, 469-481.

Buas, M. F. and Kadesch, T. (2010). Regulation of skeletal myogenesis by Notch. *Exp. Cell Res.* **316**, 3028-3033.

Buas, M. F., Kabak, S. and Kadesch, T. (2010). The Notch effector Hey1 associates with myogenic target genes to repress myogenesis. *J. Biol. Chem.* **285**, 1249-1258.

Buckingham, M. and Relaix, F. (2007). The role of Pax genes in the development of tissues and organs: Pax3 and Pax7 regulate muscle progenitor cell functions. *Annu. Rev. Cell Dev. Biol.* **23**, 645-673.

Cao, Y., Yao, Z., Sarkar, D., Lawrence, M., Sanchez, G. J., Parker, M. H., MacQuarrie, K. L., Davison, J., Morgan, M. T., Ruzzo, W. L. et al. (2010). Genome-wide MyoD binding in skeletal muscle cells: a potential for broad cellular reprogramming. *Dev. Cell* **18**, 662-674.

Carlson, M. E. and Conboy, I. M. (2007). Regulating the Notch pathway in embryonic, adult and old stem cells. *Curr. Opin. Pharmacol.* **7**, 303-309.

Carlson, M. E., Hsu, M. and Conboy, I. M. (2008). Imbalance between pSmad3 and Notch induces CDK inhibitors in old muscle stem cells. *Nature* **454**, 528-532.

Cherrett, C., Furutani-Seiki, M. and Bagby, S. (2012). The Hippo pathway: key interaction and catalytic domains in organ growth control, stem cell self-renewal and tissue regeneration. *Essays Biochem.* **53**, 111-127.

Cook, M. and Tyers, M. (2007). Size control goes global. *Curr. Opin. Biotechnol.* **18**, 341-350.

Delfini, M. C., Hirsinger, E., Pourquie, O. and Duprez, D. (2000). Delta 1-activated notch inhibits muscle differentiation without affecting Myf5 and Pax3 expression in chick limb myogenesis. *Development* **127**, 5213-5224.

Deng, C., Zhang, P., Harper, J. W., Elledge, S. J. and Leder, P. (1995). Mice lacking p21CIP1/WAF1 undergo normal development, but are defective in G1 checkpoint control. *Cell* **82**, 675-684.

Engleka, K. A., Gitler, A. D., Zhang, M., Zhou, D. D., High, F. A. and Epstein, J. A. (2005). Insertion of Cre into the Pax3 locus creates a new allele of Splotch and identifies unexpected Pax3 derivatives. *Dev. Biol.* **280**, 396-406.

Fortini, M. E. and Artavanis-Tsakonas, S. (1994). The suppressor of hairless protein participates in notch receptor signaling. *Cell* **79**, 273-282.

Fukada, S.-i., Uezumi, A., Ikemoto, M., Masuda, S., Segawa, M., Tanimura, N., Yamamoto, H., Miyagoe-Suzuki, Y. and Takeda, S. (2007). Molecular signature of quiescent satellite cells in adult skeletal muscle. *Stem Cells* **25**, 2448-2459.

Fukada, S.-i., Yamaguchi, M., Kokubo, H., Ogawa, R., Uezumi, A., Yoneda, T., Matev, M. M., Motohashi, N., Ito, T., Zolkiewska, A. et al. (2011). Hesr1 and Hesr3 are essential to generate undifferentiated quiescent satellite cells and to maintain satellite cell numbers. *Development* **138**, 4609-4619.

Furutachi, S., Matsumoto, A., Nakayama, K. I. and Gotoh, Y. (2013). p57 controls adult neural stem cell quiescence and modulates the pace of lifelong neurogenesis. *EMBO J.* **32**, 970-981.

Georgia, S., Soliz, R., Li, M., Zhang, P. and Bhushan, A. (2006). p57 and Hes1 coordinate cell cycle exit with self-renewal of pancreatic progenitors. *Dev. Biol.* **298**, 22-31.

Gros, J., Manceau, M., Thomé, V. and Marcelle, C. (2005). A common somitic origin for embryonic muscle progenitors and satellite cells. *Nature* **435**, 954-958.

Hadchouel, J., Tajbakhsh, S., Primig, M., Chang, T. H., Daubas, P., Rocancourt, D. and Buckingham, M. (2000). Modular long-range regulation of Myf5 reveals unexpected heterogeneity between skeletal muscles in the mouse embryo. *Development* **127**, 4455-4467.

Halevy, O., Novitch, B. G., Spicer, D. B., Skapek, S. X., Rhee, J., Hannon, G. J., Beach, D. and Lassar, A. B. (1995). Correlation of terminal cell cycle arrest of skeletal muscle with induction of p21 by MyoD. *Science* **267**, 1018-1021.

Han, H., Tanigaki, K., Yamamoto, N., Kuroda, K., Yoshimoto, M., Nakahata, T., Ikuta, K. and Honjo, T. (2002). Inducible gene knockout of transcription factor recombination signal binding protein-J reveals its essential role in T versus B lineage decision. *Int. Immunol.* **14**, 637-645.

Hawke, T. J., Meeson, A. P., Jiang, N., Graham, S., Hutcheson, K., DiMaio, J. M. and Garry, D. J. (2003). p21 is essential for normal myogenic progenitor cell function in regenerating skeletal muscle. *Am. J. Physiol. Cell Physiol.* **285**, C1019-C1027.

Hirsinger, E., Malapert, P., Dubrulle, J., Delfini, M. C., Duprez, D., Henrique, D., Ish-Horowicz, D. and Pourquie, O. (2001). Notch signalling acts in postmitotic avian myogenic cells to control MyoD activation. *Development* **128**, 107-116.

Imayoshi, I., Sakamoto, M., Yamaguchi, M., Mori, K. and Kageyama, R. (2010). Essential roles of Notch signaling in maintenance of neural stem cells in developing and adult brains. *J. Neurosci.* **30**, 3489-3498.

Iso, T., Kedes, L. and Hamamori, Y. (2003). HES and HERP families: multiple effectors of the Notch signaling pathway. *J. Cell Physiol.* **194**, 237-255.

Jarriault, S., Brou, C., Logeat, F., Schroeter, E. H., Kopan, R. and Israel, A. (1995). Signalling downstream of activated mammalian Notch. *Nature* **377**, 355-358.

John, R. M., Ainscough, J. F.-X., Barton, S. C. and Surani, M. A. (2001). Distant cis-elements regulate imprinted expression of the mouse p57(Kip2) (Cdkn1c) gene: implications for the human disorder, Beckwith–Wiedemann syndrome. *Hum. Mol. Genet.* **10**, 1601-1609.

Kablar, B., Krastel, K., Ying, C., Asakura, A., Tapscott, S. J. and Rudnicki, M. A. (1997). MyoD and Myf-5 differentially regulate the development of limb versus trunk skeletal muscle. *Development* **124**, 4729-4738.

Kablar, B., Asakura, A., Krastel, K., Ying, C., May, L. L., Goldhamer, D. J. and Rudnicki, M. A. (1998). MyoD and Myf-5 define the specification of musculature of distinct embryonic origin. *Biochem. Cell Biol.* **76**, 1079-1091.

Kassar-Duchossoy, L., Giacone, E., Gayraud-Morel, B., Jory, A., Gomès, D. and Tajbakhsh, S. (2005). Pax3/Pax7 mark a novel population of primitive myogenic cells during development. *Genes Dev.* **19**, 1426-1431.

Kitamoto, T. and Hanaoka, K. (2010). Notch3 null mutation in mice causes muscle hyperplasia by repetitive muscle regeneration. *Stem Cells* **28**, 2205-2216.

Kopan, R. and Ilagan, M. X. G. (2009). The canonical Notch signaling pathway: unfolding the activation mechanism. *Cell* **137**, 216-233.

Lagha, M., Kormish, J. D., Rocancourt, D., Manceau, M., Epstein, J. A., Zaret, K. S., Relaix, F. and Buckingham, M. E. (2008). Pax3 regulation of FGF signaling affects the progression of embryonic progenitor cells into the myogenic program. *Genes Dev.* **22**, 1828-1837.

Lepper, C. and Fan, C.-M. (2010). Inducible lineage tracing of Pax7-descendant cells reveals embryonic origin of adult satellite cells. *Genesis* **48**, 424-436.

Manceau, M., Gros, J., Savage, K., Thome, V., McPherron, A., Paterson, B. and Marcelle, C. (2008). Myostatin promotes the terminal differentiation of embryonic muscle progenitors. *Genes Dev.* **22**, 668-681.

Matsumoto, A., Takeishi, S., Kanie, T., Susaki, E., Onoyama, I., Tateishi, Y., Nakayama, K. and Nakayama, K. I. (2011). p57 is required for quiescence and maintenance of adult hematopoietic stem cells. *Cell Stem Cell* **9**, 262-271.

Megason, S. and McMahon, A. (2002). A mitogen gradient of dorsal midline Wnts organizes growth in the CNS. *Development* **129**, 2087-2098.

Monahan, P., Rybak, S. and Raetzman, L. T. (2009). The notch target gene HES1 regulates cell cycle inhibitor expression in the developing pituitary. *Endocrinology* **150**, 4386-4394.

Mourikis, P. and Tajbakhsh, S. (2014). Distinct contextual roles for Notch signalling in skeletal muscle stem cells. *BMC Dev. Biol.* **14**, 2.

Mourikis, P., Gopalakrishnan, S., Sambasivan, R. and Tajbakhsh, S. (2012a). Cell-autonomous Notch activity maintains the temporal specification potential of skeletal muscle stem cells. *Development* **139**, 4536-4548.

Mourikis, P., Sambasivan, R., Castel, D., Rocheteau, P., Bizzarro, V. and Tajbakhsh, S. (2012b). A critical requirement for notch signaling in maintenance of the quiescent skeletal muscle stem cell state. *Stem Cells* **30**, 243-252.

Murphy, M. and Kardon, G. (2011). Origin of vertebrate limb muscle: the role of progenitor and myoblast populations. *Curr. Top. Dev. Biol.* **96**, 1-32.

Osborn, D. P. S., Li, K., Hinits, Y. and Hughes, S. M. (2010). Cdkn1c drives muscle differentiation through a positive feedback loop with Myod. *Dev. Biol.* **350**, 464-475.

Picard, C. A. and Marcelle, C. (2013). Two distinct muscle progenitor populations coexist throughout amniote development. *Dev. Biol.* **373**, 141-148.

Relaix, F., Rocancourt, D., Mansouri, A. and Buckingham, M. (2005). A Pax3/Pax7-dependent population of skeletal muscle progenitor cells. *Nature* **435**, 948-953.

Development (2014) 141, 2780-2790 doi:10.1242/dev.110155

Relaix, F., Montarras, D., Zaffran, S., Gayraud-Morel, B., Rocancourt, D., Tajbakhsh, S., Mansouri, A., Cumano, A. and Buckingham, M. (2006). Pax3 and Pax7 have distinct and overlapping functions in adult muscle progenitor cells. *J. Cell Biol.* **172**, 91-102.

Reynaud, E. G., Leibovitch, M. P., Tintignac, L. A. J., Pelpel, K., Guillier, M. and Leibovitch, S. A. (2000). Stabilization of MyoD by direct binding to p57(Kip2). *J. Biol. Chem.* **275**, 18767-18776.

Riccio, O., van Gijn, M. E., Bezdek, A. C., Pellegrinet, L., van Es, J. H., Zimber-Strobl, U., Strobl, L. J., Honjo, T., Clevers, H. and Radtke, F. (2008). Loss of intestinal crypt progenitor cells owing to inactivation of both Notch1 and Notch2 is accompanied by derepression of CDK inhibitors p27Kip1 and p57Kip2. *EMBO Rep.* **9**, 377-383.

Rios, A. C., Serralbo, O., Salgado, D. and Marcelle, C. (2011). Neural crest regulates myogenesis through the transient activation of NOTCH. *Nature* **473**, 532-535.

Rudnicki, M. A., Braun, T., Hinuma, S. and Jaenisch, R. (1992). Inactivation of MyoD in mice leads to up-regulation of the myogenic HLH gene Myf-5 and results in apparently normal muscle development. *Cell* **71**, 383-390.

Rudnicki, M. A., Schnegelsberg, P. N. J., Stead, R. H., Braun, T., Arnold, H.-H. and Jaenisch, R. (1993). MyoD or Myf-5 is required for the formation of skeletal muscle. *Cell* **75**, 1351-1359.

Schienda, J., Engleka, K. A., Jun, S., Hansen, M. S., Epstein, J. A., Tabin, C. J., Kunkel, L. M. and Kardon, G. (2006). Somitic origin of limb muscle satellite and side population cells. *Proc. Natl. Acad. Sci. U.S.A.* **103**, 945-950.

Schuster-Gossler, K., Cordes, R. and Gossler, A. (2007). Premature myogenic differentiation and depletion of progenitor cells cause severe muscle hypotrophy in Delta1 mutants. *Proc. Natl. Acad. Sci. U.S.A.* **104**, 537-542.

Schweisguth, F. and Posakony, J. W. (1992). Suppressor of Hairless, the Drosophila homolog of the mouse recombination signal-binding protein gene, controls sensory organ cell fates. *Cell* **69**, 1199-1212.

Tajbakhsh, S., Rocancourt, D., Cossu, G. and Buckingham, M. (1997). Redefining the genetic hierarchies controlling skeletal myogenesis: Pax-3 and Myf-5 act upstream of MyoD. *Cell* **89**, 127-138.

Tumaneng, K., Russell, R. C. and Guan, K.-L. (2012). Organ size control by Hippo and TOR pathways. *Curr. Biol.* **22**, R368-R379.

Umbhauer, M., Boucaut, J.-C. and Shi, D.-L. (2001). Repression of XMyoD expression and myogenesis by Xhairy-1 in Xenopus early embryo. *Mech. Dev.* **109**, 61-68.

Vasyutina, E., Lenhard, D. C., Wende, H., Erdmann, B., Epstein, J. A. and Birchmeier, C. (2007). RBP-J (Rbpsuh) is essential to maintain muscle progenitor cells and to generate satellite cells. *Proc. Natl. Acad. Sci. U.S.A.* **104**, 4443-4448.

Westbury, J., Watkins, M., Ferguson-Smith, A. C. and Smith, J. (2001). Dynamic temporal and spatial regulation of the cdk inhibitor p57(kip2) during embryo morphogenesis. *Mech. Dev.* **109**, 83-89.

Wittenberger, T., Steinbach, O. C., Authaler, A., Kopan, R. and Rupp, R. A. W. (1999). MyoD stimulates delta-1 transcription and triggers notch signaling in the Xenopus gastrula. *EMBO J.* **18**, 1915-1922.

Yan, Y., Frisen, J., Lee, M. H., Massague, J. and Barbacid, M. (1997). Ablation of the CDK inhibitor p57Kip2 results in increased apoptosis and delayed differentiation during mouse development. *Genes Dev.* **11**, 973-983.

Zacharek, S. J., Fillmore, C. M., Lau, A. N., Gludish, D. W., Chou, A., Ho, J. W., Zamponi, R., Gazit, R., Bock, C., Jäger, N. et al. (2011). Lung stem cell self-renewal relies on BMI1-dependent control of expression at imprinted loci. *Cell Stem Cell* **9**, 272-281.

Zhang, P., Wong, C., Liu, D., Finegold, M., Harper, J. W. and Elledge, S. J. (1999). p21(CIP1) and p57(KIP2) control muscle differentiation at the myogenin step. *Genes Dev.* **13**, 213-224.

Zúñiga, A., Haramis, A.-P. G., McMahon, A. P. and Zeller, R. (1999). Signal relay by BMP antagonism controls the SHH/FGF4 feedback loop in vertebrate limb buds. *Nature* **401**, 598-602.

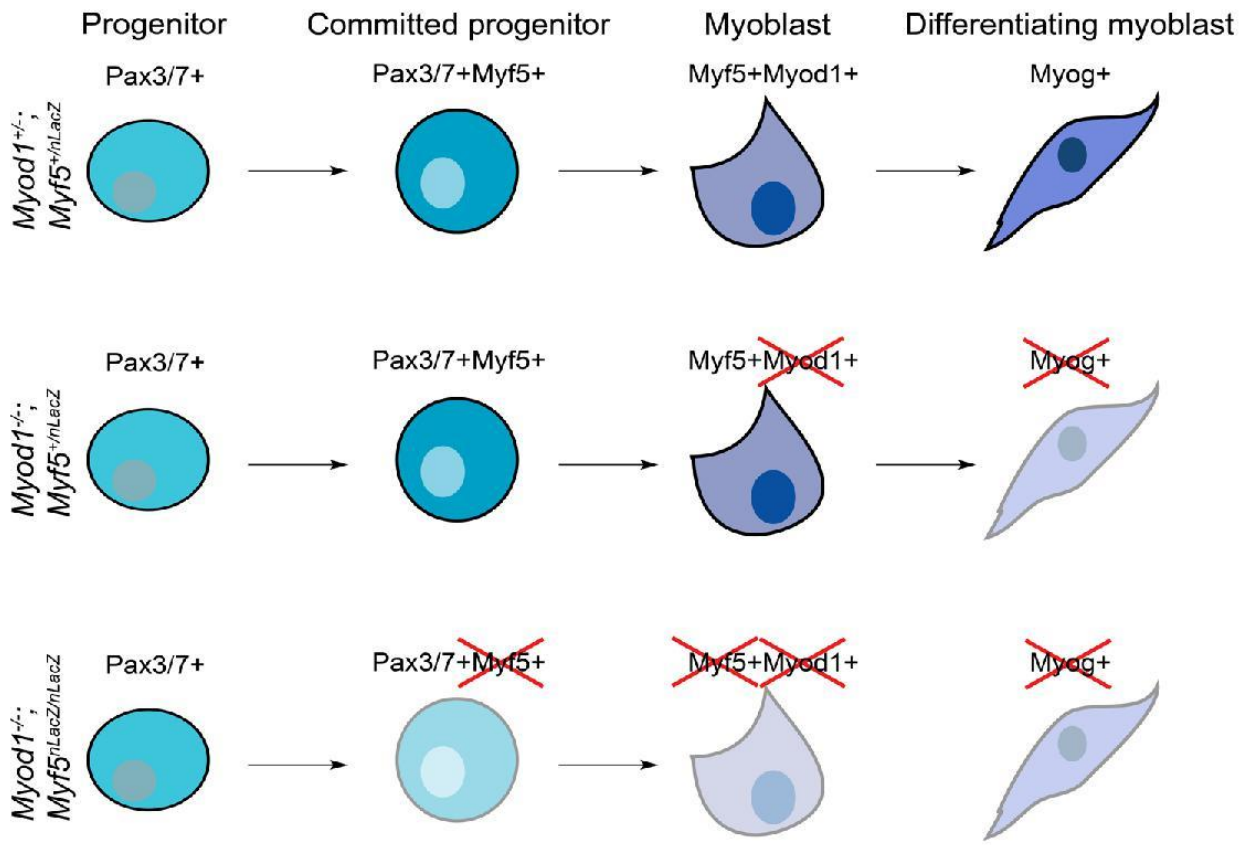

Supplementary Figure 1. Stages of myogenic differentiation impairment using the different *Myod1: Myf5* mutant compounds.

Supplementary Figure 2. Genomic sequence of p57MRE enhancer cloned in p57MRE-tk-nlacZ reporter.

Putative E-boxes are underlined with grey background. To generate *p57MREΔE-Boxes* mutant construct, every CANNTG motif has been replaced by CGNNAG.

Preface

Recent studies from us and others showed that the CDKI p57 participates in cell cycle control during muscle development. The perinatal lethality of p57 mutants precludes postnatal functional analyses to elucidate its role in adult muscle and, thus, we generated a conditional knock-out allele. We inserted loxP sites encompassing the coding region of p57 to allow tissue-specific and adult-specific excision of p57 using the loxP/Cre recombination system. By using the ubiquitous PGK-Cre, we uniformly ablated p57 and showed that the resulting mice exhibited the same defects as previously reported for the null allele. Specifically, we observed perinatal lethality and growth defects in several tissues, including the palate, the gastro-intestinal tract, the abdominal wall, and the skeletal system. Furthermore, in the new p57 allele we inserted an IRES-linked β-galactosidase reporter, to allow tracking of p57-expressing cells. We confirmed that the reporter faithfully recapitulates the expression profile of p57 in embryonic and adult tissues. Hence, we here describe a new genetic tool for expression and functional analyses of p57.

A *p57* conditional mutant allele that allows tracking of *p57*-expressing cells

Despoina Mademtzoglou[a,b*], Sonia Alonso-Martin[a,b,c*], Ted Hung-Tse Chang[a,b,d], Keren Bismuth[e], Bernadette Drayton[a,b], Frédéric Aurade[a,b,e], Frédéric Relaix[a,b,f,g1].

a. Inserm, IMRB U955-E10, F-94010, Creteil, France
b. Université Paris Est, Faculté de medecine, F-94000, Creteil, & Ecole Nationale Veterinaire d'Alfort, 94700, Maison Alfort, France
c. Present address: Tissue Regeneration Laboratory, Centro Nacional de Investigaciones Cardiovasculares (CNIC), Madrid, Spain
d. Present address: International Centre for Genetic Engineering and Biotechnology, Cancer Genomics group, Anzio Road, Cape Town, South Africa 7925
e. Sorbonne Universités, UPMC Univ Paris 06, INSERM UMRS974, Center for Research in Myology, Paris, France
f. Etablissement Français du Sang, 94017, Creteil, France
g. APHP, Hopitaux Universitaires Henri Mondor, DHU Pepsy & Centre de Référence des Maladies Neuromusculaires GNMH, 94000 Créteil France

* Contributed equally to this work

1. Correspondence: Pr Frederic Relaix
IMRB-E10, 8 rue du General Sarrail 94010 Creteil France
Frederic.relaix@inserm.fr
+33 (0) 1 49 81 39 40

Short title: p57 conditional ablation and reporter

Keywords: Cell cycle exit, CDKIs, β-galactosidase reporter, Cre-inducible ablation, post-natal survival

ABSTRACT

p57^{Kip2} (*p57*) is a maternally expressed imprinted gene regulating growth arrest which belongs to the CIP/KIP family of Cyclin-Dependent Kinase Inhibitors. While initially identified as a cell cycle arrest protein through inhibition of cyclin and cyclin-dependent kinase complexes, p57 activity has also been linked to differentiation, apoptosis, and senescence. In addition, p57 has recently been shown to be involved in tumorigenesis and cell fate decisions in stem cells. Yet, p57 function in adult tissues remains poorly characterized due to the perinatal lethality of *p57* knock-out mice. In order to analyze p57 tissue-specific activity, we generated a conditional mouse line (*p57*$^{FL\text{-}ILZ/+}$) by flanking the coding exons 2-3 by LoxP sites. In order to track *p57*-expressing or mutant cells, the *p57*$^{FL\text{-}ILZ}$ allele also contains an IRES-linked β-galactosidase reporter inserted in the 3' UTR of the gene. Here, we show that the β-galactosidase reporter expression pattern recapitulates p57 tissue-specificity during development and in postnatal mice. Furthermore, we crossed the *p57*$^{FL\text{-}ILZ/+}$ mice with *PGK-Cre* mice to generate *p57*$^{cKO\text{-}ILZ/+}$ animals with ubiquitous loss of p57. *p57*$^{cKO\text{-}ILZ/+}$ mice display developmental phenotypes analogous to previously described *p57* knock-outs. Thus, *p57*$^{FL\text{-}ILZ/+}$ is a new genetic tool allowing expression and functional conditional analyses of p57.

INTRODUCTION

Tightly controlling cell cycle is imperative for development and tissue homeostasis of complex organisms. Cell cycle progression is primarily achieved via an array of Cyclin-Dependent Kinases (CDKs) and their activating subunits named cyclins (Malumbres, 2014). Growth arrest is mediated by the interaction of these CDK-cyclin complexes with Cyclin-Dependent Kinase Inhibitors (CDKIs). CDKIs are subdivided into two families based on their structural homology and specificity of action (Borriello et al., 2011): INK4 [including $p15^{Ink4b}$ (p15), $p16^{Ink4a}$ (p16), $p18^{Inc4c}$ (p18), $p19^{Ink4d}$ (p19)] and Cip/Kip [including $p21^{Cip1}$ (p21), $p27^{Kip1}$ (p27), $p57^{Kip2}$ (p57)]. The latter counteracts cell cycle progression more broadly by inhibiting all CDK-cyclin complexes, in addition to activities outside of cell cycle regulation (Borriello et al., 2011).

p57 is the most recently discovered and least studied member of the Cip/Kip family of CDKIs. It is distinguished from its siblings, p21 and p27, by its unique structure (including a divergent central domain), distinct distribution pattern, and imprinting status. It is emerging as a multifaceted protein involved in several cellular processes, such as proliferation, differentiation, senescence, apoptosis, and motility (reviewed in Pateras et al., 2009; Rossi & Antonangeli, 2015). The gross developmental defects and perinatal lethality of mice that lack or overexpress p57 highlight its critical role during organogenesis (Yan et al., 1997; Zhang et al., 1997; Andrews et al., 2007). In addition to its role in growth arrest during differentiation, p57 plays distinct functions in several organs, including quiescence acquisition in hematopoeietic and neural stem cells (Matsumoto et al., 2011; Zou et al., 2011; Furutachi et al., 2013). Its impact on human pathology is illustrated by p57 implication in carcinogenesis, which was initially hypothesized due to its capacity to prevent proliferation. Remarkably, p57 is downregulated in several malignancies and loss of p57 is associated with poor patient prognosis. Noticeably, p57 is mutated or inactivated in the cancer-predisposing disorder Beckwith-Wiedemann syndrome (reviewed in Guo et al., 2010; Borriello et al., 2011).

In order to perform tissue-specific functional studies coupled with analysis of p57 expression, we generated a *p57* allele ($p57^{FL\text{-}ILZ/+}$), allowing LacZ-dependent visualization and Cre-inducible ablation of p57. Moreover, in contrast to a previously reported conditional *p57* mutant mice (Matsumoto et al., 2011), $p57^{FL\text{-}ILZ}$ allele allows complete ablation of the coding region, while preserving potential regulatory elements of the surrounding sequences. Here, we describe the generation of the $p57^{FL\text{-}ILZ/+}$ mouse line and demonstrate that the LacZ reporter recapitulates the p57 expression profile during development and in the adult. We also show the

efficiency of Cre-dependent ubiquitous removal of p57 function and the subsequent recapitulation of knock-out phenotypes.

RESULTS AND DISCUSSION

We generated a mouse line ($p57^{FL\text{-}N\text{-}ILZ/+}$), in which the entire p57 coding region (exons 2 and 3) is flanked by LoxP sites, to allow spatial and temporal conditional ablation of p57 by Cre recombinase (Fig.1A-D). A *FRT-neo* cassette was introduced for selection and subsequently excised using mice containing FLP recombinase activity, generating the $p57^{FL\text{-}ILZ}$ allele (Fig. 1C). The $p57^{FL\text{-}ILZ}$ allele also contains a downstream *IRES-nLacZ* gene inserted in exon 4, encoding a nuclear-localized β-galactosidase (Fig. 1C). To evaluate the LacZ expression profile, we used $p57^{FL\text{-}ILZ/+}$ heterozygotes with maternal inheritance of the targeted allele, since p57 is subjected to genomic imprinting and the paternal allele is silenced (Hatada & Mukai, 1995). Co-immunostaining experiments demonstrated that p57 and β-galactosidase co-localized in forming bone tissues during development and in postnatal kidney (Fig. 1E), two sites where p57 expression was previously documented (Yan et al., 1997; Zhang et al., 1997; Westbury et al., 2001).

Next, we performed an analysis of the *nLacZ* reporter expression in embryonic (Fig. 2) and adult (Fig. 3) tissues. During development, *p57* is widely expressed during organogenesis with high levels peaking at key differentiation steps of specific organs (Matsuoka et al., 1995; Westbury et al., 2001). Specifically, we detected high reporter expression in the developing musculoskeletal system, neural tissues and parenchymal organs of X-Gal-stained whole mount embryos (Fig. 2). At early stages (E10.5-E11.5), we observed a strong expression in brain, heart, and limbs as well as in the somites (Fig. 2A, B). Sensory organs, including the developing ears, lens and nasal processes, are also stained (Fig. 2A, B). Remarkably, the reporter pattern thoroughly mirrors p57 expression visualized by *in situ* hybridization (ISH) (Fig. 2A', B'). In the developing limbs the reporter and p57 transcripts are initially concentrated in central masses, which contain differentiating muscle and skeletal cells (Fig. 2A-B'). Strong reporter expression extends to the forming digits at later stages (Fig. 2C, D). From E13.5 the staining becomes more widespread and less intense, covering almost the entire exterior of the embryos (Fig. 2D-H). Sections of E13.5 $p57^{FL\text{-}ILZ/+}$ embryos revealed numerous X-Gal-positive cells in the heart, lung, body wall, musculoskeletal parts of the limb, and neural tissues, including the neural tube, dorsal root ganglia and thoracic vertebral body (Fig. 2I), consistent with previous reports of p57 expression (Matsuoka et al., 1995; Yan et al., 1997; Zhang et al., 1997; Westbury et al., 2001). β-galactosidase-positive cells likely correspond to cell cycle exit linked with terminal differentiation.

In contrast to embryonic tissues, p57-LacZ expression was more restricted in adult tissues. Strikingly, LacZ expression was limited to small regions or cell populations of specific organs, including the kidney, testis, skeletal muscle, heart, brain, intestine, and lung (Fig. 3), in agreement with previous studies (Matsuoka et al., 1995; Zhang et al., 1997). Specifically, we observed robust expression in the glomeruli of the kidney (Fig. 3A), where p57 is expressed at essential stages of glomerulogenesis and during the establishment of the mature phenotype (Nagata et al., 1998; Hiromura et al., 2001). β-galactosidase is also detected in the seminiferous tubules of the testis, where p57 was previously suggested to promote the meiotic progression of early spermatocytes along with cell cycle arrest and differentiation of spermatids (Kim et al., 2006). In general, β-galactosidase signal is highly localized and is, for instance, not detected in the spleen or the liver (data not shown), in line with previous reports (Matsuoka et al., 1995; Yanagida et al., 2015). Strikingly, β-galactosidase expression was also observed in organs where p57 expression was not previously described, such as the salivary gland (Fig. 3D).

We further wanted to evaluate the ability to recombine the $p57^{FL\text{-}ILZ}$ allele (via the LoxP sites) to generate p57 loss of function animals ($p57^{cko\text{-}ILZ}$). To this end, we used *PGK-Cre* mice, which induce ubiquitous recombination (Lallemand et al., 1998). We focused our study on heterozygotes with a maternally transmitted *p57*-null allele (*PGK-Cre*;$p57^{cKO\text{-}ILZ\ (m)/+}$), since the paternal allele is transcriptionally repressed (Hatada & Mukai, 1995), and previous studies revealed indistinguishable phenotypes between heterozygote and homozygote knock-outs (Yan et al., 1997; Zhang et al., 1997; Takahashi et al., 2000). As expected, p57 protein was no longer detected in all tissues examined from recombined *PGK-Cre*;$p57^{cKO\text{-}ILZ\ (m)/+}$ fetuses (Fig. 4). As we crossed the $p57^{cKO\text{-}ILZ}$ allele with a *PGK-Cre* allele inducing early and ubiquitous recombination, we expected to phenocopy previously reported *p57* knock-out mice. Indeed, as previously reported (Yan et al., 1997; Zhang et al., 1997; Takahashi et al., 2000), we observed a prominent perinatal lethality of mutants (Fig. 5A), associated with a marked size reduction of the fetus (Fig. 5B, C), similarly to the knock-out mice reported by Nakayama and colleagues (Takahashi et al., 2000). Perinatal death of *p57* mutants has been attributed to cleft palate that leaves the oral and nasal cavities connected along with difficulties in suckling/breathing and an abnormal gastrointestinal tract (Yan et al., 1997; Zhang et al., 1997; Takahashi et al., 2000). Likewise, in $p57^{cKO\text{-}ILZ\ (m)/+}$ mutants the two palatal shelves failed to grow and meet in the midline (Fig. 5D), associated with inflated stomach and intestine in a number of cases (Fig. 5E). We also observed body wall dysplasia associated with abdominal slit at birth or with thin body wall during development (Fig. 5F), in agreement with previous studies on mice lacking p57 (Zhang et al., 1997). Finally, we noticed embryonic and perinatal skeletal deformities evidenced by sternum

fusion defects, limb shortening and thickening, and delayed ossification (Fig. 5G), consistent with the skeletal defects of previous reports (Yan et al., 1997; Zhang et al., 1997; Susaki et al., 2009). Thus, we were able to successfully recombine the *p57*$^{FL\text{-}ILZ/+}$ allele, ablating p57 expression and reproducing the spectrum of p57 knock-out phenotypes. However, β-galactosidase activity is hardly detected in recombined *p57*$^{cKO\text{-}ILZ\ (m)/+}$ mutants embryos, likely due to destabilized mRNA in the deleted allele (Fig. S1).

In conclusion, the *p57*$^{FL\text{-}ILZ/+}$ allele provides a genetic tool that allows conditional ablation of p57 by removal of the complete coding region, encoded by exons 2-3, in a spatiotemporal manner using tissue-specific and/or inducible Cre lines. Moreover, the *p57*$^{FL\text{-}ILZ/+}$ allele provides a faithful reporter to track the expression pattern of p57, including the possibility to follow epigenetic effects and imprinting changes, and identify new sites of expression that may require p57 activity.

MATERIALS AND METHODS

Generation of cKO mice

A 61.8kb BAC clone from a mouse 129Sv (129S7AB2.2; Adams et al., 2005) genomic library centered around the p57 locus (bMQ-38L12; SourceBioscience #WTSIB741L1238Q) has been chosen to carry out locus modifications using λ-red recombination (Lee et al., 2001). A LoxP site has first been inserted into p57 5'UTR in exon 1 and then a *LoxP-FRT-PGK-NEO-BGHpA-FRT-IRESnlsLacZ* cassette into p57 3'UTR in exon 4. Finally, the 19.5kb cKO targeting cassette containing recombined p57 locus, 5.8kb of genomic sequence upstream of exon 1, and 5kb downstream of exon 4, has been extracted from the BAC clone by gap repair.

BAC targeting vectors construction

The first BAC targeting construct was generated by PCR amplification of two homology arms, using bMQ-38L12 as template DNA. The first arm upstream of ATG contained 98bp of 5' exon 1; the second 21bp of 3' exon 1, intron 1, and 173bp of exon 2 including beginning of CDS (pair 1: 5'-CATTATGCTAATCGTGAGGAGGC-3' and 5'-CTTAAGTCTGGATCGCTTGTCCTG-3', 203bp; pair 2: 5'-CTTAAGAGCCGTCCATCACCAATCAG-3' and 5'-AAGTTGAAGTCCCAGCGGTTGTAGAC-3', 380bp). Amplicons were subcloned in *pGEMTeasy* (Promega, # A3610) with a newly introduced AflII site in-between. Then a *LoxP-kanamycin-LoxP* cassette was inserted blunt in AflII. Similarly, homology arms for the second BAC targeting construct were amplified from the BAC DNA and

subcloned in *pGEMTeasy* with a HindIII site in-between. The first arm contains 119bp at the end of exon 3, including STOP codon, intron 3 and 216bp of 5' exon 4. The second homology arm contains the following 361bp of exon 4 (pair3: 5'-GAGAACTGCGCAGGAGAACAAG-3' and 5'-AAGCTTTACACCTTGGGACCAGC-3', 424bp; pair 4: 5'-AAGCTTTAAATCATTTATGTAAAATGTTTAATCTCTACTCG-3' and 5'-GCAATCTAATGAAGTGGGGGAC-3', 361bp). In parallel, a 1.9kb EcoRV-SacII *FRT-PGK-Neo-BGHpA-FRT-LoxP* fragment from *pL451* (Liu et al., 2003) was cloned blunt into SalI of *pIRES-nLacZ* (Relaix et al., 2003). Then, the 5.9kb NotI fragment-containing *LoxP-FRT-PGK-Neo-BGHpA-FRT-IRESnLacZ* was inserted blunt into the homology arms carrying vector in HindIII. The complete 1.8kb and 6.8kb BAC targeting linear cassettes directed against exon 1 and exon 4, respectively, were released by NotI digestion and gel purified (Macherey-Nagel, NucleoSpin® Gel and PCR Clean-up, #740609).

The gap repair plasmid was built from PCR generated homology arms (5.9kb upstream of exon 1 and 5kb downstream of exon 4) using bMQ-38L12 as template, assembled in *pGEMTeasy* with EcoRV created in central position (pair 5: 5'-CTACTTACCAGCCTCTGAGGA-3' and 5'-GATATCCAAGCCAGACCTCCCTGC-3', 529bp; pair 6: 5'-GATATCCTGGTTTCCCACCTTGTGATG-3' and 5'-GTTGTGATCCACACCTGACTCC-3', 520bp). The full insert was then excised with EcoRI and cloned blunt in *pBluescriptSK-* (*pBSK-*, Stratagene) to give *p57-gap-repair* plasmid. An hygromycin resistance cassette was PCR amplified from *pSKT.HygroBACe3.6Lox511* (kindly given by Dr. J. Hadchouel) with SacI introduced at each extremities and cloned into *p57-gap-repair* SacI site to give the gap repair plasmid *p57gaprepairHygro(-)*.

All cloning PCR were carried out using Advantage-2 (Clontech, #639201) or PHUSION DNA polymerases (Thermoscientific, #F530L). All DNA digestions were performed using NEB enzymes.

<u>*BAC recombinations*</u>

BAC recombinations were performed by first electroporation of bMQ-38L12 BAC DNA (BTX ECM399 electroporator; 0.1cm cuvettes, 1.3kV, 100ng DNA) into the *E. coli* Cre-inducible SW106 strain and selection on chloramphenicol (cam^R; 10µg/ml) LB plates. DNA from five transformants was analyzed by restriction profiling using NotI + SpeI on 0.6% large agarose gels ran overnight. One clone, L12A, with the expected restriction profile, satisfactorily completed a deeper restriction profiling with EagI, XhoI+NruI, Aat2, AgeI+NotI, HpaI+NotI, RsrII+NotI. To perform DNA recombination, 500µl of this clone's overnight culture were used to inoculate 25ml of LB+cam^R, further grown for 135 minutes at 32°C. Then, the λ-red recombinase was induced by 15 minute-incubation of the culture at 42°C. Bacteria were made electro-competent by two washes

in 10ml cold dH_2O and gentle resuspension on ice. The 1.8kb purified exon 1 targeting cassette was introduced by electroporation (0.2cm cuvettes, 1.75kV, 20ng DNA), and transformants were selected on kanamycin (kan^R; 25μg/ml) plates. Extracted DNA from four kan^R clones, L12AK1 to 4, and analyzed with NotI+SpeI was effectively recombined. To pop-out the kanamycin cassette located between the two LoxP sites and leave one LoxP site at the wanted location, Cre recombinase expression was induced in L12AK1 clone using 0.1% L(+) arabinose (Sigma-Aldrich, #A3256) in liquid culture for 2 hours. Bacteria were then plated on cam^R LB plates. Three clones were positively tested for loss of kanamycin resistance, BglII restriction profiling and PCR across deletion on BAC extracted DNA, and one of them was then chosen for further modifications. L12AK#NE1 DNA was electroporated in *E. coli* Flp-inducible SW105 strain as described above, and DNA from two clones growing on cam^R, L12AK#OF1 and OF2, were subjected to BglII restriction profiling to assess integrity following the transformation process. A L12AK#OF1 culture was induced for λ-red recombinase expression and made electro-competent and, then, it was transformed with the 6.8kb purified exon 4 targeting cassette (0.2cm cuvettes, 1.75kV, 25ng). DNA from three kan^R transformants, L12A#FC1-3, was extracted and tested for NotI+RsrII restriction profiling, showing successful recombination for clones L12A#FC1 and 2, further confirmed by PCR at 5' and 3' extremities of the insertion, and deep restriction profiling of L12A#FC1 DNA with NheI, NdeI, SpeI, NruI, AgeI, EcoRI, and AseI+NotI. To assess FRT sites functionality (*FRT-PGK-Neo-pA-FRT* cassette), Flp recombinase was induced in L12A#FC1 bacterial clone with arabinose as described above. DNA from five clones, which have lost kanamycin resistance, was extracted and subjected to AatII profiling and showed that *PGK-Neo-pA* sequence was missing and FRT sites were functional. Similarly, LoxP sites functionality was tested. DNA from L12A#FC1 was electroporated in SW106, then Cre recombinase was induced with arabinose, and DNA from five cam^R-kanamycin sensitive clones was extracted and profiled with AatII. Again, the analysis showed that the sequence from the 3'end of exon 1 to 5' of exon 4 was properly floxed-out, thus proving that LoxP sites are functional.

<u>*Gap repair and final cKO construct*</u>

Bacterial clone L12A#FC1 was made electro-competent, λ-Red recombinase induced as described above, and transformed with 10ng of circular *p57gaprepairHygro(-)*, and then selected on hygromycin (hyg^R; 125μg/ml) LB plates. 22 out of the 24 DNA extracted (Macherey-Nagel, NucleoSpin® plasmid #740588) from hyg^R clones showed that the expected 19.5kb insert was present following gap repair. To provide a negative selectable marker in ES cells, a 1.6kb cassette containing the PGK promoter driving the expression of the Diphteria toxin A subunit (*Pgk-DTApA*) was PCR amplified from a *pSK-pDTA* plasmid (Relaix et al., 2003) with SalI and XhoI

introduced in 5' and 3', respectively, and subcloned in one of the gap repair clones into SalI site. Resulting transformants were screened for *PGK-DTA-pA* in reverse orientation.

Generation of the p57$^{FL\text{-}N\text{-}ILZ/+}$ mouse model

The targeting vector was electroporated in CK35 embryonic stem (ES) cells of 129S2 genetic background (Kress et al. 1998). 30 µg of a Pme1-linearized construct were electroporated (240 V, 500 µF - Gene Pulser II, Biorad) into 5x10^7 cells in 0.8ml PBS. Cells were then seeded on a layer of embryonic fibroblast feeders in DMEM (Life Technologies, #31966047) supplemented with 15% ES-culture-tested FBS (Life Technologies #10270-106), non-essential amino acids (Life Technologies, #11140-035), Penicillin-Streptomycin (Life Technologies, #15140-114), 10^{-4} M ß-mercaptoethanol (Sigma-Aldrich, #M6250); 1000 UI LIF (Merck-Millipore, #ESG1107). Geneticin (300 µg/ml) selection started on day 2 (Life Technologies, #10131-019) and picking was done on day 9.

ES cells were preselected by two 3' external PCRs (pair 7: 5'-CACTGCATTCTAGTTGTGGTTTGTCCAAAC-3' and 5'-GGGACAGTTGCTAGCTGTGA -3', 5.6kb product; pair 8: 5'- CCCCCTGAACCTGAAACATA-3' and 5'-GGTCGCTACCATTACCAGTTGGTCTGG-3', 6kb). The first PCR product was digested with BglII into two bands of 3.3kb and 2.3kb. Clones were then screened for recombination events by Southern blot analysis using HindII digestion and a 5'-flanking probe (wt allele: 10.8kb, KO: 8.6kb). The positive clones were further verified by SacI digestion and LacZ internal probes. Targeted ES cells were recovered with 9.3% frequency. Positive clones were caryotyped and euploïde clones were used to produce chimeras and germline transmission.

The resulting mice are kept in a mixed 129S2 X C57Bl/6N background and will be available to the research community upon manuscript acceptance.

Mouse lines

FLP and *PGK-Cre* transgenic mice have been previously described (Lallemand et al., 1998; Rodriguez et al., 2000). For *in situ* hybridization experiments C57BL/6N (Janvier) embryos were used.

Embryo harvest

Female and male mice were crossed overnight and separated the following morning after macroscopical vaginal examination for plug presence. In case of plug, that morning was defined as embryonic day (E) 0.5. At least three embryos per genotype and per time point were analyzed.

Immunohistochemistry and X-Gal staining

Whole mount samples: Embryos and adult organs were harvested and fixed for 30 minutes to 2 hours (depending on the stage) in 4% paraformaldehyde/PBS at 4°C. Incubation with X-Gal solution (0.4 mg/ml X-Gal in 2 mM $MgCl_2$, 0.1% Tween20, 1X PBS, 4 mM $K_4Fe(CN)_6$, and 4 mM $K_3Fe(CN)_6$; Sigma-Aldrich) was performed at 37^{o}C on a rotary shaker. Incubation duration varied from 2 hours to overnight depending on the age. Specimens were placed in 4% paraformaldehyde/PBS at 4^{o}C for long-term storage.

Sections: Embryos and newborns were harvested and fixed for 25 minutes to 2 hours (depending on the age) in 4% paraformaldehyde/PBS at 4°C, followed by overnight incubation in 15% sucrose/PBS for cryoprotection before freezing. Organs of adult mice were frozen fresh and fixation was performed directly on sections with 4% paraformaldehyde/PBS for 20 minutes at room temperature. For X-Gal staining, frozen sections were incubated with X-Gal solution as previously mentioned overnight at 37^{o}C. Adult tissues were counterstained with eosin (ThermoFisher Scientific, #6766007) for 30 seconds to highlight their structure. For hematoxylin-eosin staining, frozen sections were incubated with hematoxylin (Sigma-Aldrich, # MHS32) for 11 minutes to stain nuclei, counterstained with eosin for 30 seconds to highlight cytoplasm, and dehydrated with passages through increasing concentrations of ethanol (30%, 50%, 70%, 85%, 95%, 100%) and two washes in xylene. For immunofluorescence, frozen sections were permeabilized in 0.1% Triton X-100/PBS and blocked in 1% bovine serum albumin/PBS at room temperature. Immunolabeling was performed overnight at 4^{o}C for primary antibodies and 1 hour at room temperature for secondary antibodies. Nuclei were counterstained with DAPI. The following antibodies were used: mouse anti-β-galactosidase 1:200 (Promega, #Z378), rabbit anti-p57 1:150 (Santa Cruz, #sc-8298), Fluorescein (FITC)-AffiniPure goat anti-mouse IgG2a secondary antibody (Jackson ImmunoResearch, #115095206), and AlexaFluor594-conjugated F(ab')2-goat anti-rabbit IgG (H+L) secondary antibody (ThermoFisher Scientific, #A11072).

At least three animals were analyzed in each experiment.

Skeleton staining

E14.5 and newborn mice were eviscerated and fixed in 100% ethanol for 48 hours. The carcasses were stained with alcian blue (0.15% in 4:1 ethanol / acetic acid; "alcian blue 8GX", Sigma-Aldrich, # A3157) for 48 hours, postfixed in ethanol for 24 hours, cleared in 2% KOH, stained with alizarin red (0.15% in 0.5% KOH; "alizarin red S monohydrate", Riedel-de Haën, #33010), and decolorized in increasing concentrations of glycerol (20%, 50%, 70%) for one week. Specimens were stored in 70% glycerol. At least three animals per genotype and per time point were analyzed.

Whole-Mount *in situ* hybridization

p57 (Genbank accession number: BC005412.1) riboprobe was synthesized using PstII/T7. Primers for probe amplification were designed with the NCBI-Primer BLAST tool and ordered from Eurogentec. The probes were amplified using as template one of the BAC repair clones described above. The PCR product was purified with the NucleoSpin Gel and PCR Clean-up kit (Macherey-Nagel, #740609) and inserted into the *pGEM-T Easy* vector (Promega, #A1360) according to the manufacturer's instructions. Following overnight transformation of competent cells, colonies were analyzed by restriction digestion and verified by sequencing. 2µg of the plasmid was linearized with appropriate restrictions enzymes at 37^{o}C for 30 minutes and purified with the NucleoSpin Gel and PCR Clean-up kit. Transcription and Digoxigenin-labeling were performed with the DIG RNA labeling Kit (SP6/T7) (Roche, #11175025910) and the product was purified with illustra MicroSpin G-50 Columns (GE Healthcare, #27533001) following the manufacturer's protocol.

Harvested embryos were fixed in 4% paraformaldehyde/PBS overnight, dehydrated through 25%, 50%, 75% methanol/0.1% Tween20/PBS and stored in 100% methanol at -20^{o}C. Before use, embryos were rehydrated with descending concentrations of methanol, treated with 10µg/ml proteinase-K in 0.1% Tween20/PBS (15 minutes at E10.5, 25 minutes at E11.5), post-fixed with 4% paraformaldehyde/0.1% glutaraldehyde/PBS for 20 minutes and incubated with 1µg/ml DIG-labeled RNA probe overnight at 68^{o}C. After several steps of washes, the embryos were incubated with 1:2000 anti-DIG-AP Fab fragment (Roche, #11175025910) overnight at 4^{o}C. Following three days of intense washes, the embryos were incubated with BM purple AP substrate (Roche, #11442074001) until color was developed to the desired extent. For long-term storage, specimens were kept in 4% paraformaldehyde/PBS at 4^{o}C. Three animals per time point were analyzed.

Graphic editing

Graphs and representative photos were arranged in Figure format with the graphics editor Photoshop CS5. Uniform background was added in whole mount sample photos to cover shadows or background differences.

Statistical test

Body weight differences were compared with the Mann-Whitney U-test. Differences at $p<0.05$ were considered significant.

ACKNOWLEDGEMENTS

The authors thank Dr. P.Mourikis for constructive comments to improve the study and Dr. M.Borok for critically reading the manuscript. This work was supported by funding from INSERM Avenir Program, Association Française contre les Myopathies (AFM) via TRANSLAMUSCLE (PROJECT 19507), Labex REVIVE (ANR-10-LABX-73), Fondation pour la Recherche Médicale (FRM; Grant FDT20130928236 and DEQ20130326526), Agence Nationale pour la Recherche (ANR) grant Epimuscle (ANR 11 BSV2 017 02), Bone-muscle-repair (ANR-13-BSV1-0011-02), BMP-biomass (ANR-12-BSV1-0038- 04), Satnet (ANR-15-CE13-0011-01), RHU CARMMA (ANR-15-RHUS-0003), and the Agence Nationale pour la Recherche Maladies Rares (MRAR) grant Pax3 in WS (ANR-06-MRAR-32-01).

REFERENCES

Adams DJ, Quail MA, Cox T, van der Weyden L, Gorick BD, Su Q, Chan WI, Davies R, Bonfield JK, Law F, Humphray S, Plumb B, Liu P, Rogers J, Bradley A. 2005. A genome-wide, end-sequenced 129Sv BAC library resource for targeting vector construction. Genomics 86: 753-758.

Andrews SC, Wood MD, Tunster SJ, Barton SC, Surani MA, John RM. 2007. Cdkn1c (p57Kip2) is the major regulator of embryonic growth within its imprinted domain on mouse distal chromosome 7. BMC Dev Biol 7: 53-67.

Borriello A, Caldarelli I, Bencivenga D, Criscuolo M, Cucciolla V, Tramontano A, Oliva A, Perrotta S, Della Ragione F. 2011. p57(Kip2) and cancer: time for a critical appraisal. Mol Cancer Res 9: 1269-1284.

Furutachi S, Matsumoto A, Nakayama KI, Gotoh Y. 2013. p57 controls adult neural stem cell quiescence and modulates the pace of lifelong neurogenesis. EMBO J 32: 970-981.

Guo H, Tian T, Nan K, Wang W. 2010. p57: A multifunctional protein in cancer (Review). Int J Oncol 36: 1321-1329.

Hatada I, Mukai T. 1995. Genomic imprinting of p57KIP2, a cyclin-dependent kinase inhibitor, in mouse. Nat Genet 11: 204-206.

idney Int. 2001 Dec;60(6):2235-46.

Hiromura K, Haseley LA, Zhang P, Monkawa T, Durvasula R, Petermann AT, Alpers CE, Mundel P, Shankland SJ. 2001. Podocyte expression of the CDK-inhibitor p57 during development and disease. Kidney Int 60: 2235-2246.

Arch Androl. 2006 Nov-Dec;52(6):463-9.

Kim ST, Park NC, Yi LS, Gye MC. 2006. Expression of p57kip2 in germ cells and Leydig cells in human testis. Arch Androl 52: 463-469.

Kress C, Vandormael-Pournin S, Baldacci P, Cohen-Tannoudji M, Babinet C. 1998. Nonpermissiveness for mouse embryonic stem (ES) cell derivation circumvented by a single backcross to 129/Sv strain: establishment of ES cell lines bearing the Omd conditional lethal mutation. Mamm Genome 9: 998-1001.

Lallemand Y, Luria V, Haffner-Krausz R, Lonai P. 1998. Maternally expressed PGK-Cre transgene as a tool for early and uniform activation of the Cre site-specific recombinase. Transgenic Res 7: 105-112.

Lee EC, Yu D, Martinez de Velasco J, Tessarollo L, Swing DA, Court DL, Jenkins NA, Copeland NG. 2001. A highly efficient *Escherichia coli*-based chromosome engineering system adapted for recombinogenic targeting and subcloning of BAC DNA. Genomics 73: 56-65.

Liu P, Jenkins NA, Copeland NG. 2003. A highly efficient recombineering-based method for generating conditional knockout mutations. Genome Res 13: 476-484.

Malumbres M. 2014. Cyclin-dependent kinases. Genome Biol 15: 122-132.

Matsuoka S, Edwards MC, Bai C, Parker S, Zhang P, Baldini A, Harper JW, Elledge SJ. 1995. p57KIP2, a structurally distinct member of the p21CIP1 Cdk inhibitor family, is a candidate tumor suppressor gene. Genes Dev 9: 650-652.

Matsumoto A, Takeishi S, Kanie T, Susaki E, Onoyama I, Tateishi Y, Nakayama K, Nakayama KI. 2011. p57 is required for quiescence and maintenance of adult hematopoietic stem cells. Cell Stem Cell 9: 262-271.

Nagata M, Nakayama K, Terada Y, Hoshi S, Watanabe T. 1998. Cell cycle regulation and differentiation in the human podocyte lineage. Am J Pathol 153: 1511-1520.

Mol Cancer Res. 2009 Dec;7(12):1902-19. doi: 10.1158/1541-7786.MCR-09-0317. Epub 2009 Nov 24.

Pateras IS, Apostolopoulou K, Niforou K, Kotsinas A, Gorgoulis VG. 2009. p57KIP2: "Kip"ing the cell under control. Mol Cancer Res 7: 1902-1919.

Relaix F, Polimeni M, Rocancourt D, Ponzetto C, Schäfer BW, Buckingham M. 2003. The transcriptional activator PAX3-FKHR rescues the defects of Pax3 mutant mice but induces a myogenic gain-of-function phenotype with ligand-independent activation of Met signaling *in vivo*. Genes Dev 17: 2950-2965.

Rodriguez CI, Buchholz F, Galloway J, Sequerra R, Kasper J, Ayala R, Stewart AF, Dymecki SM. 2000. High-efficiency deleter mice show that FLPe is an alternative to Cre-loxP. Nat Genet 25: 139-140.

Rossi MN, Antonangeli F. 2015. Cellular Response upon Stress: p57 Contribution to the Final Outcome. Mediators Inflamm 2015: 259325.

Susaki E, Nakayama K, Yamasaki L, Nakayama KI. 2009. Common and specific roles of the related CDK inhibitors p27 and p57 revealed by a knock-in mouse model. Proc Natl Acad Sci USA 106: 5192-5197.

Takahashi K, Nakayama K, Nakayama K.2000. Mice lacking a CDK inhibitor, p57Kip2, exhibit skeletal abnormalities and growth retardation. J Biochem 127: 73-83.

Westbury J, Watkins M, Ferguson-Smith AC, Smith J. 2001. Dynamic temporal and spatial regulation of the cdk inhibitor p57(kip2) during embryo morphogenesis. Mech Dev 109: 83-89.

Yan Y, Frisén J, Lee MH, Massagué J, Barbacid M. 1997. Ablation of the CDK inhibitor p57Kip2 results in increased apoptosis and delayed differentiation during mouse development. Genes Dev 11: 973-983.

Yanagida A, Chikada H2, Ito K1, Umino A1, Kato-Itoh M1, Yamazaki Y1, Sato H1, Kobayashi T1, Yamaguchi T1, Nakayama KI3, Nakauchi H4, Kamiya A5. 2015. Liver maturation deficiency in p57(Kip2)-/- mice occurs in a hepatocytic p57(Kip2) expression-independent manner. Dev Biol 407: 331-343.

Zhang P, Liégeois NJ, Wong C, Finegold M, Hou H, Thompson JC, Silverman A, Harper JW, DePinho RA, Elledge SJ. 1997. Altered cell differentiation and proliferation in mice lacking p57KIP2 indicates a role in Beckwith-Wiedemann syndrome. Nature 387: 151-158.

Zou P, Yoshihara H, Hosokawa K, Tai I, Shinmyozu K, Tsukahara F, Maru Y, Nakayama K, Nakayama KI, Suda T. 2011. p57(Kip2) and p27(Kip1) cooperate to maintain hematopoietic stem cell quiescence through interactions with Hsc70. Cell Stem Cell 9: 247-261.

FIGURE LEGENDS

Figure 1. Generation of *p57$^{FL\text{-}ILZ/+}$* mice

(A-D) Schematic representation of wild-type (wt) mouse *p57^{Kip2}* (p57) allele (A), floxed *p57* allele with *Neo*-selection cassette (*p57$^{FL\text{-}N\text{-}ILZ}$*; B), floxed *p57* allele after removal of the *Neo*-selection cassette by FLP recombinase (*p57$^{FL\text{-}ILZ}$*; C), and recombined *p57* allele after removal of the floxed fragment by Cre recombinase (*p57$^{cKO\text{-}ILZ}$*; D). The four exons are represented by empty boxes, marked as E1-E4. Exons 2 and 3 contain the

coding regions (black box), with start codons (arrowheads) and stop codon (asterisk) indicated below the exons. LoxP and FRT sites are also shown as indicated. (E) Immunofluorescence analysis of β-galactosidase (green) and p57 (red) showing forming skeletal elements of the vertebral column (upper panel), and perinatal kidney section (lower panel). Heterozygote animals with maternally transmitted transgene were used, due to imprinting silencing of the paternally transmitted *p57* allele. Maternal inheritance is indicated with superscript (m). Nuclei were counterstained blue with DAPI. Scale bars: 50μm.

Figure 2. Time-course of *LacZ* expression in $p57^{FL\text{-}ILZ/+}$ *embryos*

(A-H) Whole mount X-Gal staining on $p57^{FL\text{-}ILZ\ (m)/+}$ embryos at E10.5 (A), E11.5 (B), E12.5 (C), E13.5 (D), E14.5 (E), E15.5 (F), E16.5 (G), E17.5 (H). Heterozygous animals with maternal inheritance of the transgene were used, due to imprinted silencing of the paternally transmitted *p57* allele. Maternal transmission is indicated by superscript (m). The skin was removed from E15.5 onwards, while small remaining pieces in the limb and tail tip resulted in lack of staining. (I-J) Whole mount *in situ* hybridization for *p57* at E10.5 (I) and E11.5 (J), wild type embryos are provided for comparison with X-Gal profiles. Scale bars: 2mm. (K) Representative X-Gal stained sections at trunk level of E13.5 $p57^{FL\text{-}ILZ\ (m)/+}$ embryo. Scale bar: 400μm. bw: body wall; di: digits; E: embryonic day; ea: ear; fb: forebrain, FL: forelimb; h: heart; HL: hindlimb; le: lens; mb: midbrain, nt: neural tube; som: somites; sv: sensory vibrissae; tvb-nc: thoracic vertebral body and notochord.

Figure 3. $p57^{FL\text{-}ILZ/+}$ adult mice display tissue-specific LacZ reporter expression.

(A-H) Heterozygote $p57^{FL\text{-}ILZ/+}$ animals with maternal inheritance of the transgene were used to evaluate postnatal LacZ reporter in kidney (A-A'), testis (B-B'), skeletal muscle (C-C'), salivary gland (D-D'), heart (E), brain (F), intestine (G) and lung (H) of adult mice (8-12 weeks of age). (A-H) Whole mount X-Gal staining. Asterisks indicate the magnified part appearing within the dashed box on the lower right corner. Scale bars: 2mm in non-magnified whole mount organs; 100μm in magnified panels of whole mount organs. (A'-D') X-Gal and eosin-stained sections of the corresponding organ. Scale bars: 100μm.

Figure 4. p57 protein loss in $p57^{cKO\text{-}ILZ/+}$ mice

(A-D) X-Gal staining of $p57^{FL\text{-}ILZ(m)/+}$ mice for thoracic vertebral body (A), forelimb cartilage (B), heart (C) and body wall (D). Asterisks indicate the magnified panel shown on the right of each photo. (E-L') Immunofluorescence for p57 (red) in control (E-H') and $p57^{cKO\text{-}ILZ(m)/+}$ (I-L') E13.5 tissues, corresponding to (A-D). Nuclei were counterstained blue with DAPI in (E-H) and (I-L). Scale bars: 100μm.

Figure 5. Phenotypes of *p57*$^{cKO\text{-}ILZ/+}$ mice

(A-F) Comparison of *p57*$^{cKO\text{-}ILZ\ (m)/+}$ mutants to control littermates. Heterozygote *p57*$^{cKO\text{-}ILZ\ (m)/+}$ animals with maternal inheritance of the transgene were used due to epigenetic silencing of the paternally transmitted p57 allele. Maternal transmission is indicated by superscript (m). (A) *In utero* and perinatal frequencies (fraction of control per total animals) of the indicated genotypes are shown. (B-C) Average body weight (B) and representative animals (C) for the indicated genotypes at birth. Error bars represent SD. Asterisk indicates significance; $p<0.05$. (D) Closed and cleft palate in control (upper panel) and *p57*$^{cKO\text{-}ILZ\ (m)/+}$ (lower panel) mice, respectively, at birth. Sections were stained with hematoxylin (nuclei) and eosin (cytoplasm). Scale bars: 2mm *in toto* samples; 100μm in sections. (E) Representative images of control gastrointestinal tract with milk in stomach and intestine (control, upper panel) and *p57*$^{cKO\text{-}ILZ\ (m)/+}$ inflated gastrointestinal tract (lower panel) at birth. Scale bar: 5mm. (F) Umbilical region of control (upper panel) and *p57*$^{cKO\text{-}ILZ\ (m)/+}$ mice (lower panel) at embryonic stages (E13.5; left panel) and at birth (P0; right panel). Sections were stained with hematoxylin and eosin. Scale bars: 2mm *in toto* samples; 100μm in sections. (G) Sternum and limb (forelimb, foot) of control (upper panel) and *p57*$^{cKO\text{-}ILZ\ (m)/+}$ mice (lower panel) at embryonic stages (E14.5; left panel) and at birth (P0; central and right panels). Skeletons were stained with alcian blue (cartilage) and alizarin red (bone). Black (E14.5) or white (P0) asterisk indicates sternum fusion defects. Arrows indicate limb thickening and shortening. Arrowheads indicate delayed ossification. Scale bars: 2mm at E14.5 sternum and P0 foot; 5mm at P0 sternum and forelimb. E13.5: embryonic day 13.5; Int: intestine; P: palate; PS: palatal shelve; P0: post-natal day 0; P1: post-natal day 1; S: stomach.

Supplementary figure 1. LacZ expression in *p57*$^{FL\text{-}ILZ/+}$ and *p57*$^{cKO\text{-}ILZ/+}$ mice

Reporter expression in the indicated tissues of *p57*$^{FL\text{-}ILZ/+}$ (left panel) and *p57*$^{cKO\text{-}ILZ\ (m)/+}$ (right panel) animals. Arrowheads indicate X-Gal-stained glomeruli in perinatal kidney cortex. Scale bars: 200μm. E13.5: embryonic day 13.5; P0: post-natal day 0.

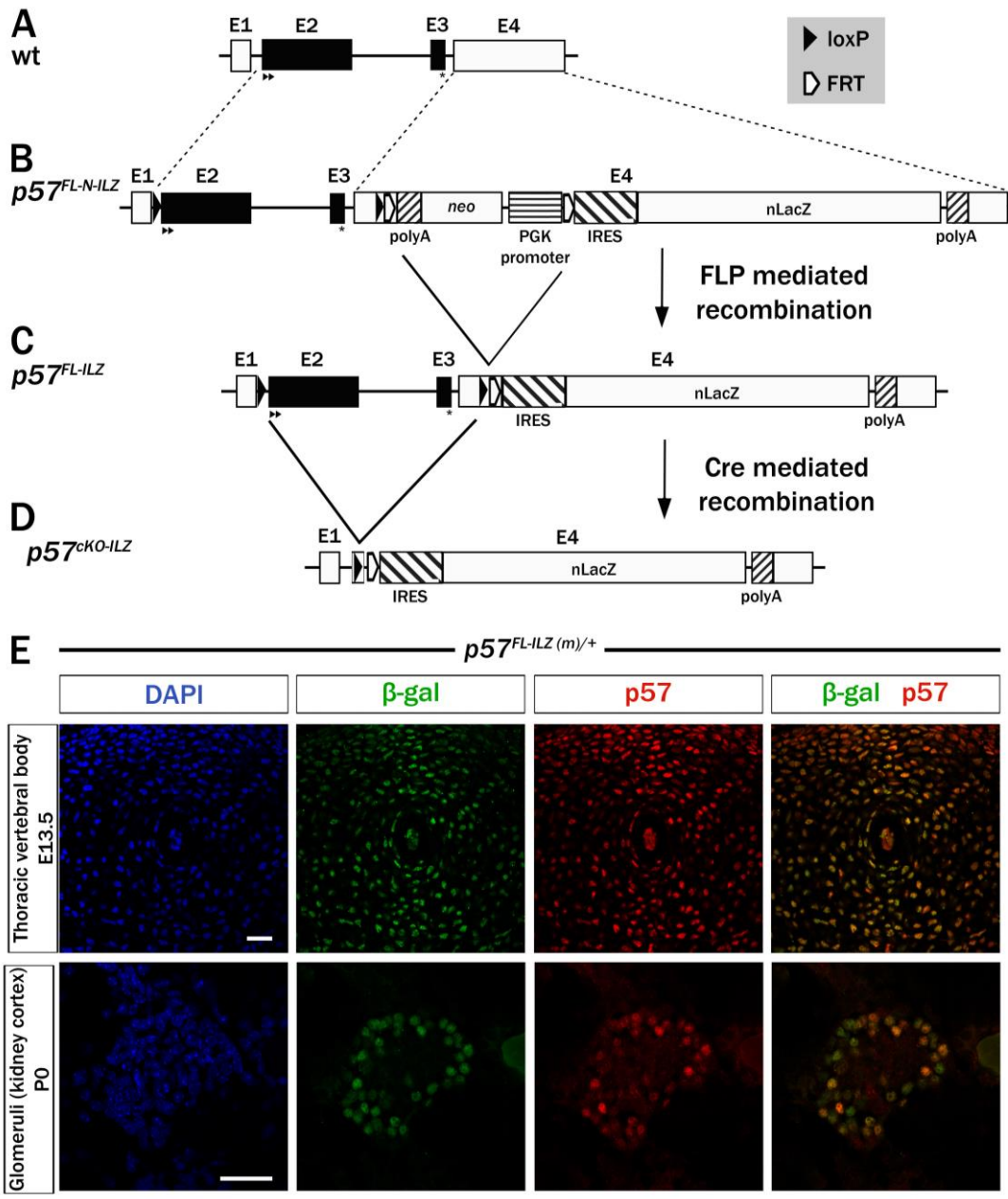
A
wt
E1
E2
E3
E4
loxP
FRT
B
p57FL-N-ILZ
neo
polyA
PGK promoter
IRES
nLacZ
polyA
FLP mediated recombination
C
p57FL-ILZ
IRES
nLacZ
polyA
Cre mediated recombination
D
p57cKO-ILZ
IRES
nLacZ
polyA
E
p57FL-ILZ (m)/+
DAPI
β-gal
p57
β-gal p57
Thoracic vertebral body E13.5
Glomeruli (kidney cortex) P0

Figure 1

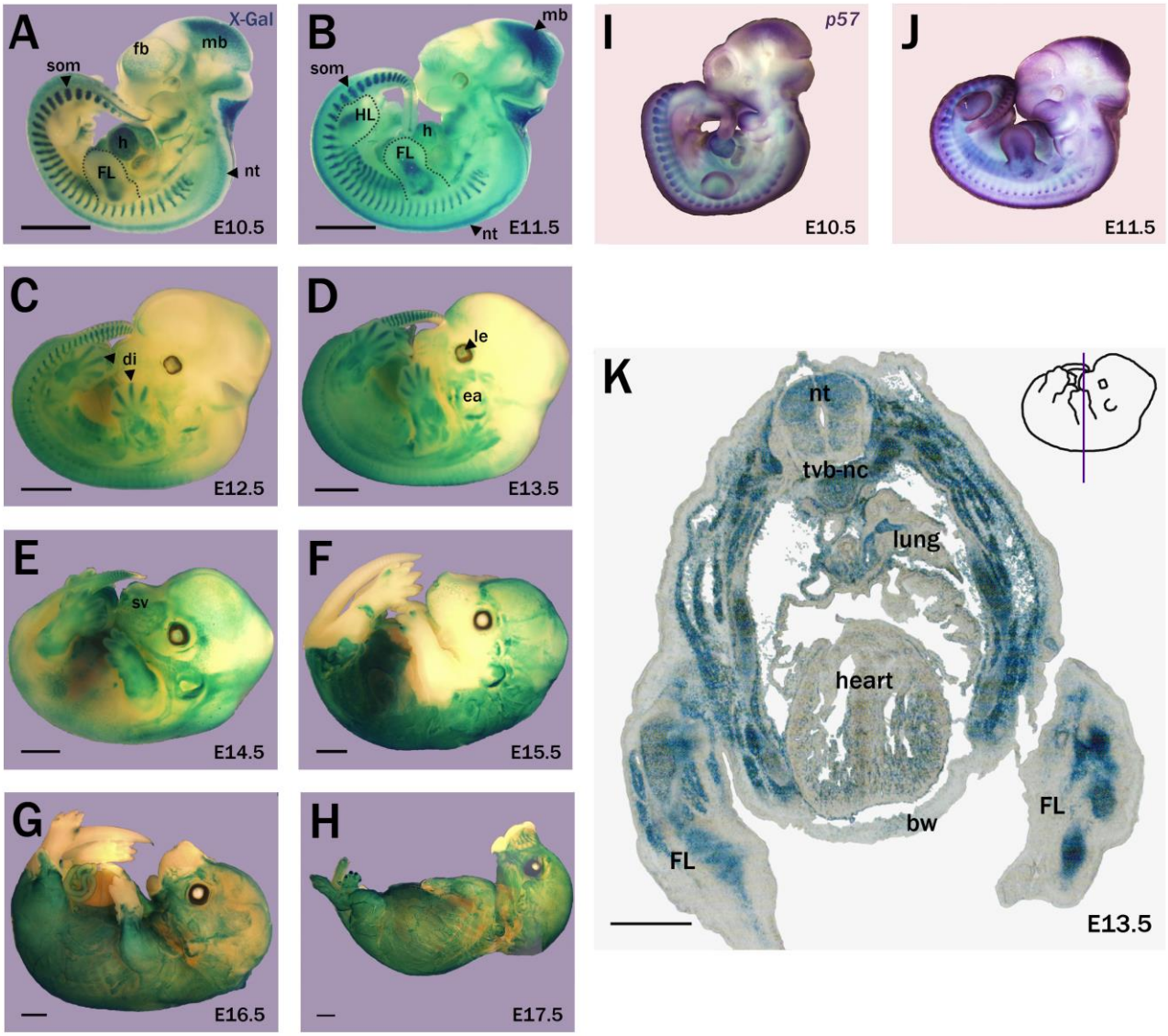
A
X-Gal
som
fb
mb
h
FL
nt
E10.5
B
mb
som
HL
h
FL
nt
E11.5
I
p57
E10.5
J
E11.5
C
di
E12.5
D
le
ea
E13.5
K
nt
tvb-nc
lung
heart
bw
FL
FL
E13.5
E
sv
E14.5
F
E15.5
G
E16.5
H
E17.5

Figure 2

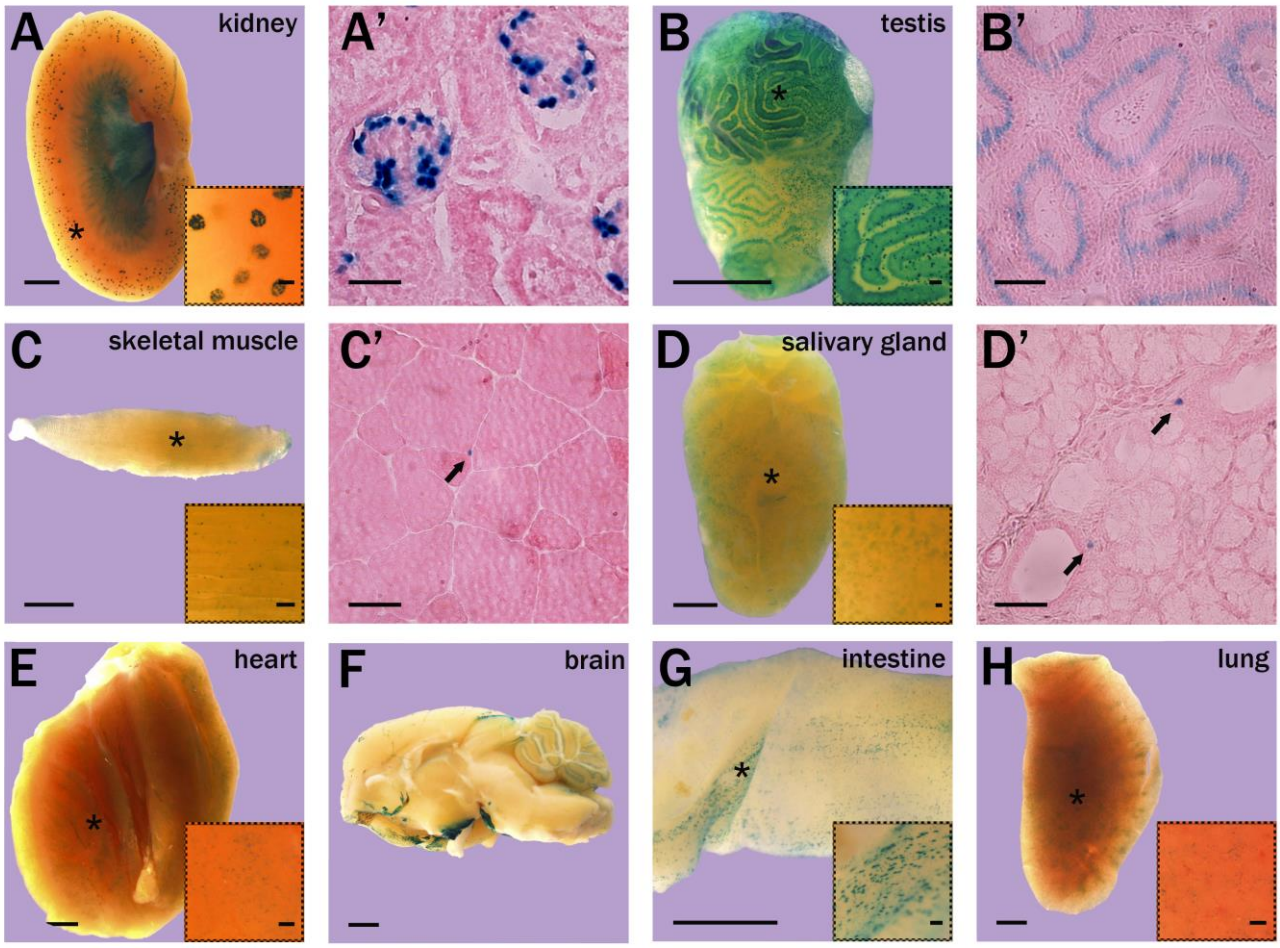
A
kidney
A'
B
testis
B'
C
skeletal muscle
C'
D
salivary gland
D'
E
heart
F
brain
G
intestine
H
lung

Figure 3

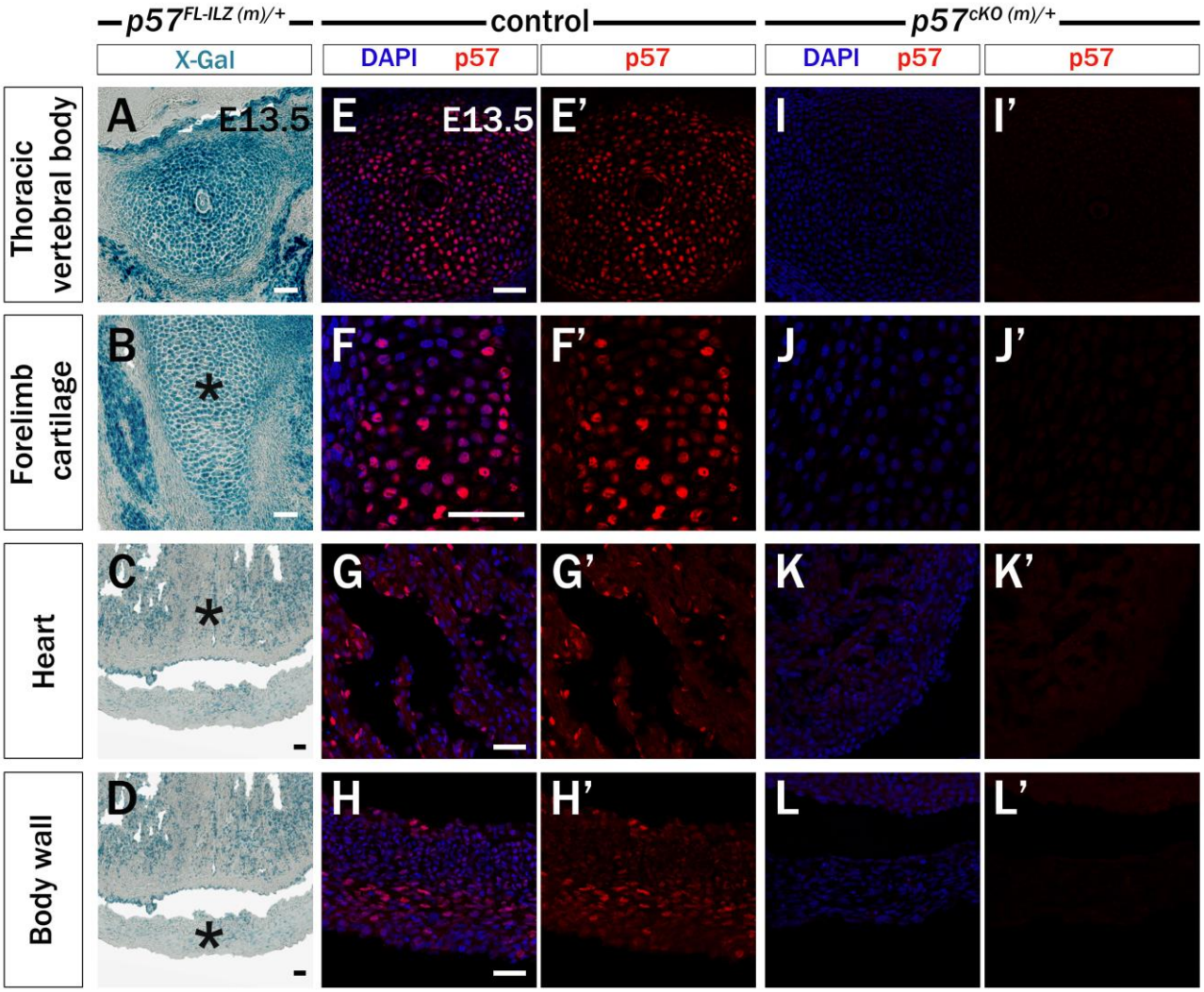
p57FL-ILZ (m)/+
control
p57cKO (m)/+
X-Gal
DAPI p57
p57
DAPI p57
p57
Thoracic vertebral body
Forelimb cartilage
Heart
Body wall
A
E13.5
E
E13.5
E'
I
I'
B
F
F'
J
J'
C
G
G'
K
K'
D
H
H'
L
L'

Figure 4

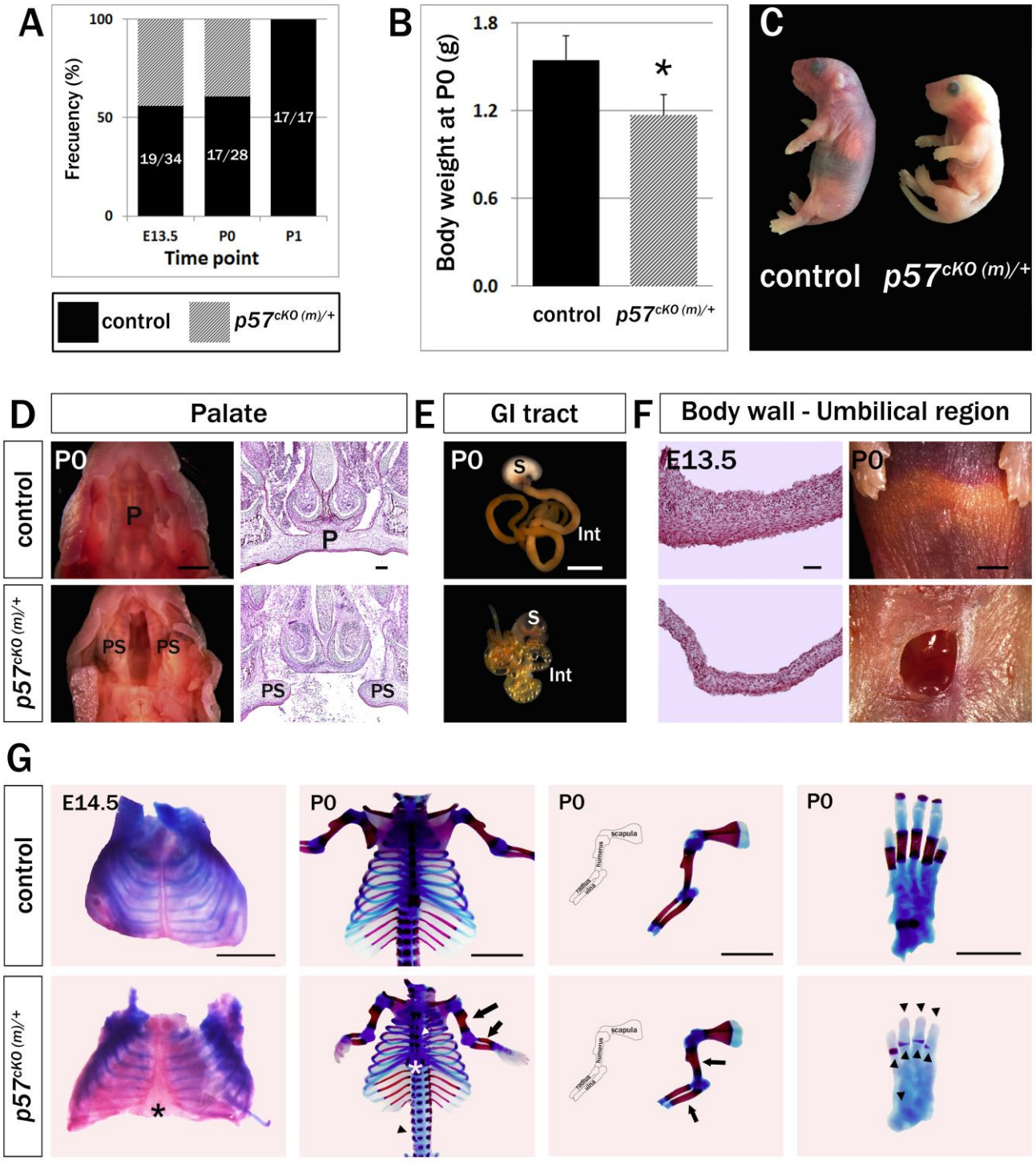
A
100
50
0
Frecuency (%)
19/34
17/28
17/17
E13.5
P0
P1
Time point
control
p57cKO (m)/+
B
1.8
1.2
0.6
0.0
Body weight at P0 (g)
*
control
p57cKO (m)/+
C
control
p57cKO (m)/+
D
Palate
E
GI tract
F
Body wall - Umbilical region
control
p57cKO (m)/+
P0
P
PS
S
Int
E13.5
G
E14.5
scapula
humerus
radius
ulna

Figure 5

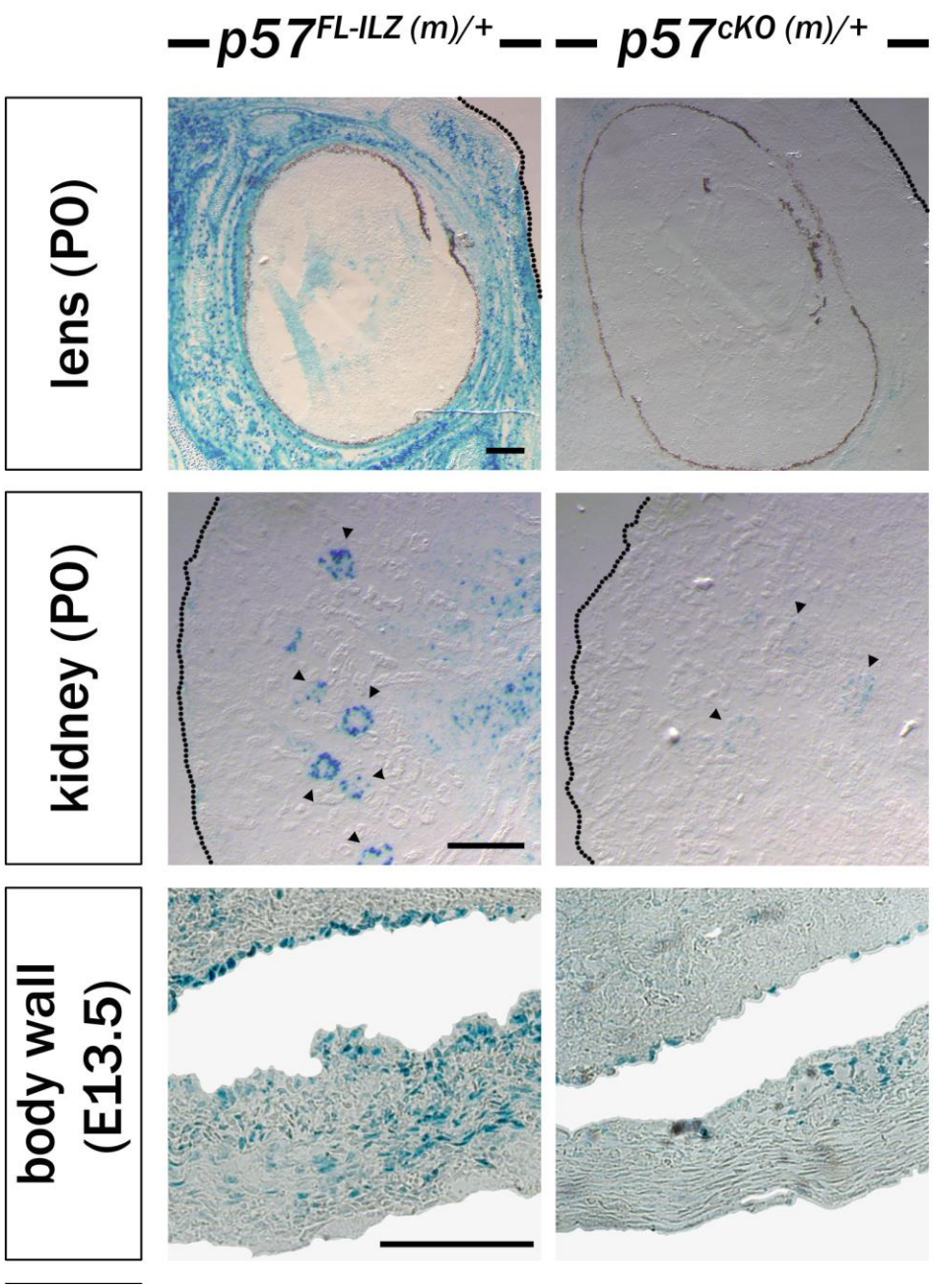

Figure S1

Preface

The CDKIs p57 and p21 have been shown to play crucial roles in cell cycle regulation of the nascent musculature. To identify their role in postnatal myogenesis we investigated their expression, function, and regulation in adult muscle stem cells, called satellite cells. The quiescent satellite cells that reside in resting adult muscles were devoid of p21, while this factor was upregulated following satellite cell activation (even in proliferating myoblasts) and differentiation. In single myofiber cultures and at early post-injury muscle regeneration time points, p21 deficiency affected the dynamics of satellite cells, indicating p21 importance in the early post-activation events. Specifically, *ex vivo*, proliferation/activation were increased at the expense of differentiation, while *in vivo*, the satellite cell compartment was significantly reduced. However, both the satellite cell numbers and the muscle architecture were restored at the end of injury-induced regeneration. Given p21 and p57 overlapping function in embryonic myogenesis, we have investigated p57 in the adult context. Same as for p21, p57 was absent from quiescent satellite cells. In contrast, we detected it in the cytoplasm of activated cells with increasing nuclear translocation upon differentiation. Using the new conditional p57 knock-out, we induced satellite cell-specific p57 ablation and observed a marked differentiation deficit of satellite cell-derived myoblasts *in vitro*. Thus, our data implicate p21 and p57 in muscle cell cycle dynamics postnatally.

Distinct regulation and function of p21 and p57 during muscle stem cell activation and differentiation

Despoina Mademtzoglou[a,b], Sonia Alonso-Martin [a,b,c], Philippos Mourikis [a,b], Frédéric Relaix [a,b,d,e*]

a. Inserm, IMRB U955-E10, F-94010, Creteil, France
b. Université Paris Est, Faculté de medecine, F-94000, Creteil, & Ecole Nationale Veterinaire d'Alfort, 94700, Maison Alfort, France
c. Present address : Tissue Regeneration Laboratory, Centro Nacional de Investigaciones Cardiovasculares (CNIC), Madrid, Spain
d. Etablissement Français du Sang, 94017, Creteil, France
e. APHP, Hopitaux Universitaires Henri Mondor, DHU Pepsy & Centre de Référence des Maladies Neuromusculaires GNMH, 94000 Créteil France

* Correspondence : Pr Frederic Relaix
IMRB-E10, 8 rue du General Sarrail 94010 Creteil France
Frederic.relaix@inserm.fr
+33 (0) 1 49 81 39 40

KEYWORDS

Satellite cells, cyclin-dependent kinase inhibitors, p21, p57, cell cycle, muscle regeneration.

ABSTRACT

Adult tissue maintenance and regeneration depends on efficient stem cell self-renewal and differentiation. In skeletal muscle the contributors to postnatal muscle growth, maintenance, and repair are the muscle satellite cells (mSCs), residing on the periphery of the syncytial post-mitotic myofibers. The mechanisms coordinating the regulation of cell cycle exit with activation, renewal and differentiation of the mSCs remain poorly understood in adult muscle. Here, we investigated the role of specific cyclin-dependent kinase inhibitors in adult mSCs that up to date have been linked to embryonic myogenesis. We show that p21 is not detected in quiescent adult mSCs, but it is induced in activated and differentiating myoblasts. Using an *ex vivo* single myofiber explant system, we examined the kinetics of myoblast production/differentiation of p21-null mice, and we observed an increase in activation and proliferation accompanied by a diminution of differentiation. *In vivo* muscle regeneration studies in the absence of p21 revealed a decrease in mSCs at day 5 post-injury, confirming a role of p21 in the early activation phase of mSCs. On the contrary, muscle architecture and mSC numbers were restored by day 28, indicative of complete regeneration. Since p21 and p57 have been shown to redundantly control embryonic myogenesis, we evaluated if p57 functions in adult myogenesis. Although p57 was absent from quiescent mSCs, it was expressed in their activated and differentiating progeny. We further demonstrate that p57 expression and subcellular localization are dynamic; exclusively cytoplasmic p57 is first observed in activated/proliferating myoblasts, while progressive nuclear translocation is associated with differentiation and growth arrest. p57-deficient myoblasts displayed a marked differentiation deficit, manifested by reduction in MYOGENIN+ cells and, subsequently, formation of smaller myotubes. Our data suggest that p21 and p57 play distinct functions both at the early steps of mSC activation and during differentiation.

INTRODUCTION

Adult regeneration is of vital importance for restoring tissue structure and function following damage. Skeletal muscle has a remarkable capacity to self-repair after severe injuries, a process dependent on muscle stem cells, the so-called muscle satellite cells (mSCs) [Relaix & Zammit, 2012]. mSCs originate from a PAX3/7+ progenitor population that in late fetal life acquires their characteristic anatomical position between the basal lamina and the plasma membrane of muscle fibers [Mauro, 1961; Relaix et al., 2005]. mSCs are involved in postnatal muscle growth [White et al., 2010; Pawlikowski et al., 2015], maintenance [Keefe et al., 2015; Pawlikowski et al., 2015], and regeneration upon injury or in many neuromuscular disorders [Lepper et al., 2011; McCarthy et al., 2011; Murphy et al., 2011; Sambasivan et al., 2011]. Juvenile mSCs acquire a non-proliferative, quiescent state around three weeks of post-natal life to preserve key functions [White et al., 2010; Cheung & Rando, 2013]. However, once stimulated by homeostatic demand or damage, mSCs become activated, re-enter cell cycle and provide differentiated progeny for muscle repair, while a subpopulation self-renews the quiescent pool [Relaix & Zammit, 2012]. The myogenic regulatory factors MYOD and MYOGENIN orchestrate mSC commitment and progression through the myogenic lineage [Wang et al., 2014], while the signals that trigger cell cycle exit and (re-)entry into quiescence remain more elusive.

Cell cycle is a synchronized process responding to positive and negative signals, while inappropriate growth arrest can result in cancer, in malformations during development, and in defective stem cell renewal [Zhang et al., 1997; Matsumoto et al., 2011; Sherr, 2012]. The common negative cell cycle regulators are Cyclin-Dependent Kinase Inhibitors (CDKIs). CDKIs are classified in two structurally and functionally defined families [Borriello et al., 2011]: the INK4 family [including $p15^{Ink4b}$ (p15), $p16^{Ink4a}$ (p16), $p18^{Inc4c}$ (p18), $p19^{Ink4d}$ (p19)] and the Cip/Kip family [including $p21^{Cip1}$ (p21), $p27^{Kip1}$ (p27), $p57^{Kip2}$ (p57)]. Although members of the Cip/Kip family have been shown to control proliferation and differentiation in embryonic muscle or in myoblasts *in vitro*, their potential involvement in mSC quiescence and cell fate decisions has not been documented [Halevy et al., 1995; Reynaud et al., 1999; Zhang et al., 1999; Messina et al., 2005; Chakkalakal et al., 2014; Zalc et al., 2014].

Given that p21 and p57 redundantly control embryonic skeletal muscle differentiation (Zhang et al., 1999), we explored their role in adult myogenesis and regeneration. We show here that p21 and p57 are not detected in quiescent mSCs, but are induced upon activation and maintained in differentiating myogenic cells. We further show that p57 subcellular localization is specifically regulated during adult myogenesis, with a progressive cytoplasmic to nuclear translocation as activated myoblasts proceed to differentiation. Using mouse mutants

and *ex vivo* analysis, we provide evidence that both p21 and p57 are distinctly involved in the early activation events, while their genetic ablation led to decreased differentiation, increased proliferation, and mSC pool diminution. Our results imply that growth arrest is dynamically controlled, with p21 and p57 playing distinct functions during adult myogenesis.

RESULTS

p21 is expressed in mSCs following their activation

To analyze the expression of p21 in muscle satellite cells (mSCs) in different states, including self-renewal and differentiation, while they are still exposed to their physical niche, we used the well-established myofiber culture system [Zammit et al., 2004; Moyle & Zammit, 2014]. We isolated single myofibers with their associated PAX7+ mSCs from *Extensor digitorum longus* (EDL) muscles of adult wildtype mice (Figs. 1A). Quiescent mSCs of freshly isolated fibers (time point 0; T0) were not labeled using antibodies against p21 (Fig. 1A-B, I). In line with this, we could not detect expression of p21 in the PAX7+ mSCs in cross-sections of resting adult *Tibialis anterior* (TA) muscles (Fig. 1C-D).

To evaluate the expression of p21 during activation, self-renewal and differentiation, we performed myofiber culture for 24-72 hours. The culture conditions allow the mSCs to get activated at T24-48 and proceed to myogenic differentiation or self-renewal of the quiescent pool (T72) [Zammit et al., 2004]. During the initial proliferation state (T24-T48) the activated mSCs co-express PAX7 and MYOD [Zammit et al., 2004]. In contrast to the quiescent population, we detected increasing levels of p21 in activated mSCs (Fig. 1I-J). By 24 hours nearly half the activated PAX7+/MYOD+ cells express p21, while almost all the PAX7+ or MYOD+ cells are p21+ at 48 hours. At T72 divergent mSC fates can be monitored including differentiation (downregulation of *Pax7* associated with expression of *MyoD* and *Myogenin*) and self-renewal (maintenance of PAX7, loss of MYOD, and lack of MYOGENIN) [Zammit et al., 2004]. p21 remained high at that time point of the culture (Fig. 1E-L). PAX7+MYOD+ cells at T72 represent activated cells [Zammit et al., 2004], suggesting that some p21+PAX7+ and p21+MYOD+ cells are proliferating myoblasts which express a cell growth arrest factor as in T48 (Fig. 1I-J). To confirm this unexpected observation, we labelled cycling cells with an antibody against KI67 and observed that indeed a high percentage of KI67+ myoblasts were co-expressing p21 (Fig. 1L). Finally, as expected, p21 presented a solid expression in differentiating MYOD+ and MYOGENIN+ cells at T72 (Fig. 1G-H, J-K).

Loss of p21 affects early phase of mSC activation

To evaluate the role of p21 on muscle homeostasis, we quantified the ratio of muscle weight per body weight and the relative number of mSCs in *p21* mutant mice compared to controls. We did not observe significant variations in the size and weight of limb muscles or diaphragm in mutant mice compared to controls (Fig. 2A). Trunk muscles did not exhibit any difference either (data not shown), although dissection limitations render this comparison less reliable. The number PAX7+ cells per 100 fibers was similar in *p21* mutant mice compared to controls, suggesting that the mSC compartment has been correctly established in the absence of p21 (Fig. 2B-D). We did not observe centrally located nuclei, indicative of ongoing regeneration, in muscle cross-sections (data not shown). Furthermore, freshly isolated myofibers of mutant and control EDLs had comparable amounts of mSCs and no PAX7+ cells were expressing KI67 at T0 (data not shown), implying that mSCs correctly exited cell cycle postnatally and entered into quiescence.

We then examined the kinetics of myoblast production and differentiation upon p21 depletion using single myofiber cultures. At T72, mSC-derived myoblasts represent a mixed population (see above) and PAX7/MYOD immunostaining can reveal self-renewing (PAX7+MYOD-), activated/proliferating (PAX7+MYOD+), and differentiating (PAX7-MYOD+) myoblasts [Zammit et al., 2004]. In the absence of p21, we observed an increased proliferation, as evidenced by the fraction of activated PAX7+MYOD+ myoblasts (Fig.2E) and confirmed by quantification of the cycling, KI67+ myoblasts per fiber (Fig. 2F). Self-renewal (PAX7+MYOD-) did not seem to be affected (Fig. 2E), but we observed prolonged activation (PAX7+MYOD+) at the expense of differentiation (PAX7-MYOD+) (Fig. 2E). Moreover, we found less MYOGENIN+ differentiating myoblasts per fiber in *p21* mutants (Fig. 2G). These data suggest that p21 functions at the early phase of satellite cell activation to limit proliferation during the proliferative phase, and p21 deficiency affects their proliferation and differentiation.

Next, we evaluated the impact of p21 loss of function for skeletal muscle regeneration. We performed intra-muscular cardiotoxin injections into the TA and sacrificed the mice at 5, 10 and 28 days post-injury, to evaluate early, intermediate and late time points of the regeneration procedure. Once muscle degeneration is induced, mSCs undergo a sequence of events similar to the myofiber culture: (1) get activated, (2) proliferate to expand their population, and (3) self-renew their quiescent pool for future needs and provide differentiated progeny for new fiber formation and muscle repair [Relaix & Zammit, 2012]. Our histological analysis of injured muscle did not show abnormalities in *p21* mutant mice (Fig. 3A-F). During the first post-injury days, damaged muscle show extensive inflammatory cell infiltration and muscle progenitor proliferation [Paylor et al., 2011]. Accordingly, we observed increased cellular content of control and mutant muscles at D5 of regeneration (Fig.

3A-B). Normal tissue structure, with well-formed myofibers and diminished interstitial space, was restored at similar time in controls and mutants (Fig. 4C-F). Deposition of fibrotic and adipose tissue was similar between controls and mutants at all time points analyzed (data not shown). Since our *ex vivo* data suggest an early activation defect upon p21 ablation (Fig. 3), we evaluated the mSC population throughout regeneration. Injury-triggered mSC pool amplification led to a remarkable increase of the PAX7+ population at D5 post-cardiotoxin in controls and mutants (Fig. 3M). However, significantly less mSCs were present in the *p21*-null animals at D5 (Fig. 3G-H, M). At later time points no significant difference was observed (Fig. 3I-M). In both controls and mutants, mSC numbers decreased back to baseline levels once their contribution to muscle regeneration was finished at D28 (Fig. 2D, 3M).

Combining the observed *ex vivo* defective differentiation/proliferation with the *in vivo* normal muscle regeneration and mSC pool restoration, we conclude that p21 regulates the early phase of mSC activation, leading to a delay but not a complete impairment of their performance. Our results suggest that p21 is involved in the fine tuning of activated satellite cells proliferation.

p57 is expressed in activated but not quiescent mSCs

Since embryonic muscle growth arrest was redundantly controlled by p21 and p57, we next evaluated if p57 also operates during adult myogenesis. We first examined p57 expression in mSCs in myofiber cultures and *in vivo* resting muscle (Fig. 4). On freshly isolated myofibers (T0), quiescent PAX7+ mSCs did not express p57 (Fig. 4A), while culture-mediated mSC activation induced p57 expression in PAX7/MYOD+ myoblasts at T24-T48 (Fig 4A-B). In line with this, mSCs of resting adult TA muscles were p57-negative (Fig. 4C). However, p57 was detected in non-myogenic interstitial cells, consistently with previous reports of p57 presence in adult muscle extracts [Matsuoka et al., 1995; Park & Chung, 2001].

We next evaluated the kinetics of p57 expression in mSCs upon *ex vivo* activation in myofiber cultures. Activated PAX7+ (Fig. 5A) and MYOD+ (Fig. 5B) myoblasts at T24-T48 presented with increasing amounts of p57. Remarkably, during the early activation/proliferation phase, p57 was restricted to the cytoplasm (Figs. 4A-B, 5A-B). At T72, there is a mixed population of self-renewing (corresponding to part of Pax7+ cells), activated/proliferating (part of PAX7+ and MYOD+ cells), and differentiating (MYOGENIN+ and part of MYOD+ cells) myoblasts [Zammit et al., 2004]. We observed high percentages of p57 in each of these populations (Fig. 5A-C). Of note, as differentiation proceeded (MYOD+ followed by MYOGENIN+ at T72), p57 expression was becoming increasingly nuclear (Fig. 5B-C). Although p57 was mostly cytoplasmic in PAX7+p57+ T72 myoblasts,

p57 exhibited nuclear presence in around 25% of MYOD+p57+ and 55% of MYOGENIN+p57+ T72 myoblasts (Fig. 5A-C). Finally, similarly to the T24-T48 activated/cycling populations, p57 continued to be present in KI67+ proliferating cells at T72, yet limited to their cytoplasm (Fig. 5D). These results suggest that in contrast to p21, nuclear expression of p57 is not compatible with the proliferative status of activated satellite cells.

Loss of p57 affects myogenic differentiation

To circumvent the early perinatal lethality of *p57* knock-out mice, we have generated a floxed *p57* allele ($p57^{Flox\text{-}ILZ}$) to enable conditional abrogation of p57 using the Cre/loxP system [Mademtzoglou et al., submitted]. To selectively ablate p57 from the mSCs and their progeny, we intercrossed $p57^{Flox\text{-}ILZ}$ mice with the $Pax7^{CreERT2}$ line [Lepper et al., 2009]. In the resulting mice, Cre expression and p57 excision are dependent on tamoxifen (TMX) induction. Administration of TMX (intraperitoneal injections) or 4-hydroxytamoxifen (in culture) failed to efficiently recombine *p57* locus (Fig. S1A-C), hindering subsequent *in vivo* analyses of *p57*-deficient muscles in $Pax7^{CreERT2}$; $p57^{Flox\text{-}ILZ}$ animals. To improve the efficiency of recombination, we crossed floxed animals with $Pax3^{Cre}$ mice [Engleka et al., 2005], targeting the muscle lineage from early embryonic stages. However, high levels of p57 protein in the mSC progeny were still observed in myofiber cultures (Fig. S1D). We then inserted $p57^{Flox\text{-}ILZ}$ and $Pax7^{CreERT2}$ in the background of the Cre-responsive two-color fluorescent reporter $ROSA^{mT/mG}$, to allow the selection of recombined GFP+ cells. FACS-sorted cells grew in high serum conditions and then were serum-deprived to differentiate for 1 or 3 days and stained with early (e.g. Myogenin) or late (i.e. Myosin Heavy Chain-MyHC) differentiation markers, respectively (Fig 6A). p57 transcript and protein were induced by differentiation in the control cells (Fig. 6B-C, E). On the contrary, they were almost undetectable in cells from mutant animals (Fig. 6B, D-E), while p21 showed same levels in controls and mutants (Fig. 6B). In primary cultures of FACS-sorted satellite cells from *p57*-deficient mice, myogenic differentiation was impaired. One-day post-differentiation, myogenin expression was significantly decreased (Fig. 6F-H). Furthermore, myotube formation three days-post-differentiation was severely compromised (Fig. 3G-H). In conclusion, muscle regeneration in the absence of p57 could not be evaluated, despite promising *in vitro* results (Fig. 6) which strongly implicated p57 in the regulation of postnatal myogenesis.

DISCUSSION

Regenerative adult myogenesis is crucial for recovery from injuries, but can be compromised by degenerative or disease states that affect the functional capacity of skeletal muscle stem cells, the satellite cells (mSCs). The maintenance of mSCs functions largely depends on the entry and maintenance of a non-cycling, reversible

quiescent state. The molecular mechanisms that control mSC cell cycle transitions and adult myogenesis have gained significant interest in recent years, as a way to understand post-trauma tissue restoration and, subsequently, to design efficient innovative therapies when it is defective.

Given the essential, yet redundant, role of p21 and p57 in embryonic and fetal myogenesis [Zhang et al., 1999], we hypothesized that they may also control cell cycle and differentiation of mSCs in adult muscle. We found that p21 protein is not expressed in resting muscle cells, including quiescent mSCs (Fig. 1). This observation is in agreement with previous reports for negligible p21 mRNA [Macleod et al., 1995] or protein [Franklin & Xiong, 1996] in adult muscle, but contradicts reports for high *p21* transcripts [Parker et al., 1995; Park & Chung, 2001]; variance in analyzed muscles, mouse background, age window, and probes, could account for these differences. *p21* null mice do not exhibit any muscle phenotypes during development [Zhang et al., 1999], and as we did not observe p21 expression in resting adult muscles (Fig. 1C-D), we expected no differences in resting muscles of mutant and control animals. Indeed, muscle weight, architecture, and mSC numbers were not affected in the absence of p21 (Fig. 2A-D), consistent with previous reports [Deng et al., 1995; Hawke et al., 2003; Chakkalakal et al., 2014; Chinzei et al., 2015].

Similarly to p21, we did not detect p57 in quiescent mSCs on sections or isolated myofibers of resting adult (8-12 weeks) muscle (Fig. 4A, C), while it was abundant in interstitial cells (Fig. 4C). Our finding is consistent with previous reports of high p57 levels in adult muscle [Matsuoka et al., 1995; Park & Chung, 2001] and lack of p57 in FACS-sorted postnatal mSC populations at different ages and dormancy states [Chakkalakal et al., 2014]. In contrast, an early study detected p57 in quiescent mSCs [Fukada et al., 2007] which were isolated with a FACS protocol using an antibody previously described by the same group [Fukada et al., 2004]. However, this antibody immuno-reacts with bone marrow cells [Fukada et al., 2004], where p57 has a well-established role and presence in the hematopoietic lineage [Matsumoto et al, 2011; Zou et al., 2011]. Furthermore, p57 immunostaining in Fukada et al. [2007] were performed with an antibody against the p57 carboxy-terminus, which might cross-react with the respective domain of p27 [Matsuoka et al., 1995; Galea et al., 2008; Pateras et al., 2009]. Combining our observation with previous reports [Fukada et al., 2004; 2007; Chakkalakal et al., 2014; present study], we conclude that quiescent mSCs do not express p57. Instead, it is established that they express p27, the other CDKI of the family including p21 and p57 [Chakkalakal et al., 2014; our unpublished data]. However, this observation does not preclude p21 and p57 participation in mSC cell cycle dynamics; in the pituitary p57 was found to promote cell cycle exit, while p27 prevented cell cycle re-entry [Bilodeau et al., 2009].

Previous reports demonstrated that p21 and p57 are required to drive embryonic muscle progenitors out of the cell cycle during terminal differentiation [Zhang et al., 1999]. Consistently, we found that p21 and p57 are not expressed in quiescent mSCs (Figs. 1, 4, 5). Yet we show that they are unexpectedly upregulated upon *in vitro* activation in proliferating mSCs (Figs. 1, 4, 5). Although T24-T48 cells are still cycling [Zammit et al., 2004], they were expressing cell cycle inhibitors, such as p57 (Fig. 5A-B) and p21 (Fig. 1I-J). Furthermore, many KI67+ cells at T72 expressed p57 (Fig. 1L) or p21 (Fig. 5D). Accordingly, post-regeneration activation of mSCs has been shown to induce p21 and p57 with their levels peaking at D3-4 [Yan et al., 2003; our unpublished observations]. The appearance of p21 and p57 might be associated with MYOD expression. MYOD is expressed soon after mSC activation [Zammit et al., 2004; Zhang et al., 2010] and sustains the transition from quiescence to cell cycle via the replication-related factor CDC6 [Zhang et al., 2010]. MYOD induces growth arrest in non-myogenic cell lines [Crescenzi et al., 1990; Sorrentino et al., 1990] and has a well-established role for the entry into the myogenic lineage. Remarkably, despite MYOD robust expression, myoblasts continue to proliferate and do not proceed to differentiation for several days [Tajbakhsh, 2009]. In fact, in dividing myoblasts MYOD activity is inhibited by Id proteins and CDK/Cyclin complexes [Wei & Paterson, 2001]. Furthermore, additional factors, including MYOGENIN, were suggested to initiate or enhance transcription in part of MYOD targets [Blais et al., 2005; Cao et al., 2006].

Both p21 and p57 have been implicated in positive feedback loops with MYOD, whereby MYOD induces them and they in turn enhance MYOD activity and stabilization in cultured cells or *in vivo*. Specifically, MYOD promoted *p21* transcription [Halevy et al., 1995; Tintignac et al., 2004], while in its absence p21 expression was delayed during muscle development [Parker et al., 1995]. p21 stabilized MYOD by inhibiting its phosphorylation [Reynaud et al., 1999], while non-phosphorylable MYOD sustained p21 expression [Tintignac et al., 2004]. MYOD induced *p57* both by disrupting a chromatin loop to release the *p57* promoter and by upregulating intermediate factors [Vaccarello et al., 2006; Figliola et al., 2008; Busanello et al., 2012; Battistelli et al., 2014]. Furthermore, we previously identified a muscle-specific *p57* regulatory element that MYOD binds and transactivates [Zalc et al., 2014]. Co-immunoprecipitation assays revealed direct p57-MYOD binding [Reynaud et al., 2000]. Loss- and gain-of-function experiments in zebrafish embryos established a positive feedback loop between p57 and MYOD [Osborn et al., 2011].

Upon mSC activation, p21 and p57 were expressed in proliferating myoblasts in single myofiber cultures (Figs. 1, 4, 5), including T24-T48 cycling populations as well as KI67+ cells at T72. These observations might contradict

their traditional role as cell cycle exit factors [Gu et al., 1993; Harper et al., 1993; Xiong et al., 1993; Lee et al., 1995; Matsuoka et al., 1995]. However, at low concentrations, p21 promotes assembly and nuclear localization of CDK/Cyclin complexes, whereas at high amounts it exhibits its inhibitory activity towards them [Michieli et al., 1994; Harper et al., 1995; LaBaer et al., 1997]. Similarly, p21 is involved in nuclear accumulation and activity of CDK/Cyclin complexes in fibroblasts converted to myogenic fate [Peschiaroli et al., 2002], while differentiation of the C2C12 myogenic cell line leads to increased inhibition of CDK4 by p21 [Wang & Walsh, 1996]. It remains to be verified whether these interactions are at play in our experimental system. The fact that p21 ablation caused increased proliferation in the myofiber cultures (Fig. 4) suggests that p21 is involved in restraining the cell cycle.

The role of p57 in cycling myoblasts of isolated myofiber cultures seems to be more complex. p57 is cytosolically restricted in activated myoblasts but translocates to the nucleus as differentiation progresses (Fig. 5). We have not identified the molecular events underlying this shuttling, although some observations might explain this subcellular localization pattern. Firstly, p57 might be regulated on the cellular level, by cytoplasmic restriction during proliferation. A similar mechanism was shown for ERK signaling in muscle progenitors, whereby switching from proliferation to differentiation was associated with subcellular ERK localization [Michailovici et al., 2014]. Secondly, p57 could be implicated in cell cycle progression through CDK/Cyclin assembly, similarly to its Cip/Kip siblings (see above). In the absence of p21 and p27, p57 resumes their role in CDK/Cyclin complex stabilization in mouse embryonic fibroblasts [Cerqueira et al., 2014]. However, this might be less likely in myoblasts, where p57-MYOD binding engages the p57 helix domain [Reynaud et al., 2000] that was found indispensable for CDK/Cyclin binding and inhibition [Hashimoto et al., 1998; Reynaud et al., 2000]. Thirdly, p57 could be involved in nucleo-cytoplasmic distribution of cyclins or CDKs, as previously observed in other cell types. p57 has been shown to interfere with the nuclear translocation of cyclin D1 [Zou et al., 2011] and to relocalize fraction of CDK2 in the cytoplasm [Figliola & Maione, 2004]. Fourthly, while in the cytoplasm, p57 might participate in mSC mobilization, one of the earliest manifestations of their activation [Siegel et al., 2009]. Cytoplasmic p57 was described to regulate cell motility together with LIM-kinase1 [Vlachos & Joseph, 2009; Chow et al., 2011; Guo et al., 2015]. Although we did not detect LIM-kinase1 in our myofiber cultures, we cannot exclude association with other, yet uncharacterized, partners. Future studies are expected to elucidate the roles of p57 in different sub-cellular compartments of myoblasts.

p21 did not undergo nucleo-cytoplasmic translocation in myoblasts of myofiber cultures (Fig. 1). Similarly, p21 is strictly nuclear in forming myotubes [Figliola & Maione, 2004] and p21, but not p57 or p27, appears in the

nucleus of KI67+ proliferating b-cells [Fiaschi-Taesch et al., 2013]. Moreover, cytoplasmic presence of p21 is linked to degradation [Hwang et al., 2009] or oncogenesis [Besson et al., 2004; Besson et al., 2008]. Finally, p21 might not be subjected to regulation on the cellular level (e.g. initial cytoplasmic restriction), because of its role in the early events following mSC activation phase (Figs. 2-3), and at a moderate level, p21 expression is compatible with proliferation, which might not be the case for p57.

p21 and p57 were shown to function in a redundant manner during differentiation of embryonic myogenic cells. On the contrary, in the adult we observed early differentiation and proliferation defects in single mutants, implying lack of such compensation in the initial post-activation phase. Monitoring of myoblast kinetics at the early post-activation period showed that in the absence of p21 there was a differentiation deficit and proliferation increase *in vitro* as well as diminution of the mSC pool *in vivo* (Figs. 2-3). However, muscle regeneration was completed by 28 days post-injury, leading to indistinguishable muscle structure and mSC numbers between controls and mutants (Fig. 3). Similarly, mSCs and muscle architecture were restored by 28-30 days post-injury in previous studies [Hawke et al., 2003; Chakkalakal et al., 2014; Chinzei et al., 2015], despite occasional defects at earlier time points [Hawke et al., 2003; Chinzei et al., 2015]. This implies a crucial role during the early activation events, while at later stages p21 either becomes dispensable or its role is masked by compensatory upregulation of other factors. Future studies with *p21/p57* double knock-out mice are expected to be more enlightening. In contrast to the myogenic differentiation defects observed with *p21*-null mice, siRNA-mediated p21 knock-down in primary myoblast cultures left myogenic differentiation unaffected [Biferi et al., 2015]. The difference was attributed to the effect of acute versus chronic p21 loss, while conditional genetic ablation of p21 with the loxP-Cre system would allow test this hypothesis.

p57 deficiency hindered myoblast differentiation and myotube formation (Fig. 6). p57 correlates with differentiation in many tissues [Westbury et al., 2001], while in myogenic cultures is sometimes considered as a differentiation marker [Reynaud et al., 1999; Mounier et al., 2011]. Nevertheless, the consequences of its ablation on adult muscle have not been examined, notably because of the perinatal lethality of p57 mutant mice, which our new conditional knock-out allele should allow to bypass [Mademtzoglou et al., submitted]. Flanking the coding exons 2-3 by LoxP sites ensured postnatal survival while leaving the possibility of Cre-induced excision [Mademtzoglou et al., submitted]. Our data implicate p57 in adult myogenesis, with the caveat that such observations are limited to an *in vitro* system lacking the structural, neurogenic, and metabolic fidelity of the muscle tissue [Grounds, 2014]. *In vivo* regeneration studies would decipher if and how p57 influences the re-establishment of mSC pool post-injury, given its emerging importance in the quiescence

and renewal of other stem cells [Matsumoto et a., 2011; Zacharek et al., 2011; Furutachi et al., 2013]. However, *in vivo* analysis was hindered by inefficient recombination (Fig. S1). Previous studies suggest that recombination resistance/success in mSCs is related to the cell cycle state (quiescence versus activation/proliferation) [Lepper et al., 2009; Günther et al., 2013; von Maltzahn et al., 2013]. In our set, various schemes TMX or 4-hydroxytamoxifen administration failed to recombine p57 locus (Fig. S1A-C). p57 is an imprinted gene with preferential expression of the maternal allele [Hatada & Mukai, 1995]. Thus, to exclude the possibility of paternal allele reactivation, we produced animals in which both p57 alleles were floxed, but we again could not observe successful recombination following tamoxifen treatment (Fig. S1B-C). Inefficient recombination persisted when we used $Pax3^{Cre}$;$p57^{Flox\text{-}ILZ}$ mice (Fig. S1D), while no homozygous $p57^{cKO/cKO}$ animals were obtained in the crosses with $Pax3^{Cre}$ mice. In addition, mice from the $Pax3^{Cre}$ crosses did not follow mendelian frequencies at genotyping age and part of the mutants died at birth due to cleft palate, in agreement with Pax3 and p57 involvement in the development of craniofacial structures [Yan et al., 1997; Zhang et al., 1997; Zalc et al., 2015; Mademtzoglou et al., submitted].

In conclusion, our data indicate that p21 and p57 play essential roles at the early phase following mSC activation. The presence of p21 and p57 is compatible with activation/ proliferation and possibly represents an early activation event. Their loss profoundly affects *ex vivo* myogenic differentiation. Our data so far indicate that p21 and p57 function in distinct ways during adult and embryonic myogenesis, in terms of early versus continuous myogenesis support and (possibly) compensation for each other's loss. It remains to be established whether at later stages of differentiation/regeneration p21 and p57 take a leading role in *p57* and *p21* mutants, respectively, to rescue the observed preliminary defects. mSC-specific double *p21/p57* knock-out will elucidate their relative contributions and putative redundancies in the adult.

ACKNOWLEDGEMENTS

This work was supported by funding from INSERM Avenir Program, Association Française contre les Myopathies (AFM) via TRANSLAMUSCLE (PROJECT 19507), Labex REVIVE (ANR-10-LABX-73), Fondation pour la Recherche Médicale (FRM; Grant FDT20130928236 and DEQ20130326526), Agence Nationale pour la Recherche (ANR) grant Epimuscle (ANR 11 BSV2 017 02), Bone-muscle-repair (ANR-13-BSV1-0011-02), BMP-biomass (ANR-12-BSV1-0038- 04), Satnet (ANR-15-CE13-0011-01), RHU CARMMA (ANR-15-RHUS-0003), and the Agence Nationale pour la Recherche Maladies Rares (MRAR) grant Pax3 in WS (ANR-06-MRAR-32-01). We wish to acknowledge Bénédicte Hoareau (Flow Cytometry Core CyPS, Pierre and Marie Curie University),

Serban Morosan, and the animal care facility (Centre d'Expérimentation Fonctionnelle, School of Medicine Pierre et Marie Curie).

MATERIALS AND METHODS

Mouse lines

The following mouse lines have been previously described: *Pax3*$^{Cre/+}$, *Pax7*$^{CreERT2/+}$, *Rosa*^{mTmG} (The Jackson Laboratory, stock 007576), p21$^{+/-}$, p57$^{cKO\ (m)/+}$ (p57 is imprinted with preferential expression of the maternal allele; superscript (m) indicates maternal inheritance) [Brugarolas et al., 1995; Engleka et al., 2005; Lepper et al., 2009; Mademtzoglou et al., submitted]. Non-mutant littermates were used as controls. For recombination induction with the *Pax7*^{CreERT2} allele, mice were injected with tamoxifen (T5648, Sigma-Aldrich) as recommended [Lepper et al., 2009]. C57BL/6J (Janvier) mice were used as wildtype animals for Figs. 1, 4, 5. Adult mice of 8 to 12 weeks of age were used. At least three mice per genotype were assessed.

All animals were maintained inside a barrier facility, and all *in vivo* experiments were performed in accordance with the French and European Community guidelines for the care and use of laboratory animals.

Single myofiber isolation and culture

Single muscle fibers were isolated by enzymatic digestion and mechanical disruption of *EDL* muscles [Moyle & Zammit, 2014]. For enzymatic digestion muscles were incubated for 90 minutes at 37^{o}C with 0.2% collagenase type I (C0130, Sigma-Aldrich) in Penicillin/Streptomycin(P/S)-supplemented DMEM (41966, ThermoFisher Scientific). For mechanical disruption, muscles were transferred to 5%-horse-serum-coated deep petri dishes (Z692301, Sigma-Aldrich) with P/S-supplemented DMEM and medium was flushed against the muscle. Detached fibers were transferred into new dishes with P/S-supplemented DMEM. For timed culture, all fibers were transferred after finishing isolation into 5%-horse-serum-coated 6-well plates and cultured in the presence of 10% horse serum and 1% chicken embryo extract (#092850145, MP Biomedicals). If indicated, 5µM 4-hydroxytamoxifen (H6278, Sigma-Aldrich) was added at the beginning of the culture and renewed 48 hours later.

Cell sorting and culture

Using the tamoxifen-inducible Cre line *Pax7*^{CreERT2}, membrane-GFP is expressed in muscle satellite cells (mSCs) of *Rosa*^{mTmG} mice. Hindlimb muscles were dissociated by 0.2% w/v collagenase A (11088793001, Roche) and 2.4U/ml dispase II (04942078001, Roche) in digestion buffer [HBSS (14025, Thermo Scientific), 1%

Penicillin/Streptomycin, 0.1µg/ml DNase I (11284932001, Sigma), 0.4mM $CaCl_2$, 5mM $MgCl_2$, 0.2% bovine serum albumin (BSA; 0010001620, Jackson ImmunoResearch)] with 90 minute incubation at 37°C. Dissociated muscles were filtered through 100µm and 40µm cell strainers. GFP+ cells were collected with FACS Aria II based on gating of GFP signal.

Sorted cells were plated on matrigel (354230, Corning Life Sciences)-coated chamber slides (177445, Nalge Nunc International). They were initially cultured in high-serum conditions (referred to as "growth phase") with 20% fetal bovine serum, 10% horse serum and 2.5pg/ml bFGF (450-33B, PeproTech) in DMEM+Glutamax (61925, ThermoFisher Scientific) supplemented with 1% P/S, 20mM L-glutamine (25030, Thermo Scientific), 10mM pyruvate (11360, Thermo Scientific), and 0.1M Hepes (15630, Thermo Scientific). Upon reaching 70% confluence, they were switched to low-serum conditions (5% horse serum in P/S-supplemented DMEM+Glutamax) to differentiate (referred to as "differentiation phase").

Gene expression analysis

RNA was extracted with the RNeasy Micro kit (74004, Qiagen), according to the manufacturer's instructions. cDNA was synthetized with the Transcriptor First Strand cDNA Synthesis kit (04379012001, Roche). RT-qPCR reactions were carried out in triplicate using the LightCycler 480 Sy Green Master (04887352001, Roche). Hypoxanthine Phosphoribosyltransferase 1 (HPRT) transcripts were used for normalization. Oligonucleotides sequences are available upon request.

Muscle regeneration

Adult (8-12 week old) mice were intramuscularly injected with 45 µl of cardiotoxin solution (10 µM; L8102, Latoxan) into the *Tibialis Anterior* (TA) after being anesthetized. Muscles were recovered 5, 10 or 28 days post-injury.

Immunohistochemistry

Sections: Muscles were frozen fresh in liquid nitrogen-cooled isopentane and sectioned at 8um. Frozen sections were fixed with 4% paraformaldehyde/PBS for 20 minutes at room temperature. For hematoxylin-eosin staining, nuclei were stained with hematoxylin (MHS32, Sigma-Aldrich) for 11 minutes and cytoplasmes were counter-stained with eosin (6766007, Thermo Scientific) for 30 seconds. The sections were then dehydrated with brief passages through increasing concentrations of ethanol (30%, 50%, 70%, 85%, 95%, 100%). For two-color immunofluorescence, frozen sections were treated with methanol for 6 minutes at -20°C,

immersed to 0.01M citric acid pH 6.0 at 90°C for antigen retrieval and blocked with 5% BSA/PBS at room temperature. For three-color immunofluorescence, sections were permeabilized and blocked with 3% BSA, 10% lamb serum, 0.25% TritonX-100/PBS for 30 minutes at room temperature. In both cases, immunolabeling was performed at 4°C overnight for primary antibodies and at room temperature for 1h for secondary antibodies. When fibers were outlined with Alexa-conjugated anti-laminin, incubation was performed for 3 hours at room temperature, after washing out the secondary antibody. Nuclei were counterstained blue with DAPI. When mouse-raised antibodies were applied, endogenous mouse IgG was blocked by incubation with goat anti-mouse fab fragment affinity-purified antibody (115-007-003, Jackson Immunoresearch) for 30 minutes at room temperature.

Single myofibers: After isolation (T0) or following culture (T24, T48, T72), myofibers were fixed with 37°C-preheated 4% paraformaldehyde/PBS for 10 minutes at room temperature. Fixed fibers were permeabilized with 0.5% TritonX-100/PBS for 8 minutes, blocked with 10% goat serum, 10% swine serum in 0.025% Tween20/PBS for 45 minutes and incubated with primary antibody (overnight at 4°C) and secondary antibody (1h at room temperature). Nuclei were counterstained blue with DAPI.

Primary myoblast culture: Cell cultures were fixed with 4% paraformaldehyde/PBS for 15 minutes at room temperature, permeabilized with 0.5% TritonX-100/PBS for 5 minutes, blocked with 5% BSA, 10% goat serum and immunolabeled with primary antibody (overnight at 4°C) and secondary antibody (1h at room temperature). Nuclei were counterstained blue with DAPI.

Antibodies

The following antibodies were used: mouse anti-Ki67 1:80 (#556003, BD Pharmingen), mouse anti-PAX7 1:100 (Pax7-c, DSHB), mouse anti-MYOD 1:80 (M3512, DAKO), rabbit anti-MYOD 1:100 (sc769, Santa Cruz), mouse anti- MYOGENIN 1:100 (F5D-c, DSHB), rabbit anti-p57 1:100 (sc8298, Santa Cruz), goat anti-p57 1:50 (sc1039, Santa Cruz), rabbit anti-p21 1:100 (ab 2961, Abcam), mouse anti-MyHC 1:100 (mf20-c, DSHB), rabbit anti-laminin 1:400 (L9393, Sigma-Aldrich), rabbit AlexaFluor647-conjugated anti-laminin 1:200 (NB300-144AF647, Novus Biological), AlexaFluor-coupled secondary antibodies (Life Technologies, Jackson ImmunoResearch).

Graphic editing

Graphs and representative photos were arranged in Figure format with the graphics editor Photoshop CS5. Color intensities of hematoxylin-eosin photos were adjusted to acquire uniform result among different sections.

Statistical test

Data of control and mutant mice in Figs. 3-4 were compared with the Mann-Whitney U-test. Differences at $p<0.05$ were considered significant.

FIGURE LEGENDS

Figure 1. p21 expression during muscle satellite cell (mSC) activation and differentiation.

(A-B) Quiescent PAX7+ (green) mSCs satellite cells (A) lack p21 (red; B) in single myofibers of *Extensor digitorum longus* (EDL) muscle. (C-D) Lack of p21 (red; D) in sections of *Tibialis anterior* muscle. Arrowhead indicates mSC, marked with PAX7 (green; C). Myofibers are outlined with laminin (gray). (E-H) p21 expression (red; F, H) 72 hours post-culture of single myofibers of *Extensor digitorum longus* muscle. Myoblasts were stained with PAX7 (E) or MYOD (G) in green. (I-L) Quantification of p21 expression in myoblasts stained for PAX7+ (I), MYOD+ (J), MYOGENIN+ (K) or KI67+ (L) cells. Single myofibers of EDL and their associated mSCs were cultured and fixed at 24-hour intervals. Data show mean+SD, n=3 animals (20-33 fibers/animal). Nuclei were counter-stained with DAPI (blue). Scale bars 40μm.

Figure 2. p21 deficiency affects early activation phase of muscle satellite cells (mSCs).

(A) Muscle weight per body weight ratios for *p21* mutants and control littermates. Analyzed muscles were from hindlimbs (*Extensor digitorum longus*, EDL; *Tibialis anterior*, TA; gastrocnemius, GCN), forelimbs (biceps, BC; triceps, TC), and diaphragm (DIA). (B-C) TA sections of control (B) and *p21*-null (C) animals stained with PAX7 (red) and laminin (green) to mark mSCs (arrowheads) and fiber outline, respectively. Nuclei were counter-stained with DAPI (blue). (D) Quantification of (B-C). (E-G) Myoblast kinetics in single myofiber cultures of EDLs of *p21* mutant and control animals at 72 hours. Proportions of PAX7+ and/or MYOD+ myoblasts (E), proliferating KI67+ myoblasts (F), and differentiating Myogenin+ cells (G) were quantified. Data show mean+SD (A-D: n≥4 animals, E-G: n≥3 animals, 18-28 fibers/animal). Asterisks indicate significance; $p<0.01$ (**) or $p<0.001$ (***). Scale bars 50μm.

Figure 3. Muscle regeneration time-course in the absence of p21.

(A-F) Hematoxylin (nuclei)-eosin (cytoplasm) stained sections of regenerating TA muscles of controls (A, C, E) and *p21* mutants (B, D, F) at 5 (A, B), 10 (C, D), and 28 (E, F) days post-cardiotoxin injury. (G-L) Regenerating muscles of controls (G, I, K) and *p21* mutants (H, J, L) were stained with PAX7 (red) and laminin (green) to mark muscle satellite cells (mSCs) and myofibers, respectively, at 5 (G, H), 10 (I, J), and 28 (K, L) days post-cardiotoxin. Arrowheads indicate mSCs at D28 (K, L). (M) Quantification of (G-L). Data show mean+SD, n≥3 animals. Asterisks indicate significance; p<0.001 (***). Scale bars 50μm.

Figure 4. p57 expression in single myofiber culture and muscle sections.

(A) Muscle satellite cells (mSCs; T0) and myoblasts (T24-T48) stained with PAX7 (green) and p57 (red) in single myofiber cultures of *Extensor digitorum longus* (EDL) muscles. Arrowheads indicate Pax7+ cells. (B) Myoblasts of single EDL myofibers stained with MYOD (green) and p57 (red). Arrowheads indicate MYOD+ cells. (C) p57 (red) presence in *Tibialis anterior* muscle section. mSCs were marked with PAX7 (green) and fibers were outlined with laminin (gray). Arrowheads indicate p57+ cells. Asterisks indicate satellite cells. Nuclei were counter-stained with DAPI. Scale bars 40μm.

Figure 5. p57 expression and subcellular localization during satellite cell activation and differentiation.

(A) Immunofluorescence for PAX7 (green) and p57 (red) at T72 in single myofiber cultures of *Extensor digitorum longus* muscles and quantification of PAX7+ cells that co-expressed over the time-course of the culture. (B) Immunofluorescence for MYOD (green) and p57 (red) at T72 in single myofiber cultures and quantification of MYOD+ cells that co-expressed p57 over the time course of the culture. (C) Immunofluorescence for MYOGENIN (green) and p57 (red) at T72 in single myofiber cultures and quantification of MYOGENIN+ cells that co-expressed p57 at T72, when MYOGENIN+ cells are abundant. (D) Immunofluorescence for KI67 (green) and p57 (red) at T72 in single myofiber cultures and quantification of Ki67+cells that co-express p57 at T72. Nuclei were counter-stained with DAPI (blue). Cytoplasmic (light gray) or nuclear (dark gray) localization of p57 is indicated in the graphs. Data show mean+SD, n≥3 animals, 20-32 fibers/animal. Scale bars 40μm.

Figure 6. p57 deficiency impairs myogenic differentiation.

(A) Time-course of intraperitoneal tamoxifen injections (TMX arrows), chase, and muscle satellite cell harvest (FACS arrow) and culture (light gray bar for growth culture conditions, dark gray bar for differentiation culture conditions). Analyzed animals were *Pax7*$^{CreERT2/+}$;*p57*$^{flox/flox}$; *Rosa*^{mTmG} (*p57* cKO) and *Pax7*$^{CreERT2/+}$;*p57*$^{+/+}$;*Rosa*^{mTmG} (control). (B) *p57* and *p21* transcript levels of control and *p57* cKO myoblast cultures three days post-

differentiation. (C-K) Control (C, F, I) and *p57* cKO (D, G, J) myoblast cultures were examined for p57 protein (red) three days post-differentiation (C, D), MYOGENIN+ cells (green) one day post-differentiation. (F, G), and myotube formation three days post-differentiation (I, J). Nascent myotubes were marked with myosin heavy chain (MyHC; green; I, J). Nuclei were counter-stained with DAPI (blue). Graphs show quantification of p57 expression (E), Myogenin expression (H), and nuclei/myotube (K). Data show mean+SD, n=3 animals. Asterisks indicate significance; $p<0.001$. Scale bar 40μm.

Supplementary Figure 1. Cre-mediated recombination strategies of floxed *p57* allele.

(A-C) Animals with *p57* floxed allele(s) ($p57^{cKO/+}$ or $p57^{cKO/cKO}$) were crossed with tamoxifen-inducible $Pax7^{CreERT2}$ mice. Schemes show the tamoxifen (TMX) or 4-hydroxytamoxifen (4-OHT) regimens and chase periods before (TMX) or during (4-OHT) single myofiber culture of *Extensor digitorum longus* (EDL) muscle. Photos show p57 (red) expression in single myofibers at 72 hours, implying insufficient recombination. (D) Single myofiber from $Pax3^{Cre/+};p57^{cKO/+}$ mouse, showing p57 expression (red) at 72 hours post-culture of EDL myofibers. (E-F) Heads of $Pax3^{+/+};p57^{cKO/+}$ (control) and $Pax3^{Cre/+};p57^{cKO/+}$ (cKO) animals at birth showing closed (control; E) or cleft (cKO; F) palate. When heterozygous *p57* animals ($p57^{cKO/+}$) were used, they had maternally transmitted transgene, due to imprinting silencing of the paternally transmitted *p57* allele. Homozygous animals were used to exclude possible paternal allele activation in the crosses with $Pax7^{CreERT2}$ mice. Nuclei in (A-D) were counter-stained with DAPI (blue). P: palate; PS: palatal shelf. Scale bars 40μm (myofibers) or 2mm (head).

REFERENCES

Battistelli C, Busanello A, Maione R. Functional interplay between MyoD and CTCF in regulating long-range chromatin interactions during differentiation. J Cell Sci 2014;127:3757-67.

Besson A, Assoian RK, Roberts JM. Regulation of the cytoskeleton: an oncogenic function for CDK inhibitors? Nat Rev Cancer 2004;4:948-55.

Besson A, Dowdy SF, Roberts JM. CDK inhibitors: cell cycle regulators and beyond. Dev Cell 2008;14:159-69.

Biferi MG, Nicoletti C, Falcone G, Puggioni EM, Passaro N, Mazzola A, Pajalunga D, Zaccagnini G, Rizzuto E, Auricchio A, Zentilin L, De Luca G, Giacca M, Martelli F, Musio A, Musarò A, Crescenzi M. Proliferation of Multiple Cell Types in the Skeletal Muscle Tissue Elicited by Acute p21 Suppression. Mol Ther 2015;23:885-95.

Bilodeau S, Roussel-Gervais A, Drouin J. Distinct developmental roles of cell cycle inhibitors p57Kip2 and p27Kip1 distinguish pituitary progenitor cell cycle exit from cell cycle reentry of differentiated cells. Mol Cell Biol 2009;29:1895-1908.

564 **Blais** A, Tsikitis M, Acosta-Alvear D, Sharan R, Kluger Y, Dynlacht BD. An initial blueprint for myogenic
565 differentiation. Genes Dev 2005;19:553-69.
566 **Borriello** A, Caldarelli I, Bencivenga D, Criscuolo M, Cucciolla V, Tramontano A, Oliva A, Perrotta S, Della
567 Ragione F. p57(Kip2) and cancer: time for a critical appraisal. Mol Cancer Res 2011;9:1269-84.
568 **Brugarolas** J, Chandrasekaran C, Gordon JI, Beach D, Jacks T, Hannon GJ. Radiation-induced cell cycle arrest
569 compromised by p21 deficiency. Nature 1995;377:552-7.
570 **Busanello** A, Battistelli C, Carbone M, Mostocotto C, Maione R. MyoD regulates p57kip2 expression by
571 interacting with a distant cis-element and modifying a higher order chromatin structure. Nuclei Acids Res
572 2012;40:8266-75.
573 **Cao** Y, Kumar RM, Penn BH, Berkes CA, Kooperberg C, Boyer LA, Young RA, Tapscott SJ. Global and gene-
574 specific analyses show distinct roles for Myod and Myog at a common set of promoters. EMBO J 2006;25:502-
575 11.
576 **Cerqueira** A, Martín A, Symonds CE, Odajima J, Dubus P, Barbacid M, Santamaría D. Genetic characterization of
577 the role of the Cip/Kip family of proteins as cyclin-dependent kinase inhibitors and assembly factors. Mol Cell
578 Biol 2014;34:1452-59.
579 **Chakkalakal** JV, Christensen J, Xiang W, Tierney MT, Boscolo FS, Sacco A, Brack AS. Early forming label-
580 retaining muscle stem cells require p27kip1 for maintenance of the primitive state. Development
581 2014;141:1649-59.
582 **Cheung** TH, Rando TA. Molecular regulation of stem cell quiescence. Nat Rev Mol Cell Biol 2013;14:329-40.
583 **Chinzei** N, Hayashi S, Ueha T, Fujishiro T, Kanzaki N, Hashimoto S, Sakata S, Kihara S, Haneda M, Sakai Y,
584 Kuroda R, Kurosaka M. P21 deficiency delays regeneration of skeletal muscular tissue. PLoS One
585 2015;10:e0125765.
586 **Chow** SE, Wang JS, Lin MR, Lee CL. Downregulation of p57kip² promotes cell invasion via LIMK/cofilin pathway
587 in human nasopharyngeal carcinoma cells. J Cell Biochem 2011;112:3459-68.
588 **Crescenzi** M, Fleming TP, Lassar AB, Weintraub H, Aaronson SA. MyoD induces growth arrest independent of
589 differentiation in normal and transformed cells. Proc Natl Acad Sci USA 1990;87:8442-46.
590 **Deng** C, Zhang P, Harper JW, Elledge SJ, Leder P. Mice lacking p21CIP1/WAF1 undergo normal development,
591 but are defective in G1 checkpoint control. Cell 1995;82:675-84.
592 **Engleka** KA, Gitler AD, Zhang M, Zhou DD, High FA, Epstein JA. Insertion of Cre into the Pax3 locus creates a
593 new allele of Splotch and identifies unexpected Pax3 derivatives. Dev Biol 2005;280:396-406.

Fiaschi-Taesch NM, Kleinberger JW, Salim FG, Troxell R, Wills R, Tanwir M, Casinelli G, Cox AE, Takane KK, Srinivas H, Scott DK, Stewart AF. Cytoplasmic-nuclear trafficking of G1/S cell cycle molecules and adult human β-cell replication: a revised model of human β-cell G1/S control. Diabetes 2013;62:2460-70.

Figliola R, Maione R. MyoD induces the expression of p57Kip2 in cells lacking p21Cip1/Waf1: overlapping and distinct functions of the two cdk inhibitors. J Cell Physiol 2004;200:468-75.

Figliola R, Busanello A, Vaccarello G, Maione R. Regulation of p57(KIP2) during muscle differentiation: role of Egr1, Sp1 and DNA hypomethylation. J Mol Biol 2008;380:265-77.

Franklin DS, Xiong Y. Induction of p18INK4c and its predominant association with CDK4 and CDK6 during myogenic differentiation. Mol Biol Cell 1996;7:1587-99.

Fukada S, Higuchi S, Segawa M, Koda K, Yamamoto Y, Tsujikawa K, Kohama Y, Uezumi A, Imamura M, Miyagoe-Suzuki Y, Takeda S, Yamamoto H. Purification and cell-surface marker characterization of quiescent satellite cells from murine skeletal muscle by a novel monoclonal antibody. Exp Cell Res 2004;296:245-55.

Fukada S, Uezumi A, Ikemoto M, Masuda S, Segawa M, Tanimura N, Yamamoto H, Miyagoe-Suzuki Y, Takeda S. Molecular signature of quiescent satellite cells in adult skeletal muscle. Stem Cells 2007;25:2448-59.

Furutachi S, Matsumoto A, Nakayama KI, Gotoh Y. p57 controls adult neural stem cell quiescence and modulates the pace of lifelong neurogenesis. EMBO J 2013;32:970-81.

Galea CA, Wang Y, Sivakolundu SG, Kriwacki RW. Regulation of cell division by intrinsically unstructured proteins: intrinsic flexibility, modularity, and signaling conduits. Biochemistry 2008;47:7598-609.

Grounds MD. The need to more precisely define aspects of skeletal muscle regeneration. Int J Biochem Cell Biol 2014;56:56-65.

Gu Y, Turck CW, Morgan DO. Inhibition of CDK2 activity in vivo by an associated 20K regulatory subunit. Nature 1993;36:707-10.

Günther S, Kim J, Kostin S, Lepper C, Fan CM, Braun T. Myf5-positive satellite cells contribute to Pax7-dependent long-term maintenance of adult muscle stem cells. Cell Stem Cell 2013;13:590-601.

Guo H, Li Y, Tian T, Han L, Ruan Z, Liang X, Wang W, Nan K. The role of cytoplasmic p57 in invasion of hepatocellular carcinoma. BMC Gastroenterol 2015;15:104.

Halevy O, Novitch BG, Spicer DB, Skapek SX, Rhee J, Hannon GJ, Beach D, Lassar AB. Correlation of terminal cell cycle arrest of skeletal muscle with induction of p21 by MyoD. Science 1995;267:1018-21.

Harper JW, Adami GR, Wei N, Keyomarsi K, Elledge SJ. The p21 Cdk-interacting protein Cip1 is a potent inhibitor of G1 cyclin-dependent kinases. Cell 1993;75:805-16.

Harper JW, Elledge SJ, Keyomarsi K, Dynlacht B, Tsai LH, Zhang P, Dobrowolski S, Bai C, Connell-Crowley L, Swindell E, Fox MP, Wei N. Inhibition of cyclin-dependent kinases by p21. Mol Biol Cell 1995;6:387-400.

Hashimoto Y, Kohri K, Kaneko Y, Morisaki H, Kato T, Ikeda K, Nakanishi M. Critical role for the 310 helix region of p57(Kip2) in cyclin-dependent kinase 2 inhibition and growth suppression. J Biol Chem 1998;273:16544-50.

Hatada I, Mukai T. Genomic imprinting of p57KIP2, a cyclin-dependent kinase inhibitor, in mouse. Nat Genet 1995;11:204-6.

Hawke TJ, Meeson AP, Jiang N, Graham S, Hutcheson K, DiMaio JM, Garry DJ. p21 is essential for normal myogenic progenitor cell function in regenerating skeletal muscle. Am J Physiol Cell Physiol 2003;285:C1019-27.

Hwang CY, Lee C, Kwon KS. Extracellular signal-regulated kinase 2-dependent phosphorylation induces cytoplasmic localization and degradation of p21Cip1. Mol Cell Biol 2009;29:3379-89.

Keefe AC, Lawson JA, Flygare SD, Fox ZD, Colasanto MP, Mathew SJ, Yandell M, Kardon G. Muscle stem cells contribute to myofibres in sedentary adult mice. Nat Commun 2015;6:7087.

LaBaer J, Garrett MD, Stevenson LF, Slingerland JM, Sandhu C, Chou HS, Fattaey A, Harlow E. New functional activities for the p21 family of CDK inhibitors. Genes Dev 1997;11:847-62.

Lee MH, Reynisdóttir I, Massagué J. Cloning of p57KIP2, a cyclin-dependent kinase inhibitor with unique domain structure and tissue distribution. Genes Dev 1995;9:639-49.

Lepper C, Conway SJ, Fan CM. Adult satellite cells and embryonic muscle progenitors have distinct genetic requirements. Nature 2009;460:627-31.

Lepper C, Partridge TA, Fan CM. An absolute requirement for Pax7-positive satellite cells in acute injury-induced skeletal muscle regeneration. Development 2011;138:3639-46.

Macleod KF, Sherry N, Hannon G, Beach D, Tokino T, Kinzler K, Vogelstein B, Jacks T. p53-dependent and independent expression of p21 during cell growth, differentiation, and DNA damage. Genes Dev 1995;9:935-44.

Mademtzoglou D, Alonso-Martin S, Chang T, Bismuth K, Drayton B, Aurade F, Relaix F. A p57 conditional mutant allele that allows tracking of p57-expressing and mutant cells. Genesis [submitted]

Matsumoto A, Takeishi S, Kanie T, Susaki E, Onoyama I, Tateishi Y, Nakayama K, Nakayama KI. p57 is required for quiescence and maintenance of adult hematopoietic stem cells. Cell Stem Cell 2011;9:262-71.

Matsuoka S, Edwards MC, Bai C, Parker S, Zhang P, Baldini A, Harper JW, Elledge SJ. p57KIP2, a structurally distinct member of the p21CIP1 Cdk inhibitor family, is a candidate tumor suppressor gene. Genes Dev 1995;9:650-62.

Mauro A. Satellite cell of skeletal muscle fibers. J Biophys Biochem Cytol 1961;9:493-5.

McCarthy JJ, Mula J, Miyazaki M, Erfani R, Garrison K, Farooqui AB, Srikuea R, Lawson BA, Grimes B, Keller C, Van Zant G, Campbell KS, Esser KA, Dupont-Versteegden EE, Peterson CA. Effective fiber hypertrophy in satellite cell-depleted skeletal muscle. Development 2011;138:3657-66.

Megeney LA, Kablar B, Garrett K, Anderson JE, Rudnicki MA. MyoD is required for myogenic stem cell function in adult skeletal muscle. Genes Dev 1996;10:1173-83.

Messina G, Blasi C, La Rocca SA, Pompili M, Calconi A, Grossi M. p27Kip1 acts downstream of N-cadherin-mediated cell adhesion to promote myogenesis beyond cell cycle regulation. Mol Biol Cell 2005;16:1469-80.

Michailovici I, Harrington HA, Azogui HH, Yahalom-Ronen Y, Plotnikov A, Ching S, Stumpf MP, Klein OD, Seger R, Tzahor E. Nuclear to cytoplasmic shuttling of ERK promotes differentiation of muscle stem/progenitor cells. Development 2014;141:2611-20.

Michieli P, Chedid M, Lin D, Pierce JH, Mercer WE, Givol D. Induction of WAF1/CIP1 by a p53-independent pathway. Cancer Res 1994;54:3391-95.

Mounier R, Chrétien F, Chazaud B. Blood vessels and the satellite cell niche. Curr Top Dev Biol 2011;96:121-38.

Moyle LA, Zammit PS. Isolation, culture and immunostaining of skeletal muscle fibres to study myogenic progression in satellite cells. Methods Mol Biol 2014;1210:63-78.

Murphy MM, Lawson JA, Mathew SJ, Hutcheson DA, Kardon G. Satellite cells, connective tissue fibroblasts and their interactions are crucial for muscle regeneration. Development 2011;138:3625-37.

Osborn DP, Li K, Hinits Y, Hughes SM. Cdkn1c drives muscle differentiation through a positive feedback loop with Myod. Dev Biol 2011;350:464-75.

Park CW, Chung JH. Age-dependent changes of p57(Kip2) and p21(Cip1/Waf1) expression in skeletal muscle and lung of mice. Biochim Biophys Acta 2001;1520:163-8.

Parker SB, Eichele G, Zhang P, Rawls A, Sands AT, Bradley A, Olson EN, Harper JW, Elledge SJ. p53-independent expression of p21Cip1 in muscle and other terminally differentiating cells. Science 1995;267:1024-27.

Pateras IS, Apostolopoulou K, Niforou K, Kotsinas A, Gorgoulis VG. p57KIP2: "Kip"ing the cell under control. Mol Cancer Res 2009;7:1902-19.

Pawlikowski B, Pulliam C, Betta ND, Kardon G, Olwin BB. Pervasive satellite cell contribution to uninjured adult muscle fibers. Skelet Muscle 2015;5:42.

Paylor B, Natarajan A, Zhang RH, Rossi F. Nonmyogenic cells in skeletal muscle regeneration. Curr Top Dev Biol 2011;96:139-65.

Peschiaroli A, Figliola R, Coltella L, Strom A, Valentini A, D'Agnano I, Maione R. MyoD induces apoptosis in the absence of RB function through a p21(WAF1)-dependent re-localization of cyclin/cdk complexes to the nucleus. Oncogene 2002;21:8114-27.

Relaix F, Rocancourt D, Mansouri A, Buckingham M. A Pax3/Pax7-dependent population of skeletal muscle progenitor cells. Nature 2005;435:948-53.

Relaix F, Zammit PS. Satellite cells are essential for skeletal muscle regeneration: the cell on the edge returns centre stage. Development 2012;139:2845-56.

Reynaud EG, Pelpel K, Guillier M, Leibovitch MP, Leibovitch SA. p57(Kip2) stabilizes the MyoD protein by inhibiting cyclin E-Cdk2 kinase activity in growing myoblasts. Mol Cell Biol 1999;19:7621-29.

Reynaud EG, Leibovitch MP, Tintignac LA, Pelpel K, Guillier M, Leibovitch SA. Stabilization of MyoD by direct binding to p57(Kip2). J Biol Chem 2000;275:18767-76.

Sambasivan R, Yao R, Kissenpfennig A, Van Wittenberghe L, Paldi A, Gayraud-Morel B, Guenou H, Malissen B, Tajbakhsh S, Galy A. Pax7-expressing satellite cells are indispensable for adult skeletal muscle regeneration. Development 2011;138:3647-56.

Sherr CJ. Ink4-Arf locus in cancer and aging. Wiley Interdiscip Rev Dev Biol 2012;1:731-41.

Siegel AL, Atchison K, Fisher KE, Davis GE, Cornelison DD. 3D timelapse analysis of muscle satellite cell motility. Stem Cells 2009;27:2527-38.

Sorrentino V, Pepperkok R, Davis RL, Ansorge W, Philipson L. Cell proliferation inhibited by MyoD1 independently of myogenic differentiation. Nature 1990;345:813-15.

Tajbakhsh S. Skeletal muscle stem cells in developmental versus regenerative myogenesis. J Intern Med 2009;266:372-89.

Tintignac LA, Sirri V, Leibovitch MP, Lécluse Y, Castedo M, Metivier D, Kroemer G, Leibovitch SA. Mutant MyoD lacking Cdc2 phosphorylation sites delays M-phase entry. Mol Cell Biol 2004;24:1809-21.

Vaccarello G, Figliola R, Cramerotti S, Novelli F, Maione R. p57Kip2 is induced by MyoD through a p73-dependent pathway. J Mol Biol 2006;356:578-88.

Vlachos P, Joseph B. The Cdk inhibitor p57(Kip2) controls LIM-kinase 1 activity and regulates actin cytoskeleton dynamics. Oncogene 2009;28:4175-88.

von Maltzahn J, Jones AE, Parks RJ, Rudnicki MA. Pax7 is critical for the normal function of satellite cells in adult skeletal muscle. Proc Natl Acad Sci USA 2013;110:16474-9.

Wang J, Walsh K. Inhibition of retinoblastoma protein phosphorylation by myogenesis-induced changes in the subunit composition of the cyclin-dependent kinase 4 complex. Cell Growth Differ 1996;7:1471-78.

Wang YX, Dumont NA, Rudnicki MA. Muscle stem cells at a glance. J Cell Sci. 2014;127:4543-8.

Webster MT, Manor U, Lippincott-Schwartz J, Fan CM. Intravital imaging reveals ghost fibers as architectural units guiding myogenic progenitors during regeneration. Cell Stem Cell 2016;18:243-52.

Wei Q, Paterson BM. Regulation of MyoD function in the dividing myoblast. FEBS Lett 2001;490:171-178.

Westbury J, Watkins M, Ferguson-Smith AC, Smith J. Dynamic temporal and spatial regulation of the cdk inhibitor p57(kip2) during embryo morphogenesis. Mech Dev 2001;109:83-9.

White RB, Biérinx AS, Gnocchi VF, Zammit PS. Dynamics of muscle fibre growth during postnatal mouse development. BMC Dev Biol 2010;10:21.

Xiong Y, Hannon GJ, Zhang H, Casso D, Kobayashi R, Beach D. p21 is a universal inhibitor of cyclin kinases. Nature 1993;366:701-4.

Yan Y, Frisén J, Lee MH, Massagué J, Barbacid M. Ablation of the CDK inhibitor p57Kip2 results in increased apoptosis and delayed differentiation during mouse development. Genes Dev 1997;11:973-83.

Yan Z, Choi S, Liu X, Zhang M, Schageman JJ, Lee SY, Hart R, Lin L, Thurmond FA, Williams RS. Highly coordinated gene regulation in mouse skeletal muscle regeneration. J Biol Chem 2003;278:8826-36.

Zacharek SJ, Fillmore CM, Lau AN, Gludish DW, Chou A, Ho JW, Zamponi R, Gazit R, Bock C, Jäger N, Smith ZD, Kim TM, Saunders AH, Wong J, Lee JH, Roach RR, Rossi DJ, Meissner A, Gimelbrant AA, Park PJ, Kim CF. Lung stem cell self-renewal relies on BMI1-dependent control of expression at imprinted loci. Cell Stem Cell 2011;9:272-81.

Zalc A, Hayashi S, Auradé F, Bröhl D, Chang T, Mademtzoglou D, Mourikis P, Yao Z, Cao Y, Birchmeier C, Relaix F. Antagonistic regulation of p57kip2 by Hes/Hey downstream of Notch signaling and muscle regulatory factors regulates skeletal muscle growth arrest. Development 2014;141:2780-90.

Zalc A, Rattenbach R, Auradé F, Cadot B, Relaix F. Pax3 and Pax7 play essential safeguard functions against environmental stress-induced birth defects. Dev Cell 2015 ;33:56-66.

Zammit PS, Golding JP, Nagata Y, Hudon V, Partridge TA, Beauchamp JR. Muscle satellite cells adopt divergent fates: a mechanism for self-renewal? J Cell Biol 2004;166:347-57.

Zhang P, Liégeois NJ, Wong C, Finegold M, Hou H, Thompson JC, Silverman A, Harper JW, DePinho RA, Elledge SJ. Altered cell differentiation and proliferation in mice lacking p57KIP2 indicates a role in Beckwith-Wiedemann syndrome. Nature 1997;387:151-8.

Zhang P, Wong C, Liu D, Finegold M, Harper JW, Elledge SJ. p21(CIP1) and p57(KIP2) control muscle differentiation at the myogenin step. Genes Dev 1999;13:213-24.

Zhang K, Sha J, Harter ML. Activation of Cdc6 by MyoD is associated with the expansion of quiescent myogenic satellite cells. J Cell Biol 2010;188:39-48.

Zou P, Yoshihara H, Hosokawa K, Tai I, Shinmyozu K, Tsukahara F, Maru Y, Nakayama K, Nakayama KI, Suda T. p57(Kip2) and p27(Kip1) cooperate to maintain hematopoietic stem cell quiescence through interactions with Hsc70. Cell Stem Cell 2011;9:247-61.

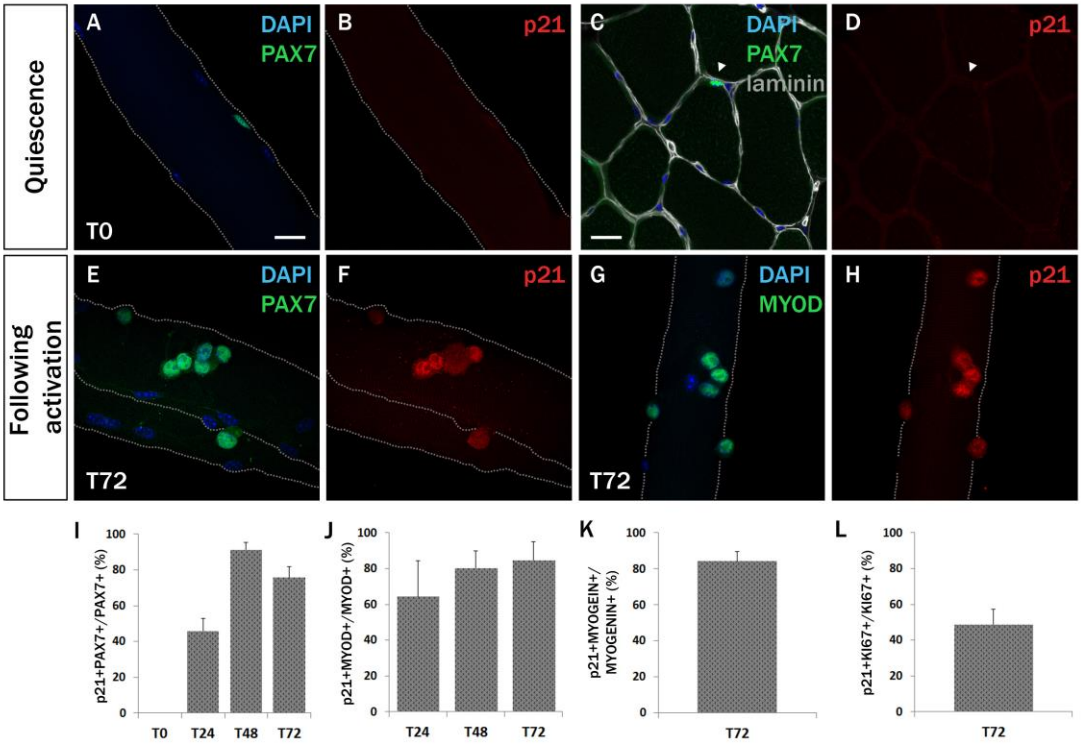

Figure 1

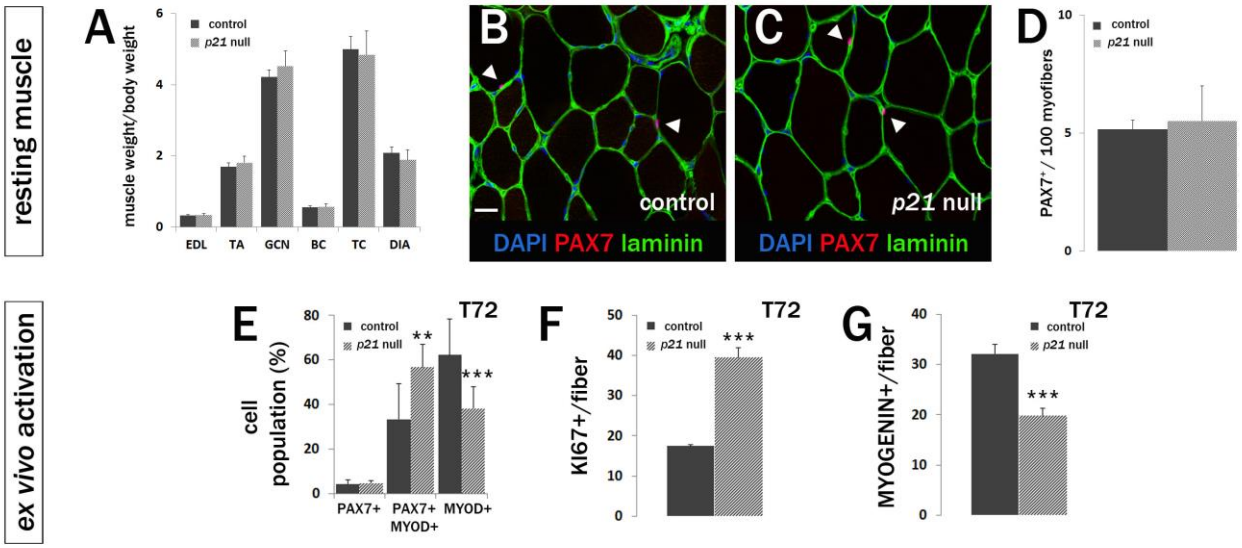

Figure 2

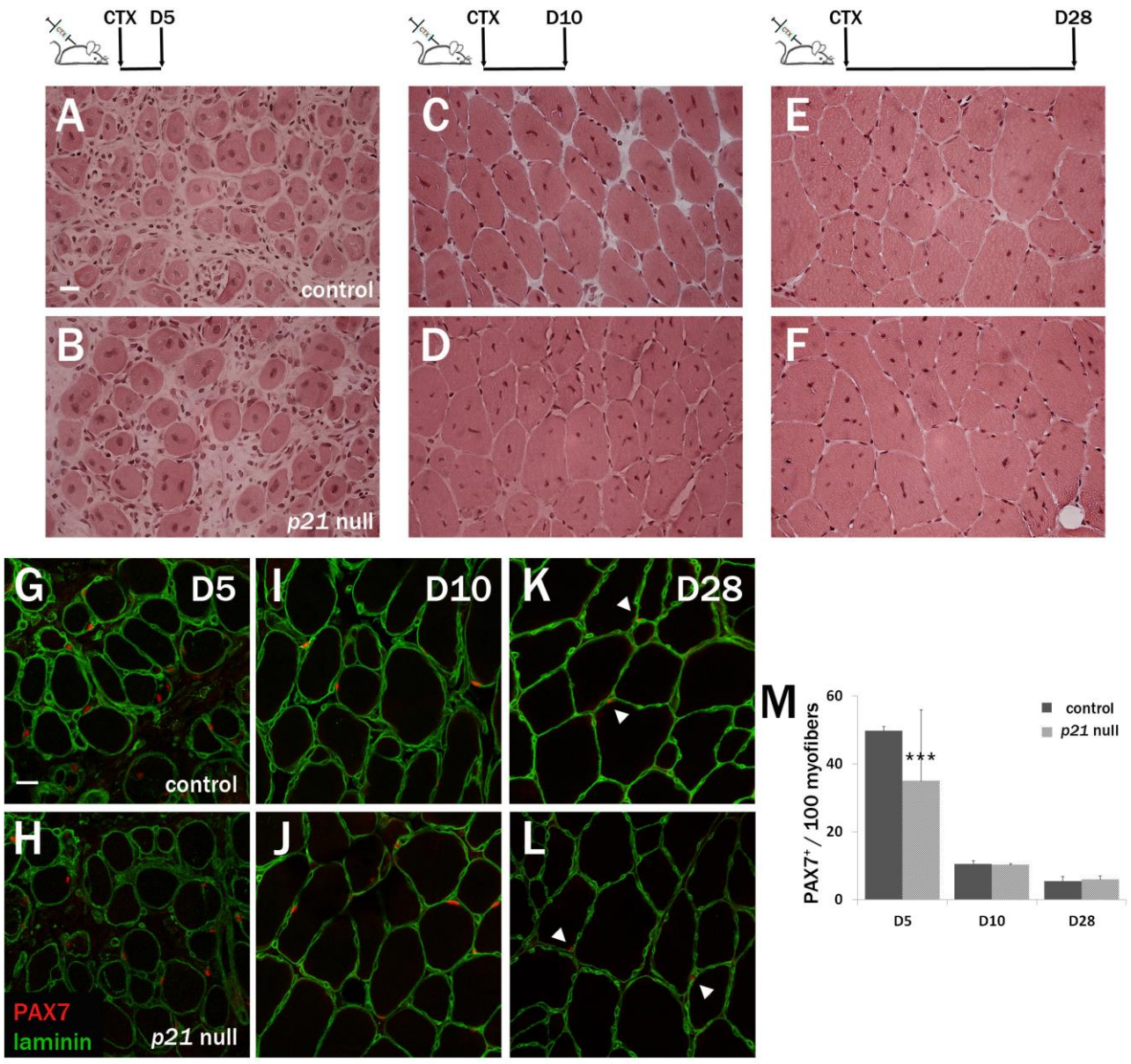
CTX D5
CTX D10
CTX D28
A
control
B
p21 null
C
D
E
F
G D5
control
I D10
K D28
H
PAX7
laminin
p21 null
J
L
M
PAX7+ / 100 myofibers
60
40
20
0
***
control
p21 null
D5
D10
D28

Figure 3

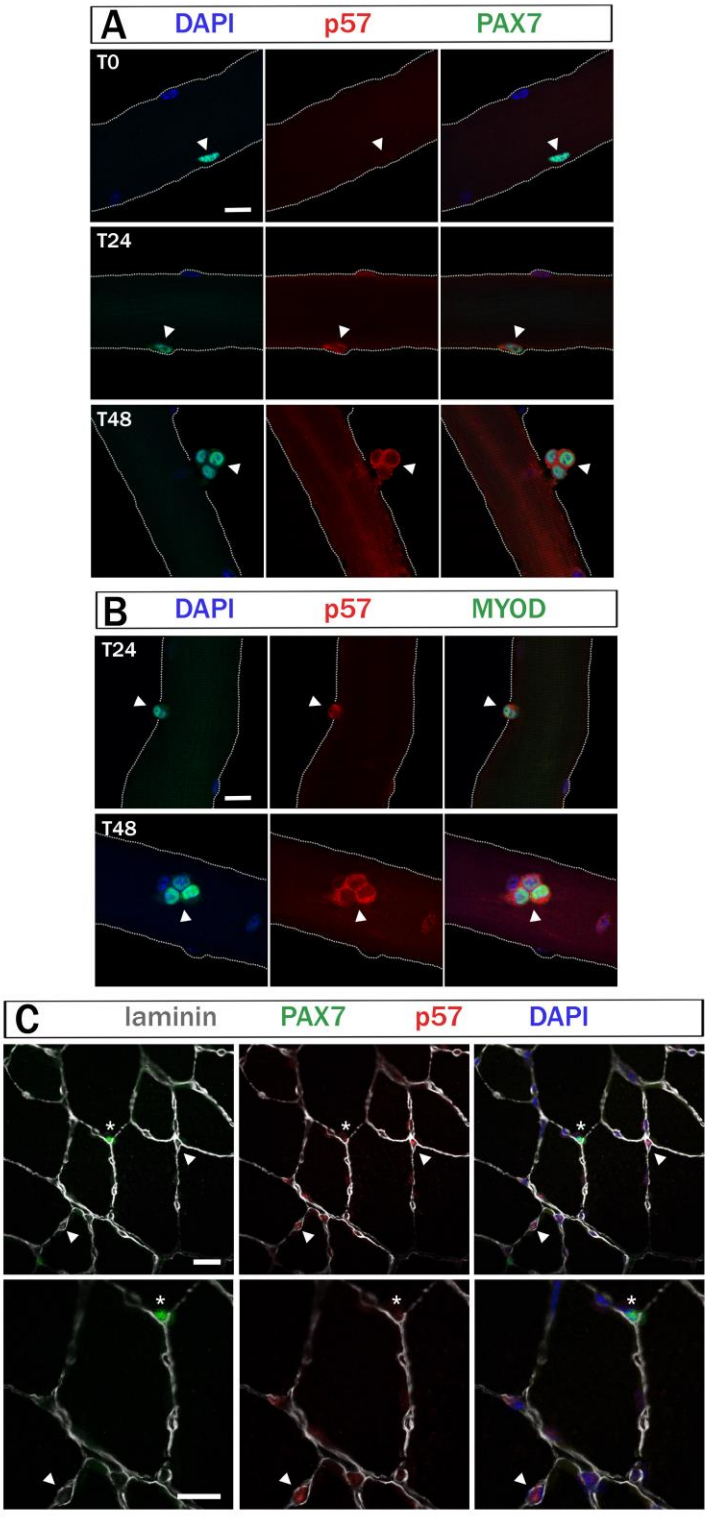
A
DAPI
p57
PAX7
T0
T24
T48
B
DAPI
p57
MYOD
T24
T48
C
laminin
PAX7
p57
DAPI

Figure 4

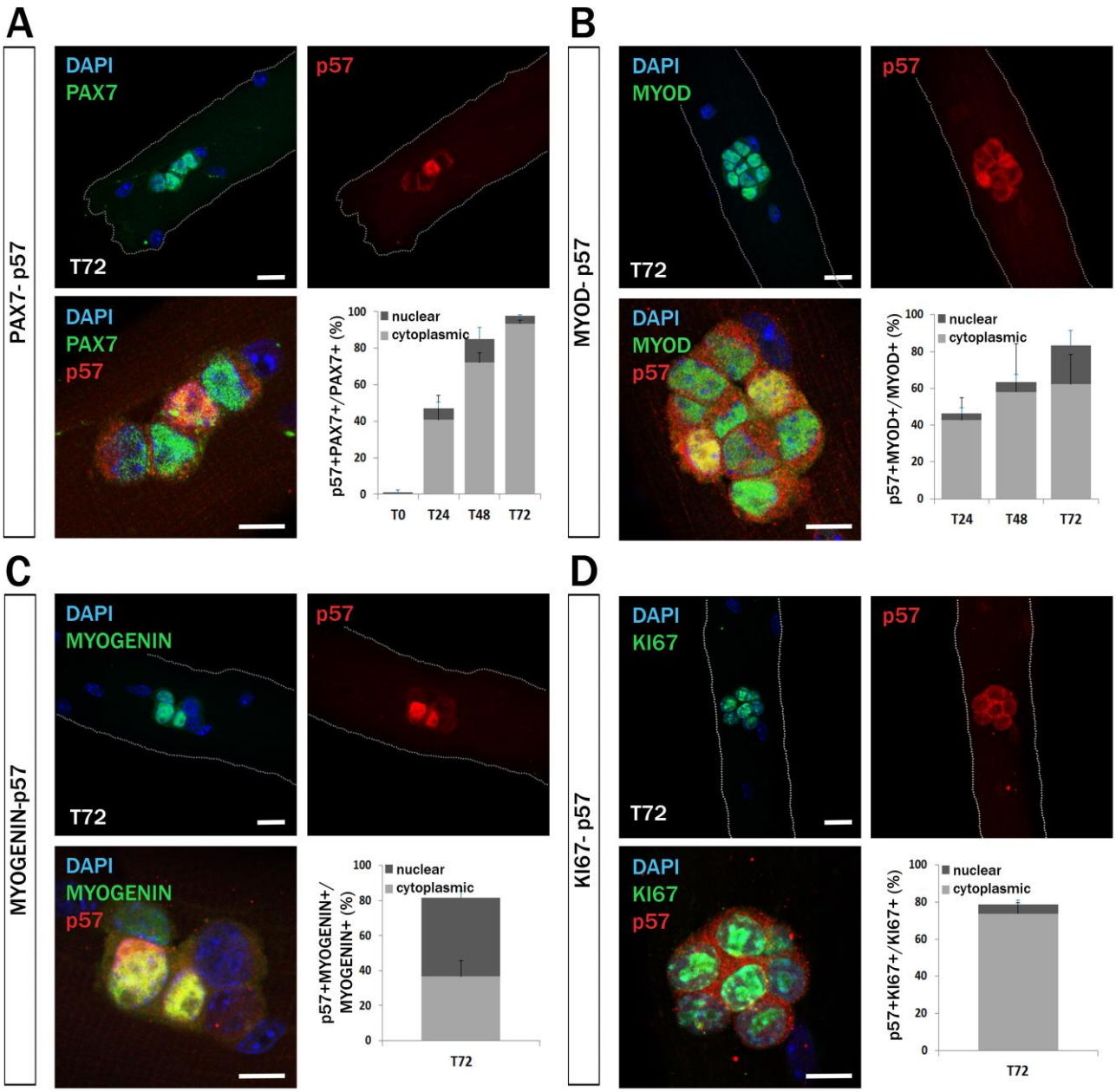
A
PAX7- p57
DAPI
PAX7
T72
p57
DAPI
PAX7
p57
nuclear
cytoplasmic
p57+PAX7+/PAX7+ (%)
T0
T24
T48
T72
B
MYOD- p57
DAPI
MYOD
T72
p57
DAPI
MYOD
p57
nuclear
cytoplasmic
p57+MYOD+/MYOD+ (%)
T24
T48
T72
C
MYOGENIN-p57
DAPI
MYOGENIN
T72
p57
DAPI
MYOGENIN
p57
nuclear
cytoplasmic
p57+MYOGENIN+/ MYOGENIN+ (%)
T72
D
KI67- p57
DAPI
KI67
T72
p57
DAPI
KI67
p57
nuclear
cytoplasmic
p57+KI67+/KI67+ (%)
T72

Figure 5

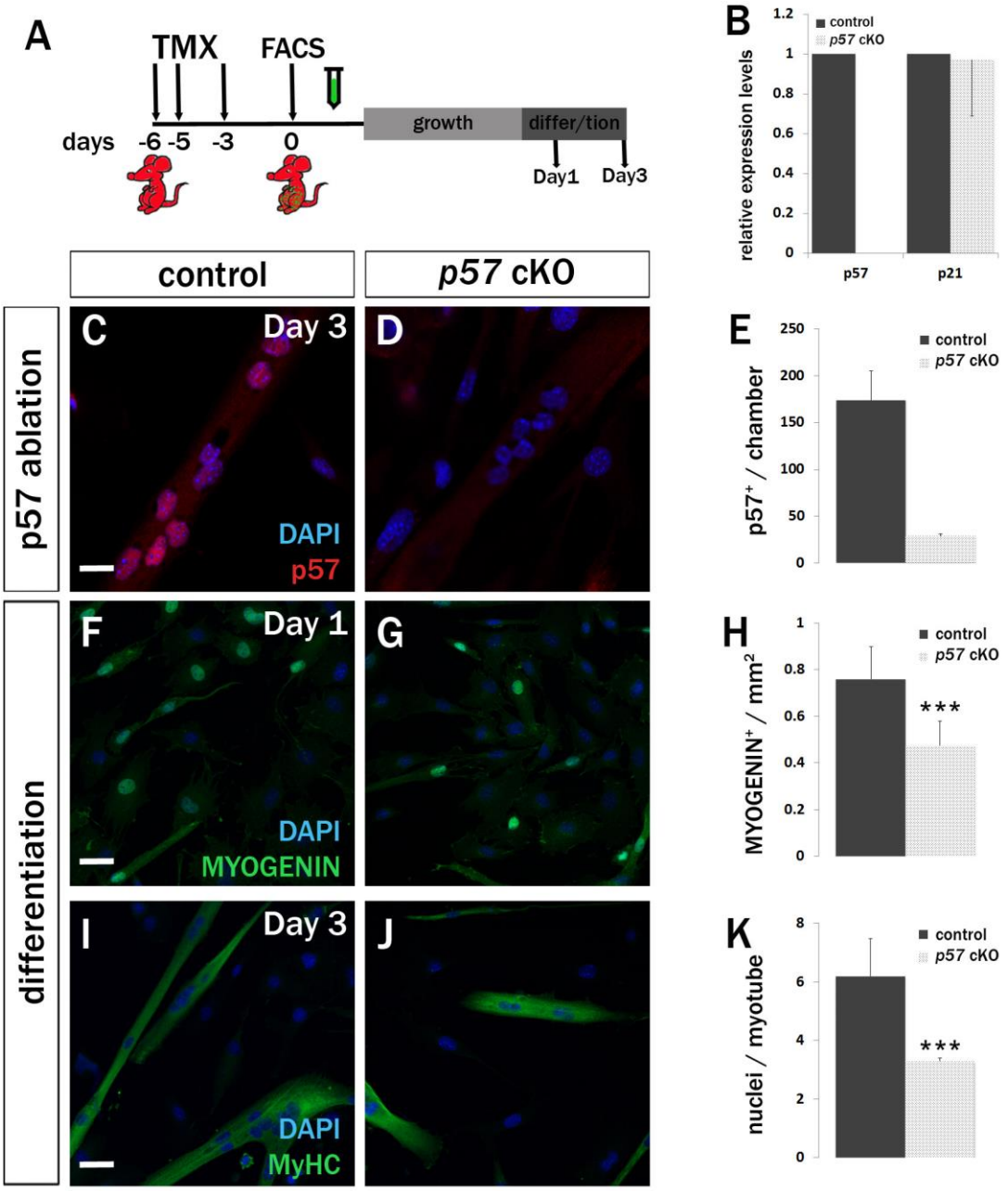
A
TMX
FACS
days
-6 -5 -3
0
growth
differ/tion
Day1
Day3
control
p57 cKO
p57 ablation
differentiation
C
Day 3
DAPI
p57
D
F
Day 1
DAPI
MYOGENIN
G
I
Day 3
DAPI
MyHC
J
B
control
p57 cKO
relative expression levels
1.2
1
0.8
0.6
0.4
0.2
0
p57
p21
E
control
p57 cKO
p57+ / chamber
250
200
150
100
50
0
H
control
p57 cKO
MYOGENIN+ / mm2
1
0.8
0.6
0.4
0.2
0
***
K
control
p57 cKO
nuclei / myotube
8
6
4
2
0
***

Figure 6

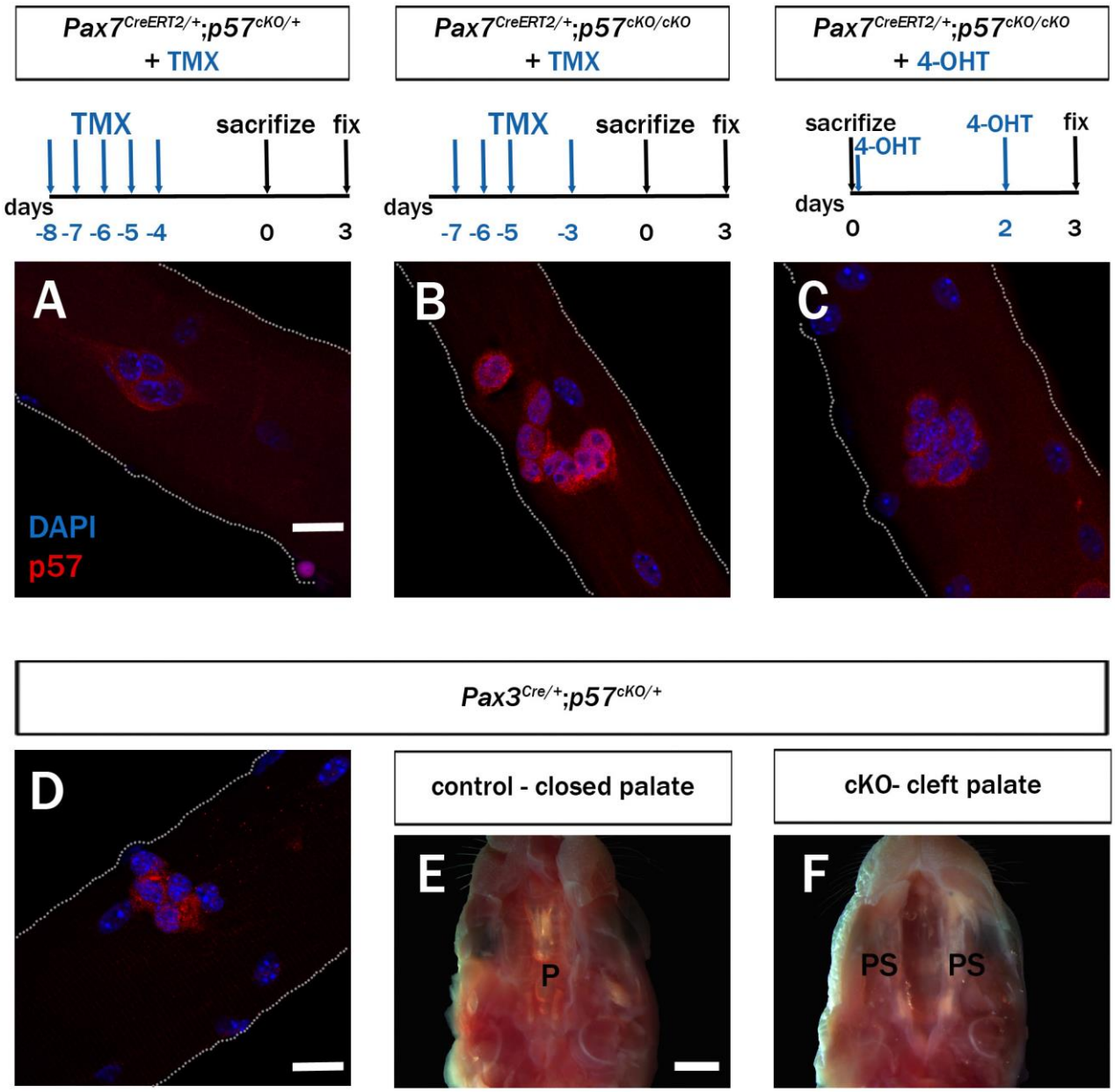
Pax7CreERT2/+;p57cKO/+
+ TMX
TMX
sacrifize
fix
days
-8 -7 -6 -5 -4
0
3
Pax7CreERT2/+;p57cKO/cKO
+ TMX
TMX
sacrifize
fix
days
-7 -6 -5
-3
0
3
Pax7CreERT2/+;p57cKO/cKO
+ 4-OHT
sacrifize
4-OHT
4-OHT
fix
days
0
2
3
A
DAPI
p57
B
C
Pax3Cre/+;p57cKO/+
D
control - closed palate
cKO- cleft palate
E
P
F
PS
PS

Figure S1

DISCUSSION

CDKIs, MRFs and Notch signaling interplay in cell cycle exit during development

The balance between proliferation and differentiation ensures normal tissue development during embryogenesis. Unregulated proliferation or premature differentiation can have deleterious defects. Thus, much effort is placed on understanding the mechanisms which define the equilibrium between sufficient propagation and differentiation, supporting the formation of morphologically and functionally correct structures. In the developing skeletal muscle, previous studies have identified key signaling pathways and factors controlling these procedures and we showed how they are coordinated in the co-existing and interacting proliferating progenitor and differentiating myoblast populations of the nascent muscle masses [Zalc et al., 2014].

One of the hallmarks of differentiation is the acquisition of a post-mitotic state, leading to the general assumption that growth arrest and differentiation are interconnected. During skeletal muscle formation in the embryo and fetus, cell cycle exit occurs at the transition from committed progenitors to determined myoblasts. Indeed, at the course of differentiation from Pax3/7+ progenitors to Myogenin+ myoblasts we observed progressively increasing expression of cyclin-dependent kinase inhibitors (CDKIs). This is consistent with the observed Hes/Hey repressive activity on Myogenic Regulator Factor (MRF)-mediated transactivation of the identified p57MRE, as our data and previous studies suggest high Notch and high MRF activity in muscle progenitors and in committed/differentiating cells, respectively. Monitoring the cell cycle status upon differentiation impairment (using MyoD mutant embryos) and vice-versa (using p21/p57 double knock-outs) showed that cell cycle exit and differentiation are synchronous, yet uncoupled [Zalc et al., 2014]. In the absence of MyoD, limb myogenesis is delayed and Myf5 is maintained at high levels [Kablar et al., 1997; Kablar et al., 1998]. We found that Myf5+Pax3/7- cells expressed p57 at E12.5 MyoD$^{-/-}$ forelimbs [Zalc et al., 2014]. Given our model whereby MyoD binds and activates p57 via the p57MRE sequence, we assume that Myf5 operates similarly. Pax7+Myf5- undifferentiated progenitors were shown to represent a slow-cycling pool, while Pax7+Myf5+ cells correspond to a committed fast-cycling population [Picard & Marcelle, 2013]. Future studies are expected to address the subtle cell cycle regulation of those populations and the role of Myf5 in cell proliferation changes.

Apart from cell cycle regulation, p57 functions in muscle through a positive feedback loop with MyoD. Evidence from myogenic cell lines and zebrafish implicate it in MyoD stabilization (see below). It is not known whether the same mechanism operates in murine embryonic myogenesis. However, it could be suggested that growth arrest and differentiation are initially independent but subsequently synergize to drive terminal differentiation. Accordingly, p21/p57 double knock-out mice show impaired Mef2c expression [Zhang et al., 1999b], implicating p21 and p57 in the regulation of terminal differentiation.

In the model of coordinated regulation that we propose, the interplay of Notch-mediated p57 repression in Pax3/7 progenitors and the MRF-mediated p57 activation in myoblasts is essential for growth arrest. A similar Notch-based interplay of progenitor and committed cells has recently been proposed for the airway epithelium [Pardo-Saganta et al., 2015]. During embryonic and postnatal myogenesis, Notch signaling is crucial for sustaining progenitors and stem cells, while myogenic differentiation requires Notch downregulation [Mourikis & Tajbakhsh, 2014]. Further studies are required to precise the molecular network among PAX/MRF regulation, cell growth arrest, and Notch switch. Even though p57 and p21 are absent from cycling cells of E11.5 forelimbs under normal conditions [Zalc et al., 2014], we observed cycling Pax3+p57+ or Pax3+p21+ progenitors in *Pax3*$^{Cre/+}$*; Rbpj*$^{flox/flox}$ E11.5 forelimbs [Zalc et al., 2014]. Although the latter might correspond to a transitory state, it is also possible that Notch regulates both cell cycle progression and arrest through a complex mechanism. As *Rbpj* ablation does not cause a complete growth arrest or differentiation of Pax3 progenitors [Zalc et al., 2014], other pathways might be involved. Indeed, in postnatal myogenesis the balance of Notch and Wnt or Notch and TGF-b/pSmad3 orchestrates proliferative expansion and differentiation [Brack et al., 2008; Carlson et al., 2008]. The opposing cell cycle effects of Notch and TGF-b are imposed through the control of CDKIs, including p21 [Carlson et al., 2008].

Our study in embryonic myogenesis and growth arrest suggests a model for Notch/MRF crosstalk through p57 regulation. Whether the same mechanism applies in postnatal myogenesis remains to be shown, but a few lines of evidence render it a possible scenario. Firstly, p57MRE was identified by a

MyoD ChIP-seq in C2C12 cells, raising the possibility that it can be reused in adult muscle cells. Secondly, Notch has a well-established role in maintenance as well as homing of satellite cells [Bjornson et al., 2012; Bröhl et al., 2012; Mourikis et al., 2012b; Wen et al., 2012]. Thirdly, p57 has an emerging role stem cell homeostasis, including hematopoietic [Matsumoto et al., 2011; Zou et al., 2011], neural [Furutachi et al., 2013], and lung [Zacharek et al., 2011] stem cells. Fourthly, p57 is transcriptionally repressed by Notch effectors in several systems, apart from the embryonic muscle [Zalc et al., 2014], including neural plate cells [Park et al., 2005], pancreatic progenitors [Georgia et al., 2006], pituitary [Monahan et al., 2009], and thyroid gland [Carre et al., 2011]. It would be interesting to speculate that CDKI modulation represents a general safeguard mechanism for fine tuning of stem/progenitor-based prenatal growth and postnatal regeneration avoiding structure malformation and/or cancer.

Conditional *p57* ablation for postnatal studies

Developmental data implicate p57 in the majority of the emerging tissues and organs [Zhang et al., 1997; Yan et al., 1997; Susaki et al., 2009], while by regulating cell cycle arrest, apoptosis, and cell mobility, p57 is a putative tumor suppressor [Kavanagh & Joseph, 2011]. However, *in vivo* p57 studies in the adult organism require the development of genetic tools that bypass the perinatal lethality of p57-deficient mice.

We generated a mouse model that allows conditional ablation of the coding region of p57 by the loxP/Cre system [Mademtzoglou et al., submitted-1]. We demonstrated that ubiquitous Cre expression results in p57 recombination and loss. Cre-induced p57 absence reproduced the phenotypes observed in p57-null mice, confirming its indispensable role during embryonic development [Zhang et al., 1997; Yan et al., 1997; Susaki et al., 2009; Mademtzoglou et al., submitted-1]. p57 expression has been associated with key differentiation steps of various organs [Matsuoka et al., 1995; Westbury et al., 2001]. Its loss caused proliferation, apoptosis, and differentiation defects in various tissues, such as skeleton, cranio-facial structures, sensory organs,

gastro-intestinal tract, and reproductive system [Yan et al., 1997; Zhang et al., 1997; Takahashi et al., 2000; Susaki et al., 2009; Mademtzoglou et al., submitted-1]. p57 ablation in a spatially- and temporally- defined manner during development will allow the characterization of the cell population(s) and time window, in which p57 function is crucial for individual structures. Furthermore, postnatal-specific p57 abrogation overcomes perinatal lethality and facilitates investigation of stem cell function and cell fate decisions.

The generated mice also contain a β-galactosidase reporter. We showed that this reporter faithfully recapitulates the expression profile that was described for p57, including widespread expression during development and highly localized in the adult [Matsuoka et al., 1995; Yan et al., 1997; Zhang et al., 1997; Westbury et al., 2001; Mademtzoglou et al., submitted-1]. Since early studies on p57 expression relied on northern and western analysis of entire organs, the new mouse provides a fast reporter-based way for screening of p57-expressing cell populations to define focused functional analyses.

Differences in genetic backgrounds in humans or model organisms affect responses to various factors, including disease susceptibility [Chow, 2016]. In our study, $p57^{FL\text{-}ILZ/+}$ mice showed improved survival in mixed 129S2 X C57Bl/6N or 129S2 X C57Bl/6J background compared to C57Bl/6J. Similarly, the effects of excessive p57 on embryonic growth retardation were responsive to genetic background [Andrews et al., 2007]. Strain background can also influence p57 imprinting, with minor expression of the paternal allele being detectable in certain crosses [Park & Chung, 2001].

CDKIs in the control of satellite cells

Regenerative myogenesis in adult skeletal muscle is of vital importance for recovery from injuries, but can be compromised by degenerative or disease states, including aging, that affect the functional capacity of satellite cells, namely the muscle stem cells. Central in their function preservation is the entry into a reversibly dormant state (i.e. quiescence) whenever they are not contributing to muscle formation, meaning when postnatal growth or post-injury repair ceases. Thus, unraveling their cell cycle transitions and (re)-acquisition of quiescence has gained significant interest in recent years.

Focusing on cell cycle exit signals, we hypothesized that p21 and p57 might drive adult satellite cells out of the cell cycle to promote myogenic differentiation or self-renewal of the quiescent pool. They have been shown to redundantly control embryonic muscle cell cycle status and differentiation [Zhang et al., 1999b], while the adult regenerative program is postulated to recapitulate features of embryonic myogenesis [Tajbakhsh, 2009]. In homeostasis, we found no p21 protein in quiescent satellite cells or any other muscle cell type [Mademtzoglou et al., submitted-2], complementing previous reports for negligible p21 mRNA [Macleod et al., 1995] or protein [Franklin & Xiong, 1996] in adult muscle. On the contrary, skeletal muscle is one of the tissues with high levels of p57 transcript in adult life [Matsuoka et al., 1995; Park & Chung, 2001] and we found p57 protein to be abundant in interstitial cells [Mademtzoglou et al., submitted-2], giving insight to its intramuscular localization. However, it was missing from the satellite cell compartment in muscle sections and in freshly isolated single myofibers [Mademtzoglou et al., submitted-2], in line with a previous study on mRNA analysis of FACS-sorted postnatal satellite cell populations at different ages and dormancy states [Chakkalakal et al., 2014]. The only report on p57 presence in quiescent satellite cells [Fukada et al., 2007] is based on FACS-sorting with a novel antibody that the same group previously described [Fukada et al., 2004]; nevertheless, this antibody is also immuno-recognizing a fraction of bone marrow cells [Fukada et al., 2004], while p57 has a well-established role and presence in the hematopoietic lineage [Matsumoto et al, 2011; Zou et al., 2011]. Furthermore, p57 immunostaining in Fukada et al. [2007] was performed with an antibody that recognizes a sequence in the carboxy-terminal region of p57, which

might cross-react with the respective homologous domain of p27 [Matsuoka et al., 1995; Galea et al., 2008; Pateras et al., 2009]. Combining our and previous observations [Fukada et al., 2004; 2007; Chakkalakal et al., 2014; Mademtzoglou et al., submitted-2], we conclude that quiescent satellite cells are p57 negative. Instead, they express p27, the last CDKI of the family encompassing p21 and p57 [Chakkalakal et al., 2014; our unpublished observation]. However, this observation does not preclude p21 and p57 participation in satellite cell cycle dynamics; in the pituitary p57 was found to promote cell cycle exit, while p27 prevented cell cycle re-entry [Bilodeau et al., 2009].

Upon satellite cell activation p21 and p57 rapidly became upregulated. Given their role in growth arrest during embryonic myogenesis [Zhang et al., 1999b], we did not expect p21 and p57 at early post-activation stages when myoblasts are dividing and no differentiation or self-renewal occurs [Zammit et al., 2004]. Their presence in actively proliferating cells seems intuitively contradictory to their role as cell cycle inhibiting molecules. However, p21 has been associated with cell cycle progression by promoting the assembly of cyclin-CDK complexes and their nuclear localization, whereas it induces growth arrest when it stoichiometrically exceeds these complexes [Xiong et al., 1993; Firpo et al., 1994; Michieli et al., 1994; Nourse et al., 1994; Zhang et al., 1994; Harper et al., 1995; Liu et al., 1996; LaBaer et al., 1997]. Thus, p21 was proposed to “titrate” proliferation by impeding it at zero/high amounts but supporting it in intermediate concentrations. In MyoD-converted fibroblasts p21 is involved in nuclear accumulation and activity of cyclin-Cdk complexes [Peschiaroli et al., 2002], possibly extending the previous observation in the myogenic context. Furthermore, experiments with C2C12, a widely used mouse myoblast cell line [Yaffe & Saxel, 1977] that can differentiate into myocytes, showed that the interaction of p21 with Cdk4 was higher in myocytes than myoblasts, leading to Cdk4 inhibition [Wang & Walsh, 1996b]. Whether these findings can be generalized to our experimental system remains to be shown. Of note, genetic ablation of p21 led to an increase in Ki67+ myoblasts in our *ex vivo* myofiber culture [Mademtzoglou et al., submitted-2], favoring a stronger contribution of p21 to the inhibition than promotion of Cdk activity and cell cycle progression.

We also found p57 in activated, proliferating cells, but mostly restricted to their cytoplasm, while in differentiating populations it became progressively nuclear. The molecular events regulating this shuttling remain to be identified. Cytoplasmic p57 was found to associate with LIM-kinase1 and regulate cell motility [Vlachos & Joseph, 2009; Chow et al., 2011; Guo et al., 2015]. We asked whether a same mechanism is found in muscle, given that one of the early manifestations of satellite cell activation is their mobilization [Siegel et al., 2009; Marg et al., 2014; Webster et al., 2016]. However, I was not able to detect *LIM-kinase1* expression in single myofiber cultures. Future studies with scratch assays in primary myoblast culture might show if it is associated with mobility with other, yet uncharacterized, partners. A second possibility is that p57 shuttling is related to cell cycle dynamics and differentiation progression. Such regulation on the cellular level, has previously been described for ERK in muscle progenitors [Michailovici et al., 2014]. Post-translational modifications of p57 protein might restrain it to the cytoplasm to allow cell cycle to progress. Alternatively, p57 might help the assembly of recently produced cyclin and CDK molecules in the cytoplasm, as p21 and p27 do (see above). In their absence, p57 was shown to resume their role in stabilizing cyclin-CDK complexes in mouse embryonic fibroblasts [Cerqueira et al., 2014]. Finally, it could be involved in the relocalization of Cdk or cyclins, as is the case for fibroblasts with ectopic MyoD and hematopoietic stem cells, respectively [Figliola & Maione, 2004; Zou et al., 2011]. Further studies are required to better understand the p57 nucleo-cytoplasmic translocation in activated and differentiating myoblasts. The fact that it persisted in the cytoplasm of half of the differentiating myoblasts [Mademtzoglou et al., submitted-2] complicates our speculation, but is consistent with previous data on p57 cytoplasmic distribution in myotubes forming from MyoD-converted fibroblasts [Figliola & Maione, 2004]. On the contrary, p21 did not undergo such nucleo-cytoplasmic shuttling [Mademtzoglou et al., submitted-2]. Similarly, when fibroblasts were induced to myogenic fate by MyoD, p21 had strictly nuclear presence in the forming myotubes [Figliola & Maione, 2004]. Moreover, p21, but not p57 or p27, appeared in the nucleus of Ki67+ proliferating b-cells, when proliferation was induced by adenoviral expression of cyclins and Cdks [Fiaschi-Taesch et al., 2013]. In general, under normal conditions, p21 is not expected to persist in the cytoplasm, as its presence there is linked to degradation [Hwang et al., 2009] or oncogenesis [Besson et al., 2004; Besson et al., 2008].

Upregulation of p21 and p57 upon satellite cell activation might be related to MyoD, which is also absent from quiescent satellite cells but appears as early as three hours post-activation *ex vivo* [Zammit et al., 2004; Zhang et al., 2010] or six hours post-injury *in vivo* [Grounds et al., 1992]. Both p21 and p57 are induced by MyoD, while later they enhance its activity and stabilization [Halevy et al., 1995; Reynaud et al., 1999; Reynaud et al., 2000b; Tintignac et al., 2004; Osborn et al., 2011; Battistelli et al., 2014; Zalc et al., 2014]. Interestingly, the p57-MyoD binding engages the p57 helix domain that was found indispensable for Cdk/cylin inhibition [Hashimoto et al., 1998; Reynaud et al., 2000b], possibly explaining p57 presence in cycling cells. MyoD is expressed in activated/proliferating myoblasts [Zammit et al., 2004; Liu et al., 2012] and has been proposed to be required for the transition from quiescence to the cell cycle, acting through the replication-related factor Cdc6 [Zhang et al., 2010]. MyoD deficient myoblasts divide in a perturbed way, with divisions taking longer and being less frequent [Megeney et al., 1996]. Curiously, despite MyoD presence in myoblasts, they continue to proliferate and do not proceed to differentiation for several days *in vitro* or *in vivo* [Tajbakhsh, 2009]. It is suggested that additional factors, including Myogenin, are needed to initiate/enhance transcription of at least a subset of MyoD targets [Blais et al., 2005; Cao et al., 2006]. This might also explain why exogenous MyoD induces growth arrest in non-myogenic cell lines [Crescenzi et al., 1990; Sorrentino et al., 1990], but not in myogenic ones or satellite cell-derived myoblasts.

p21 has been implicated at the early post-activation steps of satellite cells. Using the *ex vivo* system of floating myofibers my work shows that p21 is present in myoblasts soon after satellite cells are activated [Mademtzoglou et al., submitted-2], while during muscle regeneration, it was shown to peak at 3-4 days post-injury and then decline [Yan et al., 2003; our unpublished observation]. Conversely, resting muscle and quiescent satellite cells are devoid of p21 [Mademtzoglou et al., submitted-2], while muscle development in p21 mutants could to be rescued by p57 [Zhang et al., 1999b]. Thus, we hypothesized that under homeostatic conditions adult muscle would not be affected by p21 loss, while we expected deficits in satellite cell activation/differentiation and possibly muscle regeneration after injury. Indeed, resting muscles of p21 knock-out mice were indistinguishable from control littermates muscles in terms of muscle weight, histology, and satellite

cell compartment [Mademtzoglou et al., submitted-2], in line with previous observations [Deng et al., 1995; Hawke et al., 2003; Chakkalakal et al., 2014; Chinzei et al., 2015]. However, p21 null mice had significantly less satellite cells at an early regeneration time point (i.e. D5), although starting with similar pre-regeneration satellite cell amounts [Mademtzoglou et al., submitted-2]. Moreover, regeneration was not overtly affected, as evidenced by the restoration of the satellite cell pool as well as muscle architecture (e.g. myofiber formation, myofiber morphology, central nucleation, interstitium minimization to pre-injury levels) [Mademtzoglou et al., submitted-2]. Similarly, satellite cell numbers [Chakkalakal et al., 2014] and muscle structure [Hawke et al., 2003; Chakkalakal et al., 2014; Chinzei et al., 2015] one month post-injury revealed successful regeneration in previous studies, despite occasional defects at earlier time points [Hawke et al., 2003; Chinzei et al., 2015]. Furthermore, p21 absence did not compromise the long-term regeneration potential, as evidenced by repeated injuries and muscle recovery [Chakkalakal et al., 2014].

To get a better insight into the early activation/differentiation phase, we used single myofiber cultures. Although this systems bears the disadvantages of an *ex vivo* situation, it might reflect a more physiological activation compared to the complete degeneration that is experimentally performed but rarely occurring in nature. When we cultured isolated myofibers from p21 mutant and control mice, activated satellite cells showed increased proliferation and decreased myogenic differentiation [Mademtzoglou et al., submitted-2]. This is indicative of an early defect, in line with our *in vivo* observations and previous data [Hawke et al., 2003; Chakkalakal et al., 2014; Chinzei et al., 2015]. AAV-mediated acute p21 knock-down triggered proliferation of quiescent cells (including satellite cells) and increased cellularity; nevertheless, when the delivered siRNA was used in primary myoblast culture it did not affect differentiation [Biferi et al., 2015]. The difference with previous studies was attributed to the effect of acute versus chronic p21 loss. Future experiments, including conditional genetic ablation of p21 with the loxP-Cre system would allow testing this hypothesis.

In the absence of p57 there was a differentiation deficit *in vitro* and myoblasts did not advance through the myogenic program. p57 correlates with differentiation in various embryonic tissues [Westbury et al., 2001]. It is highly and rapidly upregulated upon *in vitro* myogenic differentiation

[Reynaud et al., 1999], while it has even been considered as synonymous to it [Mounier et al., 2011]. However, the consequences of its abrogation on adult muscle have not been estimated, partially because of the perinatal lethality of p57 mutant mice, which we overpassed with the new conditional knock-out we generated. With the caveat that our *in vitro* system lacks the structural, neurogenic, and metabolic fidelity of the muscle tissue [Grounds, 2014], our data suggest that p57 is involved in adult myogenic differentiation. Although we wished to verify these findings in the *in vivo* context, our analysis was hindered by inefficient recombination [Mademtzoglou et al., submitted-2]. Previous studies on satellite cells suggest that the cell cycle state (quiescence versus activation/proliferation) may interfere with recombination resistance/success [Lepper et al., 2009; Günther et al., 2013; von Maltzahn et al., 2013]. Given these findings, a more appropriate scheme for tamoxifen-inducible Cre-mediated p57 recombination might include administration of tamoxifen during muscle regeneration. It will be interesting to monitor how p57 influences the post-regeneration re-establishment of the satellite cell compartment, given its emerging importance in the quiescence and maintenance of other stem cells, such as hematopoietic [Matsumoto et al., 2011; Zou et al., 2011], neural [Furutachi et al., 2013], and lung stem cells [Zacharek et al., 2011].

Overall, we conclude that p21 and p57 are essential at the early steps following satellite cell activation. Their presence seems compatible with activation/proliferation and possibly represents an early activation event. Their loss profoundly affects *ex vivo* myogenic differentiation. Our data sofar indicate that p21 and p57 function in distinct ways during adult and embryonic myogenesis, in terms of early versus continuous myogenesis support. It remains to be established whether the preliminary differentiation/regeneration defects are rescued by p21 and p57 in p57 and p21 mutants, respectively. Satellite cell-specific double p21/p57 knock-out may elucidate their relative contributions and putative redundancies in the adult. A better understanding of cell cycle regulation in satellite cells is imperative to define the molecular events underlying their long-term preservation -through (re)-entry into quiescence- and their rapid response to regenerative needs -through prompt and tightly controlled activation. Defective stem cell cycle dynamics and continuous activation/proliferation can lead to DNA damage accumulation, apoptosis, pool exhaustion, and inability to support homeostatic or regenerative demands.

ANNEX

Further contribution to projects of the partner labs

Gene expression profiling of muscle stem cells identifies novel regulators of postnatal myogenesis

Alonso-Martin S, Rochat A, Mademtzoglou D, Morais J, De Reynies A, Auradé F, Chang T, Zammit PS, Relaix F

Skeletal muscle growth and regeneration require a population of muscle stem cells, the satellite cells, located in close contact to the myofiber. These cells are specified during fetal and early postnatal development in mice from a Pax3/7 population of embryonic progenitor cells. As little is known about the genetic control of their formation and maintenance, we performed a genome-wide chronological expression profile identifying the dynamic transcriptomic changes involved in establishment of muscle stem cells through life, and acquisition of muscle stem cell properties. We have identified multiple genes and pathways associated with satellite cell formation, including set of genes specifically induced (EphA1, EphA2, EfnA1, EphB1, Zbtb4, Zbtb20) or inhibited (EphA3, EphA4, EphA7, EfnA2, EfnA3, EfnA4, EfnA5, EphB2, EphB3, EphB4, EfnBs, Zfp354c, Zcchc5, Hmga2) in adult stem cells. Ephrin receptors and ephrins ligands have been implicated in cell migration and guidance in many tissues including skeletal muscle. Here we show that Ephrin receptors and ephrins ligands are also involved in regulating the adult myogenic program. Strikingly, impairment of EPHB1 function in satellite cells leads to increased differentiation at the expense of self-renewal in isolated myofiber cultures. In addition, we identified new transcription factors, including several zinc finger proteins. ZFP354C and ZCCHC5 decreased self-renewal capacity when overexpressed, whereas ZBTB4 increased it, and ZBTB20 induced myogenic progression. The architectural and transcriptional regulator HMGA2 was involved in satellite cell activation. Together, our study shows that transcriptome profiling coupled with myofiber culture analysis, provides an efficient system to identify and validate candidate genes implicated in establishment/maintenance of muscle stem cells. Furthermore, tour de force transcriptomic profiling provides a wealth of data to inform for future stem cell-based muscle therapies.

Article in press. Provisional form follows

frontiers in Cell and Developmental Biology

ORIGINAL RESEARCH
published: xx June 2016
doi: 10.3389/fcell.2016.00058

Gene Expression Profiling of Muscle Stem Cells Identifies Novel Regulators of Postnatal Myogenesis

Sonia Alonso-Martin[1, 2, 3*†], *Anne Rochat*[1], *Despoina Mademtzoglou*[1, 2, 3], *Jessica Morais*[1], *Aurelien De Reynies*[4], *Frédéric Auradé*[5], *Ted Chang*[1†], *Peter S. Zammit*[6] and *Frédéric Relaix*[1, 2, 3, 7, 8*]

[1] INSERM, IMRB U955-E10, Créteil, France, [2] Université Paris Est, Faculté de Medecine, Créteil, France, [3] Ecole Nationale Veterinaire d'Alfort, Maison Alfort, France, [4] Programme Cartes d'Identité des Tumeurs, Ligue Nationale Contre le Cancer, Paris, France, [5] Sorbonne Universités, UPMC Univ Paris 06, INSERM UMRS974, Center for Research in Myology, Paris, France, [6] Randall Division of Cell and Molecular Biophysics, King's College London, London, UK, [7] Etablissement Français du Sang, Créteil, France, [8] APHP, Hopitaux Universitaires Henri Mondor, DHU Pepsy and Centre de Référence des Maladies Neuromusculaires GNMH, Créteil, France

Skeletal muscle growth and regeneration require a population of muscle stem cells, the satellite cells, located in close contact to the myofiber. These cells are specified during fetal and early postnatal development in mice from a Pax3/7 population of embryonic progenitor cells. As little is known about the genetic control of their formation and maintenance, we performed a genome-wide chronological expression profile identifying the dynamic transcriptomic changes involved in establishment of muscle stem cells through life, and acquisition of muscle stem cell properties. We have identified multiple genes and pathways associated with satellite cell formation, including set of genes specifically induced (*EphA1*, *EphA2*, *EfnA1*, *EphB1*, *Zbtb4*, *Zbtb20*) or inhibited (*EphA3*, *EphA4*, *EphA7*, *EfnA2*, *EfnA3*, *EfnA4*, *EfnA5*, *EphB2*, *EphB3*, *EphB4*, *EfnB*s, *Zfp354c*, *Zcchc5*, *Hmga2*) in adult stem cells. Ephrin receptors and ephrins ligands have been implicated in cell migration and guidance in many tissues including skeletal muscle. Here we show that Ephrin receptors and ephrins ligands are also involved in regulating the adult myogenic program. Strikingly, impairment of EPHB1 function in satellite cells leads to increased differentiation at the expense of self-renewal in isolated myofiber cultures. In addition, we identified new transcription factors, including several zinc finger proteins. ZFP354C and ZCCHC5 decreased self-renewal capacity when overexpressed, whereas ZBTB4 increased it, and ZBTB20 induced myogenic progression. The architectural and transcriptional regulator HMGA2 was involved in satellite cell activation. Together, our study shows that transcriptome profiling coupled with myofiber culture analysis, provides an efficient system to identify and validate candidate genes implicated in establishment/maintenance of muscle stem cells. Furthermore, tour de force transcriptomic profiling provides a wealth of data to inform for future stem cell-based muscle therapies.

Keywords: skeletal muscle, myogenesis, satellite cells, ephrins, zinc fingers

OPEN ACCESS

Edited by:
Atsushi Asakura,
University of Minnesota, USA

Reviewed by:
Akiyoshi Uezumi,
Fujita Health University, Japan
Lucia Latella,
National Research Council of Italy, Italy

****Correspondence:***
Sonia Alonso-Martin
alonsomartin.s@gmail.com;
Frédéric Relaix
frederic.relaix@inserm.fr

†Present Address:
Sonia Alonso-Martin,
Tissue Regeneration Laboratory,
Centro Nacional de Investigaciones Cardiovasculares, Madrid, Spain;
Ted Chang,
International Centre for Genetic Engineering and Biotechnology, Cancer Genomics Group, Anzio Road, Cape Town, South Africa

Specialty section:
This article was submitted to Stem Cell Research, a section of the journal Frontiers in Cell and Developmental Biology

Received: *29 January 2016*
Accepted: *02 June 2016*
Published: *xx June 2016*

Citation:
Alonso-Martin S, Rochat A, Mademtzoglou D, Morais J, De Reynies A, Auradé F, Chang T, Zammit PS and Relaix F (2016) Gene Expression Profiling of Muscle Stem Cells Identifies Novel Regulators of Postnatal Myogenesis. Front. Cell Dev. Biol. 4:58. doi: 10.3389/fcell.2016.00058

INTRODUCTION

During vertebrate development, successive phases of embryonic and fetal myogenesis leads to formation and growth of skeletal muscles (Relaix et al., 2005; Relaix, 2006; Buckingham and Relaix, 2007). Skeletal muscle cells of trunk and limbs in mouse originate from the early somites, which appear at mid-gestation from undifferentiated presomitic mesoderm (Tajbakhsh and Buckingham, 2000). Following several steps of somite maturation, a population of muscle progenitor cells (MPC) that express the paired-box/homeobox transcription factors *Pax3* and *Pax7* emerge in the central region of the developing somite. Similar cell populations are also found in head muscles, though using a different set of transcriptional regulators (Sambasivan et al., 2011). MPC will both self-renew and give rise to all skeletal muscles via activation of a family of four muscle-specific bHLH transcription factors (*Myf5*, *Mrf4*, *MyoD*, and *Myog*: myogenin) that induce the myogenic program (Bismuth and Relaix, 2010; Murphy and Kardon, 2011). Around birth, while all MPC maintain the expression of *Pax7*, *Pax3* expression in only maintained in a subset of muscles (Relaix et al., 2006) (unpublished observations). MPC become in close contact with the muscle fibers in response to different signals, such as those from the Notch pathway (Seale et al., 2000; Zammit et al., 2006a; Tajbakhsh, 2009; Brohl et al., 2012). During establishment of this anatomical niche, emerging satellite cells acquire stem cell-specific characteristics, including self-renewal capacity (Mauro, 1961; Zammit et al., 2006a; Relaix and Marcelle, 2009). During postnatal muscle growth, satellite cells supply myonuclei to maturing myofibers up to postnatal day 21 (P21) before becoming mitotically quiescent (Lepper et al., 2009; White et al., 2010). Adult satellite cells can be activated from their mitotically quiescent state upon injury (Wang and Rudnicki, 2011; Relaix and Zammit, 2012), to proliferate, and co-express MYOD and PAX7. They then differentiate via activation of *Myog* (and down-regulation of *Pax7*) to repair damaged myofibers, while a subpopulation of satellite cells will self-renew to restore the pool of quiescent satellite cells by down-regulation of *MyoD* (Zammit et al., 2004; Rudnicki et al., 2008; Relaix and Zammit, 2012).

Understanding regulation of myogenic progression from MPCs to muscle stem cells is central to building a comprehensive model of satellite cell function. Many transcriptional networks that control embryogenesis are also important for myogenesis, such as Notch, BMP or WNT proteins (Linker et al., 2003; Ono et al., 2011; Brohl et al., 2012). Furthermore, a balance between extrinsic cues and intracellular signaling pathways, such as IGF, FGF, Notch, and TGF-β, is required to preserve stem cell function (Brack et al., 2008; Kuang et al., 2008; Brack and Rando, 2012; Dumont et al., 2015).

We have characterized the dynamics of skeletal muscle progenitor and postnatal stem cells from embryonic development to adult life, hence deciphering the intrinsic molecular pathways involved in specification and regulation of these muscle stem cells. Using this large microarray analysis of myogenic progenitoris and stem cells during development and adult myogenesis, we identified and evaluated several new candidate factors mediating satellite cell specification and function, with a focus here on EPHB1 and several transcriptional regulators, including four zinc finger transcription regulators (Zfp354c, Zcchc5, Zbtb4, and Zbtb20) *and* HMGA2, a transcriptional co-regulator belonging to the HMGI family of small high-mobility-group (HMG) proteins (Zhou et al., 1995).

Eph Receptors and Ephrin Ligands

Eph/ephrin signaling has been shown to regulate muscle satellite cell motility and patterning (Stark et al., 2011), but has not been linked with regulation of the myogenic program. Eph receptors belong to a large family of receptor tyrosine kinases (RTK) involved in cell contact-dependent signaling and patterning (Pitulescu and Adams, 2010). EPHs are classified as EphAs or EphBs based on their binding affinity for the ephrin ligands, ephrin-A (EFNA) or ephrin-B (EFNB) (Figures S1A,B). EFNAs are GPI (glycosylphosphatidylinositol)-anchored and lack a cytoplasmic domain while EFNBs are attached to the membrane by a single transmembrane domain containing a short cytoplasmic PDZ-binding motif (Pasquale, 2005). Interestingly, both Eph receptors and ephrin ligands are competent to signal following interaction (forward and reverse signaling, respectively), and both *trans* and *cis* signaling have been described (Arvanitis and Davy, 2008; Pitulescu and Adams, 2010). In addition, Eph/ephrin signaling is often part of a complex signaling network of regulatory pathways, for instance with adhesion molecules, other cell surface receptors or channels and pores (Arvanitis and Davy, 2008).

Eph/ephrin interaction leads to a large set of developmental processes and biological responses, including adhesion and repulsion, increased or reduced motility, cell plasticity, permeability and morphogenesis, and cell fate specification (Palmer and Klein, 2003; Arvanitis and Davy, 2008). Eph/ephrins are also implicated in regulation of stem cell niches and cancer (Genander and Frisen, 2010; Murai and Pasquale, 2010; Pasquale, 2010).

Zinc Finger Transcription Factors

Zinc finger proteins belong to a large family of transcription regulators subdivided in seven categories. There are about 800 zinc finger transcription factors in the human genome, with a third of those containing a KRAB (Krüppel Associated Box) domain, such as ZFP354C (see below) or related sequences as ZBTB4 or ZBTB20 (Lupo et al., 2013). KRAB is the most widespread family of transcription factors in the human genome, but is also found in yeast (*S. cerevisiae*) and worm (*C. elegans*) (Ganss and Jheon, 2004). The KRAB protein domain is a powerful repression region that acts as a transcriptional repressor, allowing the binding to co-repressor proteins (Urrutia, 2003). KRAB-containing proteins involved in cell proliferation, differentiation, apoptosis, and tumor formation have been described (Urrutia, 2003; Tian et al., 2006; Li et al., 2008).

Zfp354c (*Kid3, AJ18*) belongs to the *Kid* family of genes. The corresponding proteins *Kid1, Kid2,* and *Kid3*, share a very similar structure: a KRAB domain and 11–13 C2H2 motifs (Figure S1C), these last zinc finger motifs consisting in two cysteine and two histidine residues bonded tetrahedrally to a Zinc ion (Ganss and

Jheon, 2004). ZFP354c has been previously described as abundant in the brain (Watson et al., 2000), but its expression has not been tested in skeletal muscle. Interestingly, KRAB/C2H2 zinc finger protein ZFP354C participates in the BMP (bone morphogenic protein) signaling pathway (Jheon et al., 2003), a key regulator of skeletal muscle development and stem cell function (Amthor et al., 1998; Wang et al., 2010; Ono et al., 2011; Sartori et al., 2013). Given the important role of BMP signaling in skeletal muscle biology, ZFP354C is a good candidate as possible regulator of myogenesis.

Zinc finger and BTB domain-containing protein 4 (*Zbtb4*, *KAISO-L1*, *Znf903*) is a transcriptional repressor of specificity protein (Sp) transcription factors (Sreevalsan and Safe, 2013), that binds methylated DNA to repress transcription (Filion et al., 2006; Weber et al., 2008). Despite its broad distribution, ZBTB4 seems to be particularly expressed in the brain. In addition, examination of publicly available microarray data sets demonstrated an inverse relationship in the prognostic value and expression of ZBTB4 and the histone methyltransferase EZH2 in tumors from breast cancer patients (Yang et al., 2014). Indeed, polycomb group protein EZH2 controls self-renewal and safeguards the transcriptional identity of skeletal muscle stem cells (Juan et al., 2011).

Zinc finger and BTB domain-containing protein 20 (*Zbtb20*, *DPZF*, *Hof*, *Zfp288*) is a member of a subfamily of zinc finger proteins containing C2H2 Krüppel-type zinc fingers and BTB/POZ domains (Mitchelmore, 2002). ZBTB20 can function as a transcriptional repressor and plays an essential role in the specification of pyramidal neurons in the developing hippocampus (Nielsen et al., 2007), and promotes astrocytogenesis during neocortical development (Nagao et al., 2016). ZBTB20 is also a regulator of terminal differentiation of hypertrophic chondrocytes (Zhou et al., 2015). This factor has been recently described to be involved in liver regeneration (Weng et al., 2014), and promoting cell proliferation and tumor growth through repression of FOXO1 (Zhao et al., 2014; Kan et al., 2016). *Zbtb20* null mice exhibit severe postnatal growth retardation, metabolic dysfunction and lethality, suggesting that ZBTB20 plays non-redundant roles in multiple organ systems (Sutherland et al., 2009; Cao et al., 2016).

Zinc finger, CCHC domain-containing 5 (*Zcchc5*, *Mar3*, *Zhc5*) belongs to the family of the gag-like retrotransposon genes (glycosaminoglycans) exclusively found in mammals, and is considered an ortholog of Ty3/gypsy group. *Zcchc5* is located on the X chromosome, within the dystrophin (*Dmd*) locus (X21.1) in human. The retrotransposition capacity of these genes seems to have been lost, despite retaining an intact reading frame (Brandt et al., 2005). Thus, the retrotransposons of this family are considered as neogenes with new functions, but their impact and regulation is still poorly understood. *Zcchc5* encodes a nuclear protein containing a $CX_2CX_4HX_4C$ DNA-binding motif, also called CCHC domain, allowing DNA binding to regulate transcription. Furthermore, the proteins of the family of genes *Mart*, which includes *Zcchc5*, have been implicated in the control of cell proliferation and apoptosis in cell lines of liver cancer whereas some become up-regulated in regenerating mouse liver (Okabe et al., 2003; Brandt et al., 2005). Interestingly, *Zcchc5* is expressed in skeletal muscles of the limbs (Diez-Roux et al., 2011) (www.eurexpress.org).

Architectural Factor HMGA2 (HMGI-C)

HMGA2, also called HMGI-C, is a transcriptional co-regulator belonging to the HMGI family of small high-mobility-group (HMG) proteins containing AT-hook DNA binding domains (Zhou et al., 1995). HMGI proteins modulate gene expression by altering chromatin architecture and/or by recruiting other proteins to the transcription regulatory complex (Thanos and Maniatis, 1992; Zhou and Chada, 1998; Pfannkuche et al., 2009). *Hmga2* is highly expressed during embryonic development and down-regulated in most adult tissues (Zhou et al., 1995; Pfannkuche et al., 2009; Ashar et al., 2010). HMGA2 plays an important role in maintaining adult stem/progenitor cells, notably in maintaining neural stem/progenitor cells (Nishino et al., 2008). *Hmga2* is also highly expressed in proliferating skeletal myoblasts during myogenesis, modulating satellite cell activation and proliferation both *in vivo* and *in vitro* (Li et al., 2012). *Hmga2* knockout mice exhibit impaired muscle development and reduced myoblast proliferation, while overexpression of *Hmga2* promotes myoblast growth preventing myoblast differentiation (Li et al., 2012). Thus, HMGA2 is a key regulator of satellite cell activation and skeletal muscle development.

METHODS

Mice

$Pax3^{GFP/+}$ mice (Relaix et al., 2005) were used to isolate MPC by fluorescent activated cell sorting (FACS) of the GFP+ cells. $Pax3^{Cre/+}$ mutant mice were kindly provided by Jonathan A. Epstein (Engleka et al., 2005). $R26^{mT-mG}$ mice were obtained from The Jackson Laboratory (Stock No: 007576) (Muzumdar et al., 2007). For myofiber cultures C57BL/6J (Janvier®) male mice (8 weeks old) were used. For lineage tracing experiments, $Pax3^{Cre/+}$ mice were crossed with $R26^{mT-mG}$ to obtain $Pax3^{Cre/+}$; $R26^{mT-mG}$ double mutant mice.

All animals were maintained inside a barrier facility, and all *in vivo* experiments were performed in accordance with the French and European Community guidelines for the care and use of laboratory animals (Project No: 01427.03 approved by MESR and File No: 15-018 from the Ethical Committee of Anses/ENVA/UPEC).

Fluorescent Activated Cell Sorting

Trunk muscle samples (intercostal, pectoral and abdominal) were isolated from the trunk as indicated in **Figure 1A**, at different stages during development and after birth. Muscle were minced and digested in 0.1% Trypsin (Life Technologies®) and 0.1% Collagenase D (Roche®) in DMEM High Glucose without phenol red (Life Technologies®). Digested muscles after filtration were cell-sorted by flow cytometry using a FACS Aria II, using FITC channel to recover the GFP+ cells from $Pax3^{GFP/+}$ mice. GFP+ cells were stained using propidium iodide to exclude dead cells (Figure S2A).

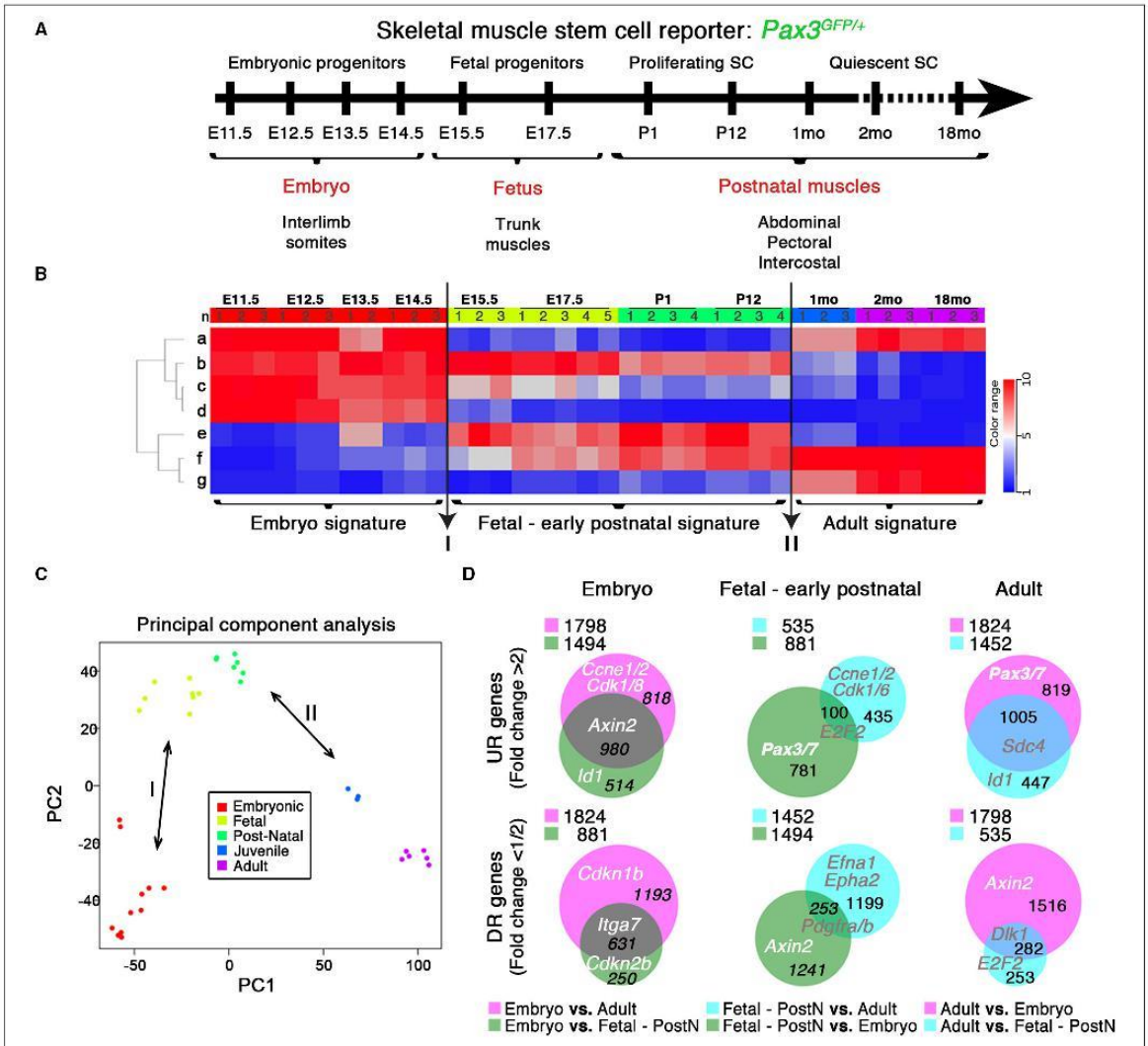

FIGURE 1 | Transcriptome dynamics from embryonic muscle development to aged mice. (A) Schematic outline of the experimental procedure illustrating the stages at which *Pax3*$^{GFP/+}$ RNA samples were harvested: E, Embryonic days; P, Postnatal days; mo, age in months. SC, satellite cells. **(B)** Genes from the microarray were organized in seven clusters ("a" to "g") according to developmental kinetics: with red indicating up-regulated (UR), and blue the down-regulated (DR) transcripts. Transition events (I and II; arrows) are indicated, highlighting the three specific signatures. n, replicate number per stage. **(C)** Principal Component Analysis (PCA) highlights these differences between the three signatures defined by the transitions events in **(B)**. **(D)** Venn diagrams show the interaction of UR (upper panels) or DR (bottom panels) genes from the different comparisons as indicated, illustrating the specific molecular signature for each developmental period. PostN, fetal-to-early postnatal. $p < 10^{-3}$ and change fold >2 (UR) or <1/2 (DR). Gene examples and the number of genes shared between groups are indicated. Legends indicate the total UR or DR genes per comparison.

qPCR Analysis

RNA from trunk muscles was isolated through the RNeasy Fibrous Tissue kit (Qiagen®). For C2C12, total RNA extraction was performed using the RNeasy mini kit from Qiagen®. Total mRNA content was transcribed into coding DNA (cDNA) according to Transcriptor First Strand cDNA Synthesis kit (Roche®) protocols. Quantitative analyzes were performed using the SYBR-Green kit (Roche®). qPCR was performed on biological duplicates (by sorting two different embryo series) with technical duplicates. The results obtained were analyzed by calculating the $2^{\wedge}$-ΔCt. *Hprt1* was used as reference gene.

Oligonucleotides of the following genes were selected, tested and verified according to their efficiencies and specificities:

EphB1: FWD 5′ - CCGTGGATGACTGGCTAAGT - 3′
REV 5′ - TACCGATGGTGACTGGTTCA - 3′
Zbtb4: FWD 5′ - CGCTTCTCCATGTTGGCTAT - 3′
REV 5′ - GTGAGCAGGGAACTTGGTGT - 3′
Zbtb20: FWD 5′ - AATGCGAAAGGGAAGCAGTA - 3′
REV 5′ - ACAGGACCCGTGGAGTAATG - 3′

RNA Preparation, cDNA Synthesis, and Microarray Hybridization

Microarray processing was performed by PartnerChip (Evry, France), according to NuGEN (http://www.nugen.com/nugen/index.cfm/products/pl/) and Affymetrix (http://www.affymetrix.com/support/technical/manuals.affx) protocols. Briefly, total RNA from FACS-sorted trunk muscle GFP+ cells was extracted from independent experiments according to the RNasy® Micro Kit (QIAGEN) RNA extraction protocol. RNA samples were cleaned using Qiagen RNAeasy mini-columns and their quality assessed by spectrophotometry (Nanodrop ND-1000). Total RNA was analyzed on Agilent microarrays (Bioanalyzer, 2100) to assess integrity of ribosomal RNA (28S and 18S peaks). Synthesis and amplification of cDNA was performed following NuGEN Ovation Pico WTA System protocol, and 100 ng of total RNA were used for first strand cDNA synthesis. Second strand was synthesized following the Ribo-SPIA technology developed by NUGEN. Five micro gram of single-stranded cDNA was fragmented and a biotin-labeled nucleotide was attached to the 3′ end of each fragment (Encore Biotin Module, NuGEN). High-density oligonucleotide arrays containing 45,000 sets of oligonucleotide probes (25 m) that cover all 30,000 genes encoded by the murine genome (Affymetrix Mouse Genome 430 2.0 Arrays, Ref 900495) were used for gene expression detection. Hybridization during 16 h at 45°C in a rotary oven (Affymetrix), washing and staining (GeneChip® Fluidics Station 450) and scanning (GeneChip Scanner 3000) were carried out according to NuGEN and Affymetrix protocols. Expression Console software (Affymetrix) was used for image analysis and to determine probe signal levels. The quality and statistical analysis of the data were finally made using the GeneSpring GX11 analysis software (Agilent Technologies).

Expression Microarray Analysis

Pre-Treatment

Expression profiles of 36 samples (Pax3GFP+ cells at different stages during development and after birth) were obtained using Affymetrix Mouse Genome 430 2.0 Arrays. Expression profiles were normalized in batch using RMA algorithm (affy R package) yielding a (probe sets, samples) matrix. As the 36 samples were obtained by merging two series including 15 and 21 samples, Combat algorithm (Johnson WE—Biostatistics—2007) was used to normalize the corresponding batch effect. Expression profiles were aggregated by Gene Symbol (mean across probe sets) using Affymetrix csv annotation file (na32 version).

Unsupervised Analysis

The gene expression matrix (GEO) was then row-mean-centered. The resulting matrix was used for unsupervised classification of the genes. Genes ($n = 21678$) were partitioned in ten clusters using the kmeans classification algorithm. The biggest cluster ($n = 8896$) contained genes showing almost no variation across all samples: it was eliminated from further analysis. Three clusters were found to be highly correlated (centroids correlation >0.95) and were merged in a unique gene cluster (cluster g, **Figure 1B**). We thus remained with seven clusters. For each sample, the mean expression of all the genes of each cluster was calculated, yielding a (seven clusters, 36 samples)-matrix shown in **Figure 1B**.

Supervised Analysis

Moderate *T*-tests (as implemented in limma R package) were used to identify differentially expressed genes.

Pathways Analysis

To analyze the pathway enrichment, hypergeometric tests were used, taking as "pathways" the terms (and related murine genes) from the Gene Ontology (GO) (http://www.geneontology.org) and the murine KEGG pathways (www.genome.jp/kegg). Pathways enrichment in the seven gene clusters: in each of the seven gene clusters, the pathway analysis was performed using (i) all the genes included in the cluster, (ii) genes selected based on their coefficient of variation and median-absolute-deviation (different thresholds were used): the minimal (hypergeometric test) *p*-value obtained from these different (sub-) lists was retained. Pathways enrichment analysis of differentially expressed genes: given a comparison between two groups of samples, yielding a *p*-value and a fold change for each gene, several lists of differentially expressed genes were selected* and the minimal (hypergeometric test) *p*-value obtained from these different lists was retained. (*) Lists of differentially expressed genes: genes yielding a (moderate *T*-test) $p >$ 1e-5 were removed from the analysis; remaining genes were ordered based on the fold change; the n genes with highest (respectively lowest) fold change were selected as a separate list; the n/2 genes with highest fold change and the n/2 genes with lowest fold change were merged in another list; this operation was performed for several values of n (200, 300, 400, 500, 750, and 1000). Principal component analysis (PCA) of the expression profiles was performed using R software. Venn diagrams and pathway interaction schemes were generated applying BioVenn (http://www.cmbi.ru.nl/cdd/biovenn/) and GOrilla—REViGO (http://cbl-gorilla.cs.technion.ac.il/) software packages, respectively. Pathway analysis was completed employing DAVID Bioinformatics Resources 6.7 (http://david.abcc.ncifcrf.gov/).

Comparative Analysis of Microarray Data with Published Available Datasets

Data normalization was performed with frozenRMA and corrected for batch effect using Combat algorithm (Johnson WE—Biostatistics—2007). Combined data series were the 36 samples from our study and those from published datasets GSE50821 (Sinha et al., 2014) and GSE47177 (Liu et al., 2013).

The three Affymetrix series were used to compared adult vs. old expression profiles (supervised meta-analysis young[2 months] vs. old[>= 18 months]). This analysis showed that the combination of the three sets found 32% significantly deregulated genes and in the same direction of deregulation (32% = proportion of the combined test under H1 = Test Stouffer).

Accession Numbers

The complete microarray data set, including the RMA data used to produce intensity maps, have been deposited in NCBI's Gene Expression Omnibus, and are accessible through GEO Series accession number GSExxx (http://www.ncbi.nlm.nih.gov/geo/query/acc.cgi?acc=GSExxx). To be requested to the editor during the revision process.

Cloning (GMO Project No: 371)

To target activated satellite cells and not myofibers in our *ex vivo* assays, a replication-deficient retrovirus, MIGR (*pMSCV-IRES-eGFP*), has been used to transduce proliferating cells and overexpress either dominant negative (DN) *EphB1*, *Zbtb4,* and *Zbtb20* or full-length cDNA for *Zfp354c*, *Zcchc5*, *Zbtb4*, *Zbtb20*, and *Hmga2* (Pear et al., 1998; Zammit et al., 2006b). The virus is composed, besides the 5′ and 3′ LTR of the MSCV virus, the latter being mutated to prevent replication, and the phi integrase, of a multicloning site followed by an IRES-eGFP sequence to track infected cells by fluorescence. This tracking cassette was later modified into MISSINCK by substituting eGFP with an insulin signal sequence-Cyan Fluorescent Protein (CFP)-KDEL sequence in order to restrict fluorescent tracker expression to the endoplasmic reticulum and Golgi.

Isolated Myofiber Cultures

Isolation of Muscular Fibers

Culture of single fibers was performed according to previously described strategies (Moyle and Zammit, 2014). Briefly, dissected EDL muscles were digested in a filtered solution of 0.2% collagenase (SIGMA-ALDRICH®) in DMEM High Glucose/1% L-Glutamine/1% Penicillin/Streptomycin (Life Technologies®) (isolation medium). After 2 h of connective tissue digestion, EDLs were mechanically dissociated fiber by fiber. Quiescent satellite cells on the isolated myofibers were activated by a solution of 10% horse serum/0.5% chicken embryo extract in filtered isolation medium. Contracted fibers were removed.

Retrovirus Production and Infection

Retroviral particles (see *Cloning*) were produced in HEK293T line cells by transfection using FuGENE® with a helper virus, which contains the necessary elements to obtain the correct encapsidation and active retrovirus (*phi integrase*, *gag*, *pol* and *env* (VSV-g) genes). We collected the supernatants after transfection at T = 72 h and T = 84 h, which displayed the highest retroviral particle titers.

After 24 h of activation, myofiber-attached satellite cells were infected with the retroviral particles diluted 1/10. 48 h afterwards (T = 72 h), fibers were fixed to proceed with immunofluorescence analysis.

C2C12 Cell Culture for Muscle Differentiation and Infection

Myogenic differentiation was induced according to previously reported protocols (McMahon et al., 1994). Murine C2C12 cells were cultured in 10% fetal bovine serum (Bio West®) in High Glucose DMEM (Life Technologies®) for proliferation assay (GM). Differentiation was induced by switching into medium supplemented with 2% horse serum (Promega®) in High Glucose DMEM (DM), generating multinucleated myotubes surrounded by mononuclear reserve cells.

For retroviral infection, 10^4 C2C12 cells were plated in GM and incubated with undiluted retroviral supernatant containing 4 μg/mL polybrene (SIGMA-ALDRICH®) for 3–4 h. Retroviral medium was then removed, and the cells washed and incubated in either proliferation (for PH3, KI67, EdU, and MYOD analysis) or differentiation (for MYOG analysis) medium.

Immunostaining

Satellite Cells on Myofibers and Cryosections

Myofibers were fixed in 4% paraformaldehyde for 10 min, treated with 0.5% triton and blocked in 10% goat serum/10% swine serum (Moyle and Zammit, 2014). The following antibodies were used: EPHB1 (Rabbit Abcam® ab5414) 1/100, PAX7 monoclonal (DSHB®, PAX7-c) 1/50, MYOD monoclonal (DAKO®, clone 5.8A, M3512) 1/60, MYOD (Rabbit Santa Cruz Biotech®, sc-760) 1/50, MYOG monoclonal (DSHB®, F5D) 1/50, CD-31 (PECAM-1) (Rat BD Pharmigen®, 550274) 1/500, and GFP (Rabbit Life Technologies®) 1/500, or (Chicken Abcam® ab13970) 1/200. Secondary antibodies employed to reveal the staining were Alexa 594 goat anti-mouse IgG (H+L), Alexa 488 goat anti-rabbit IgG (H+L) (Life Technologies®), and DyLight-405 donkey anti-chicken IgY (IgG) (H+L), and Cy5-Goat Anti-Rabbit IgG (H+L) (Jackson ImmunoResearch®). Nuclei were counterstained with DAPI.

C2C12 Cultured Myoblasts

The following antibodies were used: MYOD, MYOG, and GFP (as above), PH3 (Rabbit Merck-Millipore®, 06-570) 1/50, Ki67 (BD Pharmigen®, 556003) 1/150, HA (Rabbit Sigma-Aldrich®, H6908) 1/400, and GFP monoclonal (Sigma®) 1/50. Secondary antibodies included Alexa 488 goat anti-mouse IgG (H+L), Alexa 594 goat anti-mouse IgG (H+L), Alexa 488 goat anti-rabbit IgG (H+L), Alexa 594 goat anti-rabbit IgG (H+L) (Life Technologies®). EdU reaction was performed with Click-iT® EdU Alexa Fluor® 647 Imaging Kit (ThermoFisher Scientific®). Nuclei were counterstained with DAPI.

Imaging and Statistics

Analysis was carried out using a Leica TCS SPE confocal microscope. Images were processed with either Adobe Photoshop CS5 software (Adobe Systems) or ImageJ (version 1.47v; National Institutes of Health, USA, http://imagej.nih.gov/ij).

Infected satellite cells in myofiber cultures were directly counted under a Leica fluorescent microscope at 40x and 100x magnification.

Mean ± standard error (SEM) was given. The single (*), double (**) and triple (***) asterisks represent *p*-values $p < 0.05$,

$p < 0.01$, and $p < 0.001$ respectively by Student's unpaired *t*-test or Mann–Whitney *U*-test. All experiments have been performed on at least three independent experiments for each condition.

Supplementary Movies were performed using a DSD2 Workstation with Imaris software (ANDOR).

RESULTS

Expression Dynamics of Skeletal Muscle Stem Cells

Pax3 is expressed in fetal progenitors and satellite cells of trunk hypaxial muscles (Relaix et al., 2005; Relaix, 2006; Calhabeu et al., 2013). We used a Pax3 reporter mouse to perform a chronological global profiling in embryonic, fetal and postnatal MPC and satellite cells expressing Pax3 (**Figure 1A**; Relaix et al., 2005).

Prospective isolation of Pax3-GFP myogenic progenitors and stem cells was performed as previously described (Figure S2A; Montarras et al., 2005; Lagha et al., 2010), taking advantage of the GFP coding sequence targeting one allele of *Pax3* (Relaix et al., 2005). *Pax3* is expressed in muscle progenitors but also in early migrating neural crest cells (Epstein et al., 1993). Neural crest cells give rise to many derivatives, including the peripheral nervous system, melanocytes, and a subpopulation of venous endothelial cells (by E13.5) among other cell types (Engleka et al., 2005; Stoller et al., 2008). To exclude a possible contamination of satellite cells with endothelial cells, we performed *Pax3*-lineage tracing using $Pax3^{Cre/+}$; $R26^{mTmG}$ mice (Figure S2B). While adult myogenic cells were mGFP+ (Pax3-Cre recombined), all endothelial cells remained mTOMATO+ (not recombined) (Figure S2B and Movie S1). Moreover, all CD31 (PECAM-1) + endothelial cells were included within the mTOMATO+ population (Figure S2B and Movie S2). These results demonstrate that the *Pax3* lineage does not contribute to skeletal muscle endothelial population, and that skeletal muscle expression of PAX3 is specific to muscle stem cells.

Since *Pax3* is expressed in a subset of the *Pax7*-expressing satellite cells, we compared our gene expression data with previously published datasets of adult muscle stem cells where markers different from PAX3 were used to isolate satellite cells (Figure S3A; Liu et al., 2013; Sinha et al., 2014). *Pax3*-expressing satellite cells were not significantly divergent from previously reported datasets, while embryonic and fetal/early postnatal datasets showed different specific profiles (Figure S3A). Moreover, we compared available data from adult (3–8 month-old) and old satellite cells (18–24 month-old) with our data. We identified a similar variation in all datasets, demonstrating that *Pax3*-expressing satellite cells do not define a subpopulation of satellite cells. Our data therefore are likely representative of the whole satellite population.

Expression profiles from 11 developmental stages were normalized, generating a GEO showing the kinetics of each transcript over time (**Figures 1A,B**). Transcript variations were divided into seven clusters based on general expression profiles (**Figure 1B** and Figure S3B), which were determined to be functionally homogeneous and easily aggregated in defined GO pathways (Figure S3B, Pathways). Furthermore, this *in silico* analysis of the transcriptome through categorization of expression trends (**Figure 1B** and Figure S3B, Pathways) and specific molecular signatures (**Figures 1B–D**), yielded known myogenic and related factors (Figure S3B, Genes) (Kuang et al., 2008; Abou-Khalil et al., 2009; Boldrin et al., 2012; Conboy and Rando, 2012). Strikingly, two transition events were revealed: (I) from embryonic to fetal myogenesis (Messina and Cossu, 2009), hypothesized to mark the early onset of satellite cell formation (Kassar-Duchossoy et al., 2005); and (II) the acquisition of quiescence in satellite cells around 3 weeks of age (**Figures 1B,C**; Lepper et al., 2009; White et al., 2010). These transitions define the three major developmental states: embryonic progenitors (E11.5–E14.5), fetal-to-early postnatal (E15.5–P12) and adult quiescent satellite cells (1–18 months), each with a specific molecular signature (**Figures 1B–D**). Pairwise comparison between different signatures of up-regulated (UR) and down-regulated (DR) transcripts revealed the genes and pathways defining each developmental period, provided in Figure S4 and Tables S1–S3 (UR), and Tables S4–S6 (DR), respectively. Importantly, this *in silico* analysis also provides new markers for muscle progenitor/stem cell maturation in both UR (extracellular matrix formation, anatomical structure development, immune and inflammatory responses) and DR (cell cycle and DNA repair transcripts or developmental processes) pathways.

The dynamics of our transcriptional profiling reveal that each stage of development is molecularly defined in a more progressive manner than previously recognized.

Type A-Ephrins and Eph Receptors Expression during Myogenesis

We have identified a set of transcripts specifically associated with the embryonic and fetal stages of development or the satellite cell lineage. Interestingly, Ephrin family members showed a very dynamic behavior throughout development and postnatal myogenesis, including *EphA*s and *EfnA*s (**Figure 2**). We could distinguish two distinct behaviors: first, a set of *EphA* transcripts that are up-regulated during the acquisition of muscle stem cell properties (*EphA1* and *EphA2*, **Figures 2A,B**); second, an independent set that is down-regulated over the same period (*EphA3*, *EphA4*, *EphA5*, and *EphA7*, **Figures 2C–F**). EPHA4 has been reported to bind both EFNA and EFNB ligands subtypes (Singla et al., 2010). This receptor was expressed in the developing embryo, and repressed during postnatal growth (**Figure 2D**). We found that *EphA4* is strongly expressed during early embryonic development (E11.5) and ceases its expression at the late fetal stage. In our transcriptome data, *EfnA2*, *EfnA3*, *EfnA4*, and *EfnA5* ligands expression were also down-regulated during fetal development, being no longer expressed during aging (**Figures 2H–K**). Interestingly, only *EfnA1* became up-regulated during the perinatal transition that characterizes the emergence of satellite cells (**Figure 2G**).

Type B-Ephrins and Eph Receptors Expression during Myogenesis

Expression of *EphB*s and *EfnB*s at different stages is shown in **Figure 3**. Among those, the transmembrane receptor *EphB1*

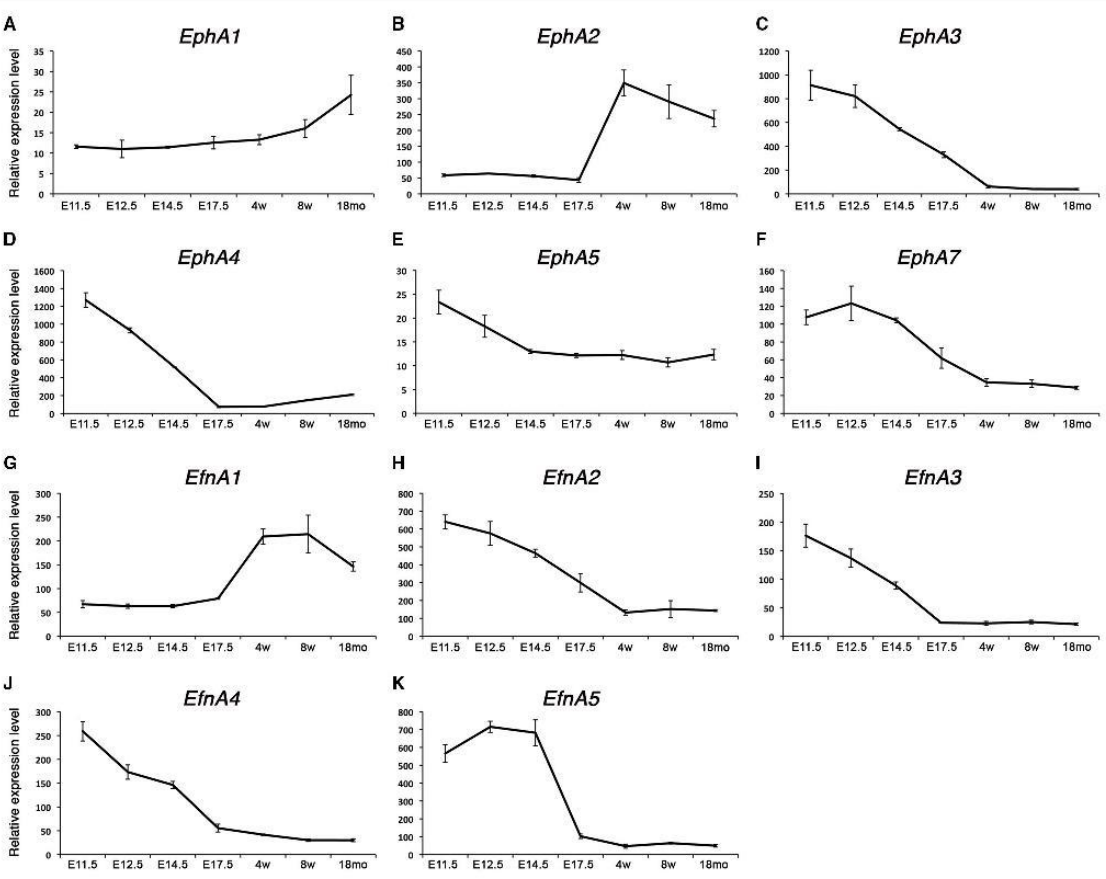

FIGURE 2 | Expression profile of *EphA* receptors and ephrins in skeletal muscle. Total RNA from FACS-sorted Pax3-GFP+ cells was used to perform microarray experiments. **(A–F)** Gene expression profiles of type-A Eph receptors from the microarray data during embryonic and postnatal myogenesis. *EphA1* and *EphA2* were up-regulated during the perinatal transition, unlike the rest of the receptors which became down-regulated. **(G–K)** Gene expression dynamics of type-A ephrins during embryonic and postnatal myogenesis. *EfnA1* was up-regulated during the perinatal transition, unlike the rest of the ligands which became down-regulated. *EphA2* and *AfnA1* decline with age. E, Embryonic days; w, age in weeks; mo, age in months.

presents a unique dynamic expression profile: initially expressed early during myogenic development, then down-regulated during the fetal stage, and finally re-expressed in postnatal satellite cells (**Figure 3A**). By contrast, *EphB2*, *EphB3,* and *EphB4* are highly expressed during early development and progressively repressed as development proceeds (**Figures 3B–D**). We confirmed that *EphB1* was first expressed during the early stages of embryonic muscle development (Figure S5A), and down-regulated in the fetal stages. While it was weakly expressed in the early immature satellite cells (i.e., P2–P4), it was strongly up-regulated by P14, with expression then maintained, albeit at a lower level, in adult satellite cells. Interestingly, aged satellite cells (18 months old) show a marked decrease in *EphB1* expression (Figure S1A), corresponding to the timing when satellite cells start losing their regenerative capacity (Sousa-Victor et al., 2014).

We used immunostaining on cultured floating myofibers to characterize expression of EPHB1 in muscle stem cells. This culture system recapitulates satellite cell activation, self-renewal and differentiation, similar to the situation observed during muscle regeneration in the adult (Zammit et al., 2004). After 72 h, satellite cells were activated and proliferating (PAX7+ and MYOD+); some cells activated myogenin (MYOG+) and down-regulated PAX7, thus differentiating, and other cells will adopt a divergent fate, withdrawing from cell cycle and maintaining the expression of PAX7 while down-regulating MYOD (Zammit et al., 2004). Co-immunostaining of EPHB1 with PAX7, a specific marker of satellite cells, was observed on isolated fibers (**Figure 3E**), in 80% of the cells. However, expression was also observed in PAX7, MYOD, and MYOG positive myogenic cells at T = 72 (Figure S5B), demonstrating that EPHB1 was not

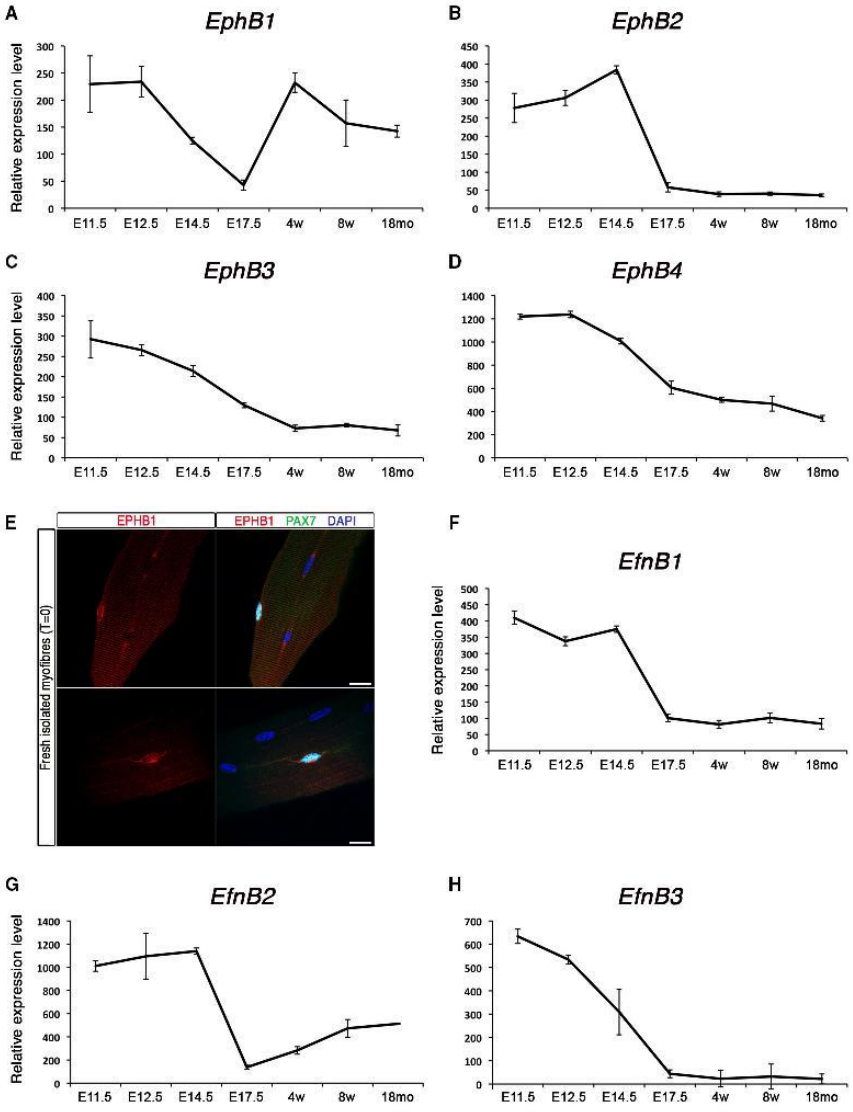

FIGURE 3 | Expression profile of *EphB* receptors and ephrins in skeletal muscle. Total RNA from FACS-sorted Pax3-GFP+ cells was used to perform microarray experiments. **(A–D)** Gene expression profiles of type-B Eph receptors during embryonic and postnatal myogenesis. *EphB1* was up-regulated during the perinatal transition, unlike the rest of the receptors which became down-regulated. **(E)** Expression of EPHB1 receptor in quiescent satellite cells on fresh isolated EDL myofibers (T = 0) by co-immunostaining for EPHB1 (red) and PAX7 (green). Nuclei were labeled in blue with DAPI. Scale bars, 10 μm. **(F–H)** Gene expression dynamics of type-B Eph receptors during embryonic and postnatal myogenesis showed that all ephrins are down-regulated during the perinatal transition. E, Embryonic days; w, age in weeks; mo, age in months.

restricted to quiescent satellite cells, but maintained during the different steps of satellite cell activation and differentiation.

Finally, the kinetics of the ligands for type B-ephrins behaved similarly to most of the type A, being down-regulated during the perinatal transition to the emergence of satellite cells (**Figures 3F–H**).

EPHB1 Regulates Myogenesis in C2C12 Cells

C2C12 myoblasts are a classic model to analyze skeletal muscle differentiation (McMahon et al., 1994). Proliferating C2C12 cells were maintained in mitogen-rich medium, but differentiation was induced by switching into a serum poor-medium, thereby

inducing MYOG expression and fusion into myotubes. Under long-term differentiation conditions, a reserve cell population emerges that shares some molecular and cellular features with quiescent satellite cells: for example, reserve cells express PAX7, are mitotically quiescent and aligned to the myotubes without fusing (Yoshida et al., 1998; Olguin and Olwin, 2004; Shefer et al., 2006).

EPHB1 is expressed in both quiescent and activated satellite cells (**Figures 3A,E** and Figure S5). The extracellular region of the Eph receptor contains a globular ligand-binding domain, a cysteine-rich region (EGF-like motif), and two fibronectin-type III repeats (Figure S1). The intracellular region contains a tyrosine kinase domain, a SAM (Sterile Alpha Motif) protein-protein interaction domain and a C-terminal PDZ-binding motif (Figure S1A). To assess EPHB1 function in myogenic cells, we generated a dominant negative form of this receptor (EphB1DN) by removing the intracellular domain of the protein (Figure S1B) (Vindis et al., 2003, 2004; Haldimann et al., 2009; Oda-Ishii et al., 2010). Binding of ephrins to Eph receptors induces heterotetramers to initiate the signal cascade, which then will oligomerize and assemble in large signaling clusters (Pitulescu and Adams, 2010). EphB1 truncated receptor (EphB1DN) is therefore able to bind ephrin ligands, but cannot forward signal (Haldimann et al., 2009; Oda-Ishii et al., 2010). We induced expression of EphB1DN or control constructs using retroviral-mediated delivery in the C2C12 myoblastic cell line (**Figure 4**). EphB1DN was cloned into a modified retroviral vector carrying either an IRES-GFP or CFP to identify transduced cells and packaged using standard methods (Pear et al., 1998; Zammit et al., 2006b). These retroviral constructs were tested in C2C12 and transduction of more than 90% of the cells was observed (**Figure S6**). Co-staining with EPHB1 antibody showed the expression of the receptor in C2C12 cells (**Figure S6A**). As our antibody is directed against the last 10 residues of the intracellular domain, a C-terminal 3HA-tagged version of EphB1DN was generated. **Figure S6B** shows a similar localization to the one of EPHB1 in transduced cells.

We then assayed whether expression of EphB1DN would impact on proliferation of C2C12 cells using an antibody detecting the phosphorylated form of histone H3 at serine 10 (PH3) (**Figures 4A,B**), and validated by KI67 and EdU incorporation (Figures S7A,B). By 24 h after infection with the EphB1DN-encoding retrovirus, C2C12 cells exhibited a significant increase in the mitotic index, suggesting either a decreased cell cycle time or a decreased myogenic commitment toward differentiation. To further characterize the role of EPHB1 during myogenic differentiation, we analyzed expression of MYOD (**Figures 4C,D**) and MYOG (**Figures 4E,F**) in C2C12 cells 48 and 72 h, respectively, after infection, and found an increased number of cells expressing these myogenic markers. We concluded that EphB1DN leads to increased proliferation and differentiation of C2C12 cells, suggesting a regulatory role for EPHB1 in satellite cell quiescence.

EPHB1 Is Required for Satellite Cell Function and Renewal

We next infected primary satellite cells on floating muscle fibers to assay the consequence of expressing EphB1DN in activated satellite cells, and assayed self-renewal, proliferation and differentiation (**Figure 5**). 48 h after infection (72 h post isolation), the number of PAX7+ cells was reduced (**Figures 5A,B**). Consistently, we observed an increase in the MYOD+ (activated/proliferating and differentiating) population (**Figures 5C,D**). The number of MYOG+ (differentiating) cells was also increased (**Figures 5E,F**). Together, these results suggest that EPHB1 is involved in the maintenance of the pool of these adult stem cells, both by promoting self-renewal and by reducing activation and differentiation. To appropriately assess self-renewal of satellite cells, Pax7/MyoD double immunostaining was performed, taking advantage of a retrovirus with a CFP reporter expression restricted to the endoplasmic reticulum and Golgi (**Figure 5G** and Figures S6, S7). We confirmed that the decrease in the self-renewing satellite cell population (Pax7) correlated to an increase in differentiation (**Figure 5G**).

Expression of Zinc Finger Containing Proteins during Myogenesis

Candidate genes coding for ZFP354c and ZCCHC5 zinc finger containing proteins were repressed during the emergence of satellite cells around birth (**Figures 6A,B**). Down-regulation of these factors was observed in muscle progenitors at the fetal stage overlapping with the emergence of satellite cells. These two zinc finger containing-proteins were not expressed in adult and aged satellite cells. While *Zfp354c* was highly expressed during early myogenesis and gradually repressed from fetal stages (**Figure 6A**), *Zcchc5* was not expressed during early embryonic myogenesis (**Figure 6B**), but appeared during early establishment/formation of the satellite cell pool, before being completely down-regulated during acquisition of satellite cell quiescence. According to the known functions of these factors, we can hypothesize their possible involvement during MPCs proliferation (*Zfp354c*), or for a correct determination of the MPC fate to become the muscle stem cells (*Zcchc5*).

By contrast, two other zinc finger containing proteins *Zbtb4* and *Zbtb20*, were not expressed during development but were induced during establishment of satellite cells and acquisition of quiescence (**Figures 6C,D**). Moreover, high expression of these zinc finger containing-proteins was maintained in adult and aged satellite cells, implicating a possible function in maintaining quiescence of muscle stem cells. Strikingly, these factors are induced during cardiotoxin-induced muscle regeneration *in vivo* (Figure S8A).

Effect of Zinc Finger Containing Proteins in Postnatal Satellite Cells

We manipulated expression of *Zfp354c*, *Zcchc5*, *Zbtb4, and Zbtb20* using retroviral-mediated delivery in single myofiber cultures as above. We generated vectors carrying either a full-length transcript for overexpression, or dominant negative forms to analyze function.

Overexpression in satellite cells of either *Zfp354c* or *Zcchc5* maintained expression in satellite cells that no longer expressed the endogenous gene (**Figures 6E–J**). Notably, overexpression of *Zfp354c* led to a decreased number of PAX7+ satellite cells compared to control (**Figure 6E**) with no apparent effect during activation (MYOD+) and differentiation (MYOG+)

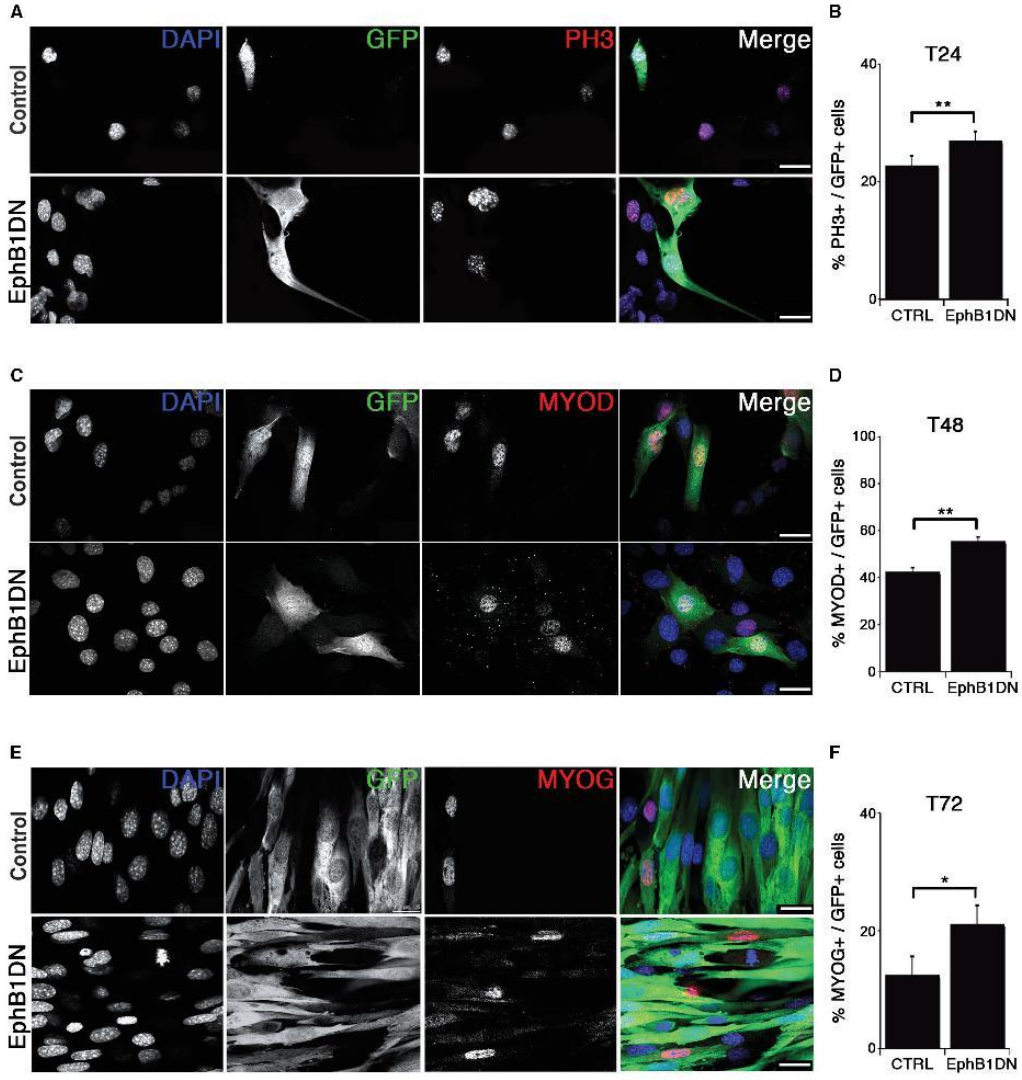

FIGURE 4 | Impairment of EPHB1 function increases proliferation and myogenic differentiation. (A–F) Overexpression of dominant negative EPHB1 (EphB1DN) using retroviruses in C2C12 cells during proliferation at T = 24 h **(A,B)**, T = 48 h **(C,D)**, and during differentiation at T = 72 h **(E,F)**. For each time point, immunostaining and the corresponding quantifications are shown. Control corresponds to infection by a GFP-expressing empty vector. Transduced cells are GFP+b (green) and nuclei are labeled with DAPI (blue). Cell percentages represent the proportion of transduced cells (GFP+) that co-express PH3 **(B)**, MYOD **(D),** or MYOG **(F)**. *p*-value $*p < 0.05$; $**p < 0.01$. Minimum number of infected cells is 250, for each marker analysis. Scale bars, 25 μm.

(**Figures 6F,G**). These results demonstrate that overexpression of *Zfp354c* resulted in a reduction of self-renewal capacity of the satellite cells.

Overexpression of *Zcchc5*in satellite cells, as *Zfp354c*, resulted in a decreased of the PAX7+ population relative to control (**Figure 6H**). Strikingly, the proportion of MYOD+ satellite cells increased without affecting MYOG-expressing differentiated cells (**Figures 6I,J**). These results showed that overexpression of *Zcchc5* induced decreased self-renewal promoting the proliferation of satellite cells. Our functional data is consistent with a specific requirement of *Zcchc5* function during the growth phase where production of MPC is needed.

We next overexpressed the other two BTB-containing zinc finger factors, *Zbtb4* and *Zbtb20* (**Figures 6K–P**). *Zbtb4* increased

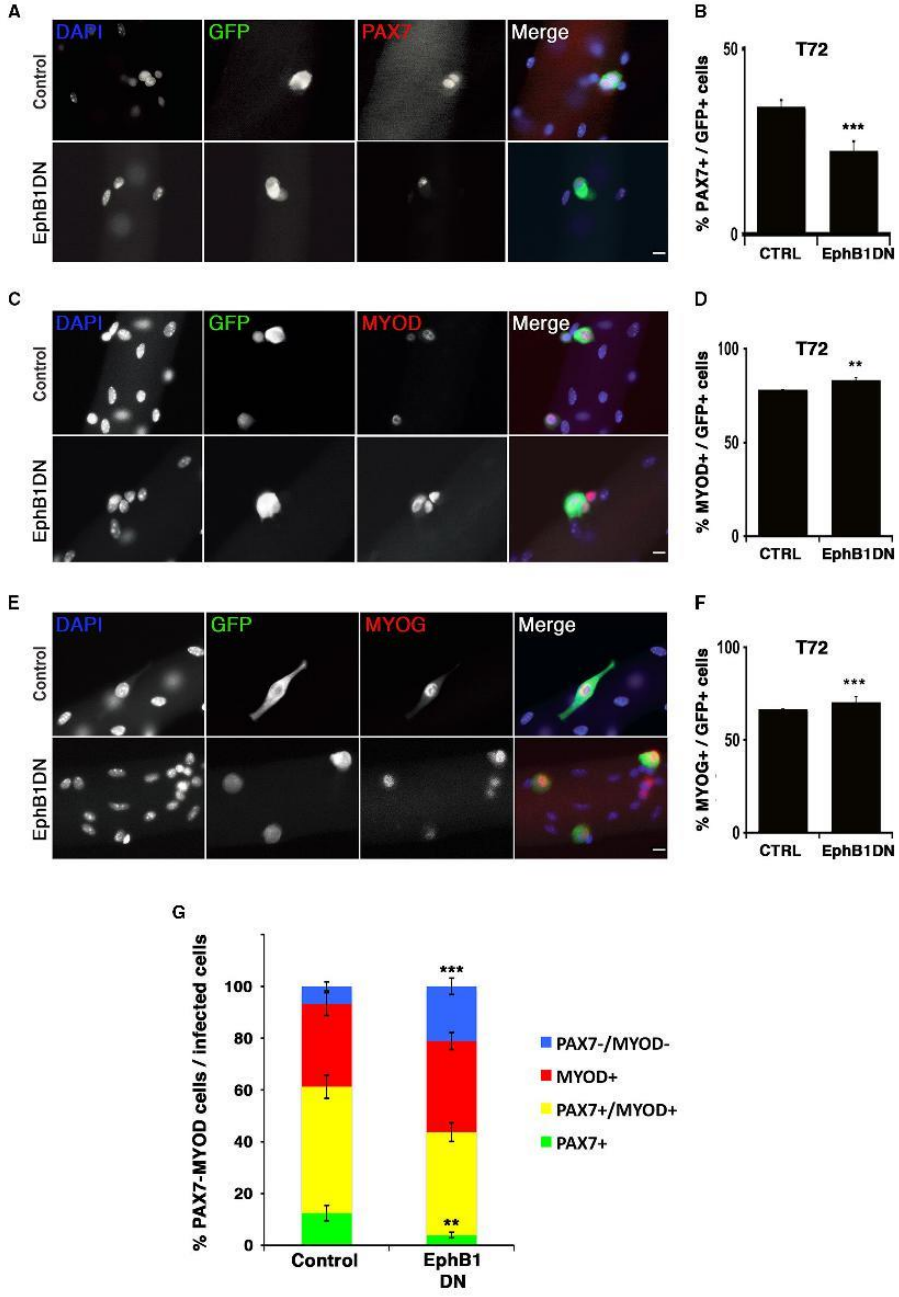

FIGURE 5 | Impairment of EPHB1 function induces satellite cell differentiation. Satellite cells were transduced to overexpress a truncated EPHB1 (EphB1DN) after 24 h in culture and analyzed 48 h later (T72). Representative immunofluorescent images are displayed for GFP, DAPI, and PAX7 **(A)**, MYOD **(C)**, and MYOG (Myogenin) **(E)** Scale bars, 20 μm. Quantifications are illustrated for quiescence/self-renewal **(B)**, activation **(D)**, and differentiation **(F)**. **(G)** Quantification of PAX7 and MYOD satellite cells 48 h after infection with EphB1DN. Control corresponds to infection by a CFP-expressing empty vector. *p*-values: $^{**}p < 0.01$ and $^{***}p < 0.001$. For each marker analysis, the minimum number of infected satellite cells is 200.

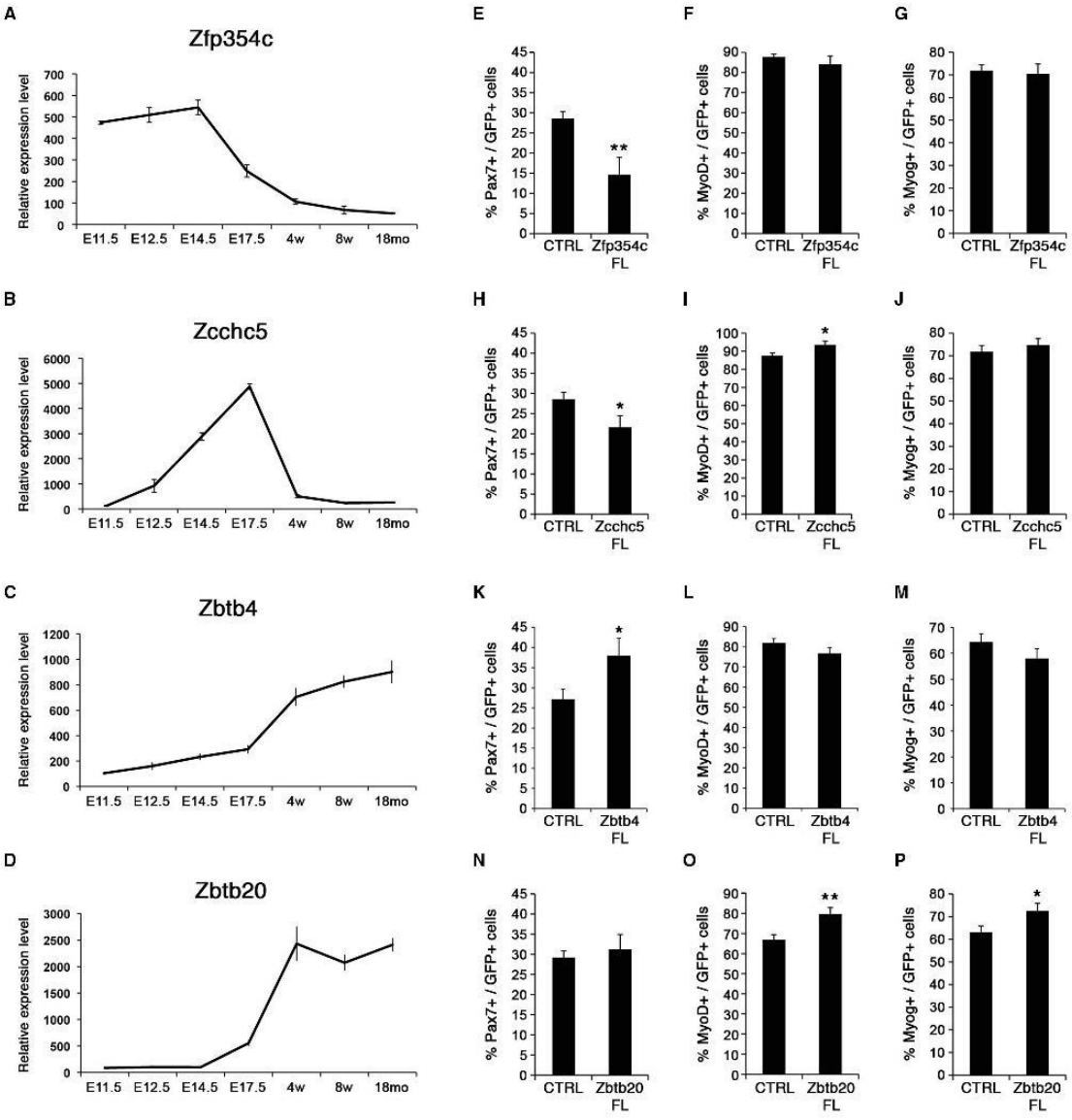

FIGURE 6 | Zinc finger proteins control satellite cell behavior. (A–D) Expression profiles for zinc finger proteins, *Zfp354c*, *Zcchc5*, *Zbtb4*, and *Zbtb20*. Whereas *Zfp354c* and *Zcchc5* are repressed in satellite cells **(A,B)**, *Zbtb4*, and *Zbtb20* are induced during satellite cell formation **(C,D)**. E, Embryonic days; w, age in weeks; mo, age in months. **(E–P)** Quantifications for quiescence/self-renewal (PAX7), activation (MYOD), and differentiation (MYOG) are shown during overexpression of the different zinc fingers: *Zfp354c* **(E–G)**, *Zcchc5* **(H–J)**, *Zbtb4* **(K–M)**, and *Zbtb20* **(N–P)**. All analyses were performed 48 h after infection. *p*-value $*p < 0.05$; $**p < 0.01$, and $***p < 0.001$. For each marker analysis, the minimum number of infected satellite cells is 200.

PAX7+ satellite cells (**Figure 6K**), whereas *Zbtb20* promoted myogenic progression by increasing the activated/proliferating (MYOD+; **Figure 6O**) and differentiating (MYOG+; **Figure 6P**) populations. These results suggested that these transcriptional repressors might be required for specification/maintenance of the muscle stem cell pool. Strikingly, inhibiting function by expression of ZBTB4 dominant negative constructs, missing the POZ DNA-binding domain, displayed an increase in

satellite cell differentiation (MYOG+) without affecting the activated/proliferating population (MYOD+) (Figures S8B,C). On the other hand, ZBTB20 could behave with a previously described phenotype in the brain of *Zbtb20* transgenic mice (Nielsen et al., 2007), where overexpression of ZBTB20 represses cell fate transitions in newborn pyramidal neurons. Moreover, overexpression of ZBTB20 has been recently described as a prognostic marker by promoting tumor growth of human hepatocellular carcinoma (Kan et al., 2016). Thus, ZBTB20 could be regulating muscle regeneration during satellite cell activation as suggested in Figure S8A.

Hmga2 Must be Repressed for Appropriate Satellite Cell Function

Hmga2 was highly expressed during early development (**Figure 7A**), when MPCs expand to populate the future skeletal muscle of the body. As development proceeds, *Hmga2* was no longer expressed, and was not detected in the emerging satellite cells prior to birth. Nishino and collaborators have described a similar behavior where *Hmga2* is highly expressed in fetal neural stem cells and declining with age (Nishino et al., 2008).

We analyzed the effect of overexpressing *Hmga2* in satellite cells (**Figures 7B–E**). A retroviral construct carrying full-length cDNA including the coding sequence for the basic and acidic region of the protein was generated (**Figure 7B**), and satellite cells infected using single myofiber culture. *Hmga2* overexpression led to a strong reduction in the pool of satellite cells expressing PAX7 (**Figures 7C,D**), with an increase on the activated/proliferating MYOD+ muscle stem cells (**Figure 7E**); data consistent with the work from Li and colleagues describing HMGA2 as a regulator of myoblast proliferation by direct interaction with the RNA-binding protein IGF2BP2 (Li et al., 2012).

DISCUSSION

PAX3 and PAX7 are key upstream regulators of skeletal myogenesis (Relaix et al., 2005; Buckingham and Relaix, 2015). Postnatally, while PAX7 labels all satellite cells (Seale et al., 2000), PAX3 is maintained in a subset of these adult muscle stem cells (Relaix et al., 2006). A complex balance between extrinsic cues and intrinsic regulatory mechanisms is needed to tightly control satellite cell determination and function. For example, defects in satellite cell regulation or in their niche, such as during postnatal growth or in degenerative conditions and aging, can impair muscle regeneration with possible fatal consequences (Dumont et al., 2015). Hence, identifying and manipulating muscle progenitor stem cells, and understanding the mechanisms underlying cell fate decision and self-renewal (Relaix, 2006; Boutet et al., 2007) are essential for development of stem cell-based therapeutic strategies.

We have developed a FACs-based chronological transcriptome profile of myogenic stem cells, sampled from embryonic and fetal progenitors, to postnatal, adult, and aging satellite cells. This provides a comprehensive description of gene expression changes throughout life of muscle stem cells and identifies two important transition events, which delimit three developmental periods of muscle stem cells with specific molecular signatures: (1) embryonic, (2) fetal to early proliferating postnatal progenitors, and (3) quiescent adult muscle stem cells (Buckingham and Relaix, 2007; Braun and Gautel, 2011). The intersection between specifically expressed genes and functional pathways defines a molecular signature unique to each developmental period. As such, our study is instrumental for a better understanding of both myogenesis and the establishment and maintenance of quiescent adult stem cells.

The dynamics of our transcriptional profiling reveal that cellular processes characterizing muscle stem cells, including transition from the fetal lineage to postnatal stem cells, establishment of quiescence and formation of a functional niche, are defined molecularly in a more progressive manner, highlighting that establishment of the satellite cell lineage is more gradual than previously recognized. For example, cell division processes (i.e., cyclins such as *Ccne1/2* or cyclin-dependent kinases such as *Cdk1*) were gradually down-regulated throughout the second transition, corresponding to the establishment of satellite cell quiescence and consistent with analysis of fetal progenitor cell proliferation (Picard and Marcelle, 2013). At the same time, known satellite cell markers such as *Sdc4* (Syndecan 4), *Itga7* (Integrin Alpha-7) or *Cav1* (Caveolin 1) were progressively up-regulated (Cornelison, 2001; Gnocchi et al., 2009).

From this large-scale myogenesis transcriptome, we functionally characterized a set of genes to provide novel intrinsic factors that regulate satellite cell behavior (**Figure 8A**).

Eph/Ephrin Pathway and Myogenesis

EPHB1 is not only involved in motility and guidance in skeletal muscle cells as previously shown (Stark et al., 2011), but also acts as a novel regulator of myogenesis. Our findings point to a function during self-renewal of satellite cells, since a dominant negative form of EPHB1 led to increased proliferation and differentiation in C2C12 myogenic cells and satellite cells in the myofiber experimental model. The increase in cell differentiation is achieved at the expense of self-renewal of the satellite cell population (**Figure 8B**). Identifying the molecular regulators of satellite cell renewal is important since it was recently shown that targeted depletion of the satellite cell pool leads to complete impairment of muscle regeneration following injury (Relaix and Zammit, 2012).

Eph/ephrin signaling takes place via direct cell-cell interaction; either as *trans* or *cis* signaling (Arvanitis and Davy, 2008; Pitulescu and Adams, 2010). This interaction could take place with the muscle fiber, between satellite cells, or via interactions with other cell types in the microenvironment (i.e., macrophages and/or microvascular cells). The satellite cell population is heterogeneous, with specific markers labeling subpopulations of the satellite cell pool and different myogenic behaviors *in vivo* or *ex vivo* (Relaix et al., 2006; Kuang et al., 2007; Rudnicki et al., 2008; Ono et al., 2010; Rocheteau et al., 2012). Whether arising through lineage or stochastic events, more "stem" satellite cells likely correspond to independently identified label-retaining satellite cells during growth and after injury (Shinin et al., 2006; Rocheteau et al., 2012; Chakkalakal

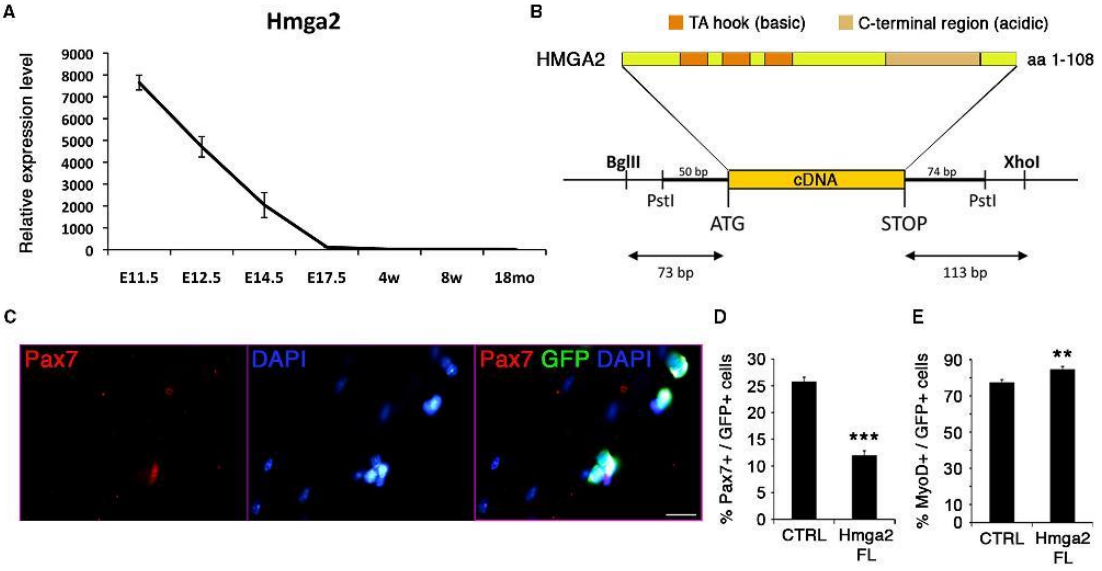

FIGURE 7 | HMGA2 reduces the pool of satellite cells. (A) Expression profile of *Hmga2* during development. E, Embryonic days; w, age in weeks; mo, age in months. **(B)** Protein structure of the non-histone, DNA-binding chromatin HMGA2 factor containing three DNA-binding sites (AT hook motifs) and the basic terminal region, which can bind various proteins. **(C)** Representative image for the co-immnofluorescence GFP (green), PAX7 (red) and DAPI (blue). Quantifications correspond to the analysis of quiescence **(D)** and activation **(E)** of the satellite cells. Forty eight hours after infection, retroviral-mediated overexpression of HMGA2 caused a reduction in the population of PAX7+ cells **(D)** and an increase MYOD+ cell population **(E)**. *p*-value $^{**}p < 0.01$ and $^{***}p < 0.001$. For each marker analysis, the minimum number of infected satellite cells is $n = 500$. Scale bar, 20 μm.

et al., 2014), or displaying different rates of cell division (Ono et al., 2012). Interestingly, satellite cells can asymmetrically divide and it will be of interest to evaluate if interaction between fibers and/or the satellite cells via the Eph/ephrin signaling plays a role in these cell fate decisions. Finally, our results are consistent with the work from Chumley and colleagues, showing that proliferative neuronal progenitor cells increase in *EphB1* mutant mice (Chumley et al., 2007), thereby demonstrating an important role of EPHB1 in maintenance of neuronal progenitors in the quiescent state.

Eph/ephrin signaling has also been shown to play a role in regulating other stem cell niches, for instance in the dental (Stokowski et al., 2007) or osteochondral (Arthur et al., 2011) system. Using an ephrin "stripe" assay revealed that satellite cells respond to a subset of ephrins with repulsive behavior *in vitro* (Stark et al., 2011). Our finding that EPHB1 is also regulating myogenesis suggests that this guidance signaling might impact multiple aspects of muscle regeneration, including escape from the niche, directed migration to sites of injury, cell-cell interactions among satellite cell progeny, and differentiation and patterning of regenerated muscle.

Identification of Novel Zinc Finger Proteins Regulating Myogenesis

We identified a set of zinc finger containing proteins with a dynamic expression profile during myogenesis. We have shown that overexpression of *Zfp354c* decreased self-renewal of satellite cells (summarized in **Figure 8**). In the skeletal system, the highest *Zfp354c* expression is in proliferating bone cells compared to mature and differentiated chondrocytes. Interestingly, ZFP354C is induced as an early response to BMP-7 (Jheon et al., 2001). It has been shown that overexpression of *Zfp354c* affects osteoblast differentiation, a lineage that is also regulated by BMP signaling (Jheon et al., 2001). Moreover, overexpression of this gene results in a decrease in osteogenic differentiation by suppressing BMP-7 induced alkaline phosphatase activity, an early marker of osteogenesis (Jheon et al., 2003). Furthermore, BMP signaling prevents myogenic differentiation of satellite cells, and is also involved in regulation of satellite cells during proliferation or differentiation (Friedrichs et al., 2011; Ono et al., 2011). In essence, there is strong evidence of a functional interaction between ZFP354C and BMP7, though the precise relationship between the two proteins is not fully understood (Jheon et al., 2002). Future studies will be necessary to evaluate whether a functional interaction between ZFP354C and BMP7 regulates myogenesis and, in general, to identify the downstream gene regulatory networks for all four zinc finger proteins presented here, ZFP354C, ZCCHC5, ZBTB4, and ZBTB20, which are able to strongly repress transcription of target genes. These zinc fingers, thus, could be used as potentially powerful tools for regulation of muscle stem cell function.

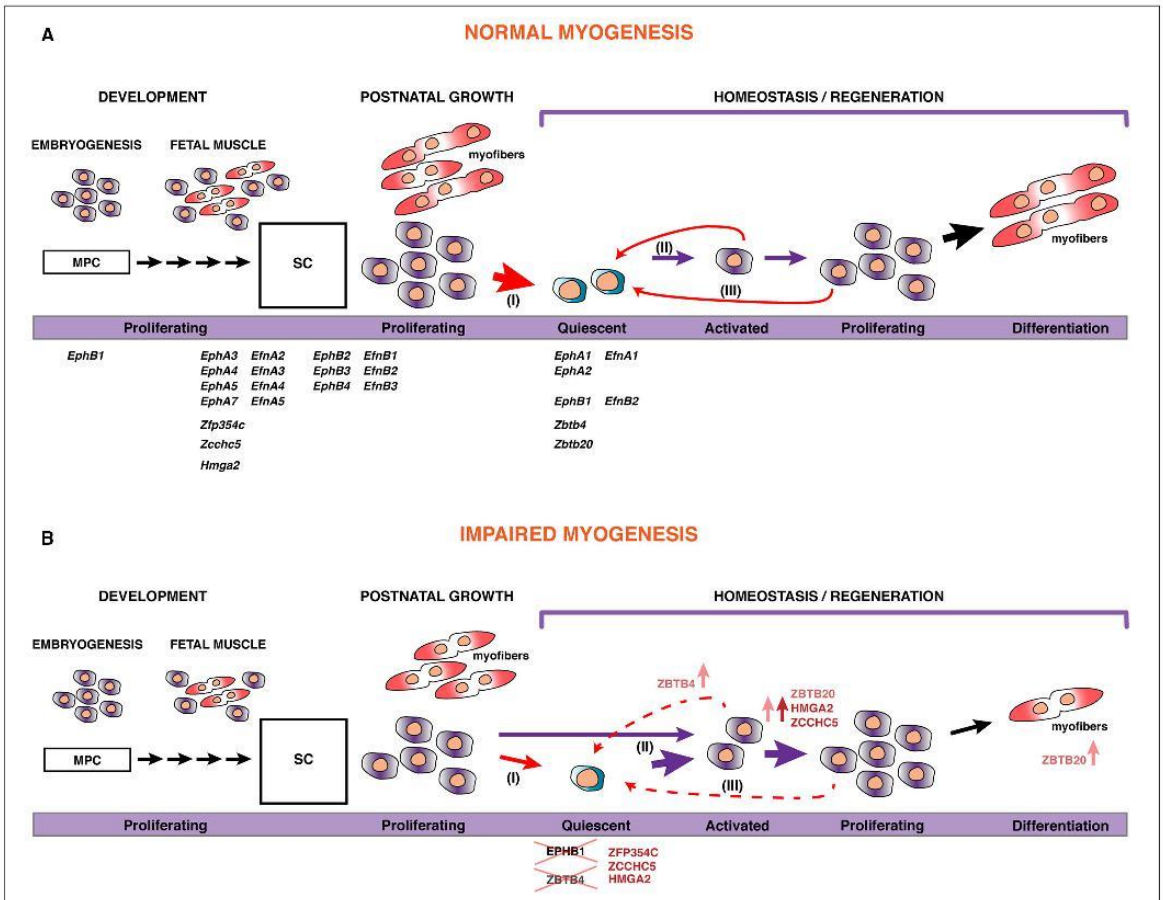

FIGURE 8 | A model for skeletal muscle stem cell behavior during myogenesis. (A) During development, embryonic and fetal progenitors are highly proliferative, augmenting the pool of MPC that will differentiate and fuse to form myofibers. As development proceeds, some of these MPCs become satellite cells (SC), the postnatal muscle stem cells. During the perinatal transition, many of these SCs will contribute to the maturation of myofibers, with a pool of stem cells maintained within the natural niche, underneath the basal lamina of the myofiber. Satellite cells become quiescent by 3 weeks after birth (I). However, in response to injury or disruption of the basal lamina, SCs become activated (II), start proliferating, and differentiate to fuse with each other or to existing myofibers for repair. Some of these will self-renew to replenish the pool of quiescent stem cells (III). The putative role and expression of the set of transcripts that we identified in this work is displayed. In addition, we show that manipulating their expression or function can lead to impaired myogenesis **(B)**, either via reduction of the pool of stem cells by promoting proliferation or cell fate determination, or through inducing precocious differentiation.

HMGA2 Function and Its Role in Myogenesis and Satellite Cell Fate Decision

HMGA2 is a co-regulator of chromatin structure and pluripotency in stem cells (Pfannkuche et al., 2009). The role of HMGA2 in myoblast proliferation has been previously described in neonatal and regenerating muscle (Li et al., 2012). *Hmga2* is sharply induced during satellite cell activation. We found that *Hmga2* is highly expressed during early muscle development and progressively down-regulated in the fetal stages, while it is not expressed during growth or aging (**Figure 7A**). It has been shown that *Hmga2* knockout mice are smaller and show defects in postnatal skeletal muscle (Zhou et al., 1995; Li et al., 2012). In addition, HMGA2/IGF2BP2 has been shown to be critical for myoblast proliferation and early myogenesis, but should be down-regulated in order for myoblasts to differentiate into multinucleated skeletal muscle. Indeed, when satellite cells are activated entering cell cycle, HMGA2 is up-regulated and activates the expression of IGF2BP2 (Li et al., 2012). Our transcriptome analysis shows that *Igf2bp2* behaves similarly to *Hmga2* before birth, but in contrast to *Hmga2*, *Igfbp2* is induced in adult stem cells, including aged satellite cells (data not shown). This suggests that IGF2BP2 could be functionally independent of HMGA2 in adult and aged satellite cells.

In conclusion, understanding the molecular signals that control and regulate the muscle stem cell population is essential in order to open new therapies strategies for muscle diseases. Here we provide a set of potential new regulators of myogenesis that improves the understanding and knowledge of the intrinsic factors controlling muscle stem cell acquisition, establishment, maintenance and function in the adult, and could be targeted to modify the regenerative capacity of endogenous skeletal muscle stem cells.

AUTHOR CONTRIBUTIONS

SA, AR, and JM designed and performed experiments, and analyzed data. SA wrote the manuscript. AD analyzed bioinformatic data. DM, FA, and TC performed experiments. PZ designed experiments. FR oversaw the entire project, designed experiments, analyzed data and wrote the manuscript. All authors read and approved the final manuscript.

ACKNOWLEDGMENTS

We thank Jonathan A. Epstein for the *Pax3*$^{Cre/+}$ mice. We thank Bernadette Drayton, Bruno Cadot, and Petra Gimpel for their input and technical assistance; Ana Cumano for her advice in FACS-sorting experiments and Olivier Poch and Julie Thompson for discussion about gene expression analysis. We thank Catherine Blanc and Bénédicte Hoareau (Flow Cytometry Core CyPS, Pierre and Marie Curie University) for their assistance. We also wish to acknowledge Serban Morosan and the animal care facility (Centre d'Expérimentation Fonctionnelle, School of Medicine Pierre et Marie Curie). SA was recipient of a postdoctoral fellowship from the Basque Community (BF106.177). This work was supported by funding to FR from INSERM Avenir Program, Association Française contre les Myopathies (AFM) via TRANSLAMUSCLE (PROJECT 19507), Association Institut de Myologie (AIM), Labex REVIVE (ANR-10-LABX-73), the European Union Sixth and Seventh Framework Program in the project MYORES and ENDOSTEM (Grant # 241440), Fondation pour la Recherche Médicale (FRM; Grant FDT20130928236), Ligue Nationale contre le Cancer, Agence Nationale pour la Recherche (ANR) grant Epimuscle (ANR 11 BSV2 017 02), RHU CARMMA (ANR-15-RHUS-0003), BMP-biomass (ANR-12-BSV1-0038- 04), Satnet (ANR-15-CE13-0011-01) and bone-muscle-repair (ANR-13-BSV1-0011-02), Decrypthon research program. This work was also funded by the German Research Foundation (DFG; Grant GK1631), French-German University (UFA-DFH; Grant CDFA-06-11) and the AFM as part of the MyoGrad International Research Training Group for Myology. PSZ wishes to acknowledge support from the Association Française contre les Myopathies grant 16050. The lab of PSZ is also supported by The Muscular Dystrophy Campaign, the Medical Research Council, FSH Society and BIODESIGN (262948-2) through EU FP7. The funders had no role in study design, data collection and analysis, decision to publish, or preparation of the manuscript. The authors declare no competing financial interests.

SUPPLEMENTARY MATERIAL

The Supplementary Material for this article can be found online at: http://journal.frontiersin.org/article/10.3389/fcell.2016.00058

REFERENCES

Abou-Khalil, R., Le Grand, F., Pallafacchina, G., Valable, S., Authier, F.-J., Rudnicki, M. A., et al. (2009). Autocrine and paracrine angiopoietin 1/Tie-2 signaling promotes muscle satellite cell self-renewal. *Cell Stem Cell* 5, 298–309. doi: 10.1016/j.stem.2009.06.001

Amthor, H., Christ, B., Weil, M., and Patel, K. (1998). The importance of timing differentiation during limb muscle development. *Curr. Biol.* 8, 642–652. doi: 10.1016/S0960-9822(98)70251-9

Arthur, A., Zannettino, A., Panagopoulos, R., Koblar, S. A., Sims, N. A., Stylianou, C., et al. (2011). EphB/ephrin-B interactions mediate human MSC attachment, migration and osteochondral differentiation. *Bone* 48, 533–542. doi: 10.1016/j.bone.2010.10.180

Arvanitis, D., and Davy, A. (2008). Eph/ephrin signaling: networks. *Genes Dev.* 22, 416–429. doi: 10.1101/gad.1630408

Ashar, H. R., Chouinard, R. A. Jr., Dokur, M., and Chada, K. (2010). *In vivo* modulation of HMGA2 expression. *Biochim. Biophys. Acta* 1799, 55–61. doi: 10.1016/j.bbagrm.2009.11.013

Bismuth, K., and Relaix, F. (2010). Genetic regulation of skeletal muscle development. *Exp. Cell Res.* 316, 3081–3086. doi: 10.1016/j.yexcr.2010.08.018

Boldrin, L., Neal, A., Zammit, P. S., Muntoni, F., and Morgan, JE. (2012). Donor satellite cell engraftment is significantlyaugmented when the host niche is preserved and endogenous satellite cells are incapacitated. *Stem Cells* 30, 1971–1984. doi: 10.1002/stem.1158

Boutet, S. C., Disatnik, M.-H., Chan, L. S., Iori, K., and Rando, TA. (2007). Regulation of Pax3 by proteasomal degradation of monoubiquitinated protein in skeletal muscle progenitors. *Cell* 130, 349–362. doi: 10.1016/j.cell.2007.05.044

Brack, A. S., Conboy, I. M., Conboy, M. J., Shen, J., and Rando, TA. (2008). A temporal switch from notch to Wnt signaling in muscle stem cells is necessary for normal adult myogenesis. *Cell Stem Cell* 2, 50–59. doi: 10.1016/j.stem.2007.10.006

Brack, A. S., and Rando, TA. (2012). Tissue-specific stem cells: lessons from the skeletal muscle satellite cell. *Cell Stem Cell* 10, 504–514. doi: 10.1016/j.stem.2012.04.001

Brandt, J., Veith, A. M., and Volff, J. N. (2005). A family of neofunctionalized Ty3/gypsy retrotransposon genes in mammalian genomes. *Cytogenet. Genome Res.* 110, 307–317. doi: 10.1159/000084963

Braun, T., and Gautel, M. (2011). Transcriptional mechanisms regulating skeletal muscle differentiation, growth and homeostasis. *Nat. Rev. Mol. Cell Biol.* 12, 349–361. doi: 10.1038/nrm3118

Brohl, D., Vasyutina, E., Czajkowski, M. T., Griger, J., Rassek, C., Rahn, H. P., et al. (2012). Colonization of the satellite cell niche by skeletal muscle progenitor cells depends on notch signals. *Dev. Cell* 23, 469–481. doi: 10.1016/j.devcel.2012.07.014

Buckingham, M., and Relaix, F. (2007). The role of Pax genes in the development of tissues and organs: Pax3 and Pax7 regulate muscle progenitor cell functions. *Annu. Rev. Cell Dev. Biol.* 23, 645–673. doi: 10.1146/annurev.cellbio.23.090506.123438

Buckingham, M., and Relaix, F. (2015). PAX3 and PAX7 as upstream regulators of myogenesis. *Semin Cell Dev. Biol.* doi: 10.1016/j.semcdb.2015.09.017

Calhabeu, F., Hayashi, S., Morgan, J. E., Relaix, F., and Zammit, P. S. (2013). Alveolar rhabdomyosarcoma-associated proteins PAX3/FOXO1A and PAX7/FOXO1A suppress the transcriptional activity of MyoD-target genes in muscle stem cells. *Oncogene* 32, 651–662. doi: 10.1038/onc.2012.73

Cao, D., Ma, X., Cai, J., Luan, J., Liu, A. J., Yang, R., et al. (2016). ZBTB20 is required for anterior pituitary development and lactotrope specification. *Nat. Commun.* 7:11121. doi: 10.1038/ncomms11121

Chakkalakal, J. V., Christensen, J., Xiang, W., Tierney, M. T., Boscolo, F. S., Sacco, A., et al. (2014). Early forming label-retaining muscle stem cells require p27kip1 for maintenance of the primitive state. *Development* 141, 1649–1659. doi: 10.1242/dev.100842

Chumley, M. J., Catchpole, T., Silvany, R. E., Kernie, S. G., and Henkemeyer, M. (2007). EphB receptors regulate stem/progenitor cell proliferation, migration, and polarity during hippocampal neurogenesis. *J. Neurosci.* 27, 13481–13490. doi: 10.1523/JNEUROSCI.4158-07.2007

Conboy, I. M., and Rando, T. A. (2012). Heterochronic parabiosis for the study of the effects of aging on stem cells and their niches. *Cell Cycle* 11, 2260–2267. doi: 10.4161/cc.20437

Cornelison, D. (2001). Syndecan-3 and syndecan-4 specifically mark skeletal muscle satellite cells and are implicated in satellite cell maintenance and muscle regeneration. *Dev. Biol.* 239, 79–94. doi: 10.1006/dbio.2001.0416

Diez-Roux, G., Banfi, S., Sultan, M., Geffers, L., Anand, S., Rozado, D., et al. (2011). A high-resolution anatomical atlas of the transcriptome in the mouse embryo. *PLoS Biol.* 9:e1000582. doi: 10.1371/journal.pbio.1000582

Dumont, N. A., Wang, Y. X., and Rudnicki, M. A. (2015). Intrinsic and extrinsic mechanisms regulating satellite cell function. *Development* 142, 1572–1581. doi: 10.1242/dev.114223

Engleka, K. A., Gitler, A. D., Zhang, M., Zhou, D. D., High, F. A., and Epstein, J. A. (2005). Insertion of Cre into the Pax3 locus creates a new allele of Splotch and identifies unexpected Pax3 derivatives. *Dev. Biol.* 280, 396–406. doi: 10.1016/j.ydbio.2005.02.002

Epstein, D. J., Vogan, K. J., Trasler, D. G., and Gros, P. (1993). A mutation within intron 3 of the Pax-3 gene produces aberrantly spliced MRNA transcripts in the splotch (Sp) mouse mutant. *Genesis* 90, 532–536. doi: 10.1073/pnas.90.2.532

Filion, G. J. P., Zhenilo, S., Salozhin, S., Yamada, D., Prokhortchouk, E., and Defossez, P. A. (2006). A family of human zinc finger proteins that bind methylated DNA and repress transcription. *Mol. Cell. Biol.* 26, 169–181. doi: 10.1128/MCB.26.1.169-181.2006

Friedrichs, M., Wirsdoerfer, F., Flohe, S. B., Schneider, S., Wuelling, M., and Vortkamp, A. (2011). BMP signaling balances proliferation and differentiation of muscle satellite cell descendants. *BMC Cell Biol.* 12:26. doi: 10.1186/1471-2121-12-26

Ganss, B., and Jheon, A. (2004). Zinc finger transcription factors in skeletal development. *Crit. Rev. Oral Biol. Med.* 15, 282–297. doi: 10.1177/154411130401500504

Genander, M., and Frisen, J. (2010). Ephrins and Eph receptors in stem cells and cancer. *Curr. Opin. Cell Biol.* 22, 611–616. doi: 10.1016/j.ceb.2010.08.005

Gnocchi, V. F., White, R. B. Ono, Y., Ellis, J. A., and Zammit, P. S. (2009). Further characterisation of the molecular signature of quiescent and activated mouse muscle satellite cells. *PLoS ONE* 4:e5205. doi: 10.1371/journal.pone.0005205

Haldimann, M., Custer, D., Munarini, N., Stirnimann, C., Zürcher, G., Rohrbach, V., et al. (2009). Deregulated ephrin-B2 expression in the mammary gland interferes with the development of both the glandular epithelium and vasculature and promotes metastasis formation. *Int. J. Oncol.* 35, 525–536.

Jheon, A., Chen, J., Teo, W., Ganss, B., Sodek, J., and Cheifetz, S. (2002). Temporal and spatial expression of a novel zinc finger transcription factor, AJ18, in developing murine skeletal tissues. *J. Histochem. Cytochem.* 50, 973–982. doi: 10.1177/002215540205000711

Jheon, A. H., Ganss, B., Cheifetz, S., and Sodek, J. (2001). Characterization of a novel KRAB/C2H2 zinc finger transcription factor involved in bone development. *J. Biol. Chem.* 276, 18282–18289. doi: 10.1074/jbc.M010885200

Jheon, A. H., Suzuki, N., Nishiyama, T., Cheifetz, S., Sodek, J., and Ganss, B. (2003). Characterization of the 5′-flanking region of the rat AJ18 gene. *Gene* 310, 203–213. doi: 10.1016/S0378-1119(03)00553-5

Juan, A. H., Derfoul, A., Feng, X., Ryall, J. G., Dell'Orso, S., Pasut, A., et al. (2011). Polycomb EZH2 controls self-renewal and safeguards the transcriptional identity of skeletal muscle stem cells. *Genes Dev.* 25, 789–794. doi: 10.1101/gad.2027911

Kan, H., Huang, Y., Li, X., Liu, D., Chen, J., and Shu, M. (2016). Zinc finger protein ZBTB20 is an independent prognostic marker and promotes tumor growth of human hepatocellular carcinoma by repressing FoxO1. *Oncotarget* 7, 14336–14349. doi: 10.18632/oncotarget.7425

Kassar-Duchossoy, L., Giacone, E., Gayraud-Morel, B., Jory, A., Gomès, D., and Tajbakhsh, S. (2005). Pax3/Pax7 mark a novel population of primitive myogenic cells during development. *Genes Dev.* 19, 1426–1431. doi: 10.1101/gad.345505

Kuang, S., Gillespie, M. A., and Rudnicki, M. A. (2008). Niche regulation of muscle satellite cell self-renewal and differentiation. *Cell Stem Cell* 2, 22–31. doi: 10.1016/j.stem.2007.12.012

Kuang, S., Kuroda, K., Le Grand, F., and Rudnicki, M. A. (2007). Asymmetric self-renewal and commitment of satellite stem cells in muscle. *Cell* 129, 999–1010. doi: 10.1016/j.cell.2007.03.044

Lagha, M., Sato, T., Regnault, B., Cumano, A., Zuniga, A., Licht, J., et al. (2010). Transcriptome analyses based on genetic screens for Pax3 myogenic targets in the mouse embryo. *BMC Genomics* 11:696. doi: 10.1186/1471-2164-11-696

Lepper, C., Conway, S. J., and Fan, C.-M. (2009). Adult satellite cells and embryonic muscle progenitors have distinct genetic requirements. *Nature* 460, 627–631. doi: 10.1038/nature08209

Li, Y., Yang, D., Bai, Y., Mo, X., Huang, W., Yuan, W., et al. (2008). ZNF418, a novel human KRAB/C2H2 zinc finger protein, suppresses MAPK signaling pathway. *Mol. Cell. Biochem.* 310, 141–151. doi: 10.1007/s11010-007-9674-4

Li, Z., Gilbert, J. A., Zhang, Y., Zhang, M., Qiu, Q., Ramanujan, K., et al. (2012). An HMGA2-IGF2BP2 axis regulates myoblast proliferation and myogenesis. *Dev. Cell* 23, 1176–1188. doi: 10.1016/j.devcel.2012.10.019

Linker, C., Lesbros, C., Stark, M. R., and Marcelle, C. (2003). Intrinsic signals regulate the initial steps of myogenesis in vertebrates. *Development* 130, 4797–4807. doi: 10.1242/dev.00688

Liu, L., Cheung, T. H., Charville, G. W., Hurgo, B. M., Leavitt, T., Shih, J., et al. (2013). Chromatin modifications as determinants of muscle stem cell quiescence and chronological aging. *Cell Rep.* 4, 189–204. doi: 10.1016/j.celrep.2013.05.043

Lupo, A., Cesaro, E., Montano, G., Zurlo, D., Izzo, P., and Costanzo, P. (2013). KRAB-zinc finger proteins: a repressor family displaying multiple biological functions. *Curr. Genomics* 14, 268–278. doi: 10.2174/13892029113149990002

Mauro, A. (1961). Satellite cell of skeletal mucle fibres. *J. Biophys. Biochem. Cytol.* 9, 493–495. doi: 10.1083/jcb.9.2.493

McMahon, D. K., Anderson, P. A., Nassar, R., Bunting, J. B., Saba, Z., Oakeley, A. E., et al. (1994). C2C12 cells: biophysical, biochemical, and immunocytochemical properties. *Am. J. Physiol. Cell Physiol.* 266, C1795–C1802.

Messina, G., and Cossu, G. (2009). The origin of embryonic and fetal myoblasts: a role of Pax3 and Pax7. *Genes Dev.* 23, 902–905. doi: 10.1101/gad.1797009

Mitchelmore, C. (2002). Characterization of two novel nuclear BTB/POZ domain zinc finger isoforms. Association with Differentiation of Hippocampal Neurons, Cerebellar Granule Cells, and Macroglia. *J. Biol. Chem.* 277, 7598–7609. doi: 10.1074/jbc.M110023200

Montarras, D., Morgan, J., Collins, C., Relaix, F., Zaffran, S., Cumano, A., et al. (2005). Direct isolation of satellite cells for skeletal muscle regeneration. *Science* 309, 2064–2067. doi: 10.1126/science.1114758

Moyle, L. A., and Zammit, P. S. (2014). Isolation, culture and immunostaining of skeletal muscle fibres to study myogenic progression in satellite cells. *Methods Mol. Biol.* 1210, 63–78. doi: 10.1007/978-1-4939-1435-7_6

Murai, K. K., and Pasquale, E. B. (2010). Restraining stem cell niche plasticity: a new talent of Eph receptors. *Cell Stem Cell* 7, 647–648. doi: 10.1016/j.stem.2010.11.023

Murphy, M., and Kardon, G. (2011). Origin of vertebrate limb muscle: the role of progenitor and myoblast populations. *Curr. Top. Dev. Biol.* 96, 1–32. doi: 10.1016/B978-0-12-385940-2.00001-2

Muzumdar, M. D., Tasic, B., Miyamichi, K., Li, L., and Luo, L. (2007). A global double-fluorescent Cre reporter mouse. *Genesis* 45, 593–605. doi: 10.1002/dvg.20335

Nagao, M., Ogata, T., Sawada, Y., and Gotoh, Y. (2016). Zbtb20 promotes astrocytogenesis during neocortical development. *Nat. Commun.* 7:11102. doi: 10.1038/ncomms11102

Nielsen, J. V., Nielsen, F. H., Ismail, R., Noraberg, J., and Jensen, N. A. (2007). Hippocampus-like corticoneurogenesis induced by two isoforms of

the BTB-zinc finger gene Zbtb20 in mice. *Development* 134, 1133–1140. doi: 10.1242/dev.000265

Nishino, J., Kim, I., Chada, K., and Morrison, S. J. (2008). Hmga2 promotes neural stem cell self-renewal in young but not old mice by reducing p16Ink4a and p19Arf expression. *Cell* 135, 227–239. doi: 10.1016/j.cell.2008.09.017

Oda-Ishii, I., Ishii, Y., and Mikawa, T. (2010). Eph regulates dorsoventral asymmetry of the notochord plate and convergent extension-mediated notochord formation. *PLoS ONE* 5:e13689. doi: 10.1371/journal.pone.0013689

Okabe, H., Satoh, S., Furukawa, Y., Kato, T., Hasegawa, S., Nakajima, Y., et al. (2003). Involvement of PEG10 in human hepatocellular carcinogenesis through interaction with SIAH1. *Cancer Res.* 63, 3043–3048.

Olguin, H. C., and Olwin, B. B. (2004). Pax-7 up-regulation inhibits myogenesis and cell cycle progression in satellite cells: a potential mechanism for self-renewal. *Dev. Biol.* 275, 375–388. doi: 10.1016/j.ydbio.2004.08.015

Ono, Y., Boldrin, L., Knopp, P., Morgan, J. E., and Zammit, P. S. (2010). Muscle satellite cells are a functionally heterogeneous population in both somite-derived and branchiomeric muscles. *Dev. Biol.* 337, 29–41. doi: 10.1016/j.ydbio.2009.10.005

Ono, Y., Calhabeu, F., Morgan, J. E., Katagiri, T., Amthor, H., and Zammit, P. S. (2011). BMP signalling permits population expansion by preventing premature myogenic differentiation in muscle satellite cells. *Cell Death Differ.* 18, 222–234. doi: 10.1038/cdd.2010.95

Ono, Y., Masuda, S., Nam, H. S., Benezra, R., Miyagoe-Suzuki, Y., and Takeda, S. (2012). Slow-dividing satellite cells retain long-term self-renewal ability in adult muscle. *J. Cell Sci.* 125, 1309–1317. doi: 10.1242/jcs.096198

Palmer, A., and Klein, R. (2003). Multiple roles of ephrins in morphogenesis, neuronal networking, and brain function. *Genes Dev.* 17, 1429–1450. doi: 10.1101/gad.1093703

Pasquale, E. B. (2005). Eph receptor signalling casts a wide net on cell behaviour. *Nat. Rev. Mol. Cell Biol.* 6, 462–475. doi: 10.1038/nrm1662

Pasquale, E. B. (2010). Eph receptors and ephrins in cancer: bidirectional signalling and beyond. *Nat. Rev. Cancer* 10, 165–180. doi: 10.1038/nrc2806

Pear, W., Miller, J., Xu, L., Pui, J., Soffer, B., Quackenbush, R., et al. (1998). Efficient and rapid induction of a chronic myelogenous leukemia-like myeloproliferative disease in mice receiving P210 bcr/abl-transduced bone marrow. *Blood* 92, 3780–3792.

Pfannkuche, K., Summer, H., Li, O., Hescheler, J., and Droge, P. (2009). The high mobility group protein HMGA2: a co-regulator of chromatin structure and pluripotency in stem cellsβ *Stem Cell Rev.* 5, 224–230. doi: 10.1007/s12015-009-9078-9

Picard, C. A., and Marcelle, C. (2013). Two distinct muscle progenitor populations coexist throughout amniote development. *Dev. Biol.* 373, 141–148. doi: 10.1016/j.ydbio.2012.10.018

Pitulescu, M. E., and Adams, R. H. (2010). Eph/ephrin molecules–a hub for signaling and endocytosis. *Genes Dev.* 24, 2480–2492. doi: 10.1101/gad.1973910

Relaix, F. (2006). Skeletal muscle progenitor cells: from embryo to adult. *Cell. Mol. Life Sci.* 63, 1221–1225. doi: 10.1007/s00018-006-6015-9

Relaix, F., and Marcelle, C. (2009). Muscle stem cells. *Curr. Opin. Cell Biol.* 21, 748–753. doi: 10.1016/j.ceb.2009.10.002

Relaix, F., Montarras, D., Zaffran, S., Gayraud-Morel, B., Rocancourt, D., Tajbakhsh, S., et al. (2006). Pax3 and Pax7 have distinct and overlapping functions in adult muscle progenitor cells. *J. Cell Biol.* 172, 91–102. doi: 10.1083/jcb.200508044

Relaix, F., Rocancourt, D., Mansouri, A., and Buckingham, M. (2005). A Pax3/Pax7-dependent population of skeletal muscle progenitor cells. *Nature* 435, 948–953. doi: 10.1038/nature03594

Relaix, F., and Zammit, P. S. (2012). Satellite cells are essential for skeletal muscle regeneration: the cell on the edge returns centre stage. *Development* 139, 2845–2856. doi: 10.1242/dev.069088

Rocheteau, P., Gayraud-Morel, B., Siegl-Cachedenier, I., Blasco, M. A., and Tajbakhsh, S. (2012). A subpopulation of adult skeletal muscle stem cells retains all template DNA strands after cell division. *Cell* 148, 112–125. doi: 10.1016/j.cell.2011.11.049

Rudnicki, M. A., Le Grand, F., McKinnell, I., and Kuang, S. (2008). The molecular regulation of muscle stem cell function. *Cold Spring Harb. Symp. Quant. Biol.* 73, 323–331. doi: 10.1101/sqb.2008.73.064

Sambasivan, R., Kuratani, S., and Tajbakhsh, S. (2011). An eye on the head: the development and evolution of craniofacial muscles. *Development* 138, 2401–2415. doi: 10.1242/dev.040972

Sartori, R., Schirwis, E., Blaauw, B., Bortolanza, S., Zhao, J., Enzo, E., et al. (2013). BMP signaling controls muscle mass. *Nat. Genet.* 45, 1309–1318. doi: 10.1038/ng.2772

Seale, P., Sabourin, L. A., Girgis-Gabardo, A., Mansouri, A., Gruss, P., and Rudnicki, M. A. (2000). Pax7 is required for the specification of myogenic satellite cells. *Cell* 102, 777–786. doi: 10.1016/S0092-8674(00)00066-0

Shefer, G., Van de Mark, D. P., Richardson, J. B., and Yablonka-Reuveni, Z. (2006). Satellite-cell pool size does matter: defining the myogenic potency of aging skeletal muscle. *Dev. Biol.* 294, 50–66. doi: 10.1016/j.ydbio.2006.02.022

Shinin, V., Gayraud-Morel, B., Gomes, D., and Tajbakhsh, S. (2006). Asymmetric division and cosegregation of template DNA strands in adult muscle satellite cells. *Nat. Cell Biol.* 8, 677–687. doi: 10.1038/ncb1425

Singla, N., Goldgur, Y., Xu, K., Paavilainen, S., Nikolov, D. B., and Himanen, J. P. (2010). Crystal structure of the ligand-binding domain of the promiscuous EphA4 receptor reveals two distinct conformations. *Biochem. Biophys. Res. Commun.* 399, 555–559. doi: 10.1016/j.bbrc.2010.07.109

Sinha, M., Jang, Y. C., Oh, J., Khong, D., Wu, E. Y., Manohar, R., et al. (2014). Restoring systemic GDF11 levels reverses age-related dysfunction in mouse skeletal muscle. *Science* 344, 649–652. doi: 10.1126/science.1251152

Sousa-Victor, P., Gutarra, S., García-Prat, L., Rodriguez-Ubreva, J., Ortet, L., Ruiz-Bonilla, V., et al. (2014). Geriatric muscle stem cells switch reversible quiescence into senescence. *Nature* 506, 316–321. doi: 10.1038/nature13013

Sreevalsan, S., and Safe, S. (2013). Reactive oxygen species and colorectal cancer. *Curr. Colorectal Cancer Rep.* 9, 350–357. doi: 10.1007/s11888-013-0190-5

Stark, D. A., Karvas, R. M., Siegel, A. L., and Cornelison, D. D. (2011). Eph/ephrin interactions modulate muscle satellite cell motility and patterning. *Development* 138, 5279–5289. doi: 10.1242/dev.068411

Stokowski, A., Shi, S., Sun, T., Bartold, P. M., Koblar, S. A., and Gronthos, S. (2007). EphB/ephrin-B interaction mediates adult stem cell attachment, spreading, and migration: implications for dental tissue repair. *Stem Cells* 25, 156–164. doi: 10.1634/stemcells.2006-0373

Stoller, J. Z., Degenhardt, K. R., Huang, L., Zhou, D. D., Lu, M. M., and Epstein, J. A. (2008). Cre reporter mouse expressing a nuclear localized fusion of GFP and β-galactosidase reveals new derivatives of Pax3-expressing precursors. *Genesis* 46, 200–204. doi: 10.1002/dvg.20384

Sutherland, A. P. R., Zhang, H., Zhang, Y., Michaud, M., Xie, Z., Patti, M. E., et al. (2009). Zinc finger protein zbtb20 is essential for postnatal survival and glucose homeostasis. *Mol. Cell. Biol.* 29, 2804–2815. doi: 10.1128/MCB.01667-08

Tajbakhsh, S. (2009). Skeletal muscle stem cells in developmental versus regenerative myogenesis. *J. Intern. Med.* 266, 372–389. doi: 10.1111/j.1365-2796.2009.02158.x

Tajbakhsh, S., and Buckingham, M. (2000). The birth of muscle progenitor cells in the mouse: spatiotemporal considerations. *Curr. Top. Dev. Biol.* 48, 225–268. doi: 10.1016/S0070-2153(08)60758-9

Thanos, D., and Maniatis, T. (1992). The high mobility group protein HMG I(Y) is required for NF-kB-dependent virus induction of the human IFN-β gene. *Cell* 71, 777–789. doi: 10.1016/0092-8674(92)90554-P

Tian, C. Y., Zhang, L. Q., and He, F. C. (2006). Progress in the study of KRAB zinc finger protein. *Yi Chuan* 28, 1451–1456. doi: 10.1360/yc-006-1451

Urrutia, R. (2003). KRAB-containing zinc-finger repressor proteins. *Genome Biol.* 4:231. doi: 10.1186/gb-2003-4-10-231

Vindis, C., Cerretti, D. P., Daniel, T. O., and Huynh-Do, U. (2003). EphB1 recruits c-Src and p52Shc to activate MAPK/ERK and promote chemotaxis. *J. Cell Biol.* 162, 661–671. doi: 10.1083/jcb.200302073

Vindis, C., Teli, T., Cerretti, D. P., Turner, C. E., and Huynh-Do, U. (2004). EphB1-mediated cell migration requires the phosphorylation of paxillin at Tyr-31/Tyr-118. *J. Biol. Chem.* 279, 27965–27970. doi: 10.1074/jbc.M401295200

Wang, H., Noulet, F., Edom-Vovard, F., Le Grand, F., and Duprez, D. (2010). Bmp signaling at the tips of skeletal muscles regulates the number of fetal muscle progenitors and satellite cells during development. *Dev. Cell* 18, 643–654. doi: 10.1016/j.devcel.2010.02.008

Wang, Y. X., and Rudnicki, M. A. (2011). Satellite cells, the engines of muscle repair. *Nat. Rev. Mol. Cell Biol.* 13, 127–133. doi: 10.1038/nrm3265

Watson, R. P., Tekki-Kessaris, N., and Boulter, C. A. (2000). Characterisation, chromosomal localisation and expression of the mouse Kid3 gene. *Biochem. Biophys. Acta* 1490, 153–158. doi: 10.1016/S0167-4781(99)00239-0

Weber, A., Marquardt, J., Elzi, D., Forster, N., Starke, S., Glaum, A., et al. (2008). Zbtb4 represses transcription of P21CIP1 and controls the cellular response to p53 activation. *EMBO J.* 27, 1563–1574. doi: 10.1038/emboj.2008.85

Weng, M.-Z., Zhuang, P.-Y., Hei, Z.-Y., Lin, P.-Y., Chen, Z.-S., Liu, Y.-B., et al. (2014). ZBTB20 is involved in liver regeneration after partial hepatectomy in mouse. *Hepatobil. Pancreatic Dis. Int.* 13, 48–54. doi: 10.1016/S1499-3872(14)60006-0

White, R. B., Biérinx, A.-S., Gnocchi, V. F., and Zammit, P. S. (2010). Dynamics of muscle fibre growth during postnatal mouse development. *BMC Dev. Biol.* 10:21. doi: 10.1186/1471-213X-10-21

Yang, W. S., Chadalapaka, G., Cho, S. G., Lee, S. O., Jin, U. H., Jutooru, I., et al. (2014). The transcriptional repressor ZBTB4 regulates EZH2 through a MicroRNA-ZBTB4-specificity protein signaling axis. *Neoplasia* 16, 1059–1069. doi: 10.1016/j.neo.2014.09.011

Yoshida, N., Yoshida, S., Koishi, K., Masuda, K., and Nabeshima, Y.-I. (1998). Cell heterogeneity upon myogenic differentiation: down-regulation of MyoD and Myf-5 generates 'reserve cells'. *J. Cell Sci.* 111, 769–779.

Zammit, P. S., Golding, J. P., Nagata, Y., Hudon, V., Partridge, T. A., and Beauchamp, J. R. (2004). Muscle satellite cells adopt divergent fates: a mechanism for self-renewal? *J. Cell Biol.* 166, 347–357. doi: 10.1083/jcb.200312007

Zammit, P. S., Partridge, T. A., and Yablonka-Reuveni, Z. (2006a). The skeletal muscle satellite cell: the stem cell that came in from the cold. *J. Histochem. Cytochem.* 54, 1177–1191. doi: 10.1369/jhc.6R6995.2006

Zammit, P. S., Relaix, F., Nagata, Y., Pérez-Ruiz, A., Collins, C., Partridge, T., et al. (2006b). Pax7 and myogenic progression in skeletal muscle satellite cells. *J. Cell Sci.* 119, 1824–1832. doi: 10.1242/jcs.02908

Zhao, J. G., Ren, K. M., and Tang, J. (2014). Zinc finger protein ZBTB20 promotes cell proliferation in non-small cell lung cancer through repression of FoxO1. *FEBS Lett.* 588, 4536–4542. doi: 10.1016/j.febslet.2014.10.005

Zhou, G., Jiang, X., Zhang, H., Lu, Y., Liu, A., Ma, X., et al. (2015). Zbtb20 regulates the terminal differentiation of hypertrophic chondrocytes via repression of Sox9. *Development* 142, 385–393. doi: 10.1242/dev.108530

Zhou, X., Benson, K. F., Ashar, H. R., and Chada, K. (1995). Mutation responsible for the mouse pygmy phenotype in the developmentally regulated factor HMGI-C. *Nature* 376, 771–774. doi: 10.1038/376771a0

Zhou, X., and Chada, K. (1998). HMGI family proteins: architectural transcription factors in mammalian development and cancer. *Keio J. Med.* 47, 73–77. doi: 10.2302/kjm.47.73

Conflict of Interest Statement: The authors declare that the research was conducted in the absence of any commercial or financial relationships that could be construed as a potential conflict of interest.

REFERENCES

Abou-Khalil R, Le Grand F, Pallafacchina G, Valable S, Authier FJ, Rudnicki MA, Gherardi RK, Germain S, Chretien F, Sotiropoulos A, Lafuste P, Montarras D, Chazaud B. **2009**. Autocrine and paracrine angiopoietin 1/Tie-2 signaling promotes muscle satellite cell self-renewal. Cell Stem Cell 5: 298-309.

Abou Khalil R, Partridge T, Chazaud B. **2010**. Les cellules du muscle chantent en choeur une berceuse pour cellules souches. Med Sci 26: 589-591.

Alexander K, Hinds PW. **2001**. Requirement for p27(KIP1) in retinoblastoma protein-mediated senescence. Mol Cell Biol 21: 3616-3631.

Allen KE, de la Luna S, Kerkhoven RM, Bernards R, La Thangue NB. **1997**. Distinct mechanisms of nuclear accumulation regulate the functional consequence of E2F transcription factors. J Cell Sci 110: 2819-2831.

Andrés V, Walsh K. **1996**. Myogenin expression, cell cycle withdrawal, and phenotypic differentiation are temporally separable events that precede cell fusion upon myogenesis. J Cell Biol 132: 657-666.

Andrews SC, Wood MD, Tunster SJ, Barton SC, Surani MA, John RM. **2007**. Cdkn1c (p57Kip2) is the major regulator of embryonic growth within its imprinted domain on mouse distal chromosome 7. BMC Dev Biol 7: 53.

Artavanis-Tsakonas S, Muskavitch MA. **2010**. Notch: the past, the present, and the future. Curr Top Dev Biol 92: 1-29.

Asakura A, Komaki M, Rudnicki M. **2001**. Muscle satellite cells are multipotential stem cells that exhibit myogenic, osteogenic, and adipogenic differentiation. Differentiation 68: 245-253.

Asp P, Acosta-Alvear D, Tsikitis M, van Oevelen C, Dynlacht BD. **2009**. E2f3b plays an essential role in myogenic differentiation through isoform-specific gene regulation. Genes Dev 23: 37-53.

Auerbach R. **1954**. Analysis of the developmental effects of a lethal mutation in the house mouse. J Exp Zool 127: 305-329.

Aulehla A, Pourquié O. **2010**. Signaling gradients during paraxial mesoderm development. Cold Spring Harb Perspect Biol 2: a000869.

Barberi L, Scicchitano BM, De Rossi M, Bigot A, Duguez S, Wielgosik A, Stewart C, McPhee J, Conte M, Narici M, Franceschi C, Mouly V, Butler-Browne G, Musarò A. **2013**. Age-dependent alteration in muscle regeneration: the critical role of tissue niche. Biogerontology 14: 273-292.

Barns M, Gondro C, Tellam RL, Radley-Crabb HG, Grounds MD, Shavlakadze T. **2014**. Molecular analyses provide insight into mechanisms underlying sarcopenia and myofibre denervation in old skeletal muscles of mice. Int J Biochem Cell Biol 53: 174-185.

Bartkova J, Lukas J, Strauss M, Bartek J. **1998**. Cyclin D3: requirement for G1/S transition and high abundance in quiescent tissues suggest a dual role in proliferation and differentiation. Oncogene 17: 1027-1037.

Battistelli C, Busanello A, Maione R. **2014**. Functional interplay between MyoD and CTCF in regulating long-range chromatin interactions during differentiation. J Cell Sci 127: 3757-3767.

Bean C, Salamon M, Raffaello A, Campanaro S, Pallavicini A, Lanfranchi G. **2005**. The Ankrd2, Cdkn1c and calcyclin genes are under the control of MyoD during myogenic differentiation. J Mol Biol 349: 349-366.

Beauchamp JR, Heslop L, Yu DS, Tajbakhsh S, Kelly RG, Wernig A, Buckingham ME, Partridge TA, Zammit PS. **2000**. Expression of CD34 and Myf5 defines the majority of quiescent adult skeletal muscle satellite cells. J Cell Biol 151: 1221-1234.

Ben-Yair R, Kalcheim C. **2005**. Lineage analysis of the avian dermomyotome sheet reveals the existence of single cells with both dermal and muscle progenitor fates. Development 132: 689-701.

Bentzinger CF, Wang YX, Rudnicki MA. **2012**. Building muscle: molecular regulation of myogenesis. Cold Spring Harb Perspect Biol 4.

Berman SD, West JC, Danielian PS, Caron AM, Stone JR, Lees JA. **2009**. Mutation of p107 exacerbates the consequences of Rb loss in embryonic tissues and causes cardiac and blood vessel defects. Proc Natl Acad Sci USA 106: 14932-14936.

Bernet JD, Doles JD, Hall JK, Kelly Tanaka K, Carter TA, Olwin BB. **2014**. p38 MAPK signaling underlies a cell-autonomous loss of stem cell self-renewal in skeletal muscle of aged mice. Nat Med 20: 265-271.

Besson A, Assoian RK, Roberts JM. **2004**. Regulation of the cytoskeleton: an oncogenic function for CDK inhibitors? Nat Rev Cancer 4: 948-955.

Besson A, Dowdy SF, Roberts JM. **2008**. CDK inhibitors: cell cycle regulators and beyond. Dev Cell 14: 159-169.

Biferi MG, Nicoletti C, Falcone G, Puggioni EM, Passaro N, Mazzola A, Pajalunga D, Zaccagnini G, Rizzuto E, Auricchio A, Zentilin L, De Luca G, Giacca M, Martelli F, Musio A, Musarò A, Crescenzi M. **2015**. Proliferation of Multiple Cell Types in the Skeletal Muscle Tissue Elicited by Acute p21 Suppression. Mol Ther 23: 885-895.

Bilodeau S, Roussel-Gervais A, Drouin J. **2009**. Distinct developmental roles of cell cycle inhibitors p57Kip2 and p27Kip1 distinguish pituitary progenitor cell cycle exit from cell cycle reentry of differentiated cells. Mol Cell Biol 29: 1895-1908.

Birchmeier C, Brohmann H. **2000**. Genes that control the development of migrating muscle precursor cells. Curr Opin Cell Biol 12: 725-730.

Biressi S, Rando TA. **2010**. Heterogeneity in the muscle satellite cell population. Semin Cell Dev Biol 21: 845-854.

Bismuth K, Relaix F. **2010**. Genetic regulation of skeletal muscle development. Exp Cell Res 316: 3081-3086.

Bjornson CR, Cheung TH, Liu L, Tripathi PV, Steeper KM, Rando TA. **2012**. Notch signaling is necessary to maintain quiescence in adult muscle stem cells. Stem Cells 30: 232-242.

Blachly JS, Byrd JC, Grever M. **2016**. Cyclin-dependent kinase inhibitors for the treatment of chronic lymphocytic leukemia. Semin Oncol 43: 265-273.

Bladt F, Riethmacher D, Isenmann S, Aguzzi A, Birchmeier C. **1995**. Essential role for the c-met receptor in the migration of myogenic precursor cells into the limb bud. Nature 376: 768-771.

Blais A, Tsikitis M, Acosta-Alvear D, Sharan R, Kluger Y, Dynlacht BD. **2005**. An initial blueprint for myogenic differentiation. Genes Dev 19: 553-569.

Bober E, Lyons GE, Braun T, Cossu G, Buckingham M, Arnold HH. **1991**. The muscle regulatory gene, Myf-6, has a biphasic pattern of expression during early mouse development. J Cell Biol 113: 1255-1265.

Bober E, Franz T, Arnold HH, Gruss P, Tremblay P. **1994**. Pax-3 is required for the development of limb muscles: a possible role for the migration of dermomyotomal muscle progenitor cells. Development 120: 603-612.

Bookstein R, Shew JY, Chen PL, Scully P, Lee WH. **1990**. Suppression of tumorigenicity of human prostate carcinoma cells by replacing a mutated RB gene. Science 247: 712-715.

Boonsanay V, Zhang T, Georgieva A, Kostin S, Qi H, Yuan X, Zhou Y, Braun T. **2016**. Regulation of skeletal muscle stem cell quiescence by suv4-20h1-dependent facultative heterochromatin formation. Cell Stem Cell 18: 229-242.

Borriello A, Caldarelli I, Bencivenga D, Criscuolo M, Cucciolla V, Tramontano A, Oliva A, Perrotta S, Della Ragione F. **2011**. p57(Kip2) and cancer: time for a critical appraisal. Mol Cancer Res 9: 1269-1284.

Brack AS, Conboy IM, Conboy MJ, Shen J, Rando TA. **2008**. A temporal switch from notch to Wnt signaling in muscle stem cells is necessary for normal adult myogenesis. Cell Stem Cell 2: 50-59.

Brack AS, Rando TA. **2012**. Tissue-specific stem cells: lessons from the skeletal muscle satellite cell. Cell Stem Cell 10: 10: 504-514.

Brack AS. **2014**. Pax7 is back. Skelet Muscle 4: 24.

Bracken AP, Ciro M, Cocito A, Helin K. **2004**. E2F target genes: unraveling the biology. Trends Biochem Sci 29: 409-417.

Braun T, Buschhausen-Denker G, Bober E, Tannich E, Arnold HH. **1989**. A novel human muscle factor related to but distinct from MyoD1 induces myogenic conversion in 10T1/2 fibroblasts. EMBO J 8: 701-709.

Braun T, Rudnicki MA, Arnold HH, Jaenisch R. **1992**. Targeted inactivation of the muscle regulatory gene Myf-5 results in abnormal rib development and perinatal death. Cell 71: 369-382.

Braun T, Bober E, Rudnicki MA, Jaenisch R, Arnold HH. **1994**. MyoD expression marks the onset of skeletal myogenesis in Myf-5 mutant mice. Develoment 120: 3083-3092.

Braun T, Arnold HH. **1995**. Inactivation of Myf-6 and Myf-5 genes in mice leads to alterations in skeletal muscle development. EMBO J 14: 1176-1186.

Braun T, Gautel M. **2011**. Transcriptional mechanisms regulating skeletal muscle differentiation, growth and homeostasis. Nat Rev Mol Cell Biol 12: 349-361.

Brent AE, Tabin CJ. **2002**. Developmental regulation of somite derivatives: muscle, cartilage and tendon. Curr Opin Genet Dev 12: 548-557.

Bringold F, Serrano M. **2000**. Tumor suppressors and oncogenes in cellular senescence. Exp Gerontol 35: 317-329.

Bröhl D, Vasyutina E, Czajkowski MT, Griger J, Rassek C, Rahn HP, Purfürst B, Wende H, Birchmeier C. **2012**. Colonization of the satellite cell niche by skeletal muscle progenitor cells depends on Notch signals. Dev Cell 23: 469-481.

Brohmann H, Jagla K, Birchmeier C. **2000**. The role of Lbx1 in migration of muscle precursor cells. Development 127: 437-445.

Brotherton DH, Dhanaraj V, Wick S, Brizuela L, Domaille PJ, Volyanik E, Xu X, Parisini E, Smith BO, Archer SJ, Serrano M, Brenner SL, Blundell TL, Laue ED. **1998**. Crystal structure of the complex of the cyclin D-dependent kinase Cdk6 bound to the cell-cycle inhibitor p19INK4d. Nature 395: 244-250.

Brzoska E, Ciemerych MA, Przewozniak M, Zimowska M. **2011**. Regulation of muscle stem cells activation: the role of growth factors and extracellular matrix. Vitam Horm 87: 239-276.

Buas MF, Kabak S, Kadesch T. **2009**. Inhibition of myogenesis by Notch: evidence for multiple pathways. J Cell Physiol 218: 84-93.

Buas MF, Kadesch T. **2010**. Regulation of skeletal myogenesis by Notch. Exp Cell Res 316: 3028-3033.

Buchkovich K, Duffy LA, Harlow E. **1989**. The retinoblastoma protein is phosphorylated during specific phases of the cell cycle. Cell 58: 1097-1105.

Buckingham M, Bajard L, Chang T, Daubas P, Hadchouel J, Meilhac S, Montarras D, Rocancourt D, Relaix F. **2003**. The formation of skeletal muscle: from somite to limb. J Anat 202: 59-68.

Buckingham M. **2007**. Skeletal muscle progenitor cells and the role of Pax genes. CR Biol 330: 530-533.

Buckingham M, Relaix F. **2007**. The role of Pax genes in the development of tissues and organs: Pax3 and Pax7 regulate muscle progenitor cell functions. Annu Rev Cell Dev Biol 23: 645-673.

Buckingham M, Mayeuf A. **2012**. Chapter 52: Skeletal Muscle Development. In: Muscle Fundamental biology and mechanisms of disease, Edited by J.A. Hill, E.N. Olson, p.749-762.

Buckingham M, Rigby PW. **2014**. Gene regulatory networks and transcriptional mechanisms that control myogenesis. Dev Cell 28: 225-238.

Buckingham M, Relaix F. **2015**. PAX3 and PAX7 as upstream regulators of myogenesis. Semin Cell Dev Biol 44: 115-125.

Burgess R, Rawls A, Brown D, Bradley A, Olson EN. **1996**. Requirement of the paraxis gene for somite formation and musculoskeletal patterning. Nature 384: 570-573.

Busanello A, Battistelli C, Carbone M, Mostocotto C, Maione R. **2012**. MyoD regulates p57kip2 expression by interacting with a distant cis-element and modifying a higher order chromatin structure. Nuclei Acids Res 40: 8266-8275.

Bustos F, de la Vega E, Cabezas F, Thompson J, Cornelison DD, Olwin BB, Yates JR 3rd, Olguín HC. **2015**. NEDD4 regulates Pax7 levels promoting activation of the differentiation program in skeletal muscle precursors. Stem Cell 33: 3138-3151.

Calhabeu F, Hayashi S, Morgan JE, Relaix F, Zammit PS. **2013**. Alveolar rhabdomyosarcoma-associated proteins PAX3/FOXO1A and PAX7/FOXO1A suppress the transcriptional activity of MyoD-target genes in muscle stem cells. Oncogene 32: 651-662.

Camarda G, Siepi F, Pajalunga D, Bernardini C, Rossi R, Montecucco A, Meccia E, Crescenzi M. **2004**. A pRb-independent mechanism preserves the postmitotic state in terminally differentiated skeletal muscle cells. J Cell Biol 167: 417-423.

Cao Y, Zhao Z, Gruszczynska-Biegala J, Zolkiewska A. **2003**. Role of metalloprotease disintegrin ADAM12 in determination of quiescent reserve cells during myogenic differentiation *in vitro*. Mol Cell Biol 23: 6725-6738.

Cao Y, Kumar RM, Penn BH, Berkes CA, Kooperberg C, Boyer LA, Young RA, Tapscott SJ. **2006**. Global and gene-specific analyses show distinct roles for Myod and Myog at a common set of promoters. EMBO J 25: 502-511.

Carlson ME, Hsu M, Conboy IM. **2008**. Imbalance between pSmad3 and Notch induces CDK inhibitors in old muscle stem cells. Nature 454: 528-532.

Carnac G, Fajas L, L'honoré A, Sardet C, Lamb NJ, Fernandez A. **2000**. The retinoblastoma-like protein p130 is involved in the determination of reserve cells in differentiating myoblasts. Curr Biol 10: 543-546.

Carre A, Rachdi L, Tron E, Richard B, Castanet M, Schlumberger M, Bidart JM, Szinnai G, Polak M. **2011**. Hes1 is required for appropriate morphogenesis and differentiation during mouse thyroid gland development. PLoS One 6: e16752.

Cenciarelli C, De Santa F, Puri PL, Mattei E, Ricci L, Bucci F, Felsani A, Caruso M. **1999**. Critical role played by cyclin D3 in the MyoD-mediated arrest of cell cycle during myoblast differentiation. Mol Cell Biol 19: 5203-5217.

Cerqueira A, Martín A, Symonds CE, Odajima J, Dubus P, Barbacid M, Santamaría D. **2014**. Genetic characterization of the role of the Cip/Kip family of proteins as cyclin-dependent kinase inhibitors and assembly factors. Mol Cell Biol 34: 1452-1459.

Chakkalakal JV, Christensen J, Xiang W, Tierney MT, Boscolo FS, Sacco A, Brack AS. **2014**. Early forming label-retaining muscle stem cells require p27kip1 for maintenance of the primitive state. Development 141: 1649-1659.

Chakravarthy MV, Abraha TW, Schwartz RJ, Fiorotto ML, Booth FW. **2000**. Insulin-like growth factor-I extends *in vitro* replicative life span of skeletal muscle satellite cells by enhancing G1/S cell cycle progression via the activation of phosphatidylinositol 3'-kinase/Akt signaling pathway. J Biol Chem 275: 35942-35952.

Chan FKM, Zhang J, Cheng L, Shapiro DN, Winoto A. **1995**. Identification of human and mouse p19, a novel CDK4 and CDK6 inhibitor with homology to $p16^{Ink4}$. Mol Cell Biol 15: 2682-2688.

Chang TS, Kim MJ, Ryoo K, Park J, Eom SJ, Shim J, Nakayama KI, Nakayama K, Tomita M, Takahashi K, Lee MJ, Choi EJ. **2003**. p57KIP2 modulates stress-activated signaling by inhibiting c-Jun NH2-terminal kinase/stress-activated protein Kinase. J Biol Chem 278: 48092-48098.

Chang NC, Rudnicki MA. **2014**. Satellite cells: the architects of skeletal muscle. Curr Top Dev Biol 107: 161-181.

Chen PL, Scully P, Shew JY, Wang JY, Lee WH. **1989**. Phosphorylation of the retinoblastoma gene product is modulated during the cell cycle and cellular differentiation. Cell 58: 1193-1198.

Chen G, Lee EY. **1999**. Phenotypic differentiation without permanent cell-cycle arrest by skeletal myocytes with deregulated E2F-1. DNA Cell Biol 18: 305-314.

Cheung TH, Rando TA. **2013**. Molecular regulation of stem cell quiescence. Nat Rev Mol Cell Biol 14: 329-340.

Chinzei N, Hayashi S, Ueha T, Fujishiro T, Kanzaki N, Hashimoto S, Sakata S, Kihara S, Haneda M, Sakai Y, Kuroda R, Kurosaka M. **2015**. P21 deficiency delays regeneration of skeletal muscular tissue. PLoS One 10: e0125765.

Chow SE, Wang JS, Lin MR, Lee CL. **2011**. Downregulation of p57kip² promotes cell invasion via LIMK/cofilin pathway in human nasopharyngeal carcinoma cells. J Cell Biochem 112: 3459-3468.

Chow CY. **2016**. Bringing genetic background into focus. Nat Rev Genet 17: 63-64.

Christ B, Brand-Saberi B. **2002**. Limb muscle development. Int J Dev Biol **2002** 4: 905-914.

Chu CY, Lim RW. **2000**. Involvement of p27(kip1) and cyclin D3 in the regulation of cdk2 activity during skeletal muscle differentiation. Biochim Biophys Acta 1497: 175-185.

Christ B, Ordahl CP. **1995**. Early stages of chick somite development. Anat Embryol (Berl) 191: 381-396.

Ciavarra G, Ho AT, Cobrinik D, Zacksenhaus E. **2011**. Critical role of the Rb family in myoblast survival and fusion. PLoS One 6: e17682.

Ciemerych MA, Archacka K, Grabowska I, Przewoźniak M. **2011**. Cell cycle regulation during proliferation and differentiation of mammalian muscle precursor cells. Results Probl Cell Differ 53:473-527.

Cobrinik D, Lee MH, Hannon G, Mulligan G, Bronson RT, Dyson N, Harlow E, Beach D, Weinberg RA, Jacks T. **1996**. Shared role of the pRB-related p130 and p107 proteins in limb development. Genes Dev 10: 1633-1644.

Cobrinik D. **2005**. Pocket proteins and cell cycle control. Oncogene 24: 2796-2809.

Collins CA, Olsen I, Zammit PS, Heslop L, Petrie A, Partridge TA, Morgan JE. **2005**. Stem cell function, self-renewal, and behavioral heterogeneity of cells from the adult muscle satellite cell niche. Cell 122: 289-301.

Comai G, Sambasivan R, Gopalakrishnan S, Tajbakhsh S. **2014**. Variations in the efficiency of lineage marking and ablation confound distinctions between myogenic cell populations. Dev Cell 31: 654-667.

Conboy IM, Rando TA. **2002**. The regulation of Notch signaling controls satellite cell activation and cell fate determination in postnatal myogenesis. Dev Cell 3: 397-409.

Conboy IM, Conboy MJ, Smythe GM, Rando TA. **2003**. Notch-mediated restoration of regenerative potential to aged muscle. Science 302: 1575-1577.

Conboy IM, Conboy MJ, Wagers AJ, Girma ER, Weissman IL, Rando TA. **2005**. Rejuvenation of aged progenitor cells by exposure to a young systemic environment. Nature 433: 760-764.

Conboy MJ, Karasov AO, Rando TA. **2007**. High incidence of non-random template strand segregation and asymmetric fate determination in dividing stem cells and their progeny. PLoS Biol 5: e102.

Cooke J, Zeeman EC. **1976**. A clock and wavefront model for control of the number of repeated structures during animal morphogenesis. J Theor Biol 58: 455-476.

Cooper RN, Tajbakhsh S, Mouly V, Cossu G, Buckingham M, Butler-Browne GS. **1999**. *In vivo* satellite cell activation via Myf5 and MyoD in regenerating mouse skeletal muscle. J Cell Sci 112: 2895-2901.

Cooper GM. **2000**. The Cell: A Molecular Approach. 2nd edition. Sunderland (MA): Sinauer Associates.

Corbeil HB, Whyte P, Branton PE. **1995**. Characterization of transcription factor E2F complexes during muscle and neuronal differentiation. Oncogene 11: 909-920.

Cosgrove BD, Gilbert PM, Porpiglia E, Mourkioti F, Lee SP, Corbel SY, Llewellyn ME, Delp SL, Blau HM. **2014**. Rejuvenation of the muscle stem cell population restores strength to injured aged muscles. Nat Med 20: 255-264.

Crescenzi M, Fleming TP, Lassar AB, Weintraub H, Aaronson SA. **1990**. MyoD induces growth arrest independent of differentiation in normal and transformed cells. Proc Natl Acad Sci USA 87: 8442-8446.

Crist CG, Montarras D, Buckingham M. **2012**. Muscle satellite cells are primed for myogenesis but maintain quiescence with sequestration of Myf5 mRNA targeted by microRNA-31 in mRNP granules. Cell Stem Cell 11: 118-126.

Davis RL, Weintraub H, Lassar AB. **1987**. Expression of a single transfected cDNA converts fibroblasts to myoblasts. Cell 51: 987-1000.

de Bondt HL, Rosenblatt J, Jancarik J, Jones HD, Morgan DO, Kim S-H. **1993**. Crystal structure of cyclin-dependent kinase 2. Nature 363:595-602.

de Bruin A, Wu L, Saavedra HI, Wilson P, Yang Y, Rosol TJ, Weinstein M, Robinson ML, Leone G. **2003**. Rb function in extraembryonic lineages suppresses apoptosis in the CNS of Rb-deficient mice. Proc Natl Acad Sci USA 100: 6546-6551.

de Falco M, De Luca A. **2006**. Involvement of cdks and cyclins in muscle differentiation. Eur J Histochem 50: 19-23.

de Luca G, Ferretti R, Bruschi M, Mezzaroma E, Caruso M. **2014**. Cyclin D3 critically regulates the balance between self-renewal and differentiation in skeletal muscle stem cells. Stem Cells 31: 2478-2491.

Delfini MC, Hirsinger E, Pourquié O, Duprez D. **2000**. Delta 1-activated notch inhibits muscle differentiation without affecting Myf5 and Pax3 expression in chick limb myogenesis. Development 127: 5213-5224.

Deng C, Zhang P, Harper JW, Elledge SJ, Leder P. **1995**. Mice lacking p21CIP1/WAF1 undergo normal development, but are defective in G1 checkpoint control. Cell 82: 675-684.

Desai D, Wessling HC, Fisher RP, Morgan DO. **1995**. Effects of phosphorylation by CAK on cyclin binding by CDC2 and CDK2. Mol Cell Biol 15: 345-350.

Dias AS, de Almeida I, Belmonte JM, Glazier JA, Stern CD. **2014**. Somites without a clock. Science 343: 791-795.

Dietrich S, Schubert FR, Healy C, Sharpe PT, Lumsden A. **1998**. Specification of the hypaxial musculature. Development 125: 2235-2249.

Dietrich S, Abou-Rebyeh F, Brohmann H, Bladt F, Sonnenberg-Riethmacher E, Yamaai T, Lumsden A, Brand-Saberi B, Birchmeier C. **1999**. The role of SF/HGF and c-Met in the development of skeletal muscle. Development 126: 1621-1629.

Draetta G, Luca F, Westendorf J, Brizuela L, Ruderman J, Beach D. **1989**. Cdc2 protein kinase is complexed with both cyclin A and B: evidence for proteolytic inactivation of MPF. Cell 56: 829-838.

Duband JL, Dufour S, Hatta K, Takeichi M, Edelman GM, Thiery JP. **1987**. Adhesion molecules during somitogenesis in the avian embryo. J Cell Biol 104: 1361-1374.

Dumont NA, Wang YX, von Maltzahn J, Pasut A, Bentzinger CF, Brun CE, Rudnicki MA. **2015**. Dystrophin expression in muscle stem cells regulates their polarity and asymmetric division. Nat Med 21: 1455-1463.

el-Deiry WS, Tokino T, Velculescu VE, Levy DB, Parsons R, Trent JM, Lin D, Mercer WE, Kinzler KW, Vogelstein B. **1993**. WAF1, a potential mediator of p53 tumor suppression. Cell 75: 817-825.

Epstein JA, Shapiro DN, Cheng J, Lam PY, Maas RL. **1996**. Pax3 modulates expression of the c-Met receptor during limb muscle development. Proc Natl Acad Sci USA 93: 4213-4218.

Erickson S, Sangfelt O, Heyman M, Castro J, Einhorn S, Grandér D. **1998**. Involvement of the Ink4 proteins p16 and p15 in T-lymphocyte senescence. Oncogene 17: 595-602.

Esteves de Lima J, Bonnin MA, Bourgeois A, Parisi A, Le Grand F, Duprez D. **2014**. Specific pattern of cell cycle during limb fetal myogenesis. Dev Biol 392: 308-323.

Fiaschi-Taesch NM, Kleinberger JW, Salim FG, Troxell R, Wills R, Tanwir M, Casinelli G, Cox AE, Takane KK, Srinivas H, Scott DK, Stewart AF. **2013**. Cytoplasmic-nuclear trafficking of G1/S cell cycle molecules and adult human β-cell replication: a revised model of human β-cell G1/S control. Diabetes 62: 2460-2470.

Figliola R, Maione R. **2004**. MyoD induces the expression of p57Kip2 in cells lacking p21Cip1/Waf1: overlapping and distinct functions of the two cdk inhibitors. J Cell Physiol 200: 468-475.

Figliola R, Busanello A, Vaccarello G, Maione R. **2008**. Regulation of p57(KIP2) during muscle differentiation: role of Egr1, Sp1 and DNA hypomethylation. J Mol Biol 380: 265-277.

Firpo EJ, Koff A, Solomon MJ, Roberts JM. **1994**. Inactivation of a Cdk2 inhibitor during interleukin 2-induced proliferation of human T lymphocytes. Mol Cell Biol 14: 4889-4901.

Flemington EK, Speck SH, Kaelin WG Jr. **1993**. E2F-1-mediated transactivation is inhibited by complex formation with the retinoblastoma susceptibility gene product. Proc Natl Acad Sci USA 90: 6914-6918.

Franklin DS, Xiong Y. **1996**. Induction of p18INK4c and its predominant association with CDK4 and CDK6 during myogenic differentiation. Mol Biol Cell 7: 1587-1599.

Fukada S, Higuchi S, Segawa M, Koda K, Yamamoto Y, Tsujikawa K, Kohama Y, Uezumi A, Imamura M, Miyagoe-Suzuki Y, Takeda S, Yamamoto H. **2004**. Purification and cell-surface marker characterization of quiescent satellite cells from murine skeletal muscle by a novel monoclonal antibody. Exp Cell Res 296: 245-255.

Fukada S, Uezumi A, Ikemoto M, Masuda S, Segawa M, Tanimura N, Yamamoto H, Miyagoe-Suzuki Y, Takeda S. **2007**. Molecular signature of quiescent satellite cells in adult skeletal muscle. Stem Cells 25: 2448-2459.

Furutachi S, Matsumoto A, Nakayama KI, Gotoh Y. **2013**. p57 controls adult neural stem cell quiescence and modulates the pace of lifelong neurogenesis. EMBO J 32: 970-981.

Gagrica S, Brookes S, Anderton E, Rowe J, Peters G. **2012**. Contrasting behavior of the p18INK4c and p16INK4a tumor suppressors in both replicative and oncogene-induced senescence. Cancer Res 72: 165-175.

Galea CA, Wang Y, Sivakolundu SG, Kriwacki RW. **2008**. Regulation of cell division by intrinsically unstructured proteins: intrinsic flexibility, modularity, and signaling conduits. Biochemistry 47: 7598-7609.

Gallant P, Fry AM, Nigg EA. **1995**. Protein kinases in the control of mitosis: focus on nucleocytoplasmic trafficking. J Cell Sci Suppl 19: 21-28.

García-Fernández RA, García-Palencia P, Suarez C, Sánchez MA, Gil-Gómez G, Sánchez B, Rollán E, Martín-Caballero J, Flores JM. **2014**. Cooperative role between p21cip1/waf1 and p27kip1 in premature senescence in glandular proliferative lesions in mice. Histol Histopathol 29: 397-406.

García-Prat L, Martínez-Vicente M, Perdiguero E, Ortet L, Rodríguez-Ubreva J, Rebollo E, Ruiz-Bonilla V, Gutarra S, Ballestar E, Serrano AL, Sandri M, Muñoz-Cánoves P. **2016**. Autophagy maintains stemness by preventing senescence. Nature 529: 37-42.

Gaubatz S, Lindeman GJ, Ishida S, Jakoi L, Nevins JR, Livingston DM, Rempel RE. **2000**. E2F4 and E2F5 play an essential role in pocket protein-mediated G1 control. Mol Cell 6: 729-735.

Gayraud-Morel B, Chrétien F, Flamant P, Gomès D, Zammit PS, Tajbakhsh S. **2007**. A role for the myogenic determination gene Myf5 in adult regenerative myogenesis. Dev Biol 312: 13-28.

Gensch N, Borchardt T, Schneider A, Riethmacher D, Braun T. **2008**. Different autonomous myogenic cell populations revealed by ablation of Myf5-expressing cells during mouse embryogenesis. Development 135: 1597-1604.

Georgia S, Soliz R, Li M, Zhang P, Bhushan A. **2006**. p57 and Hes1 coordinate cell cycle exit with self-renewal of pancreatic progenitors. Dev Biol 298: 22-31.

Gilbert PM, Havenstrite KL, Magnusson KE, Sacco A, Leonardi NA, Kraft P, Nguyen NK, Thrun S, Lutolf MP, Blau HM. **2010**. Substrate elasticity regulates skeletal muscle stem cell self-renewal in culture. Science 329: 1078-1081.

Gill RM, Hamel PA. **2000**. Subcellular compartmentalization of E2F family members is required for maintenance of the postmitotic state in terminally differentiated muscle. J Cell Biol 148: 1187-1201.

Giordani J, Bajard L, Demignon J, Daubas P, Buckingham M, Maire P. **2007**. Six proteins regulate the activation of Myf5 expression in embryonic mouse limbs. Proc Natl Acad Sci USA 104: 11310-11315.

Giovannini C, Gramantieri L, Minguzzi M, Fornari F, Chieco P, Grazi GL, Bolondi L. **2012**. CDKN1C/P57 is regulated by the Notch target gene Hes1 and induces senescence in human hepatocellular carcinoma. Am J Pathol 181: 413-422.

Gnocchi VF, White RB, Ono Y, Ellis JA, Zammit PS. **2009**. Further characterisation of the molecular signature of quiescent and activated mouse muscle satellite cells. PLoS One 4: e5205.

Goodrich DW, Wang NP, Qian YW, Lee EY, Lee WH. **1991**. The retinoblastoma gene product regulates progression through the G1 phase of the cell cycle. Cell 67: 293-302.

Gonzalez S, Perez-Perez MM, Hernando E, Serrano M, Cordon-Cardo C. **2005**. p73beta-mediated apoptosis requires p57Kip2 induction and IEX-1 inhibition. Cancer Res 65: 2186-2192.

González N, Moresco JJ, Cabezas F, de la Vega E, Bustos F, Yates JR 3rd, Olguín HC. **2016**. Ck2-dependent phosphorylation is required to maintain Pax7 protein levels in proliferating muscle progenitors. PLos One 11: e0154919.

Grifone R, Demignon J, Houbron C, Souil E, Niro C, Seller MJ, Hamard G, Maire P. **2005**. Six1 and Six4 homeoproteins are required for Pax3 and Mrf expression during myogenesis in the mouse embryo. Development 139: 2235-2249.

Grifone R, Demignon J, Giordani J, Niro C, Souil E, Bertin F, Laclef C, Xu PX, Maire P. **2007**. Eya1 and Eya2 proteins are required for hypaxial somitic myogenesis in the mouse embryo. Dev Biol 302: 602-616.

Gros J, Scaal M, Marcelle C. **2004**. A two-step mechanism for myotome formation in chick. Dev Cell 6: 875-882.

Gros J, Manceau M, Thomé V, Marcelle C. **2005**. A common somitic origin for embryonic muscle progenitors and satellite cells. Nature 435: 954-958.

Gross MK, Moran-Rivard L, Velasquez T, Nakatsu MN, Jagla K, Goulding M. **2000**. Lbx1 is required for muscle precursor migration along a lateral pathway into the limb. Development 127: 413-424.

Grounds MD, Garrett KL, Lai MC, Wright WE, Beilharz MW. **1992**. Identification of skeletal muscle precursor cells *in vivo* by use of MyoD1 and myogenin probes. Cell Tissue Res 267: 99-104.

Grounds MD, Shavlakadze T. **2011**. Growing muscle has different sarcolemmal properties from adult muscle: a proposal with scientific and clinical implications: reasons to reassess skeletal muscle molecular dynamics, cellular responses and suitability of experimental models of muscle disorders. Bioessays 33: 458-468.

Grounds MD. **2014**. The need to more precisely define aspects of skeletal muscle regeneration. Int J Biochem Cell Biol 56: 56-65.

Gu W, Schneider JW, Condorelli G, Kaushal S, Mahdavi V, Nadal-Ginard B. **1993a**. Interaction of myogenic factors and the retinoblastoma protein mediates muscle cell commitment and differentiation. Cell 72: 309-324.

Gu Y, Turck CW, Morgan DO. **1993b**. Inhibition of CDK2 activity *in vivo* by an associated 20K regulatory subunit. Nature 36: 707-710.

Guan K, Jenkins CW, Li Y, Nichols MA, Wu X, O'Keefe CL, Matera AG, Xiong Y. **1994**. Growth suppression by p18, a $p16^{INK4/MTS1}$ and $p14^{INK4B/MTS2}$-related CDK6 inhibitor, correlates with wild-type pRb function. Genes Dev 8: 2939-2952.

Guasconi V, Pritchard LL, Fritsch L, Mesner LD, Francastel C, Harel-Bellan A, Ait-Si-Ali S. **2010**. Preferential association of irreversibly silenced E2F-target genes with pericentromeric heterochromatin in differentiated muscle cells. Epigenetics 5: 704-709.

Günther S, Kim J, Kostin S, Lepper C, Fan CM, Braun T. **2013**. Myf5-positive satellite cells contribute to Pax7-dependent long-term maintenance of adult muscle stem cells. Cell Stem Cell 13: 590-601.

Guo K, Wang J, Andrés V, Smith RC, Walsh K. **1995**. MyoD-induced expression of p21 inhibits cyclin-dependent kinase activity upon myocyte terminal differentiation. Mol Cell Biol 15: 3823-3829.

Guo H, Tian T, Nan K, Wang W. **2010**. p57: A multifunctional protein in cancer (Review). Int J Oncol 36: 1321-1329.

Guo S, Liu M, Gonzalez-Perez RR. **2011a**. Role of Notch and its oncogenic signaling crosstalk in breast cancer. Biochim Biophys Acta 1815: 197-213.

Guo H, Lv Y, Tian T, Hu TH, Wang WJ, Sui X, Jiang L, Ruan ZP, Nan KJ. **2011b**. Downregulation of p57 accelerates the growth and invasion of hepatocellular carcinoma. Carcinogenesis 32: 1897-1904.

Guo H, Li Y, Tian T, Han L, Ruan Z, Liang X, Wang W, Nan K. **2015**. The role of cytoplasmic p57 in invasion of hepatocellular carcinoma. BMC Gastroenterol 15: 104.

Guruharsha KG, Kankel MW, Artavanis-Tsakonas S. **2012**. The Notch signalling system: recent insights into the complexity of a conserved pathway. Nat Rev Genet 13: 654-666.

Gurung R, Parnaik VK. **2012**. Cyclin D3 promotes myogenic differentiation and Pax7 transcription. J Cell Biochem 113: 209-219.

Haizlip KM, Harrison BC, Leinwand LA. **2015**. Sex-based differences in skeletal muscle kinetics and fiber-type composition. Physiology (Bethesda) 30: 30-39.

Haldar M, Karan G, Tvrdik P, Capecchi MR. **2008**. Two cell lineages, myf5 and myf5-independent, participate in mouse skeletal myogenesis. Dev Cell 14: 437-445.

Halevy O, Novitch BG, Spicer DB, Skapek SX, Rhee J, Hannon GJ, Beach D, Lassar AB. **1995**. Correlation of terminal cell cycle arrest of skeletal muscle with induction of p21 by MyoD. Science 267: 1018-1021.

Hannon GJ, Beach D. **1994**. p15INK4B is a potential effector of TGF-beta-induced cell cycle arrest. Nature 371: 257-261.

Hardy D, Besnard A, Latil M, Jouvion G, Briand D, Thépenier C, Pascal Q, Guguin A, Gayraud-Morel B, Cavaillon JM, Tajbakhsh S, Rocheteau P, Chrétien F. **2016**. Comparative study of injury models for studying muscle regeneration in mice. PLoS One 11: e0147198.

Harel I, Nathan E, Tirosh-Finkel L, Zigdon H, Guimarães-Camboa N, Evans SM, Tzahor E. **2009**. Distinct origins and genetic programs of head muscle satellite cells. Dev Cell 16: 822-832.

Harper JW, Adami GR, Wei N, Keyomarsi K, Elledge SJ. **1993**. The p21 Cdk-interacting protein Cip1 is a potent inhibitor of G1 cyclin-dependent kinases. Cell 75: 805-816.

Harper JW, Elledge SJ, Keyomarsi K, Dynlacht B, Tsai LH, Zhang P, Dobrowolski S, Bai C, Connell-Crowley L, Swindell E, Fox MP, Wei N. **1995**. Inhibition of cyclin-dependent kinases by p21. Mol Biol Cell 6: 387-400.

Hashimoto Y, Kohri K, Kaneko Y, Morisaki H, Kato T, Ikeda K, Nakanishi M. **1998**. Critical role for the 3_{10} helix region of p57(Kip2) in cyclin-dependent kinase 2 inhibition and growth suppression. J Biol Chem 273: 16544-16550.

Hasty P, Bradley A, Morris JH, Edmondson DG, Venuti JM, Olson EN, Klein WH. **1993**. Muscle deficiency and neonatal death in mice with a targeted mutation in the myogenin gene. Nature 364: 501-506.

Hatada I, Mukai T. **1995**. Genomic imprinting of p57KIP2, a cyclin-dependent kinase inhibitor, in mouse. Nat Genet 11: 204-206.

Hawke TJ, Meeson AP, Jiang N, Graham S, Hutcheson K, DiMaio JM, Garry DJ. **2003**. p21 is essential for normal myogenic progenitor cell function in regenerating skeletal muscle. Am J Physiol Cell Physiol 285: C1019-C1027.

Helin K, Harlow E, Fattaey A. **1993**. Inhibition of E2F-1 transactivation by direct binding of the retinoblastoma protein. Mol Cell Biol 13: 6501-6508.

Hernandez Tejada FN, Galvez Silva JR, Zweidler-McKay PA. **2014**. The challenge of targeting notch in hematologic malignancies. Front Pediatr 2: 54.

Hiebert SW, Lipp M, Nevins JR. **1989**. E1A-dependent trans-activation of the human MYC promoter is mediated by the E2F factor. Proc Natl Acad Sci USA 86: 3594-3598.

Hinterberger TJ, Sassoon DA, Rhodes SJ, Konieczny SF. **1991**. Expression of the muscle regulatory factor MRF4 during somite and skeletal myofiber development. Dev Biol 147: 144-156.

Hirai H, Roussel MF, Kato JY, Ashmun RA, Sherr C. **1995**. Novel INK4 proteins, p19 and p18, are specific inhibitors of the cyclin dependent kinases Cdk4 and Cdk6. Mol Cell Biol 15: 2672-2881.

Hirsinger E, Malapert P, Dubrulle J, Delfini MC, Duprez D, Henrique D, Ish-Horowicz D, Pourquié O. **2001**. Notch signalling acts in postmitotic avian myogenic cells to control MyoD activation. Development 128: 107-116.

Hori K, Sen A, Artavanis-Tsakonas S. **2013**. Notch signaling at a glance. J Cell Sci 126: 2135-2140.

Horikawa K, Ishimatsu K, Yoshimoto E, Kondo S, Takeda H. **2006**. Noise-resistant and synchronized oscillation of the segmentation clock. Nature 441: 719-723.

Hu T, Guo H, Wang W, Yu S, Han L, Jiang L, Ma J, Yang C, Guo Q, Nan K. **2013**. Loss of p57 expression and RhoA overexpression are associated with poor survival of patients with hepatocellular carcinoma. Oncol Rep 30: 1707-1714.

Huang HJ, Yee JK, Shew JY, Chen PL, Bookstein R, Friedmann T, Lee EY, Lee WH. **1988**. Suppression of the neoplastic phenotype by replacement of the RB gene in human cancer cells. Science 242: 1563-1566.

Hubaud A, Pourquié O. **2014**. Signalling dynamics in vertebrate segmentation. Nat Rev Mol Cell Biol 15: 709-712.

Huh MS, Parker MH, Scimè A, Parks R, Rudnicki MA. **2004**. Rb is required for progression through myogenic differentiation but not maintenance of terminal differentiation. J Cell Biol 166: 865-876.

Hwang CY, Lee C, Kwon KS. **2009**. Extracellular signal-regulated kinase 2-dependent phosphorylation induces cytoplasmic localization and degradation of p21Cip1. Mol Cell Biol 29: 3379-3389.

Iso T, Kedes L, Hamamori Y. **2003**. HES and HERP families: multiple effectors of the Notch signaling pathway. J Cell Physiol 194: 237-255.

Jaafar Marican NH, Cruz-Migoni SB, Borycki AG. **2016**. Asymmetric distribution of primary cilia allocates satellite cells for self-renewal. Stem Cell Reports doi: 10.1016 [Epub ahead of print]

Jagla K, Dollé P, Mattei MG, Jagla T, Schuhbaur B, Dretzen G, Bellard F, Bellard M. **1995**. Mouse Lbx1 and human LBX1 define a novel mammalian homeobox gene family related to the Drosophila lady bird genes. Mech Dev 53: 345-356.

Jin RJ, Lho Y, Wang Y, Ao M, Revelo MP, Hayward SW, Wills ML, Logan SK, Zhang P, Matusik RJ. **2008**. Down-regulation of p57Kip2 induces prostate cancer in the mouse. Cancer Res 68: 3601-3608.

Julian LM, Blais A. **2015**. Transcriptional control of stem cell fate by E2Fs and pocket proteins. Front Genet 6: Article 161.

Kablar B, Krastel K, Ying C, Asakura A, Tapscott SJ, Rudnicki MA. **1997**. MyoD and Myf-5 differentially regulate the development of limb versus trunk skeletal muscle. Development 124: 4729-4738.

Kablar B, Asakura A, Krastel K, Ying C, May LL, Goldhamer DJ, Rudnicki MA. **1998**. MyoD and Myf-5 define the specification of musculature of distinct embryonic origin. Biochem Cell Biol 76: 1079-1091.

Kalcheim C, Ben-Yair R. **2005**. Cell rearrangements during development of the somite and its derivatives. Curr Opin Genet Dev 15: 371-380.

Kassar-Duchossoy L, Gayraud-Morel B, Gomès D, Rocancourt D, Buckingham M, Shinin V, Tajbakhsh S. **2004**. Mrf4 determines skeletal muscle identity in Myf5:Myod double-mutant mice. Nature 431: 466-471.

Kassar-Duchossoy L, Giacone E, Gayraud-Morel B, Jory A, Gomès D, Tajbakhsh S. **2005**. Pax3/Pax7 mark a novel population of primitive myogenic cells during development. Genes Dev 19: 1426-1431.

Kato K, Gurdon JB. **1993**. Single-cell transplantation determines the time when Xenopus muscle precursor cells acquire a capacity for autonomous differentiation. Proc Natl Acad Sci USA 90: 1310-1314.

Katz B. **1961**. The terminations of the afferent nerve fibre in the muscle spindle of the frog. Phil Trans R Soc Lond Biol 243: 221-240.

Kavanagh E, Joseph B. **2011**. The hallmarks of CDKN1C (p57, KIP2) in cancer. Biochim Biophys Acta 1816: 50-56.

Kavanagh E, Vlachos P, Emourgeon V, Rodhe J, Joseph B. **2012**. p57(KIP2) control of actin cytoskeleton dynamics is responsible for its mitochondrial pro-apoptotic effect. Cell Death Dis 3: e311.

Keefe AC, Lawson JA, Flygare SD, Fox ZD, Colasanto MP, Mathew SJ, Yandell M, Kardon G. **2015**. Muscle stem cells contribute to myofibres in sedentary adult mice. Nat Commun 6: 7087.

Khabar KS. **2016**. Hallmarks of cancer and AU-rich elements. Wiley Interdiscip Rev RNA. doi: 10.1002 [Epub ahead of print]

Kharraz Y, Guerra J, Mann CJ, Serrano AL, Muñoz-Cánoves P. **2013**. Macrophage plasticity and the role of inflammation in skeletal muscle repair. Mediators Inflamm 2013: 491497.

Kiess M, Gill RM, Hamel PA. **1995**. Expression and activity of the retinoblastoma protein (pRB)-family proteins, p107 and p130, during L6 myoblast differentiation. Cell Growth Differ 6: 1287-1298.

Kishimoto T, Okumura E. **1997**. *In vivo* regulation of the entry into M-phase: initial activation and nuclear translocation of cyclin B/Cdc2. Prog Cell Cycle Res 3: 241-249.

Kitamoto T, Hanaoka K. **2010**. Notch3 null mutation in mice causes muscle hyperplasia by repetitive muscle regeneration. Stem Cells 28: 2205-2216.

Knapp JR, Davie JK, Myer A, Meadows E, Olson EN, Klein WH. **2006**. Loss of myogenin in postnatal life leads to normal skeletal muscle but reduced body size. Development 133: 601-610.

Kobayashi H, Stewart E, Poon R, Adamczewski JP, Gannon J, Hunt T. **1992**. Identification of the domains in cyclin A required for binding to, and activation of, p34cdc2 and p32cdk2 protein kinase subunits. Mol Biol Cell 3: 1279-1294.

Konstantinides N, Averof M. **2014**. A common cellular basis for muscle regeneration in arthropods and vertebrates. Science 343: 788-791.

Korzelius J, The I, Ruijtenberg S, Prinsen MB, Portegijs V, Middelkoop TC, Groot Koerkamp MJ, Holstege FC, Boxem M, van den Heuvel S. **2011**. *Caenorhabditis elegans* cyclin D/CDK4 and cyclin E/CDK2 induce distinct cell cycle re-entry programs in differentiated muscle cells. PLoS Genet 7: e1002362.

Krishnan VS, White Z, McMahon CD, Hodgetts SI, Fitzgerald M, Shavlakadze T, Harvey AR, Grounds MD. **2016**. A Neurogenic Perspective of Sarcopenia: Time Course Study of Sciatic Nerves From Aging Mice. J Neuropathol Exp Neurol 75: 464-478.

Kriwacki RW, Hengst L, Tennant L, Reed SI, Wright PE. **1996**. Structural studies of p21Waf1/Cip1/Sdi1 in the free and Cdk2-bound state: conformational disorder mediates binding diversity. Proc Natl Acad Sci USA 93: 11504-11509.

Kuang S, Chargé SB, Seale P, Huh M, Rudnicki MA. **2006**. Distinct roles for Pax7 and Pax3 in adult regenerative myogenesis. J Cell Biol 172: 103-113.

Kuang S, Kuroda K, Le Grand F, Rudnicki MA. **2007a**. Asymmetric self-renewal and commitment of satellite stem cells in muscle. Cell 129: 999-1010.

Kuang SQ, Ling X, Sanchez-Gonzalez B, Yang H, ANdreeff M, Garcia-Manero G. **2007b**. Differential tumor suppressor properties and transforming growth factor-beta responsiveness of p57KIP2 in leukemia cells with aberrant p57KIP2 promoter DNA methylation. Oncogene 26: 1439-1448.

Kuroda K, Tani S, Tamura K, Minoguchi S, Kurooka H, Honjo T. **1999**. Delta-induced Notch signaling mediated by RBP-J inhibits MyoD expression and myogenesis. J Biol Chem 274: 7238-7244.

LaBaer J, Garrett MD, Stevenson LF, Slingerland JM, Sandhu C, Chou HS, Fattaey A, Harlow E. **1997**. New functional activities for the p21 family of CDK inhibitors. Genes Dev 11: 847-862.

Lacy ER, Filippov I, Lewis WS, Otieno S, Xiao L, Weiss S, Hengst L, Kriwacki RW. **2004**. p27 binds cyclin-CDK complexes through a sequential mechanism involving binding-induced protein folding. Nat Struct Mol Biol 11: 358-364.

Latella L, Sacco A, Pajalunga D, Tiainen M, Macera D, D'Angelo M, Felici A, Sacchi A, Crescenzi M. **2001**. Reconstitution of cyclin D1-associated kinase activity drives terminally differentiated cells into the cell cycle. Mol Cell Biol 21: 5631-5643.

Lazaro JB, Bailey PJ, Lassar AB. **2002**. Cyclin D-cdk4 activity modulates the subnuclear localization and interaction of MEF2 with SRC-family coactivators during skeletal muscle differentiation. Genes Dev 16: 1792-1805.

Le Grand F, Jones AE, Seale V, Scimè A, Rudnicki MA. **2009**. Wnt7a activates the planar cell polarity pathway to drive the symmetric expansion of satellite stem cells. Cell Stem Cell 4: 535-547.

Le Roux I, Konge J1, Le Cam L2, Flamant P3, Tajbakhsh S1. **2015**. Numb is required to prevent p53-dependent senescence following skeletal muscle injury. Nat Commun 6: 8528.

LeCouter JE, Kablar B, Whyte PF, Ying C, Rudnicki MA. **1998**. Strain-dependent embryonic lethality in mice lacking the retinoblastoma-related p130 gene. Development 125: 4669-4679.

Lee MH, Reynisdóttir I, Massagué J. **1995**. Cloning of p57KIP2, a cyclin-dependent kinase inhibitor with unique domain structure and tissue distribution. Genes Dev 9: 639-649.

Lee MH, Williams BO, Mulligan G, Mukai S, Bronson RT, Dyson N, Harlow E, Jacks T. **1996**. Targeted disruption of p107: functional overlap between p107 and Rb. Genes Dev 10: 1621-1632.

Lee AS, Anderson JE, Joya JE, Head SI, Pather N, Kee AJ, Gunning PW, Hardeman EC. **2013**. Aged skeletal muscle retains the ability to fully regenerate functional architecture. Bioarchitecture 3: 25-37.

Lees EM, Harlow E. **1993**. Sequences within the conserved cyclin box of human cyclin A are sufficient for binding to and activation of cdc2 kinase. Mol Cell Biol 13:1194-1201.

Lepper C, Conway SJ, Fan CM. **2009**. Adult satellite cells and embryonic muscle progenitors have distinct genetic requirements. Nature 460: 627-631.

Lepper C, Partridge TA, Fan CM. **2011**. An absolute requirement for Pax7-positive satellite cells in acute injury-induced skeletal muscle regeneration. Development 138: 3639-3646.

Li R, Waga S, Hannon GJ, Beach D, Stillman B. 1994. Differential effects by the p21 CDK inhibitor on PCNA-dependent DNA replication and repair. Nature 371: 534-537.

Li FX, Zhu JW, Hogan CJ, DeGregori J. **2003**. Defective gene expression, S phase progression, and maturation during hematopoiesis in E2F1/E2F2 mutant mice. Mol Cell Biol 23: 3607-3622.

Li S, Li J, Tian J, Dong R, Wei J, Qiu X, Jiang C. **2012**. Characterization, tissue expression, and imprinting analysis of the porcine CDKN1C and NAP1L4 genes. J Biomed Biotechnol 2012: 946527.

Li J, Han S, Cousin W, Conboy IM. **2015**. Age-specific functional epigenetic changes in p21 and p16 in injury-activated satellite cells. Stem Cells 33: 951-961.

Lin SC, Skapek SX, Lee EY. **1996**. Genes in the RB pathway and their knockout in mice. Semin Cancer Biol 7: 279-289.

Linask KK, Ludwig C, Han MD, Liu X, Radice GL, Knudsen KA. **1998**. N-cadherin/catenin-mediated morphoregulation of somite formation. Dev Biol 202: 85-102.

Liu Y, Martindale JL, Gorospe M, Holbrook NJ. **1996**. Regulation of p21WAF1/CIP1 expression through mitogen-activated protein kinase signaling pathway. Cancer Res 56: 31-35.

Liu QC, Zha XH, Faralli H, Yin H, Louis-Jeune C, Perdiguero E, Pranckeviciene E, Muñoz-Cànoves P, Rudnicki MA, Brand M, Perez-Iratxeta C, Dilworth FJ. **2012**. Comparative expression profiling identifies differential roles for Myogenin and p38α MAPK signaling in myogenesis. J Mol Cell Biol 4: 386-397.

Liu J, Liang X, Gan Z. **2015**. Transcriptional regulatory circuits controlling muscle fiber type switching. Sci China Life Sci 58: 321-327.

Lu Z, Hunter T. **2010**. Ubiquitylation and proteasomal degradation of the p21(Cip1), p27(Kip1) and p57(Kip2) CDK inhibitors. Cell Cycle 9: 2342-2352.

Luna VM, Daikoku E, Ono F. **2015**. "Slow" skeletal muscles across vertebrate species. Cell Biosci 5: 62.

Macleod KF, Sherry N, Hannon G, Beach D, Tokino T, Kinzler K, Vogelstein B, Jacks T. **1995**. p53-dependent and independent expression of p21 during cell growth, differentiation, and DNA damage. Genes Dev 9: 935-944.

Mademtzoglou D, Alonso-Martin S, Chang T, Bismuth K, Drayton B, Aurade F, Relaix F. A p57 conditional mutant allele that allows tracking of p57-expressing and mutant cells. Submitted-1

Mademtzoglou D, Alonso-Martin S, Mourikis P, Relaix F. Distinct regulation of p21 and p57 function during muscle stem cell activation and differentiation. Submitted-2

Maina F, Casagranda F, Audero E, Simeone A, Comoglio PM, Klein R, Ponzetto C. **1996**. Uncoupling of Grb2 from the Met receptor *in vivo* reveals complex roles in muscle development. Cell 87: 531-542.

Mal A, Chattopadhyay D, Ghosh MK, Poon RY, Hunter T, Harter ML. **2000**. p21 and retinoblastoma protein control the absence of DNA replication in terminally differentiated muscle cells. J Cell Biol 149: 281-292.

Mallo M. **2016**. Revisiting the involvement of signaling gradients in somitogenesis. FEBS J 283: 1430-1437.

Malumbres M. **2014**. Cyclin-dependent kinases. Genome Biol 15: 122-132.

Mansouri A, Stoykova A, Torres M, Gruss P. **1996**. Dysgenesis of cephalic neural crest derivatives in Pax7-/- mutant mice. Development 122: 831-838.

Marg A, Escobar H, Gloy S, Kufeld M, Zacher J, Spuler A, Birchmeier C, Izsvák Z, Spuler S. **2014**. Human satellite cells have regenerative capacity and are genetically manipulable. J Clin Invest 124: 4257-4265.

Maroto M, Iimura T, Dale JK, Bessho Y. **2008**. BHLH proteins and their role in somitogenesis. Adv Exp Med Biol 638: 124-139.

Martelli F, Cenciarelli C, Santarelli G, Polikar B, Felsani A, Caruso M. **1994**. MyoD induces retinoblastoma gene expression during myogenic differentiation. Oncogene 9: 3579-3590.

Matsumoto A, Takeishi S, Kanie T, Susaki E, Onoyama I, Tateishi Y, Nakayama K, Nakayama KI. **2011**. p57 is required for quiescence and maintenance of adult hematopoietic stem cells. Cell Stem Cell 9: 262-271.

Matsuoka S, Edwards MC, Bai C, Parker S, Zhang P, Baldini A, Harper JW, Elledge SJ. **1995**. p57KIP2, a structurally distinct member of the p21CIP1 Cdk inhibitor family, is a candidate tumor suppressor gene. Genes Dev 9: 650-662.

Matsuoka S, Thompson JS, Edwards MC, Bartletta JM, Grundy P, Kalikin LM, Harper JW, Elledge SJ, Feinberg AP. **1996**. Imprinting of the gene encoding a human cyclin-dependent kinase inhibitor, p57KIP2, on chromosome 11p15. Proc Natl Acad Sci USA 93: 3026-3030.

Mauro A. **1961**. Satellite cell of skeletal muscle fibers. J Biophys Biochem Cytol 9: 493-495.

Mayeuf A, Relaix F. **2011**. La voie Notch: Du développement à la régénération du muscle squelettique. Med Sci 27: 521-526.

Mayeuf-Louchart A, Lagha M, Danckaert A, Rocancourt D, Relaix F, Vincent SD, Buckingham M. **2014**. Notch regulation of myogenic versus endothelial fates of cells that migrate from the somite to the limb. Proc Natl Acad Sci USA 111: 8844-8849.

McCarthy JJ, Mula J, Miyazaki M, Erfani R, Garrison K, Farooqui AB, Srikuea R, Lawson BA, Grimes B, Keller C, Van Zant G, Campbell KS, Esser KA, Dupont-Versteegden EE, Peterson CA. **2011**. Effective fiber hypertrophy in satellite cell-depleted skeletal muscle. Development 138: 3657-3666.

McLoon LK, Rowe J, Wirtschafter J, McCormick KM. **2004**. Continuous myofiber remodeling in uninjured extraocular myofibers: myonuclear turnover and evidence for apoptosis. Muscle Nerve 29: 707-715.

Meadows E, Cho JH, Flynn JM, Klein WH. **2008**. Myogenin regulates a distinct genetic program in adult muscle stem cells. Dev Biol 322: 406-414.

Megeney LA, Kablar B, Garrett K, Anderson JE, Rudnicki MA. **1996**. MyoD is required for myogenic stem cell function in adult skeletal muscle. Genes Dev 10: 1173-1183.

Mennerich D, Schäfer K, Braun T. **1998**. Pax-3 is necessary but not sufficient for lbx1 expression in myogenic precursor cells of the limb. Mech Dev 73: 147-158.

Messina G, Blasi C, La Rocca SA, Pompili M, Calconi A, Grossi M. **2005**. p27Kip1 acts downstream of N-cadherin-mediated cell adhesion to promote myogenesis beyond cell cycle regulation. Mol Biol Cell 16: 1469-1480.

Michaely P, Bennett V. **1992**. The ANK repeat: a ubiquitous motif involved in macromolecular recognition. Trends Cell Biol 2: 127-129.

Michailovici I, Harrington HA, Azogui HH, Yahalom-Ronen Y, Plotnikov A, Ching S, Stumpf MP, Klein OD, Seger R, Tzahor E. **2014**. Nuclear to cytoplasmic shuttling of ERK promotes differentiation of muscle stem/progenitor cells. Development 141: 2611-2620.

Michieli P, Chedid M, Lin D, Pierce JH, Mercer WE, Givol D. **1994**. Induction of WAF1/CIP1 by a p53-independent pathway. Cancer Res 54: 3391-3395.

Monahan P, Rybak S, Raetzman LT. **2009**. The notch target gene HES1 regulates cell cycle inhibitor expression in the developing pituitary. Endocrinology 150: 4386-4394.

Montarras D, Morgan J, Collins C, Relaix F, Zaffran S, Cumano A, Partridge T, Buckingham M. **2005**. Direct isolation of satellite cells for skeletal muscle regeneration. Science 309: 2064-2067.

Morgan DO. **1997**. Cyclin-dependent kinases: engines, clocks, and microprocessors. Annu Rev Cel Dev Biol. 13: 261-291.

Moss FP, Leblond CP. **1971**. Satellite cells as the source of nuclei in muscles of growing rats. Anat Rec 170: 421-435.

Mounier R, Chrétien F, Chazaud B. **2011**. Blood vessels and the satellite cell niche. Curr Top Dev Biol 96: 121-138.

Mourikis P, Gopalakrishnan S, Sambasivan R, Tajbakhsh S. **2012a**. Cell-autonomous Notch activity maintains the temporal specification potential of skeletal muscle stem cells. Development 139: 4536-4548.

Mourikis P, Sambasivan R, Castel D, Rocheteau P, Bizzarro V, Tajbakhsh S. **2012b**. A critical requirement for notch signaling in maintenance of the quiescent skeletal muscle stem cell state. Stem Cells 30: 243-252.

Mourikis P, Tajbakhsh S. **2014**. Distinct contextual roles for Notch signalling in skeletal muscle stem cells. BMC Dev Biol 14: 2.

Mueller PR, Coleman TR, Kumagai A, Dunphy WG. **1995**. Myt1: a membrane-associated inhibitory kinase that phosphorylates Cdc2 on both threonine-14 and tyrosine-15. Science 270: 86-90.

Müller K. **2010**. Prognostische relevanz von p53 und den mismatch repair genen MLH1 und MSH2 beim kolorektalen karzinom und deren bedeutung für den benefit einer adjuvanten therapie. Dissertation - Medizinischen Fakultät Charité – Universitätsmedizin Berlin.

Muñoz-Espín D, Cañamero M, Maraver A, Gómez-López G, Contreras J, Murillo-Cuesta S, Rodríguez-Baeza A, Varela-Nieto I, Ruberte J, Collado M, Serrano M. **2013**. Programmed cell senescence during mammalian embryonic development. Cell 155: 1104-1118.

Muñoz-Espín D, Serrano M. **2014**. Cellular senescence: from physiology to pathology. Nat Rev Mol Cell Biol 15: 482-496.

Murphy M, Kardon G. **2011**. Origin of vertebrate limb muscle: the role of progenitor and myoblast populations. Curr Top Dev Biol 96: 1-32.

Murphy MM, Lawson JA, Mathew SJ, Hutcheson DA, Kardon G. **2011**. Satellite cells, connective tissue fibroblasts and their interactions are crucial for muscle regeneration. Development 138: 3625-3637.

Musumeci G, Castrogiovanni P, Coleman R, Szychlinska MA, Salvatorelli L, Parenti R, Magro G, Imbesi R. **2015**. Somitogenesis: From somite to skeletal muscle. Acta Histochem 117: 313-328.

Nabeshima Y, Hanaoka K, Hayasaka M, Esumi E, Li S, Nonaka I, Nabeshima Y. **1993**. Myogenin gene disruption results in perinatal lethality because of severe muscle defect. Νατθρε 364¨532-535.

Nakaya Y, Kuroda S, Katagiri YT, Kaibuchi K, Takahashi Y. **2004**. Mesenchymal-epithelial transition during somitic segmentation is regulated by differential roles of Cdc42 and Rac1. Dev Cell 7: 425-438.

Nguyen KT, Holloway MP, Altura RA. **2012**. The CRM1 nuclear export protein in normal development and disease. Int J Biochem Mol Biol 3: 137-151.

Nofziger D, Miyamoto A, Lyons KM, Weinmaster G. **1999**. Notch signaling imposes two distinct blocks in the differentiation of C2C12 myoblasts. Development 126: 1689-1702.

Nourse J, Firpo E, Flanagan WM, Coats S, Polyak K, Lee MH, Massague J, Crabtree GR, Roberts JM. **1994**. Interleukin-2-mediated elimination of the p27Kip1 cyclin-dependent kinase inhibitor prevented by rapamycin. Nature 372: 570-573.

Novitch BG, Mulligan GJ, Jacks T, Lassar AB. **1996**. Skeletal muscle cells lacking the retinoblastoma protein display defects in muscle gene expression and accumulate in S and G2 phases of the cell cycle. J Cell Biol 135: 441-456.

Novitch BG, Spicer DB, Kim PS, Cheung WL, Lassar AB. **1999**. pRb is required for MEF2-dependent gene expression as well as cell-cycle arrest during skeletal muscle differentiation. Curr Biol 9: 449-459.

Nowicki JL, Burke AC. **2000**. Hox genes and morphological identity: axial versus lateral patterning in the vertebrate mesoderm. Development 127: 4265-4275.

Olguín HC, Olwin BB. **2004**. Pax-7 up-regulation inhibits myogenesis and cell cycle progression in satellite cells: a potential mechanism for self-renewal. Dev Biol 275: 375-388.

Olguín HC, Yang Z, Tapscott SJ, Olwin BB. **2007**. Reciprocal inhibition between Pax7 and muscle regulatory factors modulates myogenic cell fate determination. J Cell Biol 177: 769-779.

Olguín HC, Pisconti A. **2012**. Marking the tempo for myogenesis: Pax7 and the regulation of muscle stem cell fate decisions. J Cell Mol Med 16: 1013-1025.

Olson EN, Klein WH. **1994**. bHLH factors in muscle development: dead lines and commitments, what to leave in and what to leave out. Genes Dev 8: 1-8.

Olson EN, Arnold HH, Rigby PW, Wold BJ. **1996**. Know your neighbors: three phenotypes in null mutants of the myogenic bHLH gene MRF4. Cell 85: 1-4.

Ono Y, Boldrin L, Knopp P, Morgan JE, Zammit PS. **2010**. Muscle satellite cells are a functionally heterogeneous population in both somite-derived and branchiomeric muscles. Dev Biol 337: 29-41.

Orlando S, Gallastegui E, Besson A, Abril G, Aligué R, Pujol MJ, Bachs O. **2015**. p27Kip1 and p21Cip1 collaborate in the regulation of transcription by recruiting cyclin-Cdk complexes on the promoters of target genes. Nucleic Acids Res 43: 6860-6873.

Osborn DP, Li K, Hinits Y, Hughes SM. **2011**. Cdkn1c drives muscle differentiation through a positive feedback loop with Myod. Dev Biol 350: 464-475.

Ott MO, Bober E, Lyons G, Arnold H, Buckingham M. **1991**. Early expression of the myogenic regulatory gene, myf-5, in precursor cells of skeletal muscle in the mouse embryo. Development 111: 1097-1107.

Oustanina S, Hause G, Braun T. **2004**. Pax7 directs postnatal renewal and propagation of myogenic satellite cells but not their specification. EMBO J 23: 3430-3439.

Pagano M, Pepperkok R, Verde F, Ansorge W, Draetta G. **1992**. Cyclin A is required at two points in the human cell cycle. EMBO J 11: 961-971.

Pajcini KV, Corbel SY, Sage J, Pomerantz JH, Blau HM. **2010**. Transient inactivation of Rb and ARF yields regenerative cells from postmitotic mammalian muscle. Cell Stem Cell 7: 198-213.

Palmeirim I, Henrique D, Ish-Horowicz D, Pourquié O. **1997**. Avian hairy gene expression identifies a molecular clock linked to vertebrate segmentation and somitogenesis. Cell 91: 639-648.

Pannérec A, Marazzi G, Sassoon D. **2012**. Stem cells in the hood: the skeletal muscle niche. Trends Mol Med 18: 599-606.

Pardo-Saganta A, Tata PR, Law BM, Saez B, Chow RDz, Prabhu M, Gridley T, Rajagopal J. **2015**. Parent stem cells can serve as niches for their daughter cells. Nature 523: 597-601.

Park CW, Chung JH. **2001**. Age-dependent changes of p57(Kip2) and p21(Cip1/Waf1) expression in skeletal muscle and lung of mice. Biochim Biophys Acta 1520: 163-168.

Park HC, Boyce J, Shin J, Appel B. **2005**. Oligodendrocyte specification in zebrafish requires notch-regulated cyclin-dependent kinase inhibitor function. J Neurosci 25: 6836-6844.

Parker SB, Eichele G, Zhang P, Rawls A, Sands AT, Bradley A, Olson EN, Harper JW, Elledge SJ. **1995**. p53-independent expression of p21Cip1 in muscle and other terminally differentiating cells. Science 267: 1024-1027.

Patapoutian A, Yoon JK, Miner JH, Wang S, Stark K, Wold B. **1995**. Disruption of the mouse MRF4 gene identifies multiple waves of myogenesis in the myotome. Development 121: 3347-3358.

Pateras IS, Apostolopoulou K, Niforou K, Kotsinas A, Gorgoulis VG. **2009**. p57KIP2: "Kip"ing the cell under control. Mol Cancer Res 7: 1902-1919.

Pavletich NP. **1999**. Mechanisms of cyclin-dependent kinase regulation: structures of Cdks, their cyclin activators, and Cip and INK4 inhibitors. J Mol Biol 287: 821-828.

Pawlikowski B, Pulliam C, Betta ND, Kardon G, Olwin BB. **2015**. Pervasive satellite cell contribution to uninjured adult muscle fibers. Skelet Muscle 5: 42.

Peschiaroli A, Figliola R, Coltella L, Strom A, Valentini A, D'Agnano I, Maione R. **2002**. MyoD induces apoptosis in the absence of RB function through a p21(WAF1)-dependent re-localization of cyclin/cdk complexes to the nucleus. Oncogene 21: 8114-8127.

Phelps DE, Hsiao KM, Li Y, Hu N, Franklin DS, Westphal E, Lee EY, Xiong Y. **1998**. Coupled transcriptional and translational control of cyclin-dependent kinase inhibitor p18INK4c expression during myogenesis. Mol Cell Biol 18: 2334-2343.

Picard CA, Marcelle C. **2013**. Two distinct muscle progenitor populations coexist throughout amniote development. Dev Biol 373: 141-148.

Pippa R, Espinosa L, Gundem G, García-Escudero R, Dominguez A, Orlando S, Gallastegui E, Saiz C, Besson A, Pujol MJ, López-Bigas N, Paramio JM, Bigas A, Bachs O. **2012**. p27Kip1 represses transcription by direct interaction with p130/E2F4 at the promoters of target genes. Oncogene 31: 4207-4220.

Polyak K, Kato JY, Solomon MJ, Sherr CJ, Massague J, Roberts JM, Koff A. **1994a**. p27Kip1, a cyclin-Cdk inhibitor, links transforming growth factor-beta and contact inhibition to cell cycle arrest. Genes Dev 8: 9-22.

Polyak K, Lee MH, Erdjument-Bromage H, Koff A, Roberts JM, Tempst P, Massagué J. **1994b**. Cloning of p27Kip1, a cyclin-dependent kinase inhibitor and a potential mediator of extracellular antimitogenic signals. Cell 78: 59-66.

Pourquié O. **2001**. Vertebrate somitogenesis. Annu Rev Cell Dev Biol 17: 311-350.

Pourquié O. **2011**. Vertebrate segmentation: from cyclic gene networks to scoliosis. Cell 145: 650-663.

Puri PL, Balsano C, Burgio VL, Chirillo P, Natoli G, Ricci L, Mattei E, Graessmann A, Levrero M. **1997**. MyoD prevents cyclinA/cdk2 containing E2F complexes formation in terminally differentiated myocytes. Oncogene 14: 1171-1184.

Puri PL, Cimino L, Fulco M, Zimmerman C, La Thangue NB, Giordano A, Graessmann A, Levrero M. **1998**. Regulation of E2F4 mitogenic activity during terminal differentiation by its heterodimerization partners for nuclear translocation. Cancer Res 58: 1325-1331.

Qin XQ, Chittenden T, Livingston DM, Kaelin WG Jr. **1992**. Identification of a growth suppression domain within the retinoblastoma gene product. Genes Dev 6: 953-964.

Quelle DE, Ashmun RA, Shurtleff SA, Kato JY, Bar-Sagi D, Roussel MF, Sherr CJ. **1993**. Overexpression of mouse D-type cyclins accelerates G1 phase in rodent fibroblasts. Genes Dev 7: 1559-1571.

Rao SS, Chu C, Kohtz DS. **1994**. Ectopic expression of cyclin D1 prevents activation of gene transcription by myogenic basic helix-loop-helix regulators. Mol Cell Biol 14: 5259-5267.

Rawls A, Morris JH, Rudnicki M, Braun T, Arnold HH, Klein WH, Olson EN. **1995**. Myogenin's functions do not overlap with those of MyoD or Myf-5 during mouse embryogenesis. Dev Biol 172: 37-50.

Rawls A, Valdez MR, Zhang W, Richardson J, Klein WH, Olson EN. **1998**. Overlapping functions of the myogenic bHLH genes MRF4 and MyoD revealed in double mutant mice. Development 125: 2349-2358.

Relaix F, Polimeni M, Rocancourt D, Ponzetto C, Schäfer BW, Buckingham M. **2003**. The transcriptional activator PAX3-FKHR rescues the defects of Pax3 mutant mice but induces a myogenic gain-of-function phenotype with ligand-independent activation of Met signaling *in vivo*. Genes Dev 17: 2950-2965.

Relaix F, Rocancourt D, Mansouri A, Buckingham M. **2004**. Divergent functions of murine Pax3 and Pax7 in limb muscle development. Genes Dev 18: 1088-1105.

Relaix F, Rocancourt D, Mansouri A, Buckingham M. **2005**. A Pax3/Pax7-dependent population of skeletal muscle progenitor cells. Nature 435: 948-953.

Relaix F. **2006**. Skeletal muscle progenitor cells: from embryo to adult. Cell Mol Life Sci 63: 1221-1225.

Relaix F, Montarras D, Zaffran S, Gayraud-Morel B, Rocancourt D, Tajbakhsh S, Mansouri A, Cumano A, Buckingham M. **2006**. Pax3 and Pax7 have distinct and overlapping functions in adult muscle progenitor cells. J Cell Biol 172: 91-102.

Relaix F, Zammit PS. **2012**. Satellite cells are essential for skeletal muscle regeneration: the cell on the edge returns centre stage. Development 139: 2845-2856.

Relaix F, Demignon J, Laclef C, Pujol J, Santolini M, Niro C, Lagha M, Rocancourt D, Buckingham M, Maire P. **2013**. Six homeoproteins directly activate Myod expression in the gene regulatory networks that control early myogenesis. PLoS Genet 9: e1003425.

Resnitzky D, Reed SI. **1995**. Different roles for cyclins D1 and E in regulation of the G1-to-S transition. Mol Cell Biol 15: 3463-3469.

Reynaud EG, Pelpel K, Guillier M, Leibovitch MP, Leibovitch SA. **1999**. p57(Kip2) stabilizes the MyoD protein by inhibiting cyclin E-Cdk2 kinase activity in growing myoblasts. Mol Cell Biol 19: 7621-7629.

Reynaud EG, Guillier M, Leibovitch MP, Leibovitch SA. **2000a**. Dimerization of the amino terminal domain of p57Kip2 inhibits cyclin D1-cdk4 kinase activity. Oncogene 19: 1147-1152.

Reynaud EG, Leibovitch MP, Tintignac LA, Pelpel K, Guillier M, Leibovitch SA. **2000b**. Stabilization of MyoD by direct binding to p57(Kip2). J Biol Chem 275: 18767-18776.

Rhodes SJ, Konieczny SF. **1989**. Identification of MRF4: a new member of the muscle regulatory factor gene family. Genes Dev 3: 2050-2061.

Rios AC, Serralbo O, Salgado D, Marcelle C. **2011**. Neural crest regulates myogenesis through the transient activation of NOTCH. Nature 473: 532-535.

Rocheteau P, Gayraud-Morel B, Siegl-Cachedenier I, Blasco MA, Tajbakhsh S. **2012**. A subpopulation of adult skeletal muscle stem cells retains all template DNA strands after cell division. Cell 148: 112-125.

Rodgers JT, King KY, Brett JO, Cromie MJ, Charville GW, Maguire KK, Brunson C, Mastey N, Liu L, Tsai CR, Goodell MA, Rando TA. **2014**. mTORC1 controls the adaptive transition of quiescent stem cells from G0 to G(Alert). Nature 510: 393-396.

Rossi MN, Antonangeli F. **2015**. Cellular Response upon Stress: p57 Contribution to the Final Outcome. Mediators Inflamm 2015: 259325.

Rudnicki MA, Braun T, Hinuma S, Jaenisch R. **1992**. Inactivation of MyoD in mice leads to up-regulation of the myogenic HLH gene Myf-5 and results in apparently normal muscle development. Cell 71: 383-390.

Rudnicki MA, Schnegelsberg PN, Stead RH, Braun T, Arnold HH, Jaenisch R. **1993**. MyoD or Myf-5 is required for the formation of skeletal muscle. Cell 75: 1351-1359.

Russo AA, Jeffrey PD, Patten AK, Massagué J, Pavletich NP. **1996**. Crystal structure of the p27Kip1 cyclin-dependent-kinase inhibitor bound to the cyclin A-Cdk2 complex. Nature 382: 325-331.

Russo AA, Tong L, Lee JO, Jeffrey PD, Pavletich NP. **1998**. Structural basis for inhibition of the cyclin-dependent kinase Cdk6 by the tumour suppressor p16INK4a. Nature 395: 237-243.

Saab R, Bills JL, Miceli AP, Anderson CM, Khoury JD, Fry DW, Navid F, Houghton PJ, Skapek SX. **2006**. Pharmacologic inhibition of cyclin-dependent kinase 4/6 activity arrests proliferation in myoblasts and rhabdomyosarcoma-derived cells. Mol Cancer Ther 5: 1299-1308.

Saga Y. **2012**. The mechanism of somite formation in mice. Curr Opin Genet Dev 22: 331-338.

Sambasivan R, Yao R, Kissenpfennig A, Van Wittenberghe L, Paldi A, Gayraud-Morel B, Guenou H, Malissen B, Tajbakhsh S, Galy A. **2011**. Pax7-expressing satellite cells are indispensable for adult skeletal muscle regeneration. Development 138: 3647-3456.

Samuelsson MKR, Pazirandeh A, Okret S. **2002**. A proapoptotic effect of theCDK inhibitor p57kip2 on staurosporineinduced apoptosis in HeLa cells. Biochem Biophys Res Commun 296: 702-709.

Sassoon D, Lyons G, Wright WE, Lin V, Lassar A, Weintraub H, Buckingham M. **1989**. Expression of two myogenic regulatory factors myogenin and MyoD1 during mouse embryogenesis. Nature 341: 303-307.

Scaal M, Christ B. **2004**. Formation and differentiation of the avian dermomyotome. Anat Embryol (Berl) 208: 411-424.

Scadden DT. **2006**. The stem-cell niche as an entity of action. Nature 441: 1075-1079.

Schäfer K, Braun T. **1999**. Early specification of limb muscle precursor cells by the homeobox gene Lbx1h. Nat Genet 23: 213-216.

Schienda J, Engleka KA, Jun S, Hansen MS, Epstein JA, Tabin CJ, Kunkel LM, Kardon G. **2006**. Somitic origin of limb muscle satellite and side population cells. Proc Natl Acad Sci USA 103: 945-950.

Schneider JW, Gu W, Zhu L, Mahdavi V, Nadal-Ginard B. **1994**. Reversal of terminal differentiation mediated by p107 in Rb-/- muscle cells. Science 264: 1467-1471.

Schuster-Gossler K, Cordes R, Gossler A. **2007**. Premature myogenic differentiation and depletion of progenitor cells cause severe muscle hypotrophy in Delta1 mutants. Proc Natl Acad Sci 104: 537-542.

Schwarze SR, Shi Y, Fu VX, Watson PA, Jarrard DF. **2001**. Role of cyclin-dependent kinase inhibitors in the growth arrest at senescence in human prostate epithelial and uroepithelial cells. Oncogene 20: 8184-8192.

Seale P, Sabourin LA, Girgis-Gabardo A, Mansouri A, Gruss P, Rudnicki MA. **2000**. Pax7 is required for the specification of myogenic satellite cells. Cell 102: 777-786.

Serrano M, Hannon GJ, Beach D. **1993**. A new regulatory motif in cell-cycle control causing specific inhibition of cyclin D/CDK4. Nature 366: 704-707.

Shih NP, François P, Delaune EA, Amacher SL. **2015**. Dynamics of the slowing segmentation clock reveal alternating two-segment periodicity. Development 142: 1785-1793.

Shin EK, Shin A, Paulding C, Schaffhausen B, Yee AS. **1995**. Multiple change in E2F function and regulation occur upon muscle differentiation. Mol Cell Biol 15: 2252-2262.

Shinin V, Gayraud-Morel B, Gomès D, Tajbakhsh S. **2006**. Asymmetric division and cosegregation of template DNA strands in adult muscle satellite cells. Nat Cell Biol 8: 677-687.

Siegel AL, Atchison K, Fisher KE, Davis GE, Cornelison DD. **2009**. 3D timelapse analysis of muscle satellite cell motility. Stem Cells 27: 2527-2538.

Siegel AL, Kuhlmann PK, Cornelison DD. **2011**. Muscle satellite cell proliferation and association: new insights from myofiber time-lapse imaging. Skelet Muscle 1: 7.

Singh K, Dilworth FJ. **2013**. Differential modulation of cell cycle progression distinguishes members of the myogenic regulatory factor family of transcription factors. FEBS J 280: 3991-4003.

Sirbu IO, Duester G. **2006**. Retinoic-acid signalling in node ectoderm and posterior neural plate directs left-right patterning of somitic mesoderm. Nat Cell Biol 8: 271-277.

Skapek SX, Rhee J, Spicer DB, Lassar AB. **1995**. Inhibition of myogenic differentiation in proliferating myoblasts by cyclin D1-dependent kinase. Science 267: 1022-1024.

Smeriglio P, Alonso-Martin S, Masciarelli S, Madaro L, Iosue I, Marrocco V, Relaix F, Fazi F, Marazzi G, Sassoon DA, Bouché M. **2016**. Phosphotyrosine phosphatase inhibitor bisperoxovanadium endows myogenic cells with enhanced muscle stem cell functions via epigenetic modulation of Sca-1 and Pw1 promoters. FASEB J 30: 1404-1415.

Smythe GM, Grounds MD. **2001**. Absence of MyoD increases donor myoblast migration into host muscle. Exp Cell Res 267: 267-274.

Soejima H, Higashimoto K. **2013**. Epigenetic and genetic alterations of the imprinting disorder Beckwith-Wiedemann syndrome and related disorders. J Hum Genet 58: 402-409.

Soleimani VD, Punch VG, Kawabe Y, Jones AE, Palidwor GA, Porter CJ, Cross JW, Carvajal JJ, Kockx CE, van IJcken WF, Perkins TJ, Rigby PW, Grosveld F, Rudnicki MA. **2012**. Transcriptional dominance of Pax7 in adult myogenesis is due to high-affinity recognition of homeodomain motifs. Dev Cell 22: 1208-1220.

Soos TJ, Kiyokawa H, Yan JS, Rubin MS, Giordano A, DeBlasio A, Bottega S, Wong B, Mendelsohn J, Koff A. **1996**. Formation of p27-CDK complexes during the human mitotic cell cycle. Cell Growth Differ 7: 135-146.

Sorrentino V, Pepperkok R, Davis RL, Ansorge W, Philipson L. **1990**. Cell proliferation inhibited by MyoD1 independently of myogenic differentiation. Nature 345: 813-815.

Sousa-Victor P, Gutarra S, García-Prat L, Rodriguez-Ubreva J, Ortet L, Ruiz-Bonilla V, Jardí M, Ballestar E, González S, Serrano AL, Perdiguero E, Muñoz-Cánoves P. **2014**. Geriatric muscle stem cells switch reversible quiescence into senescence. Nature 506: 316-321.

Spitz F, Demignon J, Porteu A, Kahn A, Concordet JP, Daegelen D, Maire P. **1998**. Expression of myogenin during embryogenesis is controlled by Six/sine oculis homeoproteins through a conserved MEF3 binding site. Proc Natl Acad Sci USA 95: 14220-14225.

Storer M, Mas A, Robert-Moreno A, Pecoraro M, Ortells MC, Di Giacomo V, Yosef R, Pilpel N, Krizhanovsky V, Sharpe J, Keyes WM. **2013**. Senescence is a developmental mechanism that contributes to embryonic growth and patterning. Cell 155: 1119-1130.

Susaki E, Nakayama K, Yamasaki L, Nakayama KI. **2009**. Common and specific roles of the related CDK inhibitors p27 and p57 revealed by a knock-in mouse model. Proc Natl Acad Sci USA 106: 5192-5197.

Shawber C, Nofziger D, Hsieh JJ, Lindsell C, Bögler O, Hayward D, Weinmaster G. **1996**. Notch signaling inhibits muscle cell differentiation through a CBF1-independent pathway. Development 122: 3765-3773.

Tajbakhsh S, Rocancourt D, Buckingham M. **1996**. Muscle progenitor cells failing to respond to positional cues adopt non-myogenic fates in myf-5 null mice. Nature 384: 266-270.

Tajbakhsh S, Rocancourt D, Cossu G, Buckingham M. **1997**. Redefining the genetic hierarchies controlling skeletal myogenesis: Pax-3 and Myf-5 act upstream of MyoD. Cell 89: 127-138.

Tajbakhsh S. **2003**. Stem cells to tissue: molecular, cellular and anatomical heterogeneity in skeletal muscle. Curr Opin Genet Dev 13: 413-422.

Tajbakhsh S. **2009**. Skeletal muscle stem cells in developmental versus regenerative myogenesis. J Intern Med 266: 372-389.

Takahashi K, Nakayama K, Nakayama K. **2000**. Mice lacking a CDK inhibitor, p57Kip2, exhibit skeletal abnormalities and growth retardation. J Biochem 127: 73-83.

Tedesco FS, Dellavalle A, Diaz-Manera J, Messina G, Cossu G. **2010**. Repairing skeletal muscle: regenerative potential of skeletal muscle stem cells. J Clin Invest 120: 11-19.

Terada Y, Tatsuka M, Jinno S, Okayama H. **1995**. Requirement for tyrosine phosphorylation of Cdk4 in G1 arrest induced by ultraviolet irradiation. Nature 376: 358-362.

Thalmeier K, Synovzik H, Mertz R, Winnacker EL, Lipp M. **1989**. Nuclear factor E2F mediates basic transcription and trans-activation by E1a of the human MYC promoter. Genes Dev 3: 527-536.

Timchenko NA, Iakova P, Cai ZJ, Smith JR, Timchenko LT. **2001**. Molecular basis for impaired muscle differentiation in myotonic dystrophy. Mol Cell Biol 21: 6927-6938.

Tintignac LA, Sirri V, Leibovitch MP, Lécluse Y, Castedo M, Metivier D, Kroemer G, Leibovitch SA. **2004**. Mutant MyoD lacking Cdc2 phosphorylation sites delays M-phase entry. Mol Cell Biol 24: 1809-1821.

Tsivitse S. **2010**. Notch and Wnt signaling, physiological stimuli and postnatal myogenesis. Int J Biol Sci 6: 268-281.

Tsugu A, Sakai K, Dirks PB, Jung S, Weksberg R, Fei YL, Mondal S, Ivanchuk S, Ackerley C, Hamel PA, Rutka JT. **2000**. Expression of p57(KIP2) potently blocks the growth of human astrocytomas and induces cell senescence. Am J Pathol 157: 919-932.

Ustanina S, Carvajal J, Rigby P, Braun T. **2007**. The myogenic factor Myf5 supports efficient skeletal muscle regeneration by enabling transient myoblast amplification. Stem Cell 25: 2006-2016.

Vaccarello G, Figliola R, Cramerotti S, Novelli F, Maione R. **2006**. p57Kip2 is induced by MyoD through a p73-dependent pathway. J Mol Biol 356: 578-588.

Valcheva P, Cardus A, Panizo S, Parisi E, Bozic M, Lopez Novoa JM, Dusso A, Fernández E, Valdivielso JM. **2014**. Lack of vitamin D receptor causes stress-induced premature senescence in vascular smooth muscle cells through enhanced local angiotensin-II signals. Atherosclerosis 235: 247-255.

van den Heuvel S, Dyson NJ. **2008**. Conserved functions of the pRB and E2F families. Nat Rev Mol Cell Biol 9: 713-724.

Vandromme M, Chailleux C, Escaffit F, Trouche D. **2008**. Binding of the retinoblastoma protein is not the determinant for stable repression of some E2F-regulated promoters in muscle cells. Mol Cancer Res 6: 418-425.

Vasyutina E, Stebler J, Brand-Saberi B, Schulz S, Raz E, Birchmeier C. **2005**. CXCR4 and Gab1 cooperate to control the development of migrating muscle progenitor cells. Genes Dev 19: 2187-2198.

Vasyutina E, Lenhard DC, Birchmeier C. **2007a**. Notch function in myogenesis. Cell Cycle 6: 1451-1454.

Vasyutina E, Lenhard DC, Wende H, Erdmann B, Epstein JA, Birchmeier C. **2007b**. RBP-J (Rbpsuh) is essential to maintain muscle progenitor cells and to generate satellite cells. Proc Natl Acad Sci USA 104: 4443-4448.

Vlachos P, Nyman U, Hajji N, Joseph B. **2007**. The cell cycle inhibitor p57(Kip2) promotes cell death via the mitochondrial apoptotic pathway. Cell Death Differ 14: 1497-1507.

Vlachos P, Joseph B. **2009**. The Cdk inhibitor p57(Kip2) controls LIM-kinase 1 activity and regulates actin cytoskeleton dynamics. Oncogene 28: 4175-4188.

von Maltzahn J, Jones AE, Parks RJ, Rudnicki MA. **2013**. Pax7 is critical for the normal function of satellite cells in adult skeletal muscle. Proc Natl Acad Sci USA 110: 16474-16479.

Waga S, Hannon GJ, Beach D, Stillman B. **1994**. The p21 inhibitor of cyclin-dependent kinases controls DNA replication by interaction with PCNA. Nature 369: 574-578.

Wang J, Helin K, Jin P, Nadal-Ginard B. **1995**. Inhibition of *in vitro* myogenic differentiation by cellular transcription factor E2F1. Cell Growth Differ 6: 1299-1306.

Wang J, Huang Q, Tang W, Nadal-Ginard B. **1996a**. E2F1 inhibition of transcription activation by myogenic basic helix-loop-helix regulators. J Cell Biochem 62: 405-410.

Wang J, Walsh K. **1996a**. Resistance to apoptosis conferred by Cdk inhibitors during myocyte differentiation. Science 273: 359-361.

Wang J, Walsh K. **1996b**. Inhibition of retinoblastoma protein phosphorylation by myogenesis-induced changes in the subunit composition of the cyclin-dependent kinase 4 complex. Cell Growth Differ 7: 1471-1478.

Wang J, Guo K, Wills KN, Walsh K. **1997**. Rb functions to inhibit apoptosis during myocyte differentiation. Cancer Res 57: 351-354.

Wang YX, Dumont NA, Rudnicki MA. **2014**. Muscle stem cells at a glance. J Cell Sci 127: 4543-4548.

Watanabe H, Pan ZQ, Schreiber-Agus N, DePinho RA, Hurwitz J, Xiong Y. **1998**. Suppression of cell transformation by the cyclin-dependent kinase inhibitor p57KIP2 requires binding to proliferating cell nuclear antigen. Proc Natl Acad Sci USA 95: 1392-1397.

Webster MT, Manor U, Lippincott-Schwartz J, Fan CM. **2016**. Intravital imaging reveals ghost fibers as architectural units guiding myogenic progenitors during regeneration. Cell Stem Cell 18: 243-252.

Wen Y, Bi P, Liu W, Asakura A, Keller C, Kuang S. **2012**. Constitutive Notch activation upregulates Pax7 and promotes the self-renewal of skeletal muscle satellite cells. Mol Cell Biol 21: 2300-2311.

Westbury J, Watkins M, Ferguson-Smith AC, Smith J. **2001**. Dynamic temporal and spatial regulation of the cdk inhibitor p57(kip2) during embryo morphogenesis. Mech Dev 109: 83-89.

White JD, Scaffidi A, Davies M, McGeachie J, Rudnicki MA, Grounds MD. **2000**. Myotube formation is delayed but not prevented in MyoD-deficient skeletal muscle: studies in regenerating whole muscle grafts of adult mice. J Histochem Cytochem 48: 1531-1544.

White RB, Biérinx AS, Gnocchi VF, Zammit PS. **2010**. Dynamics of muscle fibre growth during postnatal mouse development. BMC Dev Biol 10: 21.

Wirt SE, Adler AS, Gebala V, Weimann JM, Schaffer BE, Saddic LA, Viatour P, Vogel H, Chang HY, Meissner A, Sage J. **2010**. G1 arrest and differentiation can occur independently of Rb family function. J Cell Biol 191: 809-825.

Wright WE, Sassoon DA, Lin VK. **1989**. Myogenin, a factor regulating myogenesis, has a domain homologous to MyoD. Cell 56: 607-617.

Xiong Y, Hannon GJ, Zhang H, Casso D, Kobayashi R, Beach D. **1993**. p21 is a universal inhibitor of cyclin kinases. Nature 366: 701-704.

Xu XY, Wang WQ, Zhang L, Li YM, Tang M, Jiang N, Cai SL, Wei L, Jin F, Chen B. **2012**. Clinical implications of p57 KIP2 expression in breast cancer. Asian Pac J Cancer Prev 13: 5033-5036.

Yablonka-Reuveni Z, Rudnicki MA, Rivera AJ, Primig M, Anderson JE, Natanson P. **1999**. The transition from proliferation to differentiation is delayed in satellite cells from mice lacking MyoD. Dev Biol 210: 440-455.

Yaffe D, Saxel O. **1997**. Serial passaging and differentiation of myogenic cells isolated from dystrophic mouse muscle. Nature 270: 725-727.

Yan Y, Frisén J, Lee MH, Massagué J, Barbacid M. **1997**. Ablation of the CDK inhibitor p57Kip2 results in increased apoptosis and delayed differentiation during mouse development. Genes Dev 11: 973-983.

Yan Z, Choi S, Liu X, Zhang M, Schageman JJ, Lee SY, Hart R, Lin L, Thurmond FA, Williams RS. **2003**. Highly coordinated gene regulation in mouse skeletal muscle regeneration. J Biol Chem 278: 8826-8836.

Yang XM, Vogan K, Gros P, Park M. **1996**. Expression of the met receptor tyrosine kinase in muscle progenitor cells in somites and limbs is absent in Splotch mice. Development 122: 2163-2171.

Yang C, Nan H, Ma J, Jiang L, Guo Q, Han L, Zhang Y, Nan K, Guo H. **2015**. High Skp2/Low p57(Kip2) Expression is Associated with Poor Prognosis in Human Breast Carcinoma. Breast Cancer (Auckl) 4: 31-21.

Yin H, Price F, Rudnicki MA. **2013**. Satellite cells and the muscle stem cell niche. Physiol Rev 93: 23-67.

Yokoo T, Toyoshima H, Miura M, Wang Y, Iida KT, Suzuki H, Sone H, Shimano H, Gotoda T, Nishimori S, Tanaka K, Yamada N. **2003**. p57Kip2 regulates actin dynamics by binding and translocating LIM-kinase 1 to the nucleus. J Biol Chem 278: 52919-52923.

Yu S, Yang F, Shen WH. **2016**. Genome maintenance in the context of 4D chromatin condensation. Cell Mol Life Sci [Epub ahead of print]

Zabludoff SD, Csete M, Wagner R, Yu X, Wold BJ. **1998**. p27Kip1 is expressed transiently in developing myotomes and enhances myogenesis. Cell Growth Differ 9: 1-11.

Zacharek SJ, Fillmore CM, Lau AN, Gludish DW, Chou A, Ho JW, Zamponi R, Gazit R, Bock C, Jäger N, Smith ZD, Kim TM, Saunders AH, Wong J, Lee JH, Roach RR, Rossi DJ, Meissner A, Gimelbrant AA, Park PJ, Kim CF. **2011**. Lung stem cell self-renewal relies on BMI1-dependent control of expression at imprinted loci. Cell Stem Cell 9: 272-281.

Zacksenhaus E, Jiang Z, Chung D, Marth JD, Phillips RA, Gallie BL. **1996**. pRb controls proliferation, differentiation, and death of skeletal muscle cells and other lineages during embryogenesis. Genes Dev 10: 3051-3064.

Zalc A, Hayashi S, Auradé F, Bröhl D, Chang T, Mademtzoglou D, Mourikis P, Yao Z, Cao Y, Birchmeier C, Relaix F. **2014**. Antagonistic regulation of p57kip2 by Hes/Hey downstream of Notch signaling and muscle regulatory factors regulates skeletal muscle growth arrest. Development 141: 2780-2790.

Zammit PS, Golding JP, Nagata Y, Hudon V, Partridge TA, Beauchamp JR. **2004**. Muscle satellite cells adopt divergent fates: a mechanism for self-renewal? J Cell Biol 166: 347-357.

Zarkowska T, Mittnacht S. **1997**. Differential phosphorylation of the retinoblastoma protein by G1/S cyclin-dependent kinases. J Biol Chem 272: 12738-12746.

Zhang H, Hannon GJ, Beach D. **1994**. p21-containing cyclin kinases exist in both active and inactive states. Genes Dev 8: 1750-1758.

Zhang W, Behringer RR, Olson EN. **1995**. Inactivation of the myogenic bHLH gene MRF4 results in up-regulation of myogenin and rib anomalies. Genes Dev 9: 1388-1399.

Zhang P, Liégeois NJ, Wong C, Finegold M, Hou H, Thompson JC, Silverman A, Harper JW, DePinho RA, Elledge SJ. **1997**. Altered cell differentiation and proliferation in mice lacking p57KIP2 indicates a role in Beckwith-Wiedemann syndrome. Nature 387: 151-158.

Zhang P, Wong C, DePinho RA, Harper JW, Elledge SJ. **1998**. Cooperation between the Cdk inhibitors p27(KIP1) and p57(KIP2) in the control of tissue growth and development. Genes Dev 12: 3162-3167.

Zhang JM, Wei Q, Zhao X, Paterson BM. **1999a**. Coupling of the cell cycle and myogenesis through the cyclin D1-dependent interaction of MyoD with cdk4. EMBO J 18: 926-933.

Zhang P, Wong C, Liu D, Finegold M, Harper JW, Elledge SJ. **1999b**. p21(CIP1) and p57(KIP2) control muscle differentiation at the myogenin step. Genes Dev 13: 213-224.

Zhang JM, Zhao X, Wei Q, Paterson BM. **1999c**. Direct inhibition of G(1) cdk kinase activity by MyoD promotes myoblast cell cycle withdrawal and terminal differentiation. EMBO J 18: 6983-6993.

Zhang K, Sha J, Harter ML. **2010**. Activation of Cdc6 by MyoD is associated with the expansion of quiescent myogenic satellite cells. J Cell Biol 188: 39-48.

Zhu L, Harlow E, Dynlacht BD. **1995**. p107 uses a p21CIP1-related domain to bind cyclin/cdk2 and regulate interactions with E2F. Genes Dev 9: 1740-1752.

Zhu J, Woods D, McMahon M, Bishop JM. **1998**. Senescence of human fibroblasts induced by oncogenic Raf. Genes Dev 12: 2997-3007.

Zindy F, Quelle DE, Roussel MF, Sherr CJ. **1997**. Expression of the p16INK4a tumor suppressor versus other INK4 family members during mouse development and aging. Oncogene 15: 203-211.

Zismanov V, Chichkov V, Colangelo V, Jamet S, Wang S, Syme A, Koromilas AE, Crist C. **2016**. Phosphorylation of eIF2α Is a Translational Control Mechanism Regulating Muscle Stem Cell Quiescence and Self-Renewal. Cell Stem Cell 18: 79-90.

Zou P, Yoshihara H, Hosokawa K, Tai I, Shinmyozu K, Tsukahara F, Maru Y, Nakayama K, Nakayama KI, Suda T. **2011**. p57(Kip2) and p27(Kip1) cooperate to maintain hematopoietic stem cell quiescence through interactions with Hsc70. Cell Stem Cell 9: 247-261.

Online resources

1. https://embryology.med.unsw.edu.au/embryology/index.php/Mouse_Timeline_Detailed
(Timeline and hallmarks of mouse embryonic development)